

In presenting this dissertation as a partial fulfillment of the requirements for an advanced degree from Emory University, I agree that the library of the University shall make it available for inspection and circulation in accordance with its regulations, governing materials of this type. I agree that permissions to copy from, or to publish, this dissertation may be granted by the professor under whose direction it was written, or in his absence, by the Dean of the Graduate School when such copying or publication is solely for scholarly purpose and does not involve potential gain. It is understood that any copying from, or publication of this dissertation which involves potential gain will not be allowed without written permission.

Rongbiao Tong

**Chapter 1. Biomimetic Total Synthesis of
ent-Durgamone, *ent*-Nakorone and *ent*-Abudinol B
Chapter 2. Biomimetic Synthesis of Fused Polypyranes**

By

Rongbiao Tong

Doctor of Philosophy

Department of Chemistry

Dr. Frank E. McDonald

Adviser

Dr. Lanny S. Liebeskind

Committee Member

Dr. Fredric M. Menger

Committee Member

Accepted:

Lisa A. Tedesco, Ph. D.
Dean of the Graduate School

Date

***Chapter 1. Biomimetic Total Synthesis of
ent-Durgamone, ent-Nakorone and ent-Abudinol B***
Chapter 2. Biomimetic Synthesis of Fused Polypyranes

By

Rongbiao Tong

B. S., Hunan University, 2000

M. S., Hunan University, 2003

Adviser: Frank E. McDonald

An Abstract of

A dissertation submitted to the Faculty of the Graduate

School of Emory University in partial fulfillment

Of the requirements for the degree of

Doctor of Philosophy

Department of Chemistry

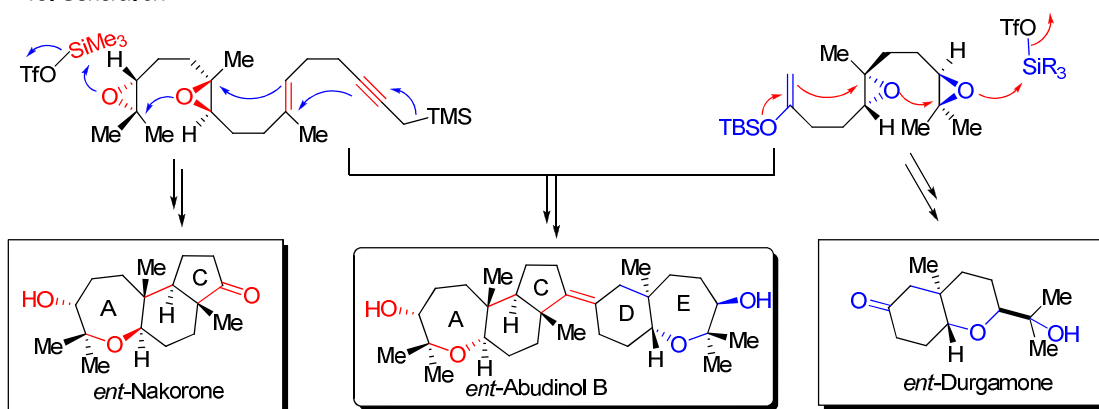
2008

Abstract

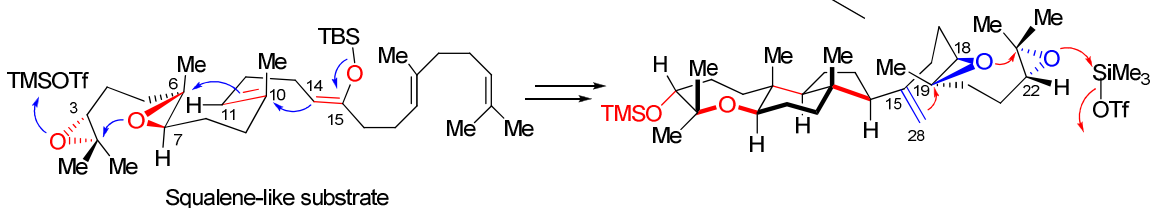
Chapter 1. Biomimetic Total Synthesis of *ent*-Durgamone, *ent*-Nakorone and *ent*-Abudinol B

The first biomimetic total syntheses of *ent*-nakorone (7 steps in 32.1% yield from farnesol), *ent*-durgamone (8 steps in 21% yield from geranylacetone), and *ent*-abudinol B (5 steps in 15.92% yield from advanced intermediates of *ent*-nakorone and *ent*-durgamone) were accomplished by combining features of tandem polyepoxide cyclization with biomimetic polyene cyclization. The present biomimetic synthesis route offers efficient access to these marine natural products. In addition, the synthesis of the tetrasubstituted alkene of *ent*-abudinol B demonstrates the application of palladium-catalyzed cross-coupling of two different polycyclic ketones via the corresponding vinyl triflates, followed by partial hydrogenation of the resulting conjugated diene.

First Generation:



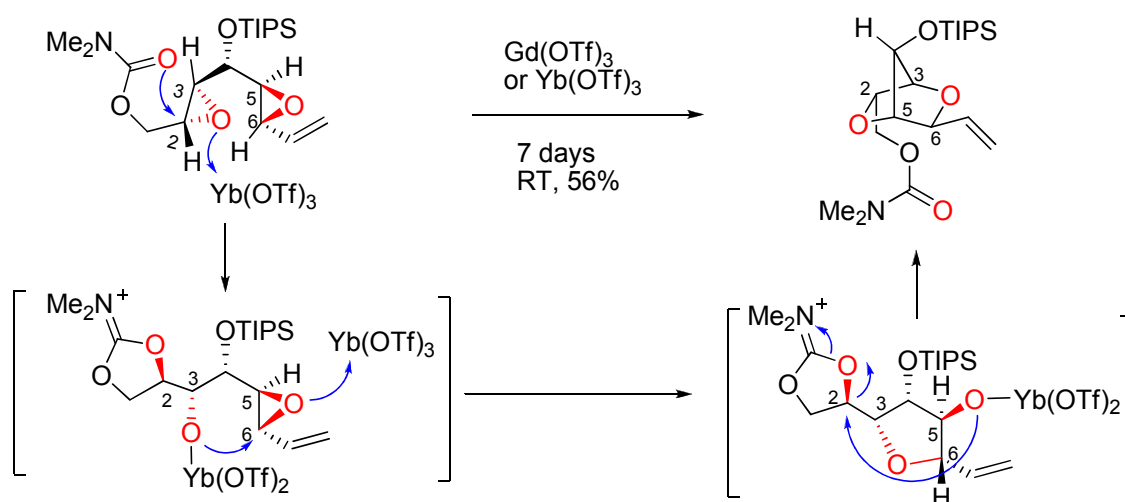
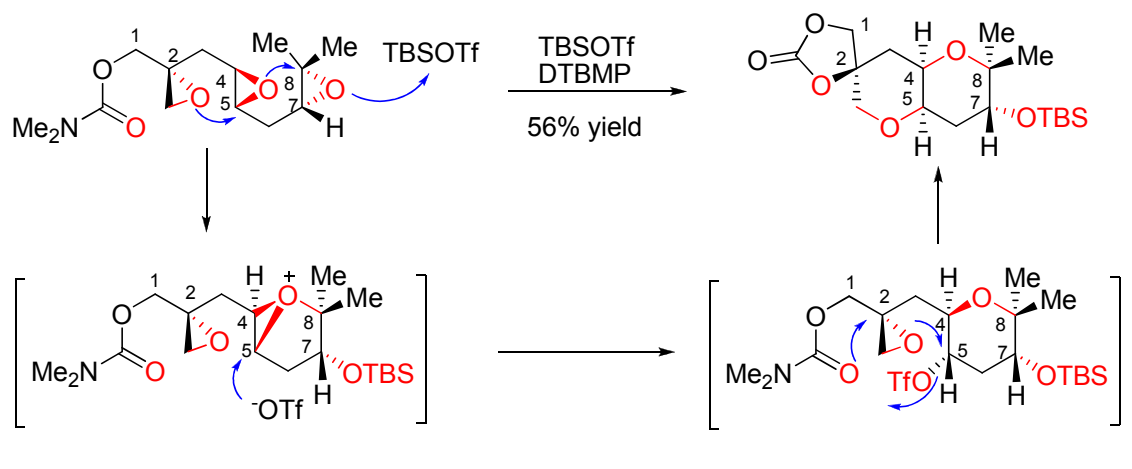
Second Generation:



The second generation of biomimetic total synthesis of the enantiomer of abudinol B was achieved in 8 steps from commercially available *trans-trans*-farnesylacetate with 0.18% overall yield, following a synthetic strategy inspired by and closely mimicking the proposed biosynthetic pathway. This synthesis demonstrates the viability of tandem oxa- and carbacyclizations of structurally complex polyepoxide-alkene substrates. This second generation synthesis features a two-directional biomimetic cyclization strategy, in which the separate polycyclic ring systems are constructed by Lewis acid-promoted tandem oxa- and carbacyclizations from a structural analog of squalene diepoxide. This demonstration of tandem cyclizations provides experimental support for the chemical viability of a proposed biogenetic pathway.

Chapter 2. Biomimetic Synthesis of Fused Polypyran

The biomimetic synthesis of fused bispyran via Lewis acid-mediated tandem oxacyclization of 1,4,7-polyepoxide is explored. Fragmentation was the main competing process for oxacyclization of skipped polyepoxides. The nature of the Lewis acid promoter is critical for the *endo*-regioselectivity of epoxide cyclization, although anomalous apparent retention of stereochemistry is observed at some reactive centers. The mechanistic interpretation leads us to hypothesize that the energy of the reaction transition state required for synchronous cyclizations to form polypyran is much higher than that in the analogous synthesis of polyoxepanes, and thus the stepwise mechanism may operate.



Oxacyclization of 2,3-disubstituted epoxide only proceeded in an *exo* mode to give cyclization products, which structures were highly dependent on the Lewis acid promoter and reaction time. These results provide the direct evidence in supporting the important role played by C3 substituent on the mode of oxacyclization of polyepoxide. These findings greatly expand our mechanistic understanding of oxacyclization of polyepoxides to polycyclic ethers and will guide our designing of novel oxacyclization in the future.

***Chapter 1. Biomimetic Total Synthesis of
ent-Durgamone, ent-Nakorone and ent-Abudinol B***
Chapter 2. Biomimetic Synthesis of Fused Polypyranes

By

Rongbiao Tong

B. S., Hunan University, 2000

M. S., Hunan University, 2003

Adviser: Frank E. McDonald

A dissertation submitted to the Faculty of the Graduate

School of Emory University in partial fulfillment

Of the requirements for the degree of

Doctor of Philosophy

Department of Chemistry

2008

Acknowledgements

I would like to convey my deepest appreciation to my adviser Dr. Frank E. McDonald for his guidance during my graduate studies at Emory University. He is an excellent mentor and provided me with a stimulating research environment and intellectual freedom. His unlimited enthusiasm for chemistry, along with interactive teaching, has greatly impressed me and will become an invaluable motivation in my future career.

I also extend my appreciation to my committee members, Dr. Lanny S. Liebeskind and Dr. Fredric M. Menger, for their creative suggestions and guidance during the past five years. The interactions with them were stimulating and were very helpful for my projects at Emory. I particularly thank Dr. Simon B. Blakey for willingness to be a committee member for my research proposal, and for his constructive criticism (along with Dr. Liebeskind and Dr. Menger) on my pre-proposal and proposal. Other organic faculty members, especially Dr. Albert Padwa and Dr. Debbie Mohler whose classes I took, taught me a great deal and I appreciated them greatly.

Dr. Shaoxiong Wu in the NMR center, Dr. Kenneth I. Hardcastle in the X-ray crystallography center, and Dr. Fred Strobel in the mass spectrometry center have been outstanding and I acknowledged their constant support.

The McDonald group members have been very friendly and created a very stimulating research environment. Special thanks goes to Jason C. Valentine, Yi-Hung Chen, Zhongbo Fei, Bonsuk Koo, Mary Smart, Brad Balthaser, John

Wiseman, Omar Robles-Resendiz, Matt Boone and Claney Pereira, for having been wonderful co-workers in the lab.

I have enjoyed my life at Emory because I made many friends here. I attended parties on weekends or holidays, discussed literatures and tough problems, chatted about routine issues in life with my new found friends. I will miss the wonderful days I spent at Emory. I thank all of you, particularly Weiqiang Zhan, Hao Yang, Hao Li, Zhihui Zhang, Yongqiang Zhang, Harry Wong, Bo Chen, Songbai Liu, Wenyong Chen and Shuangpei Liu.

Lastly, I would like to thank my wife Rong Ni for taking care of my son Terry Tong and holding our family together. It would have been impossible to accomplish my graduate research without her selfless and constant support. Thank you!

Table of Contents

Chapter 1. Biomimetic Total Synthesis of *ent*-Durgamone, *ent*-Nakorone and *ent*-Abudinol B

1.1. Introduction and Background-----	1
1.1.1. Total synthesis and biomimetic synthesis-----	1
1.1.2. Biomimetic total Synthesis of isoprenoid natural products	
from squalene-like substrates-----	3
1.1.2.1. Biogenesis of isoprenoid natural products-----	3
1.1.2.2. Stereochemistry issues in biogenesis of isoprenoid	
natural product-----	5
1.1.2.3. Biomimetic synthesis of isoprenoid natural products-----	8
1.1.3. Biomimetic synthesis of polycyclic ethers-----	12
1.1.3.1. Biogenesis of polycyclic ether natural products-----	12
1.1.3.2. Biomimetic synthesis of polycyclic ethers-----	15
1.1.3.3. Biomimetic synthesis of polycyclic ether natural products	
-----	18
1.1.4. Biogenesis of abudinol B and related natural products-----	19
1.1.5. Retrosynthetic analysis of abudinol B, durgamone and nakorone--	25
1.2. Results and discussion-----	27
1.2.1. Total synthesis of <i>ent</i> -durgamone and bicyclic ketone 77 -----	27
1.2.2. Total synthesis of <i>ent</i> -nakorone (<i>ent</i>-67) -----	35
1.2.3. Total synthesis of enantiomer of abudinol B (<i>ent</i>-64) -----	40
1.3. Biomimetic total synthesis of abudinol B from squalene-like precursor-----	52

1.3.1. Synthetic strategies-----	52
1.3.2. Synthesis of cyclization substrate 149 -----	55
1.3.3. First-stage biomimetic tricyclization-----	59
1.3.4. Second-stage biomimetic bicyclization-----	61
1.4. Conclusions-----	68
1.5. Experiments-----	70
2-D NMR spectra-----	159
X-Ray database in total synthesis of abudinol B-----	163
1.6. References-----	220

Chapter 2. Biomimetic Synthesis of Fused Polypyran

2.1. Introduction and Background-----	231
2.1.1. Reductive etherification-----	232
2.1.2. <i>Endo</i> -selective cyclization of epoxide-----	236
2.1.3. Biomimetic oxacyclization of skipped polyepoxide-----	239
2.2. Results and Discussion-----	240
2.2.1. Oxacyclization with internal disubstituted epoxide-----	240
2.2.2. Unexpected oxacyclization of skipped 2,3-disubstituted epoxides-----	247
2.3. Conclusions-----	253
2.4. Experiments-----	255
2-D NMR spectra-----	293
X-Ray database in biomimetic synthesis of fused polypyran-----	303
2.5. References-----	330

List of Figures

Chapter 1. Biomimetic Total Synthesis of *ent*-Durgamone, *ent*-Nakorone and *ent*-Abudinol B

Figure 1. Examples of polycyclic ether natural products-----	13
Figure 2. Examples of polycyclic ether terpenoid natural products-----	20
Figure 3. Oxa-carbacyclization substrates 78 , 83 and 84 -----	28
Figure 4. Intermediate or product of nonselective Shi epoxidation-----	29
Figure 5. The thermal ellipsoid diagrams for bicyclic ketones 95 and <i>epi</i> - 95 -----	32
Figure 6. The thermal ellipsoid diagram for compound 115 -----	39
Figure 7. McMurry cross coupling of arylketone-----	41
Figure 8. Thermal ellipsoid diagram for compound 117 -----	49
Figure 9. Fragments of squalene-like substrate 149 -----	55
Figure 10. NOESY NMR experiments of compounds 148a and 148b -----	60
Figure 11. Potential biomimetic synthesis of raspacionin from 149 -----	61
Figure 12. Thermal ellipsoid diagram for pentacyclic product 179 -----	66

Chapter 2. Biomimetic Synthesis of Fused Polypyrans

Figure 1. Representative core structure of polycyclic ethers-----	231
Figure 2. The thermal ellipsoid diagram for compound 51 -----	242
Figure 3. The thermal ellipsoid diagram for compound 52 -----	244
Figure 4. The thermal ellipsoid diagram for compound 56 -----	245
Figure 5. Cyclization substrate 62 and 63 -----	248

List of Schemes

Chapter 1. Biomimetic Total Synthesis of *ent*-Durgamone, *ent*-Nakorone and *ent*-Abudinol B

Scheme 1. Robinson's biomimetic synthesis of tropinone-----	2
Scheme 2. Biosynthesis of hopene and lanosterol from squalene-----	4
Scheme 3. Stork-Burgstahler's studies on the stereochemistry of polyene cyclization-----	6
Scheme 4. Schinz-Eschenmoser evidence for nonclassical cyclic carbenium ion-----	6
Scheme 5. Stereospecific cyclization of epoxy alkene-----	8
Scheme 6. Johnson's biomimetic total synthesis of sophoradiol-----	9
Scheme 7. Corey's biomimetic total synthesis of dammarenediol II-----	10
Scheme 8. Corey's biomimetic total synthesis of isoprenoid natural products---	11
Scheme 9. Nakanishi's biogenetic hypothesis of brevetoxin B-----	14
Scheme 10. Jamison's biomimetic oxacyclization of polyepoxide-----	15
Scheme 11. Valentine and McDonald's biomimetic oxacyclization of polyepoxide via epoxonium ion-----	16
Scheme 12. Holton's biomimetic total synthesis of hemibrevetoxin B-----	18
Scheme 13. Kashman's biogenetic hypothesis for abudinols-----	22
Scheme 14. Norte's biosynthesis for abudinol B-----	23
Scheme 15. Retrosynthetic analysis of abudinol B, durgamone and nakorone--	25
Scheme 16. Synthesis of diepoxy ketone 87 -----	28
Scheme 17. Synthesis of cyclization substrates-----	29

Scheme 18. TBSOTf mediated oxa-carbacyclization of 78 -----	31
Scheme 19. Oxa-carbacyclization of 83 and 84 -----	33
Scheme 20. McDonald/ Wei alkene-epoxide cyclization-----	33
Scheme 21. Total synthesis of <i>ent</i> -durgamone (ent-66)-----	34
Scheme 22. Synthesis of farnesyl sulfone 104 -----	36
Scheme 23. Synthesis of propargylic silane 109 -----	36
Scheme 24. Synthesis of cyclization substrate 81 -----	37
Scheme 25. Synthesis of enantiomer of nakorone (ent-59)-----	38
Scheme 26. McMurry coupling of 94 and 116 -----	40
Scheme 27. Takeda's method for assembly of ketones 94 and 116 -----	42
Scheme 28. Vinylolithium formation via Shapiro reaction-----	43
Scheme 29. Coupling of ketone 94 with 116 via hydrazone formation-----	44
Scheme 30. Barton's method to assemble <i>ent</i> -abudinol B from azine 127 -----	45
Scheme 31. Suzuki cross-coupling of 94 and 116 -----	46
Scheme 32. Attempts on hydrogenation of diene 137 -----	48
Scheme 33. Palladium-catalyzed hydrogenation of diene 137 -----	48
Scheme 34. Hole transfer catalyst promoted hydrogenation of diene 137 -----	50
Scheme 35. Completion of the total synthesis of <i>ent</i> -abudinol B (ent-64)-----	51
Scheme 36. Retrosynthetic analysis of <i>ent</i> -abudinol B (ent-64)-----	53
Scheme 37. Synthesis of coupling substrate 156 -----	56
Scheme 38. Synthesis of farnesyl diepoxy bromide 150 -----	56
Scheme 39. Synthesis of squalene-like substrate 149 -----	57
Scheme 40. First stage biomimetic tricyclization of 149 -----	59

Scheme 41. Olefination of tricyclic ketone 148 -----	62
Scheme 42. Double Shi diastereoselective epoxidation of 148 -----	63
Scheme 43. Bicyclization of 147a to <i>ent</i> -abudinol B (ent-64)-----	64
Scheme 44. TMSOTf-promoted cyclization of diastereomeric 147b -----	65
Scheme 45. BF ₃ -Et ₂ O promoted bicyclization of 180 -----	67

Chapter 2. Biomimetic Synthesis of Fused Polypyrans

Scheme 1. Reductive etherification for synthesis of polycyclic pyrans-----	233
Scheme 2. Intramolecular allylation of acetals-----	235
Scheme 3. Reductive etherification of carbonyl and unsaturated ester-----	236
Scheme 4. <i>Endo</i> -selective cyclizations of epoxide-----	237
Scheme 5. Biomimetic oxacyclization of skipped polyepoxide-----	239
Scheme 6. Synthesis of model substrate 41 -----	240
Scheme 7. Synthesis of skipped triepoxide 48 -----	241
Scheme 8. Oxacyclization of model substrate diepoxide 41 -----	242
Scheme 9. Trialkylsilyl triflate-promoted oxacyclization of triepoxide 48 and 53 -----	243
Scheme 10. TBSOTf-promoted oxacyclization of skipped triepoxide 48 -----	244
Scheme 11. Mechanistic explanation of oxacyclization to bispyran 56 -----	245
Scheme 12. McDonald's oxacyclization of isoprenoid-derived polyepoxide-----	247
Scheme 13. Synthesis of diepoxide 66 -----	248
Scheme 14. Synthesis of diepoxide 67 -----	249
Scheme 15. Lewis acid promoted oxacyclization of diepoxide 66 -----	250

Scheme 16. Oxacyclization of skipped triepoxide **67**-----251

Scheme 17. Transition metal promoted opening of epoxide **67**-----252

List of Tables

Chapter 1. Biomimetic Total Synthesis of *ent*-Durgamone, *ent*-Nakorone and *ent*-Abudinol B

Table 1. Crystal data and structure refinement for compound 95 -----	163
Table 2. Atomic coordinates (x 10 ⁴) and equivalent isotropic displacement parameters (Å ² x 10 ³) for compound 95 . U(eq) is defined as one third of the trace of the orthogonalized U ^{ij} tensor.-----	164
Table 3. Bond lengths [Å] and angles [°] for compound 95 -----	165
Table 4. Anisotropic displacement parameters (Å ² x 10 ³) for compound 95 . The anisotropic displacement factor exponent takes the form: $-2\pi^2[h^2 a^{*2}U^{11} + \dots + 2 h k a^* b^* U^{12}]$ -----	166
Table 5. Hydrogen coordinates (x 10 ⁴) and isotropic displacement parameters (Å ² x 10 ³) for compound 95 -----	167
Table 6. Torsion angles [°] for compound 95 -----	168
Table 7. Hydrogen bonds for compound 95 [Å and °]-----	169
Table 8. Crystal data and structure refinement for compound epi-95 -----	170
Table 9. Atomic coordinates (x 10 ⁴) and equivalent isotropic displacement parameters (Å ² x 10 ³) for epi-95 . U (eq) is defined as one third of the trace of the orthogonalized U ^{ij} tensor.-----	171
Table 10. Bond lengths [Å] and angles [°] for epi-95 -----	172

Table 11. Anisotropic displacement parameters ($\text{\AA}^2 \times 10^3$) for epi-95 . The anisotropic displacement factor exponent takes the form: $-2\pi^2 [h^2 a^{*2} U^{11} + \dots + 2 h k a^* b^* U^{12}]$	174
Table 12. Hydrogen coordinates ($\times 10^4$) and isotropic displacement parameters ($\text{\AA}^2 \times 10^3$) for epi-95 .	175
Table 13. Torsion angles [$^\circ$] for epi-95 .	176
Table 14. Hydrogen bonds for epi-95 [\AA and $^\circ$]	177
Table 15. Crystal data and structure refinement for 115 .	178
Table 16. Atomic coordinates ($\times 10^4$) and equivalent isotropic displacement parameters ($\text{\AA}^2 \times 10^3$) for 115 . $U(\text{eq})$ is defined as one third of the trace of the orthogonalized U^{ij} tensor.	179
Table 17. Bond lengths [\AA] and angles [$^\circ$] for 115 .	180
Table 18. Anisotropic displacement parameters ($\text{\AA}^2 \times 10^3$) for 115 . The anisotropic displacement factor exponent takes the form: $-2\pi^2 [h^2 a^{*2} U^{11} + \dots + 2 h k a^* b^* U^{12}]$	183
Table 19. Hydrogen coordinates ($\times 10^4$) and isotropic displacement parameters ($\text{\AA}^2 \times 10^3$) for 115 .	184
Table 20. Torsion angles [$^\circ$] for 115 .	185
Table 21. Hydrogen bonds for 115 [\AA and $^\circ$]	187
Table 22. Crystal data and structure refinement for 117 .	188

Table 23. Atomic coordinates ($\times 10^4$) and equivalent isotropic displacement parameters ($\text{\AA}^2 \times 10^3$) for 117 . $U(\text{eq})$ is defined as one third of the trace of the orthogonalized U_{ij} tensor-----	189
Table 24. Bond lengths [\AA] and angles [$^\circ$] for 117 -----	191
Table 25. Anisotropic displacement parameters ($\text{\AA}^2 \times 10^3$) for 117 . The anisotropic displacement factor exponent takes the form: $-2\pi^2 [h^2 a^{*2} U^{11} + \dots + 2 h k a^* b^* U^{12}]$ -----	197
Table 26. Hydrogen coordinates ($\times 10^4$) and isotropic displacement parameters ($\text{\AA}^2 \times 10^3$) for 117 -----	199
Table 27. Torsion angles [$^\circ$] for 117 -----	202
Table 28. Crystal data and structure refinement for 179 -----	206
Table 29. Atomic coordinates ($\times 10^4$) and equivalent isotropic displacement parameters ($\text{\AA}^2 \times 10^3$) for 179 . $U(\text{eq})$ is defined as one third of the trace of the orthogonalized U_{ij} tensor-----	207
Table 30. Bond lengths [\AA] and angles [$^\circ$] for 179 -----	209
Table 31. Anisotropic displacement parameters ($\text{\AA}^2 \times 10^3$) for 179 . The anisotropic displacement factor exponent takes the form: $-2\pi^2 [h^2 a^{*2} U^{11} + \dots + 2 h k a^* b^* U^{12}]$ -----	212
Table 32. Hydrogen coordinates ($\times 10^4$) and isotropic displacement parameters ($\text{\AA}^2 \times 10^3$) for 179 -----	214
Table 33. Torsion angles [$^\circ$] for 179 -----	216

Chapter 2. Biomimetic Synthesis of Fused Polypyranes

Table 1. Crystal data and structure refinement for 51 -----	303
Table 2. Atomic coordinates ($\times 10^4$) and equivalent isotropic displacement parameters ($\text{\AA}^2 \times 10^3$) for 51 . U(eq) is defined as one third of the trace of the orthogonalized U^{ij} tensor-----	304
Table 3. Bond lengths [\AA] and angles [$^\circ$] for 51 -----	305
Table 4. Anisotropic displacement parameters ($\text{\AA}^2 \times 10^3$) for 51 . The anisotropic displacement factor exponent takes the form: $-2\pi^2 [h^2 a^{*2} U^{11} + \dots + 2 h k a^* b^* U^{12}]$ -----	307
Table 5. Hydrogen coordinates ($\times 10^4$) and isotropic displacement parameters ($\text{\AA}^2 \times 10^3$) for 51 -----	308
Table 6. Torsion angles [$^\circ$] for 51 -----	309
Table 7. Hydrogen bonds for 51 [\AA and $^\circ$]-----	310
Table 8. Crystal data and structure refinement for 52 -----	311
Table 9. Atomic coordinates ($\times 10^4$) and equivalent isotropic displacement parameters ($\text{\AA}^2 \times 10^3$) for 52 . U(eq) is defined as one third of the trace of the orthogonalized U^{ij} tensor-----	312
Table 10. Bond lengths [\AA] and angles [$^\circ$] for 52 -----	313
Table 11. Anisotropic displacement parameters ($\text{\AA}^2 \times 10^3$) for 52 . The anisotropic displacement factor exponent takes the form: $-2\pi^2 [h^2 a^{*2} U^{11} + \dots + 2 h k a^* b^* U^{12}]$ -----	315

Table 12. Hydrogen coordinates ($\times 10^4$) and isotropic displacement parameters ($\text{\AA}^2 \times 10^3$) for 52 -----	316
Table 13. Torsion angles [$^\circ$] for 52 -----	317
Table 14. Hydrogen bonds for 52 [\AA and $^\circ$]-----	319
Table 15. Crystal data and structure refinement for 56 -----	320
Table 16. Atomic coordinates ($\times 10^4$) and equivalent isotropic displacement parameters ($\text{\AA}^2 \times 10^3$) for 56 . $U(\text{eq})$ is defined as one third of the trace of the orthogonalized U_{ij} tensor-----	321
Table 17. Bond lengths [\AA] and angles [$^\circ$] for 56 -----	322
Table 18. Anisotropic displacement parameters ($\text{\AA}^2 \times 10^3$) for 56 . The anisotropic displacement factor exponent takes the form: $-2\pi^2 [h^2 a^{*2} U^{11} + \dots + 2 h k a^* b^* U^{12}]$ -----	325
Table 19. Hydrogen coordinates ($\times 10^4$) and isotropic displacement parameters ($\text{\AA}^2 \times 10^3$) for 56 -----	326
Table 20. Torsion angles [$^\circ$] for 56 -----	328

Abbreviations

Ac	Acetyl
AIBN	2,2'-azbisisobutyronitrile
AN	acetonitrile
Aq	aqueous
Ar	aryl
Boc	<i>tert</i> -butoxycarbonyl
<i>t</i> -BOOH	<i>tert</i> -butylhydroperoxide
<i>n</i> -BuLi	<i>n</i> -butyllithium
<i>t</i> -BuLi	<i>tert</i> -butyllithium
Bz	benzoyl
Cat	catalytic
d	doublet
dppf	diphenylphosphinoferrrocene
dppp	1, 3-bis(diphenylphosphino)propane
DIBAL-H	diisobutylaluminum hydride
DIPT	diisopropyl tartrate
DMAP	<i>N, N</i> -dimethylaminopyridine
DMF	<i>N, N</i> -dimethylformamide
DMM	dimethoxymethane
DMSO	dimethylsulfoxide
DTBMP	2,6-di- <i>tert</i> -butyl-4-methylpyridine
EDTA	ethylenediaminetetraacetic acid

Equiv	equivalent
EtOAc	ethyl acetate
HMPA	Hexamethylphosphoric triamide
HRMS	high-resolution mass spectroscopy
KHMDS	potassium bis(trimethylsilyl)amide
LA	Lewis acid
LAH	lithium aluminum hydride
LDA	lithium diisopropylamide
LiHMDS	lithium bis(trimethylsilyl)amide
m	multiplet
mL	milliliter
mmol	millimole
MS	molecular sieves
Ms	methanesulfonyl
NBS	<i>N</i> -bromosuccinimide
NIS	<i>N</i> -iodosuccinimide
NMR	nuclear magnetic resonance
Ph	phenyl
PhNTf ₂	<i>N</i> -phenyltrifluoromethanesulfonimide
Pyr	pyridine
q	quartet
Red-Al	sodium bis(2-methoxyethoxy)aluminum hydride
rt	room temperature

s	singlet
Sat	saturated
t	triplet
TBAF	tetrabutylammonium fluoride
TBAI	tetrabutylammonium iodide
TBS	<i>tert</i> -butyldimethylsilyl
TEA	triethylamine
TFA	trifluoroacetic acid
THF	tetrahydrofuran
THP	tetrahydropyran
TIPS	triisopropylsilyl
TLC	thin layer chromatography
TMEDA	<i>N,N,N',N'</i> -tetramethylethylenediamine
TMS	trimethylsilyl
Tol	toluene

Chapter 1

Biomimetic Total Synthesis of *ent*-Durgamone, *ent*-Nakorone and *ent*-Abudinol B

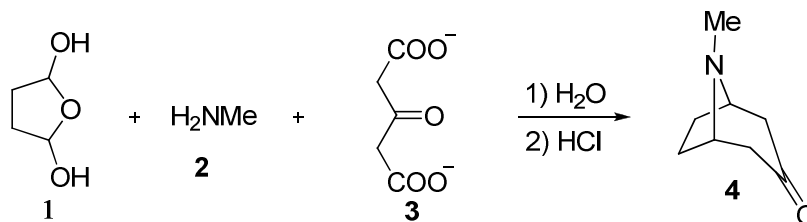
1.1. Introduction and Background

1.1.1. Total synthesis and biomimetic synthesis

As a science, total synthesis of natural products is a relatively young discipline¹, marked by the first total synthesis of strychnine (1954/Woodward), followed by many other milestones such as Vitamin B₁₂ (1973/Woodward/Eschenmoser), Ginkgolide B (1988/Corey), Calicheamicin γ_1 (1992/Nicolaou), Cytovaricin (1990/Evans), Palytoxin (1994/Kishi), Taxol (1994/Nicolaou) and brevetoxin B (1995/Nicolaou). The strategy toward the success of total synthesis of complex natural products was first practiced by R. B. Woodward and was fully developed by E. J. Corey at *Harvard University* to be a routine synthetic technology, termed as *retrosynthetic analysis*,² which revolutionized the total synthesis as a truly respected science. While mastering the logic of retrosynthetic analysis is still far from trivial, some new strategies have been widely accepted and have guided the total syntheses of an ever-increasing number of complex natural products.³ One of these important strategies is *biomimetic synthesis*, mimicking the biological process of production of natural products.⁴ Biomimetic synthesis was first coined in 1917 by Robinson⁵, who described the concept of biomimetic

synthesis through a concise total synthesis of tropinone **4** from glutaraldehyde **1**, methylamine **2** and acetone dicarboxylic acid **3** (Scheme 1).

Scheme 1. Robinson's biomimetic synthesis of tropinone.



Later, van Tamelen⁶ studied systematically different ideas and logic underlying biomimetic or biogenetic synthesis and defined biomimetic synthesis as a specific reaction or a sequence of reactions that mimic a proposed biosynthetic pathway. The process being imitated usually has a solid biochemical background. However, in some cases, biomimetic synthesis was used to describe a sequence of reactions mimicking hypothetical biogenesis. The connection of biomimetic synthesis and total synthesis of natural products is apparent, as commented by Skyler and Heathcock⁷ *“For all natural products, there exists a synthesis from ubiquitous biomolecules. The inherent interconnectivity of natural products implies that a truly biomimetic total synthesis represents a general solution not to the preparation of a compound but to the preparation of all similarly derived natural products (discovered or undiscovered).”* Exploration of chemical production process of natural products was partially driven by the understanding of their chemical formation in the biological systems. However, the biosynthetic process in nature usually involves enzyme-mediated reactions with exclusive chemo- and stereoselectivity, which poses tremendous challenges to the

chemical synthesis. These problems have to be solved by developing new synthetic strategies or chemical reactions, which will be illustrated in the following sections. But, we believe that certain chemical reaction conditions can be found to promote the exact or similar type of reactions with the natural or nonnatural substrates as nature does. Our confidence in the chemical synthesis of natural products in a biomimetic fashion has been consolidated by many successful and elegant biomimetic total syntheses and well expressed by Heathcock that *“...we think that the molecular frameworks of most natural products arise by intrinsically favorable chemical pathways—favorable enough that the skeleton could have arisen by a nonenzymic reaction in the primitive organism. If a molecule produced in this purely chemical manner was beneficial to the organism, enzymes would eventually have evolved to facilitate the production of this useful material.”*⁸

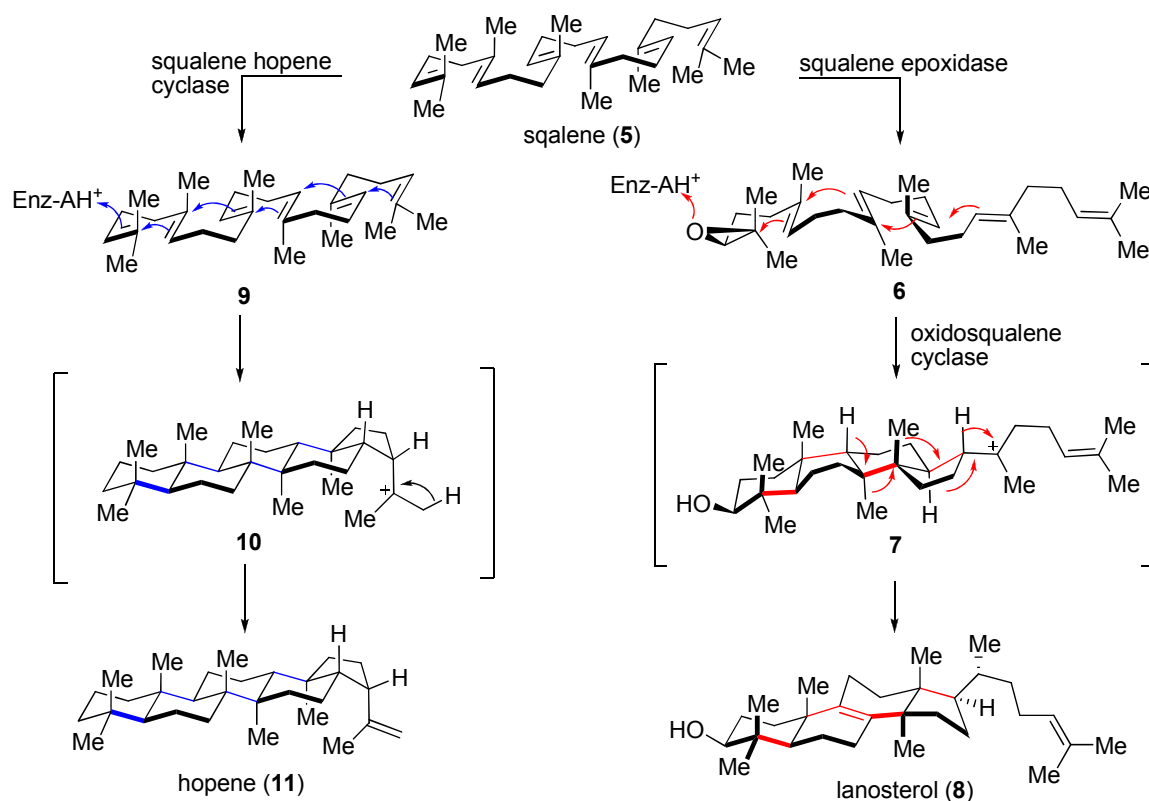
1.1.2. Biomimetic total synthesis of isoprenoid natural products from squalene-like substrates

1.1.2.1. Biogenesis of isoprenoid natural products

Since biomimetic synthesis has been recognized as an extremely efficient strategy for guiding total synthesis of natural products⁴, many efforts have been made to discover the biosynthetic pathways of natural products and develop new synthetic methods based on the hypothetical or established biogenesis. Among these efforts, biomimetic syntheses of polycyclic isoprenoid natural products⁹, such as hopene, lanosterol, cholesterol, sophoradiol and progesterone, are

among the most significant and interesting topics, probably because isoprenoid natural products not only play an important biological role in living organisms but also open a window to discover new drugs for the benefit of human beings. The biomimetic approach to total synthesis of polycyclic isoprenoids was inspired primarily by the enzyme-mediated cascade cyclization—carbacyclization of squalene (5) (scheme 2),^{9,10} which was elucidated mechanistically by site-directed mutagenesis experiments¹¹ as well as crystallographic analysis¹² of the corresponding enzymes and further supported by molecular modeling.¹³

Scheme 2. Biosynthesis of hopene and lanosterol from squalene.



Squalene (5) has been recognized to be the starting material (precisely, the intermediate) for many triterpenoid and isoprenoid natural products including hopene and lanosterol. Cascade carbacyclization of squalene (5) promoted by

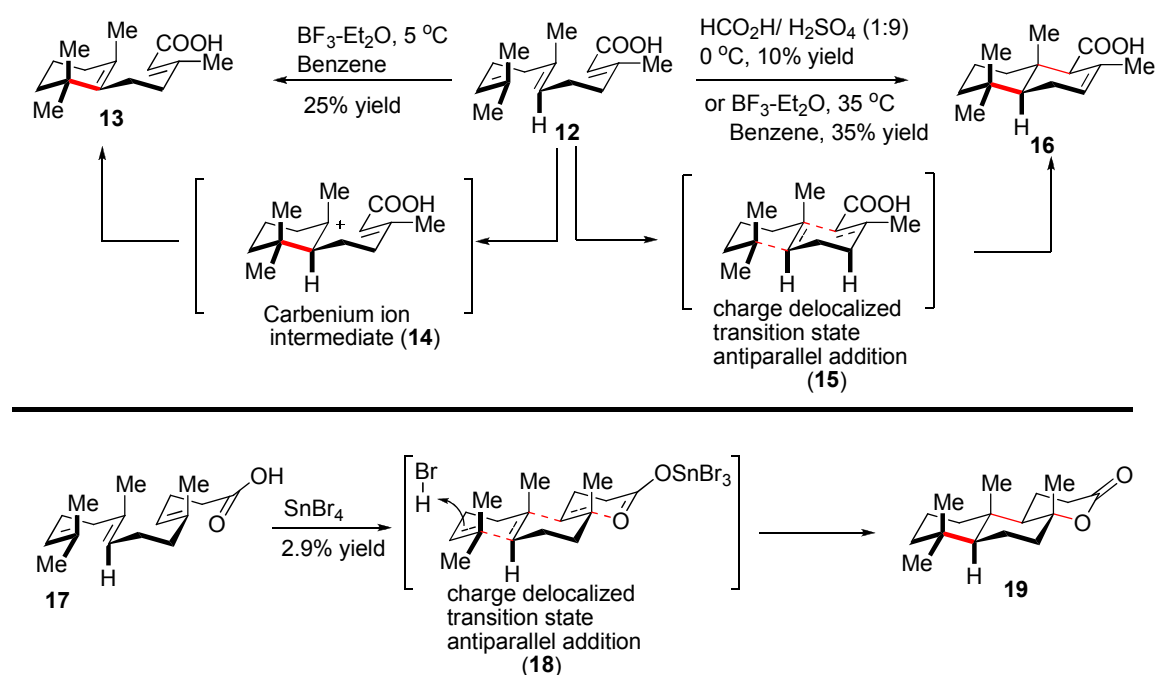
squalene-hopene cyclase produced pentacyclic hopene via beta-hydrogen elimination of carbocation intermediate **10**. Interestingly, oxidosqualene cyclase mediated carbacyclization of epoxysqualene (**6**) afforded the tetracyclic intermediate **7**, which required sequential migrations of hydrogen and methyl groups and *beta*-hydrogen elimination to complete the production of lanosterol. Mimicking such biological production process will be of significance and importance from the synthetic point of view because multiple carbon-carbon bonds will be formed in a single step and simultaneously multiple stereocenters will be set.

1.1.2.2. Stereochemistry issues in biogenesis of isoprenoid natural products

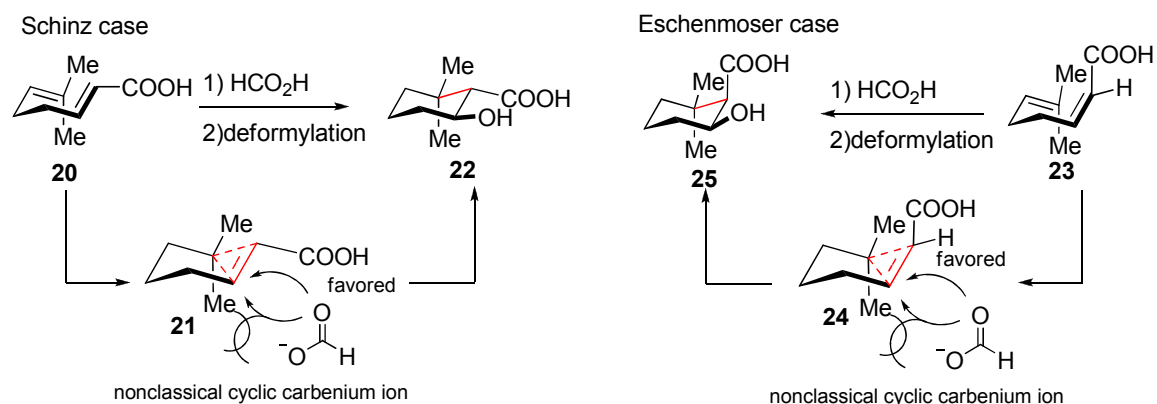
Additional impetus for the development of biomimetic polyene cyclization was provided by the “Stork-Eschenmoser” hypothesis,^{9b,14} which rationalized the stereochemical relationship between the squalene-cyclic triterpenes by using modeling substrates that underwent similar carbacyclizations. In 1955, Stork and Burgstahler¹⁵ reported the stereochemistry of cyclization of farnesic acid **12** and farnesyl acetic acid **17** (Scheme 3). Reaction of Lewis acid (BF₃-Et₂O or SnBr₄) with farnesic acid or farnesyl acetic acid generated very strong protic acid HB(O)F₃ or HBr, which induced the subsequent cyclization of **12** or **17**. Isolation of monocyclization product **13** under mild condition led them to hypothesize that the carbacyclization involved a discrete carbenium ion intermediate such as **14**, whereas formation of **16** under strong protic acidic conditions was interpreted as

a result of concerted *anti*-parallel addition through a charge delocalized transition state **15**.

Scheme 3. Stork-Burgstahler's studies on the stereochemistry of polyene cyclization.



Scheme 4. Schinz-Eschenmoser evidence for nonclassical cyclic carbenium ion.



These experiments also inspired the proposition that a weakly nucleophilic donor olefin favors a nonconcerted addition and therefore a carbenium ion intermediate.

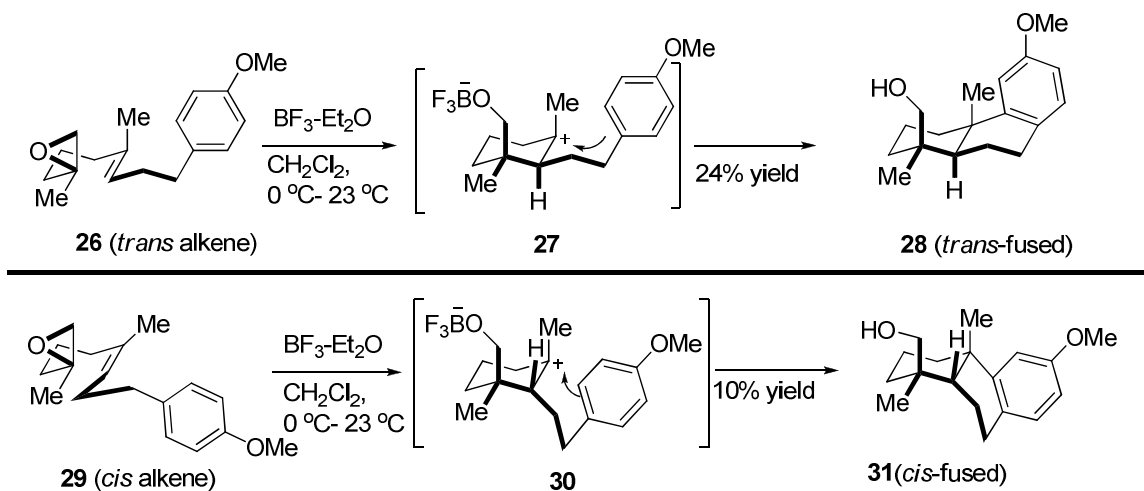
The hypothesis was examined and partially supported by studying the cyclization of farnesyl acetic acid **17** under similar conditions. Formation of ambreinolide **19** revealed a single transition state through three concerted *anti* addition to the trisubstituted alkene.

Additionally, Schinz and Eschenmoser¹⁶ provided experimental evidence to further support the *anti*-parallel addition and chair-like folding conformation during the polyene carbacyclization. A nonclassical cyclic carbenium ion was proposed as the intermediate **21** or **24** to account for the stereospecific cyclizations of geranic acid **20** and norgeranic acid **23**, respectively. Notably, in both cases formic acid underwent highly stereoselective nucleophilic additions to the intermediate nonclassical cyclic carbenium ions to generate the equatorial secondary alcohols after deformylation.

Carbacyclization of a variety of polyene compounds have been extensively studied by Stork and Eschenmoser, resulting in findings that the acid-catalyzed polyene cyclizations were nonstereospecific, but highly stereoselective. However, Goldsmith and coworkers¹⁷ at *Emory University* provided the first chemical evidence in supporting stereospecific cyclization of epoxy alkene (scheme 5). $\text{BF}_3\text{-Et}_2\text{O}$ -promoted cyclization of epoxy alkene **26** with central *trans*-substituted double bond led to tricyclic alcohol **28** with *trans*-fused A/B rings; while the corresponding *cis*-alkene **29** produced A/B *cis*-fused tricyclic alcohol **31** with lower yield under the same cyclization conditions. Intermediates **27** and **30** were proposed to account for the stereochemical outcome of the cyclization, which

were further supported by isolation of many corresponding side products. The stereochemistry of these products clearly suggested that cyclization of epoxy

Scheme 5. Stereospecific cyclization of epoxy alkene.



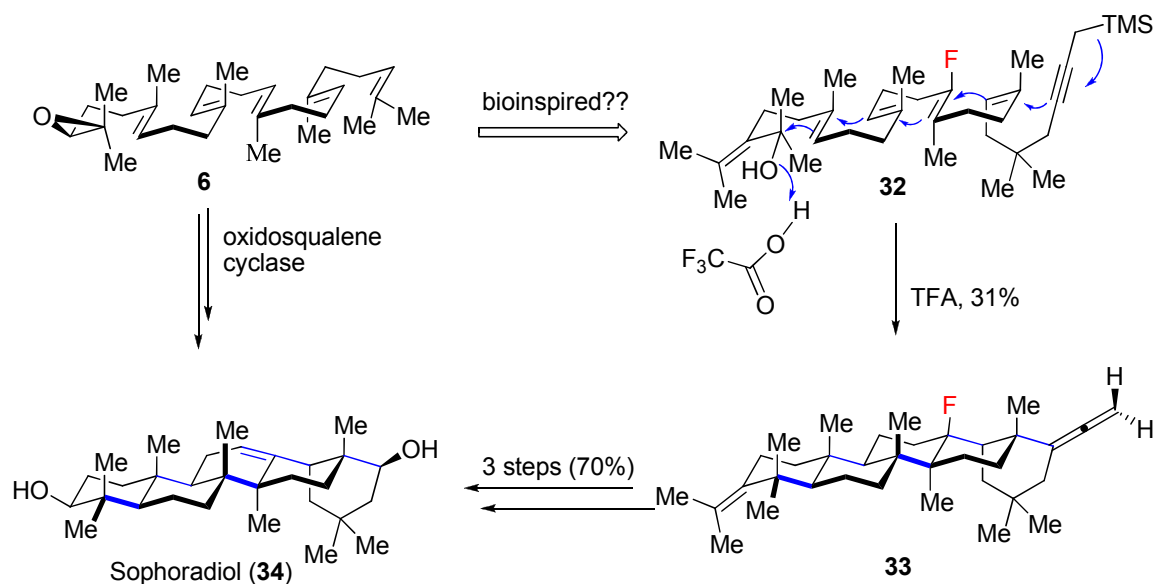
alkene occurred in a stereospecific process via cation (**27** or **30**) with conformationally fixed geometries. However, the authors have recognized that a concerted *anti*-parallel addition was also possible and could not be ruled out.

1.1.2.3. Biomimetic synthesis of isoprenoid natural products

The “Stork-Eschenmoser” hypothesis rationalized the stereochemical course of the biochemical cyclization of polyene on stereoelectronic grounds. However, direct experimental support for this hypothesis was provided by W. S. Johnson,¹⁸ who initiated the research program that developed biomimetic polyene cyclizations into viable synthetic strategies. The work¹⁸ from this laboratory culminating in the 1990s has demonstrated that the use of removable fluoride as a cation-stabilizing auxiliary and alkyne as a terminal carbon nucleophile are critical to the success of Johnson’s non-enzymatic, biomimetic pentacyclization,

which was clearly illustrated by the landmark achievement in the biomimetic total synthesis of triterpenoid natural product sophoradiol in 1994 (scheme 6).^{18e} Fish and Johnson discovered that the fluoride as cation-stabilizing auxiliary played a critical role in the formation of third cyclohexane ring (C-ring) because in the biological production process it was usually generated by cationic rearrangement

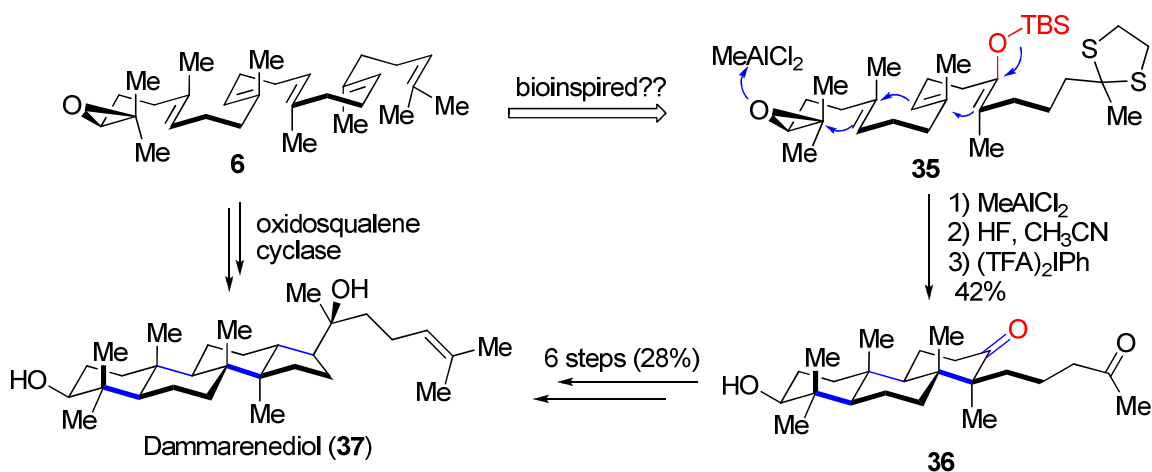
Scheme 6. Johnson's biomimetic total synthesis of sophoradiol.



of cyclopentane produced by a favorable *exo* cyclization based on Baldwin's rule (5-*exo* Markovnikov addition over 6-*endo anti*-Markovnikov addition, in agreement with results obtained by van Tamelen and Leiden utilizing the alkyne as a terminating group¹⁹). Historically significant contributions from Johnson's laboratory included the development of different initiators and terminators, which greatly expanded the scope of polyene carbacyclizations. Tertiary allylic alcohols, acetals and epoxides are good initiators in the presence of a Lewis acid (SnCl_4 or TFA), while propargylic silanes, allylic silanes and vinyl fluorides are found to be viable terminators for the cascade cyclization.

Since Johnson's pioneering synthetic work in the biomimetic polyene carbacyclization, many other elegant achievements have been made during the past decades. Contributions from E. J. Corey's laboratory are particularly noteworthy. In contrast to Johnson's use of fluoride as a cation-stabilizing auxiliary to control the regioselectivity of six-membered C-ring and alkyne as a nucleophilic terminator to facilitate the pentacyclization, Corey²⁰ utilized the enolsilane not only to direct regioselectivity for C-ring formation but also to assist the cascade cyclization due to its good nucleophilicity. The very first example that Corey used for this strategy was the first biomimetic total synthesis of dammarenediol in 1996 (scheme 7)^{20a}. Treatment of the squalene monoepoxide **35** with methyl aluminum dichloride (MeAlCl_2 , better Lewis acid in many cases) initiated the tricyclization, which was terminated with enolsilane to produce tricyclic diketone **36** as a single diastereomer in 42 % yield after desilylation and thioacetal hydrolysis. Total synthesis of dammarenediol II **37** was completed in six steps from tricyclic diketone **36** in 28% overall yield.

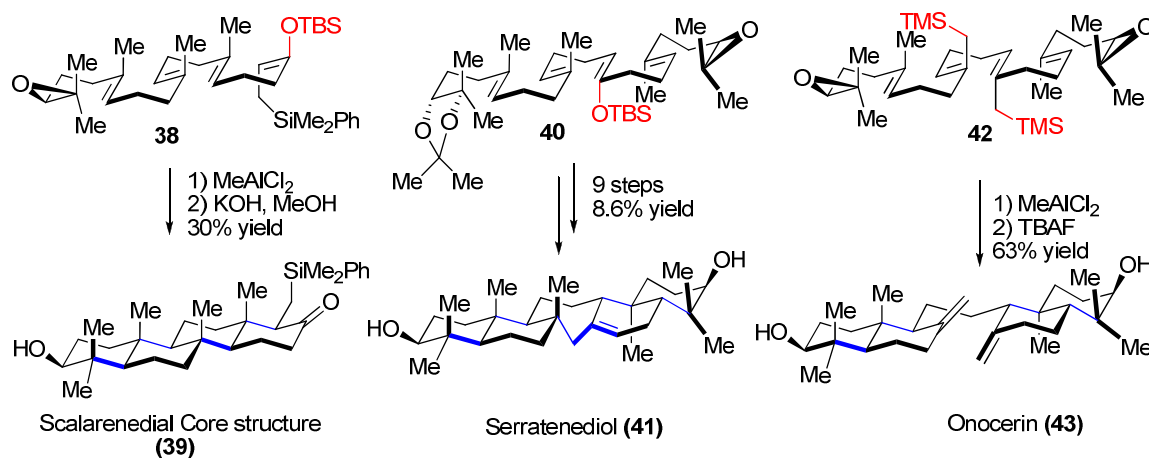
Scheme 7. Corey's biomimetic total synthesis of dammarenediol II.



Most importantly, Corey *et al.* demonstrated that epoxide was a viable initiator for the cascade carbocyclization of polyene through a chair-chair-chair transition state if a suitable Lewis acid was employed (Goldsmith^{17b} first explored BF₃-Et₂O mediated cyclization of epoxy olefins). It should be noted that epoxy squalene was found to adopt a chair-boat-chair conformation in many cyclases-catalyzed polycyclization, instead of the chair-chair-chair conformation enforced by the squalene-hopene cyclase. Again, these experiments further supported the “Stork-Eschenmoser” hypothesis.

An additional advantage of Corey’s strategy was the easy preparation of the enolsilane substrates. The power, efficiency and flexibility of Corey’s strategy are clearly demonstrated by many subsequent biomimetic total syntheses of natural products, including scalarenedial^{20b}, serratenediol^{20c} and onocerin^{20d} as shown in scheme 8.

Scheme 8. Corey’s biomimetic total synthesis of isoprenoid natural products.



Cascade carbocyclization of polyene is so successfully being emulated by chemical processes that biomimetic synthesis has revolutionized the development of chemical synthesis strategies that are similar to or inspired by

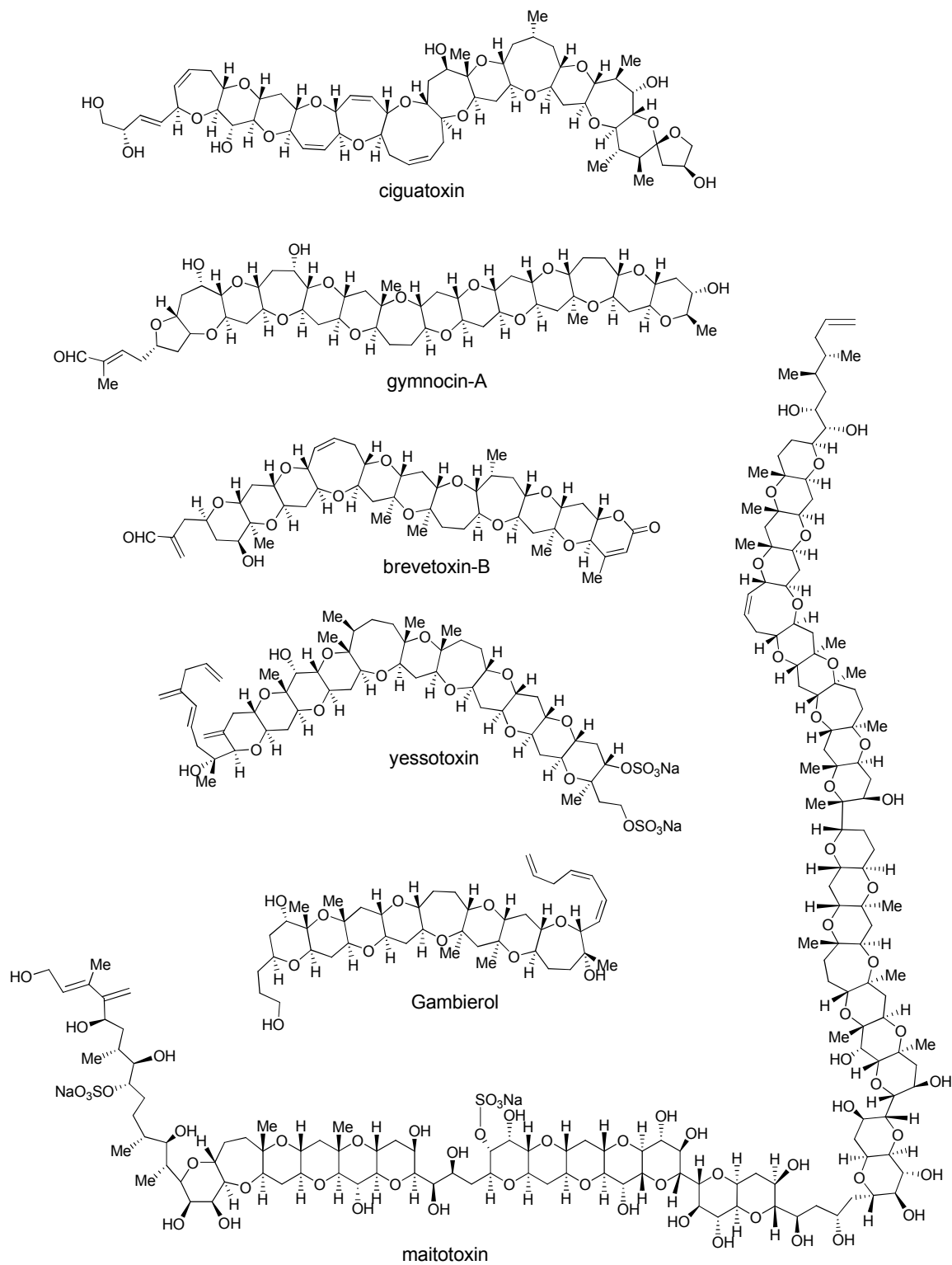
this mode of natural product biosynthesis. For instance, polycyclic ethers were proposed to arise from cascade oxacyclizations of polyepoxide, which will be reviewed briefly in the next section.

1.1.3. Biomimetic synthesis of polycyclic ethers

1.1.3.1. Biogenesis of polycyclic ether natural products

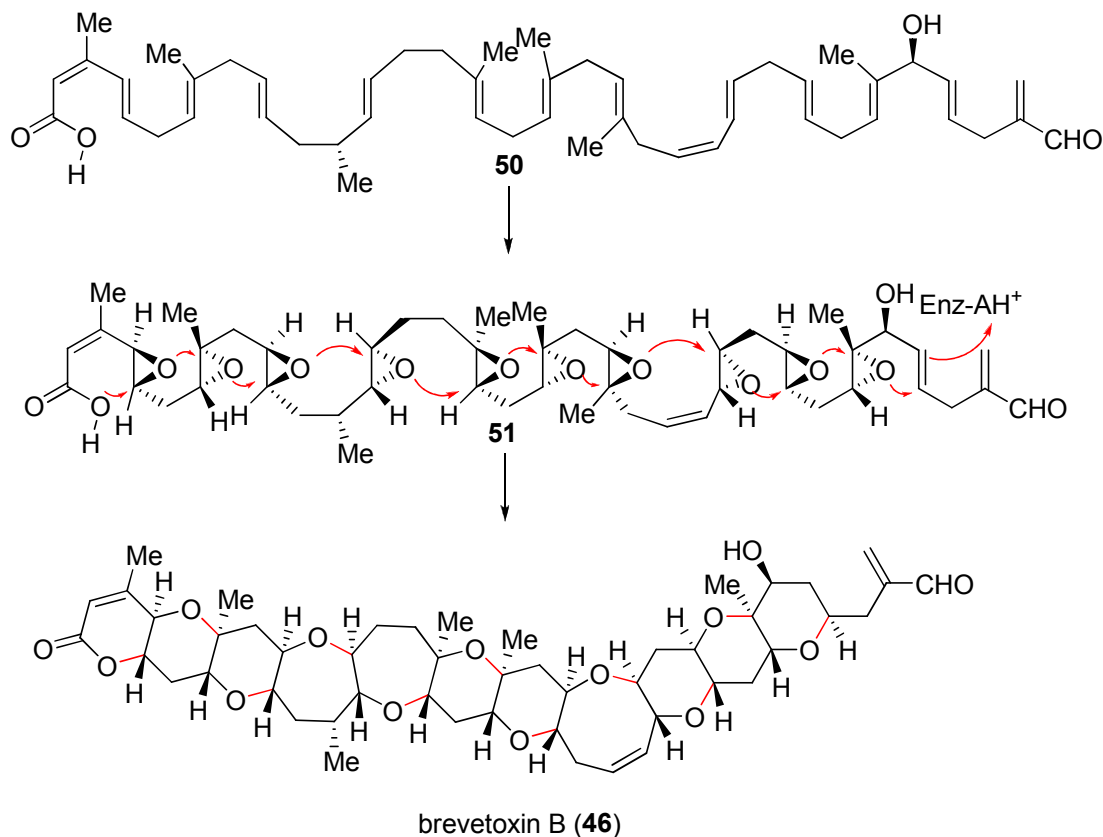
Polycyclic ether marine natural products (figure 1), such as ciguatoxin (**44**), gymnocin A (**45**), brevetoxin B (BTX-B, **46**), yessotoxin (**47**), gambierol (**48**) and maitotoxin (**49**), have attracted much attention of chemists and biochemists due to their skeletal novelty, complexity, regularity and potent biological activities.²¹ Fish poisoning was first recognized as an important biological activity of polycyclic ethers since massive fish kills was observed in the “red tide”, which produced those toxins that exert their toxicity by binding to ion channels²². The characteristic structural features of polycyclic ethers included: (1) a backbone of repeating oxygen-carbon-carbon (O-C-C) units extending from one end to the other, regardless of the ring size; (2) cyclic ethers were stacked together in a unique *trans-syn-trans*-fused fashion with alternative oxygen; (3) hydroxyl (OH) or/and methyl groups are the only functional groups on the inner ether rings. While these extremely complex structures have presented formidable challenges to synthetic organic chemists, they have provided an opportunity and also served as the inspiration for development of new synthetic methodology.^{21c, 21d, 23} Currently, the mostly accepted biogenetic hypothesis of polycyclic ethers is the Nakanishi²⁴ cascade oxacyclization of polyepoxide, a postulate that rationalized

Figure 1. Examples of polycyclic ether natural products.



the structural and stereochemical regularity of the ladder-like polycyclic ethers based on Shimizu's ^{13}C -labeling experiments (Scheme 9).

Scheme 9. Nakanishi's biogenetic hypothesis of brevetoxin B.



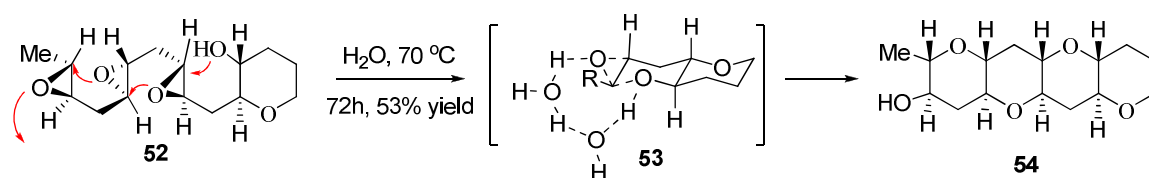
Stereoselective biogenetic epoxidation of polyene **50** would give polyepoxide **51** (first postulated by Cane, Celmer and Westley, termed as “CCW hypothesis”²⁵), which underwent *endo*-regioselective and *anti*-stereospecific oxacyclization to give brevetoxin B (**46**). This speculative biogenesis successfully explains the backbone of brevetoxin B (**46**) with *trans-syn-trans* topography so that biosynthesis of other related polycyclic ether natural products has been proposed to follow the same type of mechanism.²⁶ However, there is little direct evidence, neither site-directed mutagenesis nor molecular modeling, to support this hypothesis employing cascade oxacyclization of polyepoxides. This provides an

impetus for synthetic organic chemists to study the individual chemical transformations and to develop new chemical reactions.

1.1.3.2. Biomimetic synthesis of polycyclic ethers

Fortunately, searching for the chemical evidence of this intellectually appealing biogenesis through biomimetic synthesis was undertaken by a few research laboratories, including McDonald (Emory), Fujiwara/Murai (Hokkaido) and Jamison (MIT), resulting in development of many new chemical reactions^{23, 27}. Particularly, Vilotijevic and Jamison²⁸ recently reported that the cascade oxacyclization of polyepoxide (**52**) performed in water produced the desired polycyclic ether (**54**) with *trans-syn-trans* fusion and with exclusive *endo*-regioselectivity and *anti*-stereospecific addition (scheme 10). Notably, high *endo*-selectivity (THF vs THP) was achieved without directing groups on any of the epoxides when using water as the cyclization promoter and solvent.

Scheme 10. Jamison's biomimetic oxacyclization of polyepoxide.

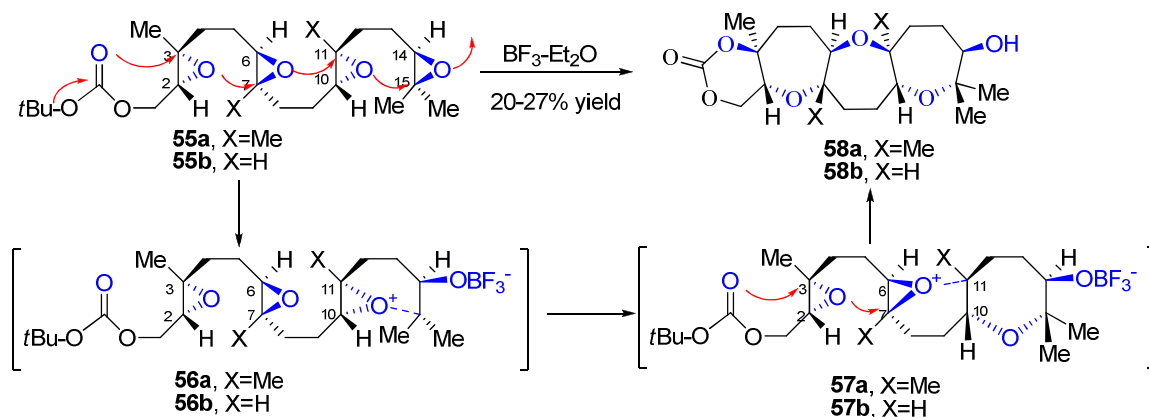


Mechanistically, two water molecules work cooperatively to activate both the nucleophile (OH group on the ether ring template) and electrophile (epoxide) through hydrogen bonding as shown in the hypothetical intermediate **53**. As recognized by the authors, this cascade oxacyclization “represents the long-

sought evidence in favor of Nakanishi's hypothesis of ladder polyether biosynthesis (or at least the feasibility)."

It is still unclear, however, that the cascade oxacyclization of polyepoxide in the Nakanishi hypothesis started from left to right (-COOH or OH as nucleophile) or from right to left (epoxide as nucleophile).²³ Experimental results from Jamison's team certainly supported the first case (left-to-right). However, an alternative mechanism (right-to-left) was also convincing and viable based on the McDonald's biomimetic oxacyclization²⁷ of polyepoxide via a bicyclic epoxonium ion intermediate (Scheme 11),²⁹ which was further elucidated by experimental and computational studies of model systems by other groups.³⁰

Scheme 11. Valentine and McDonald's biomimetic oxacyclization of polyepoxide via epoxonium ion.



Cascade oxacyclization of tetraepoxide **55** was initiated by selective activation of terminal 14,15-epoxide with Lewis acid ($\text{BF}_3\text{-Et}_2\text{O}$) to generate the hypothetical epoxonium ion intermediate **56**, which was attacked by the nearest epoxide (C10-C11) oxygen producing another epoxonium ion **57**, etc. The cyclization was finally terminated by the carbonate to afford the *trans-syn-trans* tetracyclic ethers

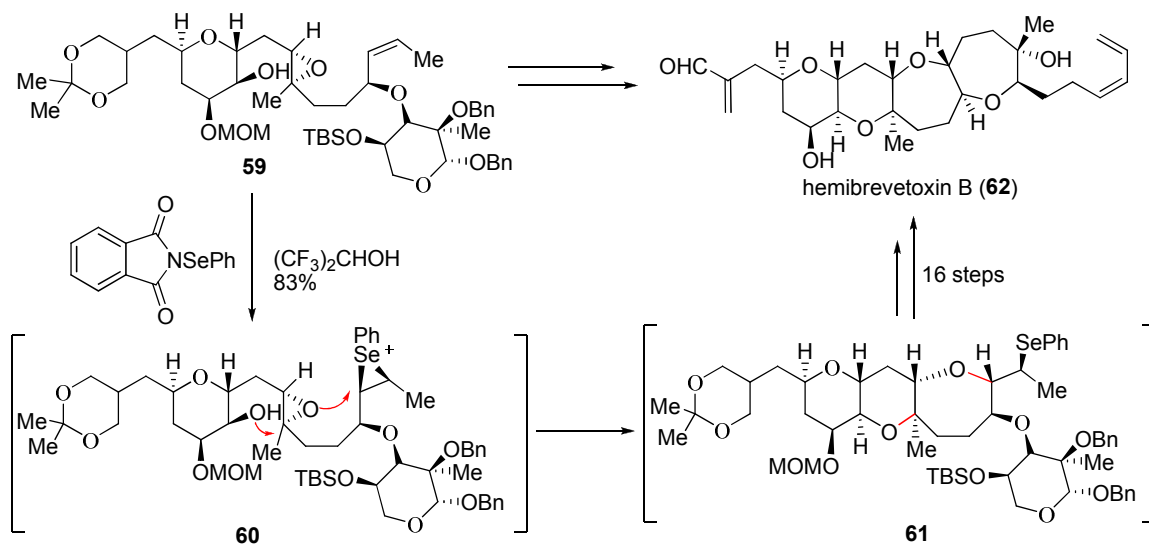
58. Both substrates (**55a** and **55b**) provided the all-*endo* oxacyclization products **58a** and **58b**, which were evidence in support of the epoxonium ion intermediate. Additionally, substituent (methyl or trimethylsilyl, not hydrogen) on C3 and C15 was found to be critical in favor of all-*endo* selectivity, which was otherwise disfavored under the Baldwin's rules.³¹

To some extent, biomimetic cascade oxacyclization of polyepoxide developed independently by Jamison and McDonald provides the direct chemical evidences in support of Nakanishi's hypothesis. Extension of these methods toward the total synthesis of polycyclic ether natural products is far from satisfactory, however, partially due to limitations of current methods, along with the difficulty in the preparation of the corresponding substrates with the current methods. In Jamison's case, the skipped polyene, a precursor of polyepoxide, was unstable and usually synthesized *in situ* by reduction of skipped polyalkyne with elemental lithium in ammonia followed immediately by oxidation; whereas in McDonald's case, biomimetic synthesis of polyoxepane (7-membered cyclic ether) was more successful than that of the polypyran (6-membered cyclic ether) synthesis. Regio-selective activation of polyepoxides was not completely solved, while substituents (such as Methyl) on both terminal epoxides are necessary to achieve the *endo*-selectivity of oxacyclization. On the other hand, the biomimetic cyclizations developed independently by McDonald's laboratory and Jamison's laboratory demonstrated the feasibility of oxacyclization of polyepoxides and would be useful in preparation of many other structurally related molecules.

1.1.3.3. Biomimetic synthesis of polycyclic ether natural products

One successful application of biomimetic synthesis to total synthesis was reported by the Holton's laboratory,³² who undertook convergent total synthesis hemibrevetoxin B, which was the first example of a total synthesis accomplished using the *endo*-selective biomimetic cascade oxacyclization of an epoxide (scheme 12).

Scheme 12. Holton's biomimetic total synthesis of hemibrevetoxin B.



In the key step of the synthesis, treatment of compound **59** with *N*-(phenylseleno)phthalimide induced the cascade cyclization to give **61** as a single diastereomer through *exo*-addition of epoxide to *epi*-selenonium **60** and subsequently *endo* opening of epoxonium ion with alcohol. The epoxide served not only as a nucleophile to open the *epi*-selenonium ion but also as an electrophile being attacked by a hydroxyl group. These results clearly

demonstrated the power and efficacy of biomimetic synthesis, since two of the four ether rings in hemibrevetoxin B were constructed in a single operation.

However, the truly biomimetic synthesis has not yet become a practical and mainstream method for synthesis of other polycyclic ether natural products. In particular, the total synthesis of maitotoxin, the largest non-biopolymer natural products known to date, still stands as a challenge to modern synthetic methodology.

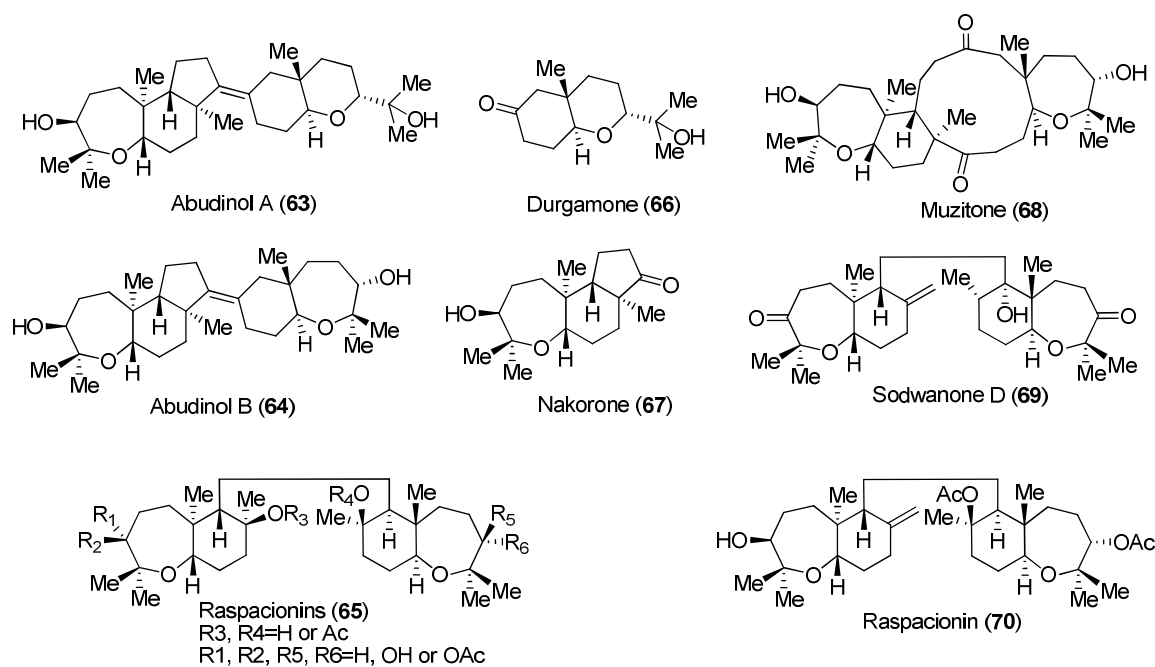
Since cascade carbacyclization and oxacyclization were proposed to be responsible for the biological production of steroids and polycyclic ethers natural products, respectively, biomimetic polycyclization was extensively explored and provided the chemical evidences to support the corresponding hypothesis. Inspired by these hypotheses and biomimetic syntheses, combination of these two processes -cascade oxa-carbacyclization, was postulated as a biosynthetic pathway³³ of polycyclic ether triterpenoids, such as abudinol B. Since there is little evidence available to support such hybrid processes, part of this thesis will focus on searching the chemical evidences in support of this hypothesis through biomimetic total synthesis of abudinol B and related natural and non-natural products, which have been proposed to be biosynthesized via cascade oxa-carbacyclization of squalene derivatives.

1.1.4. Biogenesis of abudinol B and related natural products

Polycyclic ether terpenoid marine natural products³⁴ are very abundant secondary metabolites from algae or sponges. They are one of the most

interesting families of marine natural products, not only presenting a great diversity of structural frameworks with different ring sizes and fusion, but also exhibiting strong biological activities. Recently, a family of polycyclic ether triterpenoid marine natural products, including abudinols, sodwanones and raspacionins (figure 2)³⁴⁻³⁶, has been isolated from sponges of the Axinellidae family *Ptilocaulis spiculifer*, *Axinella weltneri* and *Raspaciona aculeate*, collected from Red Sea, Indo Pacific ocean and Mediterranean sea.

Figure 2. Examples of polycyclic ether terpenoid natural products.



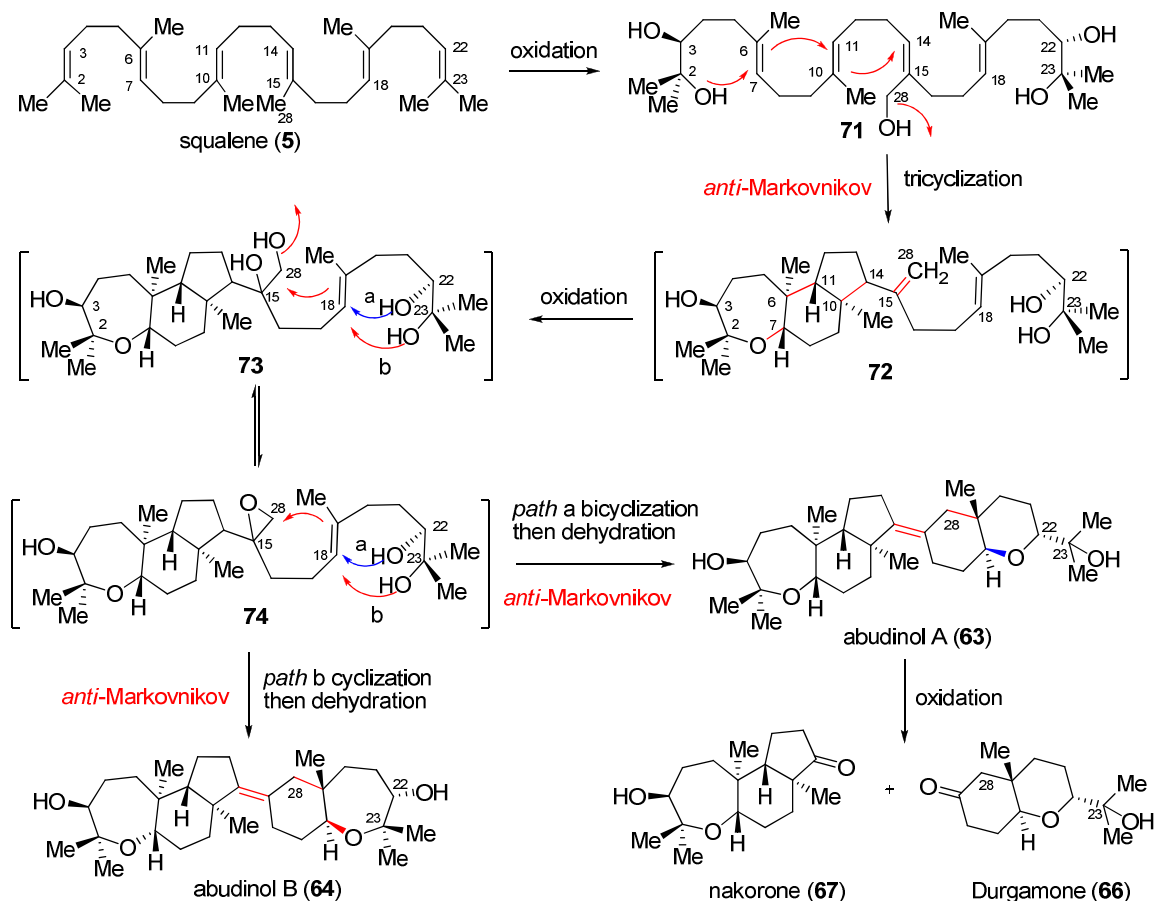
These triterpenoids constitute a big family in terms of unique and fascinating structural architectures and biological activities. In contrast to most of the triterpenoids marine natural products isolated from algae, such as thysiferol and closely related metabolites,³⁴ which display very strong cytotoxicity against tumoral or leukemia cell lines, triterpenoids isolated from sponges exhibited tremendous differences in bioactivities (mostly cytotoxicity). For instance, almost

all raspacionins³⁶ showed cytotoxicity (4-8 μ M) against MCF-7 tumoral cell line, while abudinols³⁵ and muzitone³⁵ have not been found to indicate any interesting anticancer activity so far. Even in the same class, Sodwanones^{35,37} G, I and M display good cytotoxicity (0.1-20 μ M) against Cell lines of P-388, A-549, HT-29 or MEL-28, but the other sodwanones have not yet been reported to be cytotoxic. These findings that minor structural differences result in considerable changes in biological activities stimulate the interests of synthetic organic chemists in the development of new and general methods for synthesis of these natural products and their analogs, which will offer an opportunity to study structure-activity relationships. From a synthetic point of view, particular attention has been paid to the total synthesis of abudinol B (**64**) as well as the oxidative degradation products durgamone (**66**) and nakorone (**67**), which were first reported in 1999 as isolated compounds from Red Sea sponges of the Axinellidae family *Ptilocaulis spiculifer*. The unique, highly condensed oxepane-cycloalkane skeletons of these triterpenoids were not previously synthetically explored, but given our interest in *endo*-regioselective, biomimetic tandem oxacyclizations, these structures attracted our interest for the potential of combining polyepoxide cyclizations with biomimetic polyene cyclizations.

Biogenetically, triterpenoid metabolites from sponges, featuring seven-membered cyclic ether *trans*-fused with substituted cyclohexane, in most cases, are derived from enzyme-catalyzed cascade oxidative cyclization of squalene derivatives. For instance, Kashman^{35a} proposed squalene as the starting material for the biological production of abudinols and oxidative degradation products

durgamone and nakorone (scheme 13). Regio and stereoselective enzymatic oxidation of squalene (**5**) provided intermediate **71**, which underwent *anti*-Markovnikov cyclization with *endo*-selectivity to give tricyclic ether **72**.

Scheme 13. Kashman's biogenetic hypothesis for abudinol.

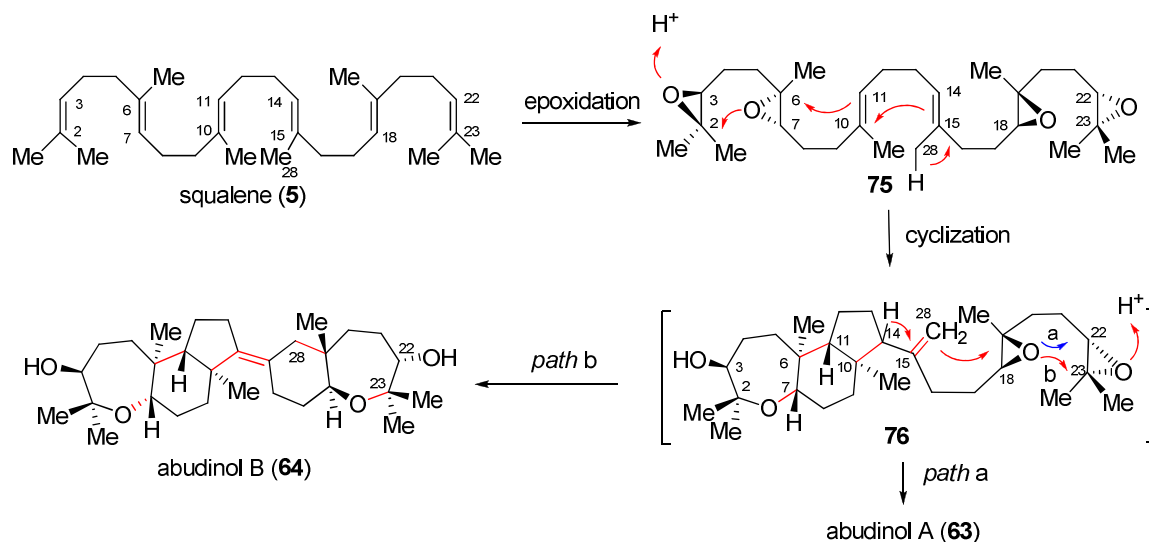


Regioselective oxidation (dihydroxylation or epoxidation) to **66** or **67** followed by another *anti*-Markovnikov cyclization and dehydration afforded the abudinol A and B. Nucleophilic attack by hydroxyl group on C22 resulted in formation of abudinol A (**63**) through path a cyclization, whereas abudinol B (**64**) was produced by cyclization terminated by tertiary alcohol on C23. Aerobic oxidation of abudinol A then provided durgamone (**66**) and nakorone (**67**). Although the

apparent violation of Markovnikov's rule in the cyclization steps has been a matter of considerable debate, many known precedents of such anomalies have been provided in the biosynthesis of tetra- and pentacyclic triterpenes. A typical example is the formation of tetrahymanol³⁸, which required three *anti*-Markovnikov additions.

Alternatively, Norte³⁴ proposed that biosynthesis of abudinol B (**64**) could be achieved by sequential tandem oxa-carbacyclization of squalene tetraepoxide (**75**) (scheme 14). Tandem oxa- and carbacyclizations of two adjacent epoxides and both alkenes of squalene tetraepoxide **75** would provide hypothetical intermediate **76** containing A, B, and C rings, and subsequent tandem cyclization with the remaining two epoxides would complete the biosynthesis of the

Scheme 14. Norte's biosynthesis for abudinol B.



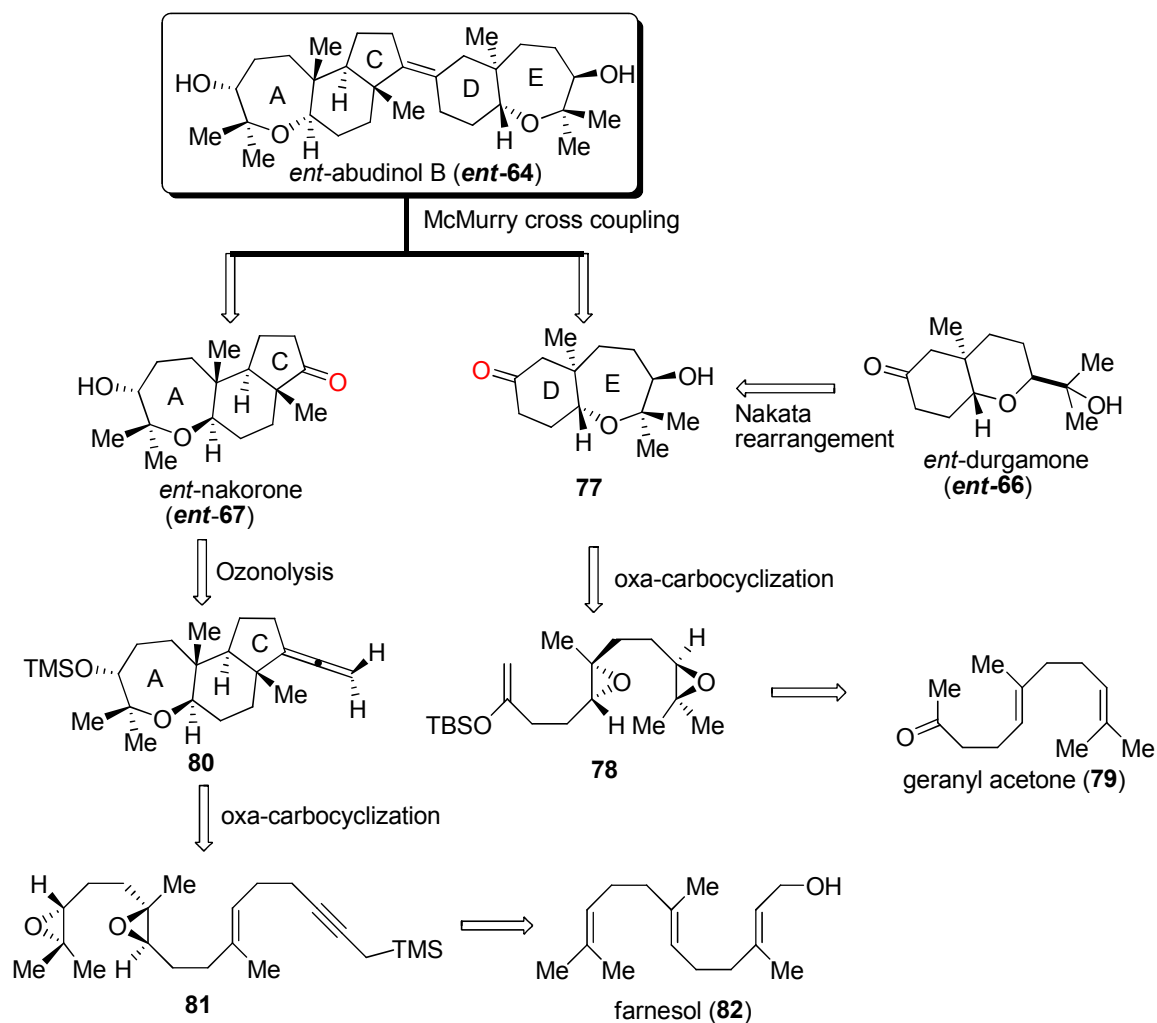
abudinol A and B. Abudinol A (**63**) corresponds to diepoxide cyclization to form carbon-oxygen bond at C22, whereas the oxepane ring of abudinol B (**64**) would arise from carbon-oxygen bond formation at the more substituted C23. In contrast to Kashman's hypothesis, Norte's cascade cyclization followed the

Markovnikov's rule, which suggests the feasibility of mimicking the cyclization under acidic conditions. In addition, Norte's proposal for the cascade cyclization is a hybrid process of the well-studied cascade carbacyclization of squalene-derived substrates and the oxacyclization of polyepoxide for the synthesis of polycyclic ethers.

1.1.5. Retrosynthetic analysis of abudinol B, durgamone and nakorone (first generation)

Our synthetic strategies toward the total synthesis of the enantiomers of abudinol B, durgamone and nakorone was inspired primarily by Norte's biosynthetic hypothesis of abudinol B and our biomimetic cascade oxacyclizations of polyepoxides (scheme 15).³⁹

Scheme 15. Retrosynthetic analysis of abudinol B, durgamone and nakorone.



Due to the ready availability of 1,2:4,5-di-*O*-isopropylidene-D-erythro-2,3-hexodiuro-2,6-pyranose “Shi catalyst” from D-fructose, we elected to prepare the enantiomers of the natural products durgamone (**66**), nakorone (**67**) and abudinol B (**64**). However, an improved preparation for the L-fructose via multiple steps is now available for preparing the enantiomeric Shi catalyst.^{41c} *Ent*-abudinol B (**ent-64**) was envisioned to be assembled by construction of the tetrasubstituted alkene via McMurry cross coupling of tricyclic *ent*-nakorone (**ent-67**) and bicyclic ketone **77**, a process conceptionally equivalent to “retro-ozonolysis”. The key oxa-carbacyclization of epoxy-alkene would be developed for the syntheses of the tricyclic ketone **ent-67** and bicyclic ketone **77** by use of propargylic silane¹⁸ and enolsilane²⁰ to terminate the cascade cyclizations, respectively. The enantiomer of durgamone (**ent-66**) could be synthesized by a ring contraction of bicyclic ketone **77** under analogous conditions for ring expansion (Nakata rearrangement).⁴⁰ Geranyl acetone (**79**) with all required carbons and methyl substituents was then proposed as the commercially available starting material for synthesis of diepoxy enolsilane **78** via two classical transformations. *Ent*-nakorone (**ent-67**) would be synthesized from the cascade oxa-carbacyclization product **80** via oxidative cleavage¹⁸ of the corresponding allene of **80**. Alkylation of farnesol (**82**) derivatives with propargylic silane followed by functional group manipulations would provide the oxacyclization substrate **81**.

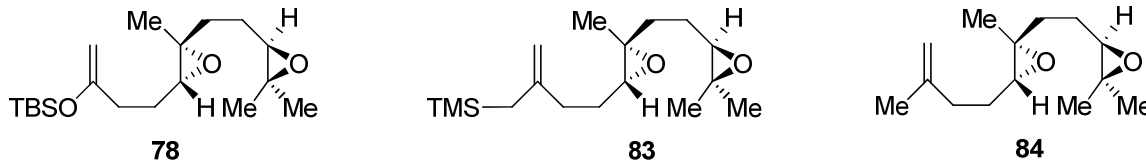
1.3. Results and discussion

While considerable accomplishments have been recorded in the biomimetic or bioinspired cascade cyclizations of polyalkene^{9,18,20} and polyepoxide cyclizations,²⁷⁻²⁹ the cyclization processes of multiple epoxides with multiple alkenes have not been previously studied. Such a hybrid process has been proposed for the biosynthesis of various triterpenoids which feature cyclic ethers fused to carbacyclic rings, including the marine triterpenoid natural product abudinol B, durgamone and nakorone. Given our interest in *endo*-regioselective and biomimetic tandem oxacyclizations,^{27,29} the structurally unique, highly condensed oxepane-cycloalkane skeleta of these terpenoids, attracted our interest for the potential of combining polyepoxide cyclizations with biomimetic polyene cyclizations. Herein, we report our studies on oxacyclization of polyepoxide-alkene³⁹ toward the total synthesis of enantiomers of abudinol B (**ent-64**), durgamone (**ent-66**) and nakorone (**ent-67**).

1.2.1. Total synthesis of *ent*-durgamone (**ent-66**) and bicyclic ketone **77**

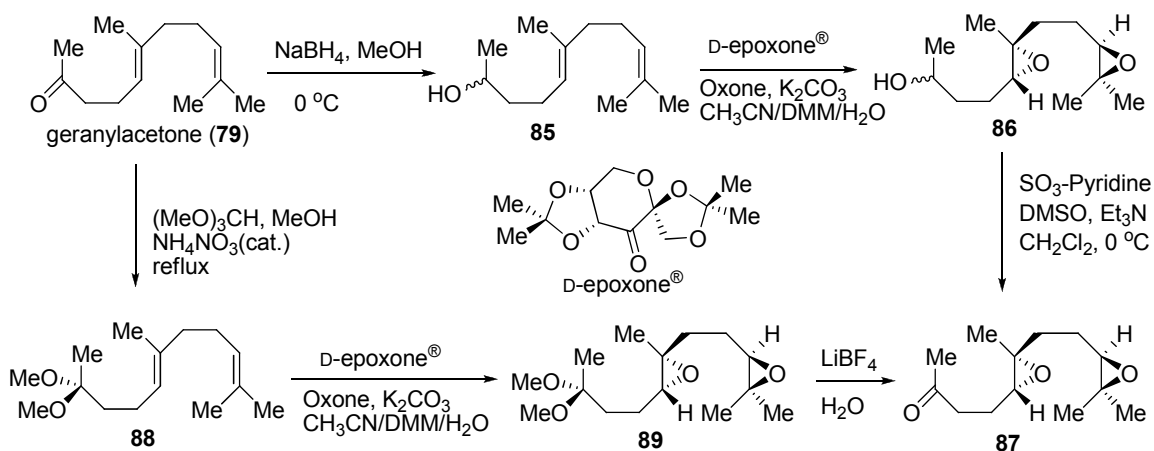
Our total synthesis of *ent*-abudinol B (**ent-64**) commenced with the biomimetic syntheses of tricyclic *ent*-nakorone (**ent-67**) and bicyclic ketone **77** via independent cascade oxa-carbacyclization. To explore the hybrid cascade oxa-carbacyclization suggested in the retrosynthetic analysis, we began our studies with the synthesis of substrates **78**, **83** and **84**, respectively (figure 3).

Figure 3. Oxa-carbacyclization substrates **78**, **83** and **84**.



Reduction of commercially available geranylacetone (**79**) with sodium borohydride in methanol (scheme 16), followed by enantioselective double Shi epoxidation⁴¹ and Parikh-Doering oxidation, afforded the keto diepoxides **87** with high overall yields and good diastereoselectivity (8:1). Alternatively, synthesis of **87** was also achieved by ketalization of geranylacetone (**79**) with trimethylorthoformate in the presence of catalytic amount of ammonium nitrate, followed by the double Shi epoxidation and acid-catalyzed deketalization⁴². A single diastereomer of **87** was obtained by the second method; however, lower yields in the ketalization of geranylacetone **79** and deketalization of **89** were obtained due to the acidic sensitivity of the dimethoxyketal diepoxide **89**.

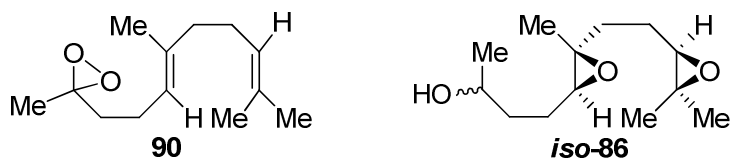
Scheme 16. Synthesis of diepoxy ketone **87**.



The “extra” two-step ketone protection/deprotection was necessary to achieve high diastereoselectivity in the double Shi epoxidation, because the ketone in **79**

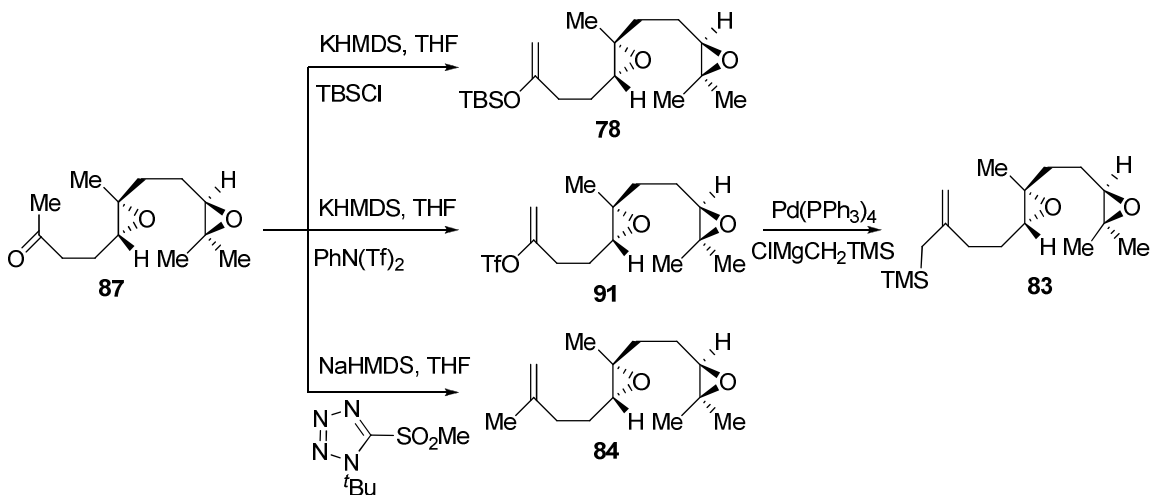
may be oxidized into dioxirane **90** that underwent nonselective epoxidation of the adjacent alkene (figure 4), which was found by previous studies in our laboratory. In contrast to the ketone, the corresponding alcohol, such as **85**, imposes little affect on the selectivity of the neighboring alkene since diepoxide **86** was found to be the major product, which was inseparable from the minor diastereomer *iso*-**86**. The ratio of **86** to *iso*-**86** was determined to be 8:1 by subsequent transformations.

Figure 4. Intermediate or product of nonselective Shi epoxidation.



In order to explore the cascade oxa-carbocyclization with different terminal carbon nucleophiles, the methyl ketone of diepoxide **87** was converted into enolsilane **78**, allylsilane **83** and 1,1-disubstituted alkene **84**, respectively (Scheme 17).

Scheme 17. Synthesis of cyclization substrates.

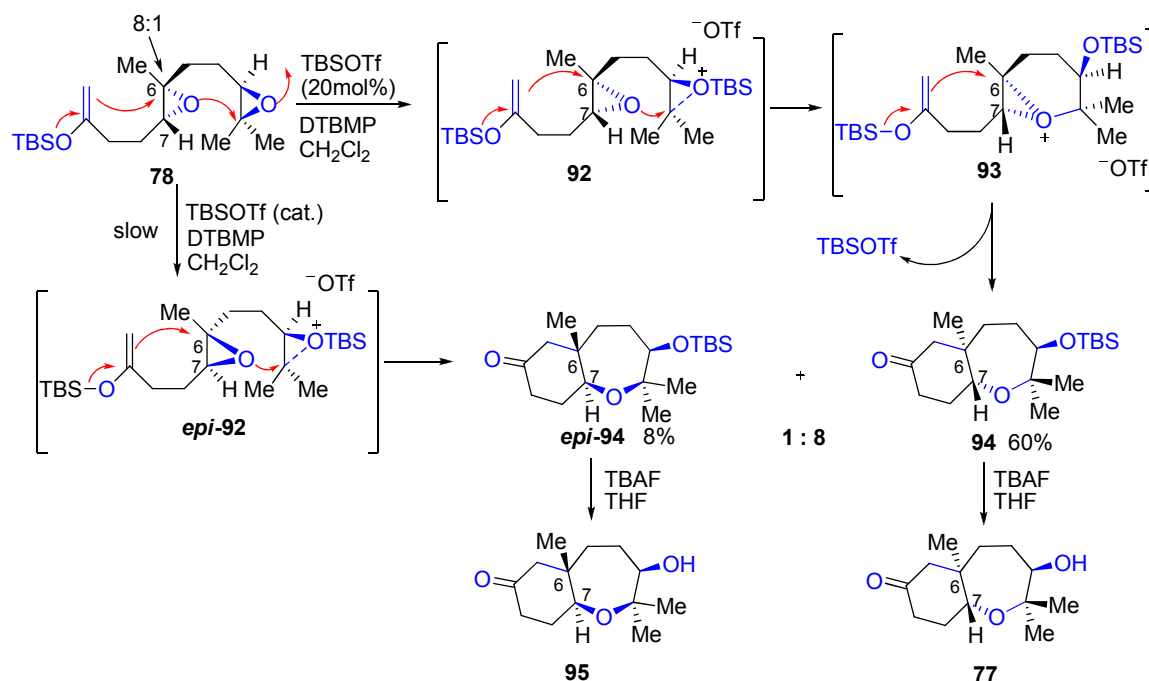


Specifically, following the general procedure⁴³ for formation of kinetic enolate⁴⁴, deprotonation of methyl ketone with potassium bis(trimethylsilyl)amide followed by capture with *tert*-butyldimethylsilyl chloride, provided diepoxy enolsilane **78**. Similarly, trapping the kinetic enolate from **87** with Comins reagent⁴⁵ [*N*-phenyl-bis(trifluoromethanesulfonimide)] gave enol triflate **91**, which underwent palladium-catalyzed Negishi cross-coupling⁴⁶ with (trimethylsilylmethyl) magnesium chloride to afford the allylsilane **83**. Particularly noteworthy is that Negishi cross-coupling proceeded much faster than the epoxide opening with the nucleophilic Grignard reagent, and due to its low Lewis acidity, the resulting side product Mg(OTf)Cl (trifluoromethanesulfonylmagnesium chloride) did not promote oxa-carbacyclization of **83**. Synthesis of diepoxy alkene **84** was achieved by following a modified Julia olefination⁴⁷ of ketone **87**.

With these substrates in hand, we began to explore the viabilities of hybrid cyclization processes, cascade oxa-carbacyclization, under abiological conditions. Oxa-carbacyclization of **78** was previously performed in our laboratory⁴⁸ using stoichiometric Lewis acid of freshly distilled trifluoroboron etherate (BF₃-Et₂O) or methylaluminum dichloride (MeAlCl₂) to provide mixtures of bicyclic ketones **94** and **95** in 40-60% yield. Reproducing such reactions, however, has never been a trivial matter if the yield is the major concern, because impurities such as HF and HCl from Lewis acid decomposition or trace amount of water in the solvent would significantly lower the yields of cyclizations. Mechanistically guided design and screen of Lewis acids led us to discover trialkylsilyl triflates⁴⁹ as potentially effective promoters of oxa-carbacyclizations. Treatment of an 8:1 mixture

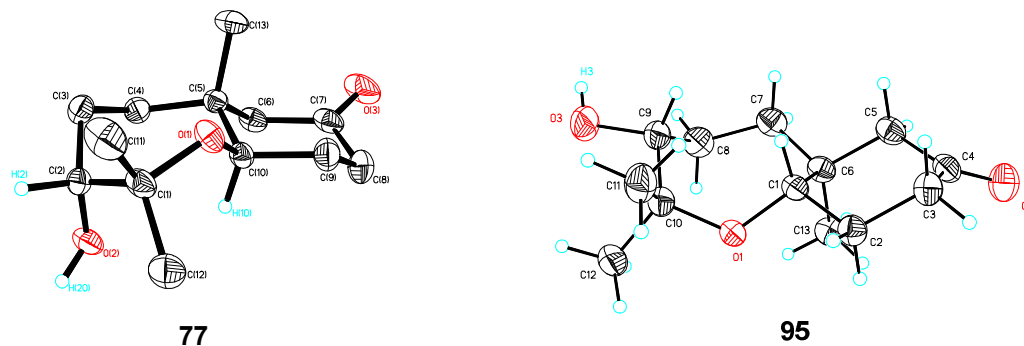
favoring diastereomer **78** with substoichiometric *tert*-butyldimethylsilyl trifluoromethanesulfonate (TBSOTf) in the presence of 2,6-di-*tert*-butyl-4-methylpyridine (DTBMP) gave chromatographically separable **94** and *epi*-**94** in excellent yield. Oxa-carbacyclization was assumed to be first induced by selective coordination of silyltriflate with the terminal epoxide **92**⁴⁹ to give bicyclo[4.1.0]epoxonium ion intermediate **93**,²⁹ which was attacked with tethered enolsilane in *anti*-parallel addition fashion¹⁵⁻¹⁷, to provide bicyclic ketone **94** corresponding to the D and E rings of *ent*-abudinol B (*ent*-**64**) (scheme 18). DTBMP was used as a bulky and non-nucleophilic base to trap any proton or triflic acid (HOTf) generated in the system for any reason. The base is also beneficial to generate the silylated cyclic products. Interestingly, bicyclic *epi*-**94** was formed in much slower rate, which was observed by monitoring the reaction

Scheme 18. TBSOTf mediated oxa-carbacyclization of **78**.



with thin layer chromatography (TLC). The stereochemistry and other structural aspects of **94** and *epi-94* were conclusively substantiated by X-ray analysis of the desilylation products **77** and **95**, respectively (figure 5).

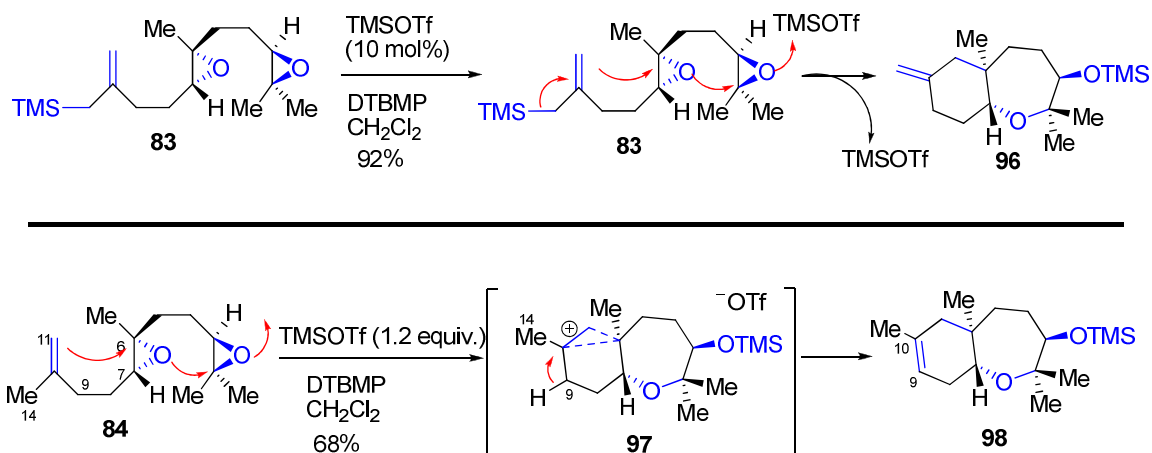
Figure 5. The thermal ellipsoid diagrams for bicyclic ketones **77** and **95**.



These results suggest that C-1 addition of alkene nucleophile is highly stereospecific with clean inversion of stereochemistry at C6 in both cyclizations. The trialkylsilyl triflate promoted oxa-carbacyclization excelled in reproducibility, bench operation and scaling up as compared with previous protocols. The ability to achieve such non-enzymatic oxa-carbacyclization clearly demonstrated the viability of cascade cyclization of polyepoxide-alkene substrates.

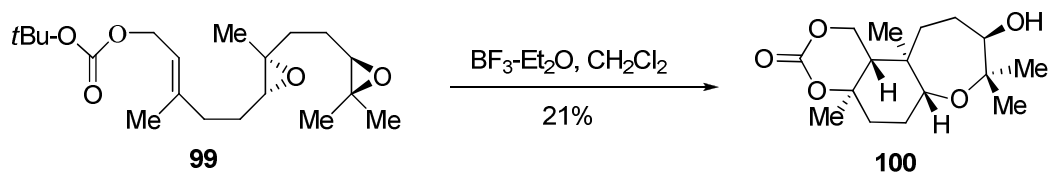
Under similarly optimized conditions, diepoxy allylsilane **83**⁴⁹ underwent similar bicyclization with a catalytic amount of TMSOTf and DTBMP to provide bicyclic alkene **98** in 92% yield, which could be transformed into bicyclic ketone **94** or **77** via ozonolysis and functional group manipulations (Scheme 19). The excellent yield with clean conversion suggests that allylsilane is an effective terminator for TMSOTf-promoted cascade oxa-carbacyclization. Other Lewis acids⁴⁹ including BF₃-Et₂O and MeAlCl₂²⁰ have been shown to promote the oxacyclization in lower yields.

Scheme 19. Oxa-carbacyclization of **83** and **84**.



Most importantly, the 1,1-disubstituted alkene of diepoxide **84** did participate in the tandem oxacyclization using 1.1 equivalent of TMSOTf and 2.0 equivalent of DTBMP at -78 °C to give bicyclic ether **98** in 68% yield. C9-C10 trisubstituted alkene of **98** was obtained as a major identified product, which was rationalized by the formation of non-classical carbenium cation intermediate **97** followed by C9 *beta*-hydrogen elimination to afford thermodynamically stable alkene. A lower yield was expected for this transformation since 1,1-disubstituted alkene was known to be less nucleophilic than the corresponding enol silane or allylic silane. In a closely related case, our laboratory previously reported the oxa-carbacyclization of farnesol-derived diepoxy alkene **99** (scheme 20)^{29a}. The low yield (21%) of oxa-carbacyclization was consistent with low nucleophilicity of allylic alkene, even with a carbonate as the terminating nucleophile.

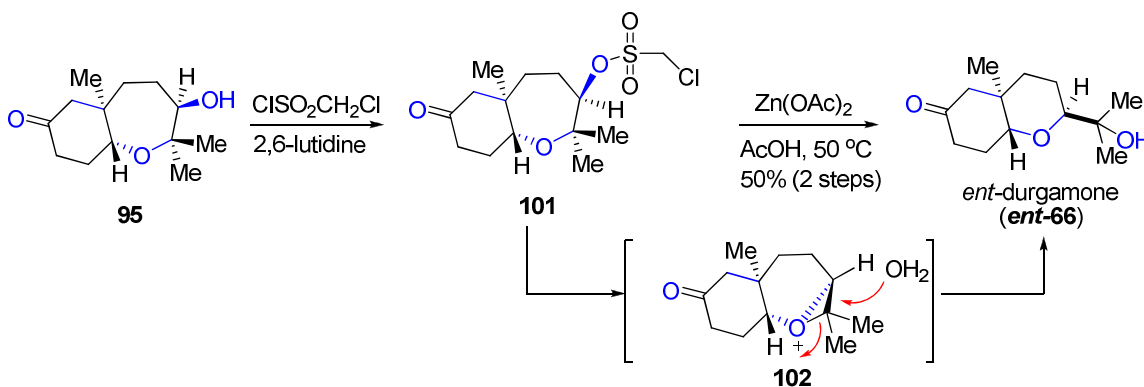
Scheme 20. McDonald/ Wei alkene-epoxide cyclization.



Comments on the oxa-carbacyclization of these diepoxy-alkenes are warranted before describing the exploration of other types of oxa-carbacyclization: 1) electron-rich alkenes are more favorable to undergo cascade mixed oxa-carbacyclizations; 2) the oxa-carbacyclization proceeds with *endo*-selectivity in *anti*-parallel addition; 3) silyl Lewis acids (TMSOTf or TBSOTf) in the presence of bulky base (DTBMP) are the choice of Lewis acid for the cascade oxa-carbacyclizations and 4) the stereochemistry of epoxides will affect the cyclization rate, but not the course, so that rate of cyclization is faster with the epoxides of all S or R configuration.

With a sufficient supply of bicyclic ketone **77** by our efficient oxa-carbacyclization, the enantiomer of durgamone (*ent*-**66**) was then synthesized by zinc acetate-mediated stereospecific ring contraction of the chloromesylate **101** (Scheme 21).

Scheme 21. Total synthesis of *ent*-durgamone (**ent**-**66**).



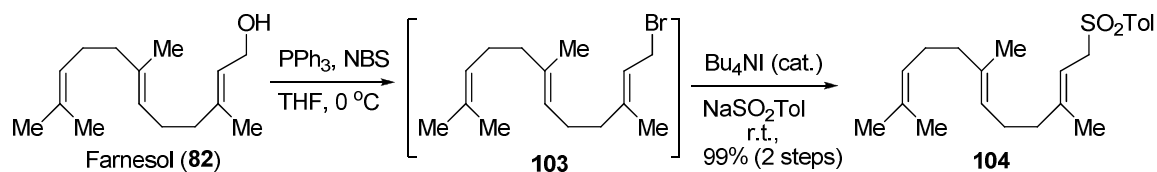
Treatment of **77** with chloromethylsulfonyl chloride in the presence of 2,6-lutidine resulted in formation of chloromesylate **101** in quantitative yield, which was subjected to zinc acetate mediated stereospecific ring contraction in acetic acid at $50\text{ }^\circ\text{C}$ to give *ent*-durgamone (**ent**-**66**) in 50% yield, presumably via epoxonium ion intermediate **102**. External nucleophilic water (or acetate ion) was expected

to attack the more substituted carbon, which has been studied by Nakata⁴⁰ for ring expansion of cyclic ethers. All of our spectroscopic data matched the very limited data reported for the natural products except for the optical rotation. The value of optical rotation of our synthetic enantiomer of durgamone (**ent-66**) is +14 (c 0.13 in methanol), whereas -28.5 (c 0.1 in methanol) of natural durgamone (**66**) was reported. The magnitude difference may be due to inaccurate measurement of concentration or impurities in the natural sample.

1.2.2. Total synthesis of *ent*-nakorone (**ent-67**)

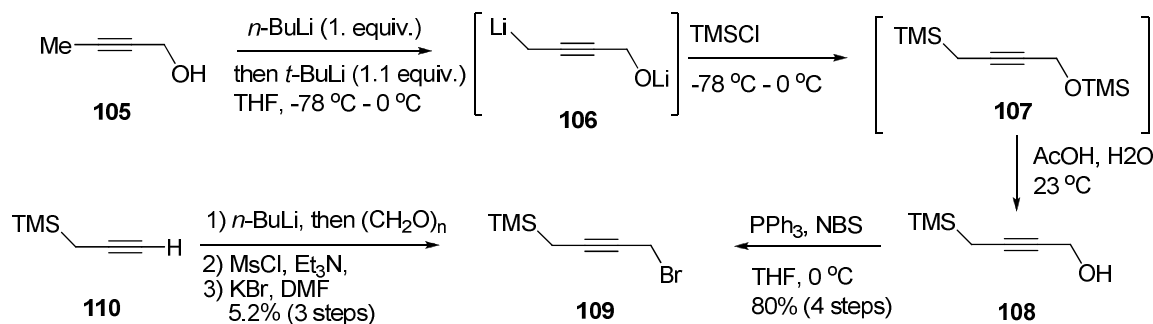
Inspired by Johnson's landmark work¹⁸ in the cascade carbocyclization of polyalkenes, propargylic silane was introduced as a terminal nucleophile for the synthesis of **ent-67** via similar oxa-carbocyclization because it is electronically rich, easily accessible and less sterically hindered. In addition, conversion of allene product by ozonolysis into the corresponding ketone was also reported to be high yielding. The synthesis of *ent*-nakorone began with preparation of coupling substrates farnesyl sulfone **104** (scheme 22)⁵¹ and propargylic bromide **109** (scheme 23)⁵². The known farnesyl sulfone was prepared using a newer procedure. Specifically, farnesol (**82**) was treated with triphenylphosphine and *N*-bromosuccinimide (NBS) in THF at 0 °C to give the unstable allylic bromide **103**, which in the same reaction pot underwent substitution with *p*-toluenesulfinic acid, sodium (NaSO₂Tol) in the presence of a catalytic amount of tetrabutylammonium iodide (Bu₄NI) for accelerating the S_N2 substitution, to provide farnesyl sulfone **104** in 99% yield.

Scheme 22. Synthesis of farnesyl sulfone **104**.



The synthesis of the known compound **109**⁵² was achieved more easily by the following sequence from 2-butyn-1-ol **105** (scheme 23). Deprotonation of alcohol **105** with butyllithium (*n*-BuLi) at -78 °C followed by deprotonation of the propargylic methyl with *tert*-butyllithium (*t*-BuLi) while slowly warming to 0 °C, generated dianion **106**, which was trapped with trimethylsilyl chloride (TMSCl) to provide **107**. Selective desilylation of **107** with acetic acid (AcOH) and water in the same reaction pot gave the desired 4-trimethylsilyl-2-butyn-1-ol (**108**) in 89% yield.

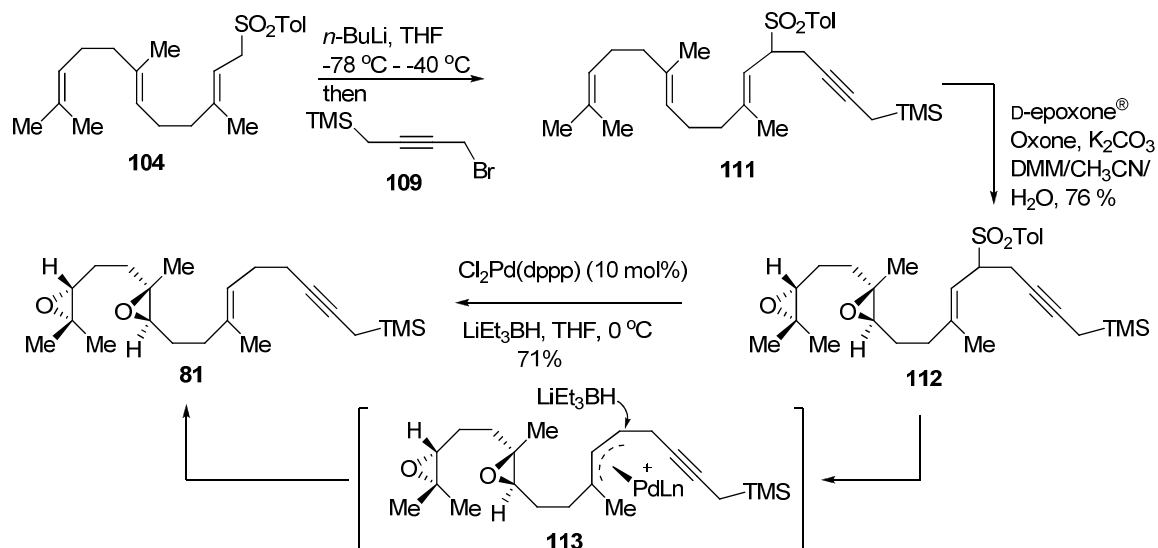
Scheme 23. Synthesis of propargylic silane **109**.



yield. Bromination of the resulting alcohol **108** was carried out with PPh_3 and NBS in THF at 0 °C to provide the desired 1-bromo-4-trimethylsilyl-2-butyne (**109**) in 90% yield. Noteworthy is that a considerably lower yield (5.2%) was obtained in our hands when following the previously reported procedure⁵² from an expensive propargylic silane **110**. Alkylation⁵³ of the lithium anion of farnesyl sulfone (**104**) with propargylic bromide **109** proceeded smoothly to afford triene-

yne **111** in 92% yield (scheme 24). Regio- and stereoselective double Shi epoxidation of **111** provided diepoxide **112** by taking advantage of the electron-withdrawing effect of the allylic sulfone to prevent epoxidation of the proximal

Scheme 24. Synthesis of cyclization substrate **81**.



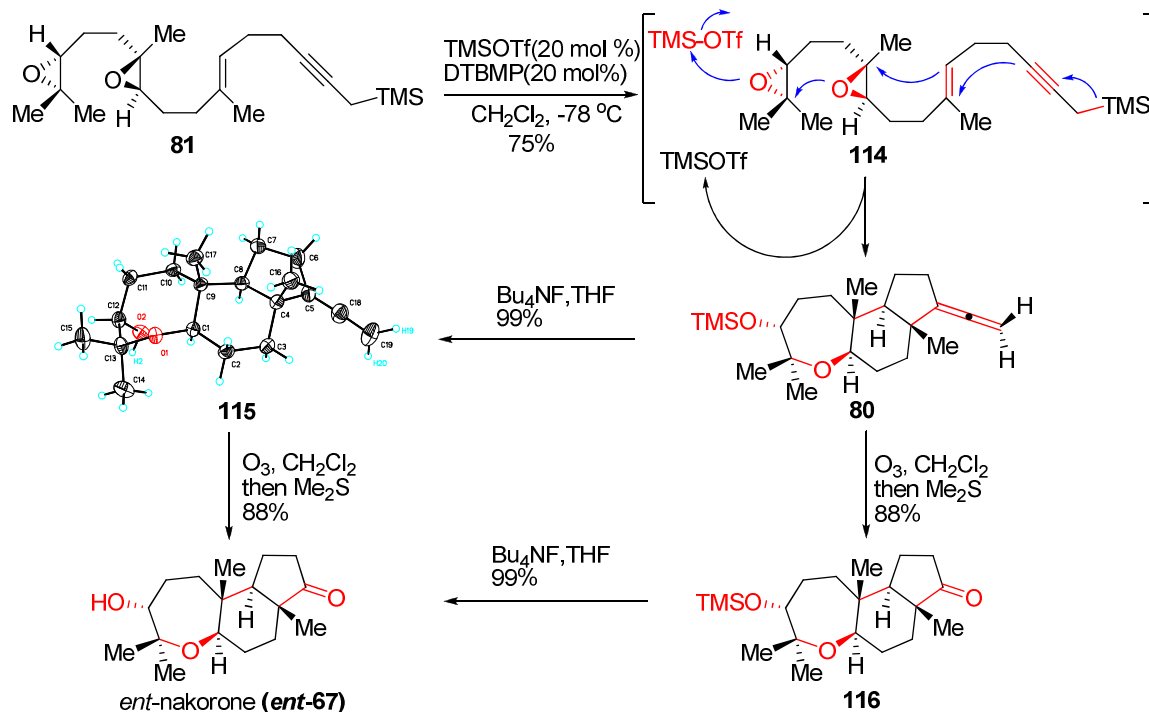
alkene. Palladium-catalyzed reductive desulfonylation⁵⁴ with Superhydride[®] (LiEt_3BH) provided the desired diepoxide enyne **81** in good yield. Mechanistically, palladium(II) was reduced by the Superhydride[®] to palladium(0), which underwent oxidative addition to allylic sulfone to generate π -allyl palladium **113**. Nucleophilic attack on the less hindered carbon with hydride resulted in formation of product **81**. The fresh preparation of palladium catalyst [$\text{Cl}_2\text{Pd}(\text{dppp})$] was imperative to successful reduction and high regioselectivity.

It is informative and instructive to comment on the desulfonylation: 1) Superhydride did not reduce or open the epoxides under the reaction conditions, which was a concern prior to conducting the reaction; 2) the electrophilic π -allyl palladium did not initiate the cascade cyclization of the remaining diepoxide, while π -allyl metal (such as Rh or Pd)⁵⁵ has been shown to be very reactive and

initiate the alkylation or cyclization to form acyclic or cyclic ethers; and 3) The nucleophilic propargylic silane survived, and palladium-catalyzed enyne cyclization or coupling⁵⁶ was not observed. The ability to achieve the regioselective desulfonylation with Superhydride in the presence of epoxides and propargylic silane has clearly revealed the stability of π -allyl palladium species from allylic sulfone.

With the substrate **81** in hand, we studied the oxa-carbacyclization terminated with propargylic silane (scheme 25). Treatment of diepoxy enyne **81** with catalytic amount of TMSOTf and DTBMP resulted in the *trans-anti-trans* tricyclic allene **80** in excellent yield, presumably via TMSOTf-activation of terminal epoxide **114**.

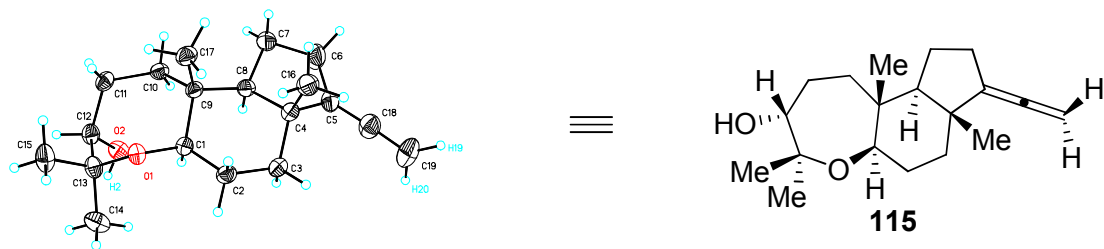
Scheme 25. Synthesis of enantiomer of nakorone (*ent-59*).



The oxa-carbacyclization proceeded smoothly in stereospecific *anti-parallel* addition fashion by following Markovnikov's rule and was usually completed in

one hour with 100% conversion of starting materials. Incredibly, the stereochemistry and tricyclic structural architecture of **80**, consistent with the enantiomers of natural product nakorone and abudinols A and B, was constructed in one single operation from a linear substrate **81**. The yield of oxacyclization of diepoxy en-yn **81** to allene **80** significantly exceeded that obtained from oxacyclization of diepoxy en-carbonate **99** to **100** shown in Scheme 20. Ozonolysis⁵⁷ of the allene of **80** to tricyclic ketone **116** was followed by desilylation with tetrabutylammonium fluoride (Bu₄NF) to furnish the *ent*-nakorone (**ent-67**), which also corresponds to the A, B and C rings of the abudinols. Alternatively, desilylation of **80** to allene **115** followed by ozonolysis also provided the *ent*-nakorone (**ent-67**) in approximately the same yields. However, oxidative cleavage of allene by the Sharpless method^{58,18f} (catalytic RuCl₃ and NaIO₄) gave mixtures of *ent*-nakorone (**ent-67**) and **116** in lower yields. The structural and stereochemical aspects of the tricyclic allene **115** were substantiated by analysis of X-ray crystallographic data (figure 6).

Figure 6. The thermal ellipsoid diagram for compound **115**.

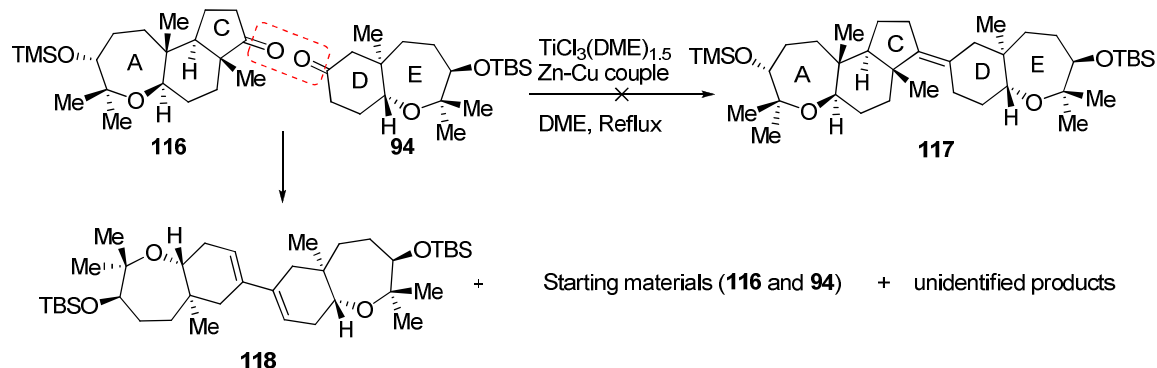


1.2.3. Total synthesis of enantiomer of abudinol B (*ent*-64)

Having demonstrated the efficient oxa-carbacyclization to provide sufficient amount of bicyclic ketone **94** and tricyclic ketone **116**, we set out to assemble these two sectors into *ent*-abudinol B (***ent*-64**). We envisioned that abudinols would arise from cross-coupling of bicyclic ketones **94** or ***ent*-66** with tricyclic **116** by a process conceptually equivalent to retro-ozonolysis. Unfortunately, the sterically hindered ketone **116** as well as the enolizable nature of **94** was incompatible with several otherwise reliable transformations of this type. In addition, it would be extremely challenging to set the right geometry of the newly-formed tetrasubstituted alkene from two cyclic ketones, since no precedents were reported to date.

A number of efforts were still made to explore this challenging transformation. First, we began to study the McMurry cross coupling⁵⁹ (Scheme 26), a retro-ozonolysis process, since only a single-step reaction was required with the ketones **94** and **116** to provide the expected *ent*-abudinol B (***ent*-64**) if it works.

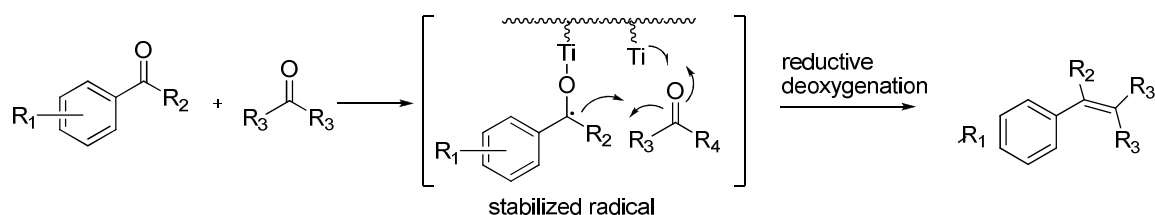
Scheme 26. McMurry coupling of **94** and **116**.



However, upon treatment of ketones **94** and **116** with classically recommended titanium trichloride and zinc-copper complex, no cross-coupling products were detected by ^1H NMR or HRMS. Diene **118** was identified by HRMS with the nonpolar products, which was explained by homocoupling of radical generated from sterically less hindered bicyclic ketone **94** followed by dehydration.

There are no precedents documenting that an aliphatic cyclic ketone will undergo intermolecular McMurry cross-coupling with another aliphatic cyclic ketone. The possibility of a bad catalyst cocktail was ruled out by successfully carrying out the control experiment with cyclohexanone. In typical intermolecular McMurry cross-coupling, the arylketone, except for excessive acetone, was the only viable coupling partner when the other is an aliphatic ketone because it would be reduced first and formed an aryl-stabilized radical, which has a lifetime long enough for coupling with external partners (Figure 7).^{59c,59d}

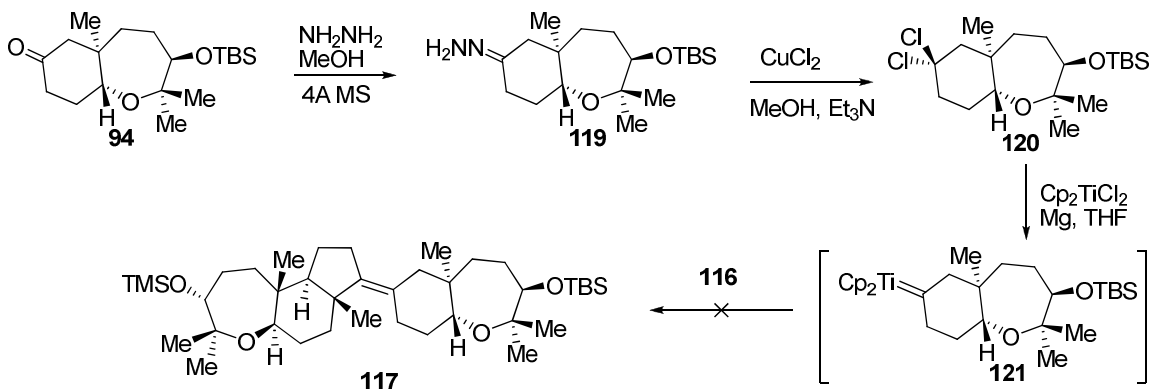
Figure 7. McMurry cross coupling of arylketone.



We next explored the reaction of one ketone with olefinating reagent derived from the other ketone, as typically polysubstituted alkenes could generally be synthesized by olefination of corresponding ketone or aldehydes with Tebbe-, Julia- or Wittig-type reagents.⁶⁰ To that end, we explored the titanocene-mediated olefination developed by Takeda, due to its efficiency and power to

construct the crowded tetrasubstituted alkene from two different aliphatic ketones (scheme 27).

Scheme 27. Takeda's method for assembly of ketones **94** and **116**.

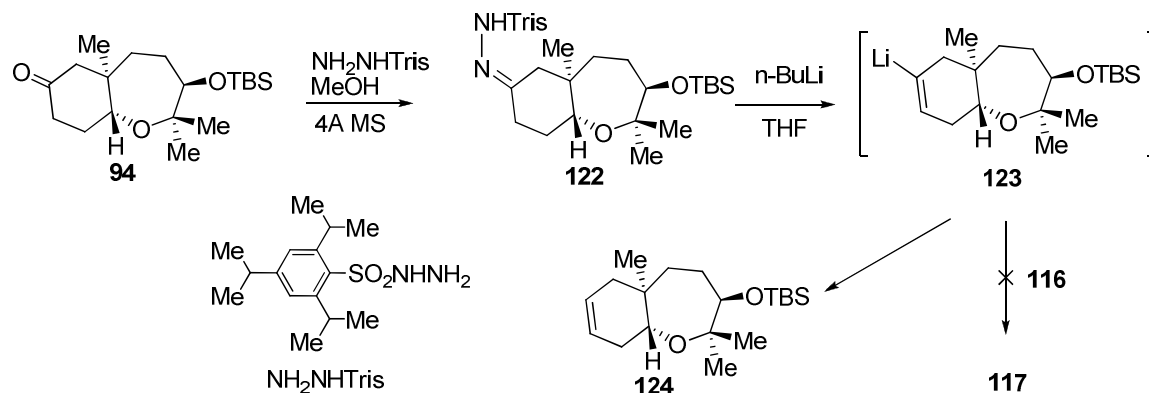


Ketone **94** was then converted into *gem*-dichloride **120** by following the Takeda protocol for *gem*-dihalide synthesis.⁶¹ Unfortunately, titanocene carbene **121**, prepared *in situ* from *gem*-dichloride **120**, Cp₂TiCl₂ and magnesium, did not undergo olefination with ketone **116**, probably because of the steric hindrance presented by the ketone **116** and/or instability of titanocene carbene **121**. Complex mixtures were observed by TLC and crude ¹H NMR. Ketone **116** could not be transformed into the corresponding *gem*-dichloride species due to the easy elimination of HCl of the *gem*-dichloride product as well as desilylation.

Therefore, we turned our attention to the other methods that are not obvious or direct to abudinol B, for example, alkylation of ketone **116** and reductive deoxygenation. We decided to make the carbon carbon single bond first via alkylation of **116** with vinyl lithium (**123**) prepared *in situ* by Shapiro Reaction (scheme 28).⁶² Condensation of ketone **94** with hydrazine produced the hydrazone **122** in good yield. Deprotonation of **122** with three equivalents of *n*-

BuLi at low temperature caused Shapiro reaction to generate vinyl lithium **123** when warming up to 0 °C.

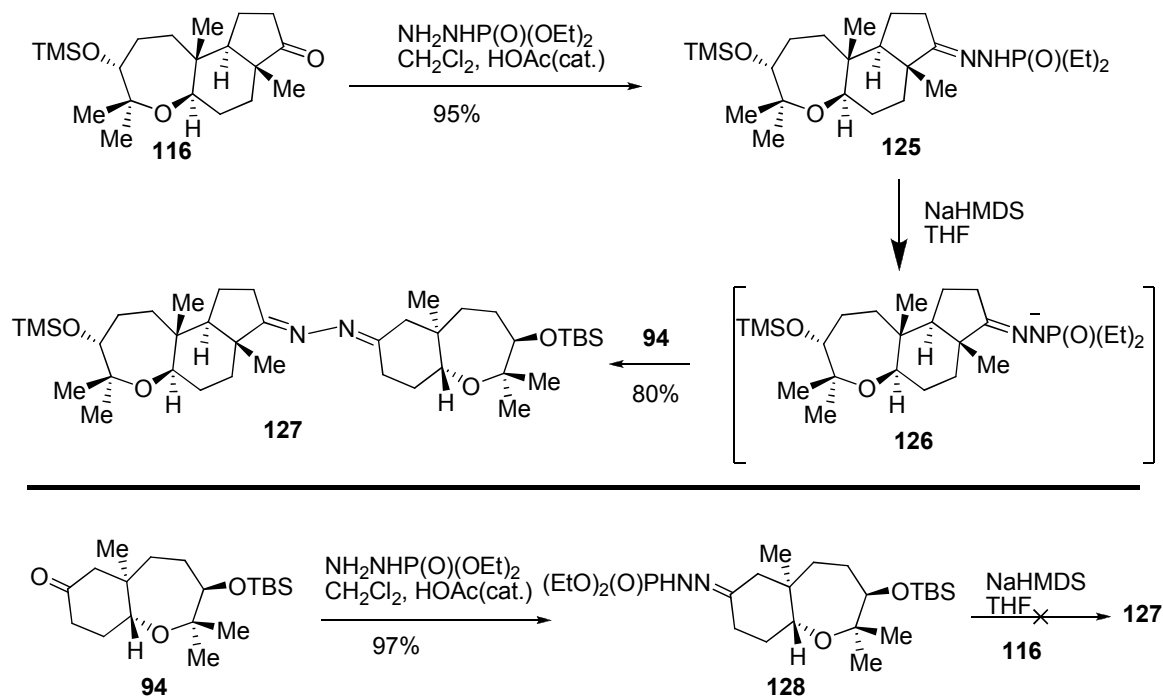
Scheme 28. Vinyl lithium formation via Shapiro reaction.



Unfortunately, the vinyl lithium **123** was not to react with the tricyclic ketone **116**, but to be protonated by THF solvent^{62d} while warming. Difficulty in preparing the vinyl lithium **123** at low temperature (-78 °C) with a high yield as well as its strong basicity^{62d} for potential enolization of ketone **116** made this route less attractive, given the fact that few precedents in the literature were documented for the stereospecific reductive deoxygenation⁶³ of allylic alcohol with migration of the double bond.

Considering the successful application of Barton's two fold molecule extrusion⁶⁴ for synthesis of tetrasubstituted alkene from two different cyclic ketones, we expected that the tetrasubstituted alkene in the *ent*-abudinol B could be constructed from ketones **94** and **116** by following similar sequences (scheme 29 and Scheme 30). We synthesized the azine (bishydrazone) **127** by following Jenneskens's procedure^{64c} for synthesis of asymmetric bishydrazone from two different ketones.

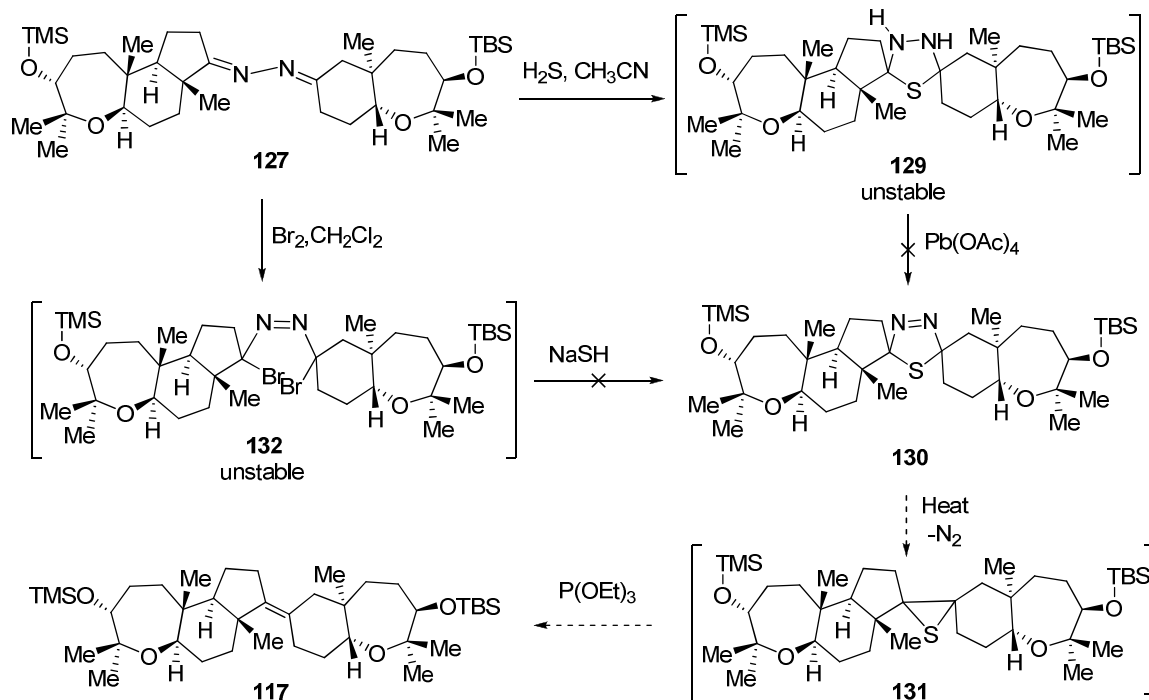
Scheme 29. Coupling of ketone **94** with **116** via hydrazone formation.



Condensation of ketone **116** with phosphite hydrazine⁶⁵ in the presence of catalytic amount of acetic acid provided the required hydrazone phosphate **125**. Deprotonation of the resulting hydrazone **125** with NaHMDS followed by reaction with ketone **94** afforded desired azine **127**. Surprisingly, azine **127** could not be synthesized by reaction of ketone **116** with hydrazone **128** under the same reaction conditions probably because the steric hindrance of the tricyclic ketone **116** disfavors nucleophilic addition upon it.

Following Barton's protocol, treatment of **127** with H_2S gas in sealed tube gave heterocycle **129**, which, unexpectedly, is unstable and decomposes on TLC when monitoring the reaction progress with TLC (Scheme 30). Subsequent subjecting of the crude **129** to lead tetraacetate $[\text{Pb}(\text{OAc})_4]$ oxidation did not afford the desired heterocycle **130**. Reversing these two steps, oxidation followed

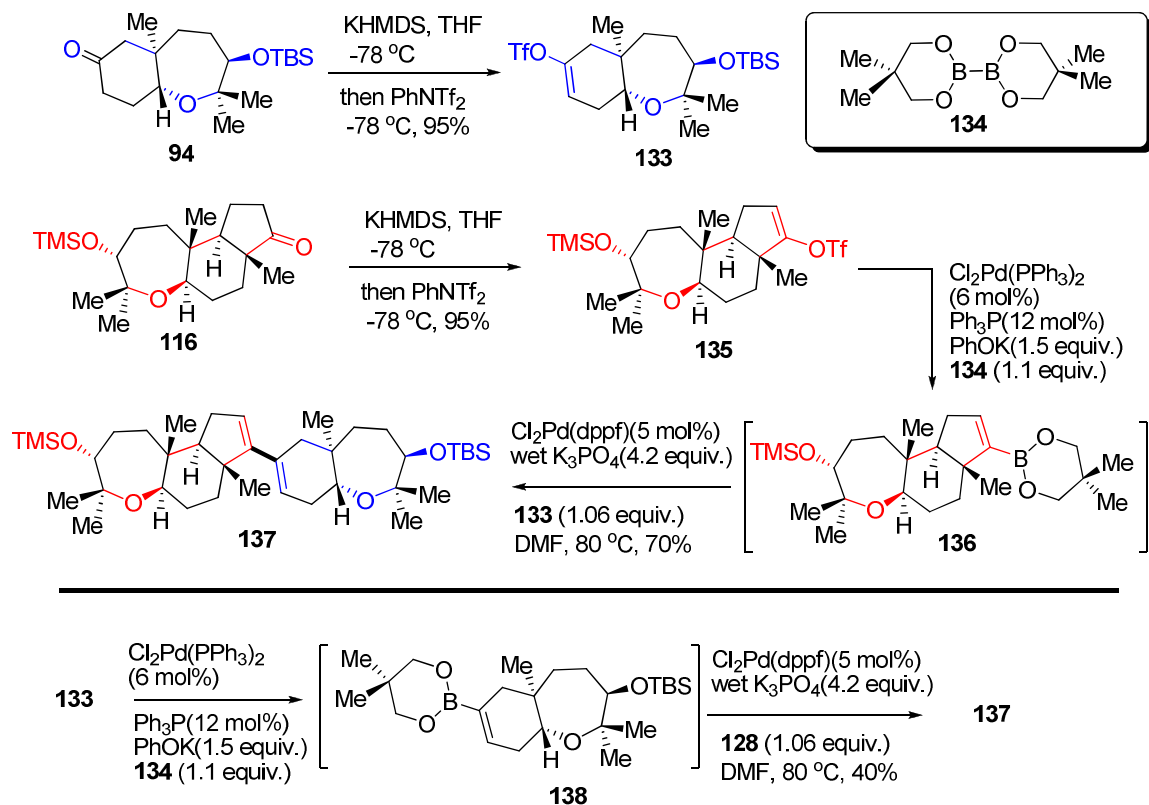
Scheme 30. Barton's method to assemble *ent*-abudinol B from azine **127**.



by substitution, still did not change the fate of instability of intermediate. Oxidative bromination⁶⁶ of **127** also resulted in unstable product **132**, which did not undergo substitution reaction with hydrogen sulfide salt. Neither **117** nor its derivatives (desilylation products) were detected by ^1H NMR or TLC when the one-pot procedure was attempted to avoid decomposition and isolation of unstable intermediates. The unpleasant odor and high toxicity of sulfur compounds associated in this transformation discouraged other attempts on this Barton-Kellogg olefin synthesis. Other fruitless efforts on utilizing bishydrazone chemistry of **127** included the AIBN-initiated radical reaction, thermal decomposition (heating) and photo decomposition (sunlight exposure for days to month in a sealed tube).

Because palladium-mediated cross-coupling reactions⁶⁷ were well established in making a C-C bond with exceeding efficiency and mild conditions, we next set out to explore palladium catalyzed cross-coupling reactions with the derivatives of ketone substrates **94** and **116**. Fortunately, numerous efforts on this new

Scheme 31. Suzuki cross-coupling of **94** and **116**.



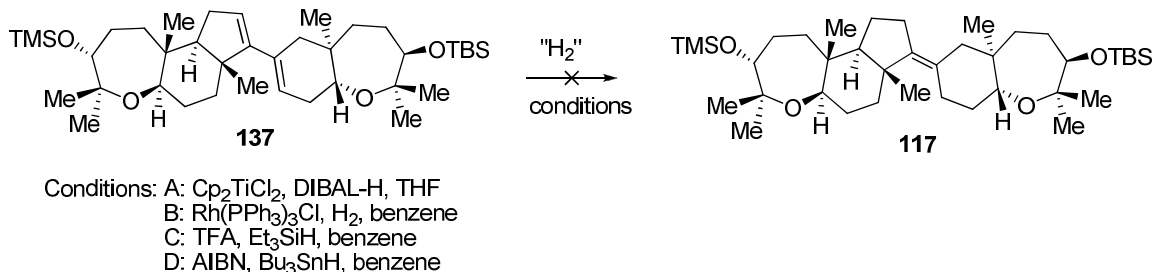
strategy were eventually rewarded by efficiently uniting **94** (DE rings) and **116** (ABC rings) sectors (Scheme 31). Using conditions developed by Miyaura,⁶⁸ the ketone **94** and **116** could be efficiently converted to the corresponding coupling partners. Trapping the kinetic enolate from **94** with Comins reagent (PhNTf₂) produced vinyltriflate **133**. Similarly, **116** was converted into vinyl triflate **135**. Palladium-catalyzed cross-coupling of **136** with **133** proceeded effectively and united the ABC and DE ring sectors through a one-pot sequence, in which

tricyclic enol triflate **135** was first converted into the vinyl boronate **136** by palladium catalysis, and then coupled with bicyclic enol triflate **133** in the presence of $\text{Cl}_2\text{Pd}(\text{dppf})$ and wet K_3PO_4 , to provide pentacyclic diene **137** in good yield. Isolation of the vinylborate **136** was not necessary in terms of yields and bench operation. Trace of water seemed beneficial to the second-step cross-coupling (**133** and **136**), because dry potassium triphosphate (K_3PO_4) gave lower yields. Under optimized conditions, Suzuki cross-coupling of boronate **138** with vinyl triflate **135** gave lower yield of diene **137**, probably because initial oxidative addition product Pd (II) is too bulky to favor the subsequent transmetalation with boronate **138**. Homocoupling and protonation of **138** were found to be two main competing processes that accounted for the moderate yield.

Surprisingly, more challenges were encountered in the partial hydrogenation of diene **137** due to the poor regio- and stereoselectivity of the very limited methods⁶⁹ available. It was well known that conjugated diene coordinated by chromium^{69c} or other metal^{69b-f} could be partially hydrogenated in 1,4-*cis*-addition manner⁶⁹, however, it was expected to give “wrong” Z-alkene geometry instead of the E-alkene in abudinol B. The faith that luck always goes to the well-prepared person gave me the courage and power to try various methods available.

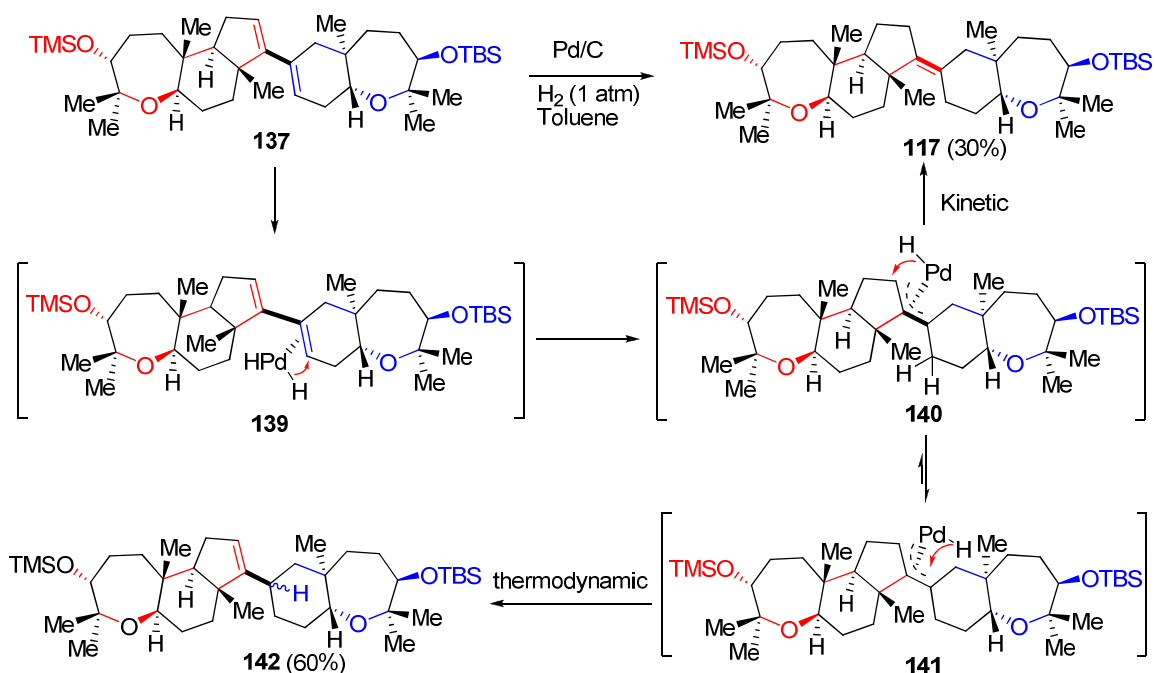
No reaction occurred when diene **137** was subjected to the partial hydrogenation conditions including titanocene-mediated reduction (A)⁷⁰, rhodium-catalyzed hydrogenation (B)⁷¹, trifluoroacetic acid (TFA) promoted reduction (C)⁷² and AIBN-initiated radical reaction (D) (scheme 32).

Scheme 32. Attempts on hydrogenation of diene **137**.



Fortunately, palladium-catalyzed hydrogenation of diene **137** in toluene at 0 °C, utilizing conditions developed by Shibasaki⁷³ for stereoselective synthesis of an exocyclic tetrasubstituted enol ether and olefin in 1, 4-addition manner, gave the desired product **117**, along with a substantial amount of the regioisomeric alkene **142** (3:5) in 95% yield (scheme 33). Mechanistically, PdH_2 coordinating the less

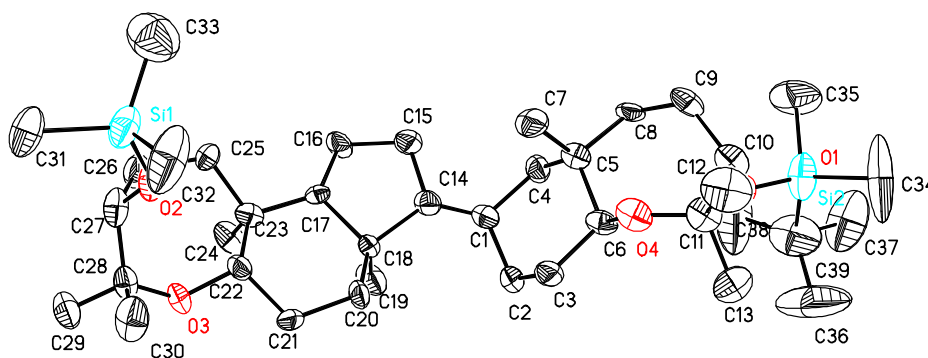
Scheme 33. Palladium-catalyzed hydrogenation of diene **137**.



hindered cyclohexene (**139**) underwent regio- and stereoselective carbopalladation to provide π -allyl palladium **140** that underwent kinetic reductive

elimination to afford the long-sought **117** in 30 % yield. Whereas **141**, conformationally equilibrated with π -allyl palladium **140**, provided thermodynamic product **142** after reductive elimination. Solvent effect on the regio- and stereoselectivity was substantial since polar solvents such as methanol, ethanol or ethyl acetate provided only trace desired product **117**. Reaction temperature was another important factor that affected the regio- and stereoselectivity of palladium-catalyzed hydrogenation. The newly-formed alkene geometry and all other structural aspects of our synthetic material were conclusively confirmed by crystallographic analysis of the bis-silyl abudinol B **117** (figure 8).

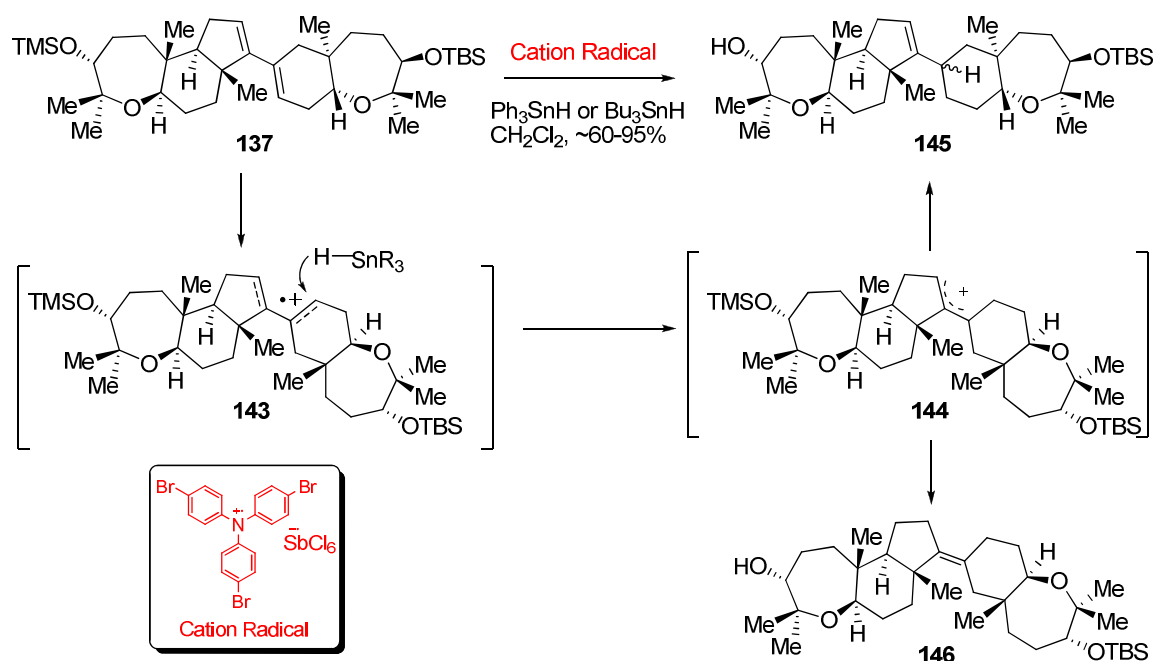
Figure 8. Thermal ellipsoid diagram for compound **117**.



Several attempts,⁷⁴ including acid-catalyzed (H_2SO_4), base-promoted ($\text{KNH}(\text{CH}_2)_3\text{NH}_2$) and transition metal-mediated $\{\text{Pd}/\text{C}$, PdCl_2 , $\text{PdCl}_2/\text{AgBF}_4$, $[\text{Pd}(\text{CH}_3\text{CN})_4](\text{BF}_4)_2\}$ isomerizations, were made to isomerize the regioisomeric alkenes **142**, but without success. In an effort to improve the overall conversion of **137** to **117**, we undertook studies on hole transfer catalyst promoted hydrogenation⁷⁵ (scheme 34), a partial reduction process developed by Bauld.

Treatment of **137** with cation radical initiator [tri(4-bromophenyl)ammonium hexachloroantimonate]^{75c}, a hole transfer catalyst, in the presence of tributyltin hydride or triphenyltin hydride gave predominantly alkene **145** after simultaneous removal of trimethylsilyl group, along with approximately 5% tetrasubstituted alkene **146** with the “wrong” alkene geometry. The *cis*-diene cation radical **143** was proposed to account for regioselective formation of **146** via unfavorable 1,4-addition of dihydrogen, which was in sharp contrast to Bauld’s case that 1,4-addition hydrogenation product was obtained exclusively.

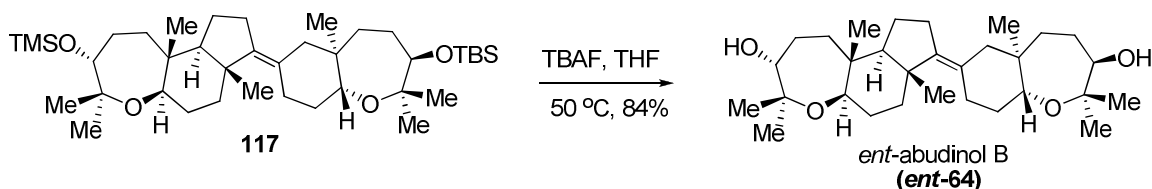
Scheme 34. Hole transfer catalyst promoted hydrogenation of diene **137**.



Although the improvement of conversion of diene **137** to monoene **117** was not achieved, the short and efficient synthetic route for preparation of diene **137** guaranteed a sufficient supply of **117** for completing the total synthesis of *ent*-abudinol B. Desilylation of **117** with tetrabutylammonium fluoride (TBAF) in THF at 60 °C provided the structure corresponding to antipode of naturally occurring

abudinol B (*ent*-**64**) in 84% yield (scheme 35). All spectroscopic data for the synthetic enantiomer of abudinol B was well matched with that of the limited data reported for the natural abudinol B. The alkene geometry and all other structural aspects of our synthetic material were conclusively confirmed by crystallographic analysis of **117**.

Scheme 35. Completion of the total synthesis of *ent*-abudinol B (*ent*-**64**).



In conclusion, the biomimetic total synthesis of *ent*-durgamone (*ent*-**66**) was achieved in 8 steps from commercially available geranylacetone (**79**) with 21% overall yield, and *ent*-nakorone (*ent*-**67**) was accomplished in 7 steps from commercial starting material farnesol (**82**) with 32.1% overall yield. Convergent and biomimetic total synthesis of *ent*-abudinol B (*ent*-**64**) was achieved in 5 steps from bicyclic ketone **94** and tricyclic ketone **116** with 15.9% overall yield. Most importantly, cascade cyclizations of diepoxides tethered to enolsilane and to ene-propargylsilane were developed and could be applied to the efficient, potentially biomimetic syntheses of several structurally related terpenoid natural product structures. These findings led to additional exploration on the possibility of the direct formation of abudinol and other oxacyclic triterpenoid natural products from polyepoxide substrates similar to squalene tetraepoxide.

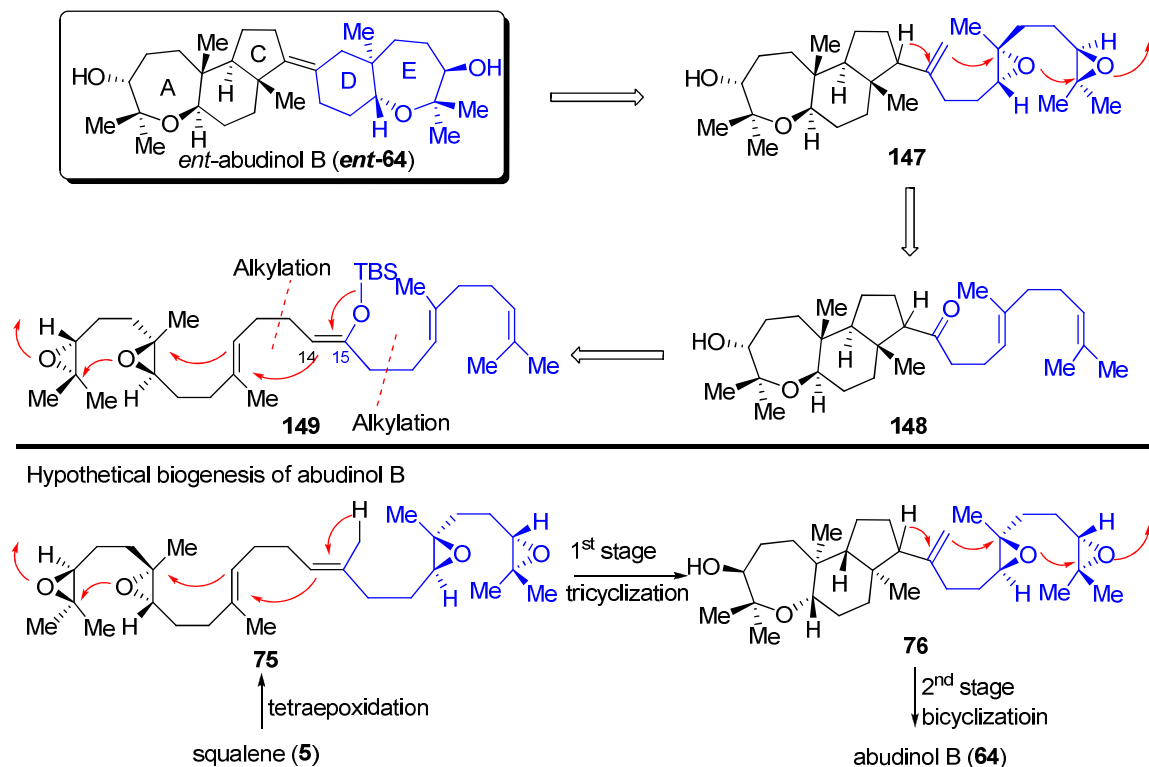
1.3. Biomimetic total synthesis of *ent*-abudinol B from squalene-like precursor

1.3.1. Synthetic strategies

Upon completion of the first total synthesis³⁹ of abudinol B, we undertook studies of the much more risky biomimetic synthesis: total synthesis of this triterpene natural product from a squalene-like precursor. Squalene (**5**) and the (*S*)-2,3-monoepoxide of squalene are precursors for the biogenesis of many 30-carbon terpenoid natural products, including steroids and hopanoids.^{9a} The demonstrated cascade polycyclization nature of the biosynthetic processes for these important natural products from squalene and squalene epoxide has also revolutionized the development of chemical synthesis strategies^{9b} that are similar to or inspired by this mode of natural product biosynthesis. More recently, a variety of triterpenoid natural products containing cyclic ethers have been discovered in marine sources including algae and sponges.^{34,35} The biosynthetic pathway for these compounds can be envisioned to arise from additional oxidations of squalene, accompanied by oxacyclizations to form the cyclic ether structures. While considerable accomplishments have been recorded in biomimetic or bioinspired cascade cyclizations of polyalkene and polyepoxide cyclizations, the cyclization processes of multiple epoxides with multiple alkenes have not been extensively studied. Such a hybrid process has been proposed for the biosynthesis of various triterpenoids which feature cyclic ethers fused to carbocyclic rings, including the marine triterpenoid natural product abudinol B (**64**)

(Scheme 14). The 30-carbon skeleton of abudinol B as well as the position of methyl substituents is consistent with a triterpene arising from biogenetic

Scheme 36. Retrosynthetic analysis of *ent*-abudinol B (*ent*-**64**).



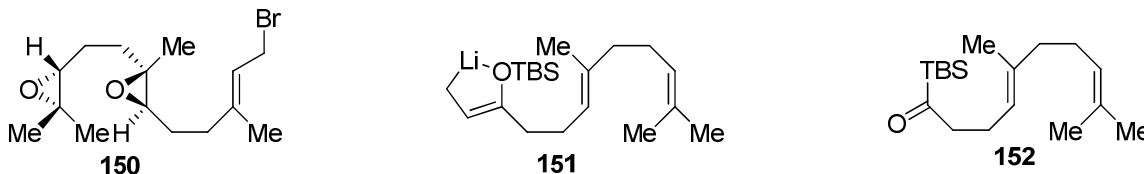
oxidative polycyclization of squalene (**5**), and also shares several structural features with other cyclic ether triterpene natural products.^{34,35} Although the nature of the biosynthetic polycyclization process has not yet been demonstrated, Norte³⁴ has proposed that tandem oxa- and carbacyclization of two adjacent epoxides and both alkenes of squalene tetraepoxide (**75**) could provide the hypothetical intermediate **76** containing the fused tricyclic sector in an initial tricyclization stage, followed by subsequent stage featuring bicyclization of the remaining two epoxides to afford the structure of abudinol B via *beta*-elimination of hydrogen to form the tetrasubstituted alkene.

Our second generation of biomimetic total synthesis of abudinol B was primarily inspired by the biogenesis proposed by Norte and highly based on the striking findings from our first generation synthesis³⁹ (Scheme 36). We envisioned that the D and E rings of *ent*-abudinol B could be formed via Lewis acid-initiated tandem oxa-carbacyclization of diepoxy alkene **147** as well as simultaneous construction of the congested tetrasubstituted alkene by loss of one equivalent of proton, a process that mirrored the second stage of biogenesis of abudinol B. Stereochemically defined **147** could be synthesized by sequential functional group manipulations of **148**, including regio- and diastereoselective double Shi epoxidation⁴¹ of the trisubstituted alkene and methylenation of the corresponding ketone. The first stage of biosynthesis of abudinol B was simulated by Lewis acid mediated tandem oxa-carbacyclization of diepoxides **149**. In order to more effectively promote the initial tricyclization cascade to afford the fused tricyclic network of abudinol B as observed in the proposed biogenetic intermediate **76**, the enolsilane at C14-C15 of **149** was designed as a good nucleophile for efficient termination of the cascade cyclization. The epoxides of compounds **149** and **147** were antipodal to those required for abudinol B, due to the ready availability of the D-fructose-derived chiral ketone⁴¹ (D-epoxone[®]) for enantioselective epoxidation.

1.3.2. Synthesis of cyclization substrate 149

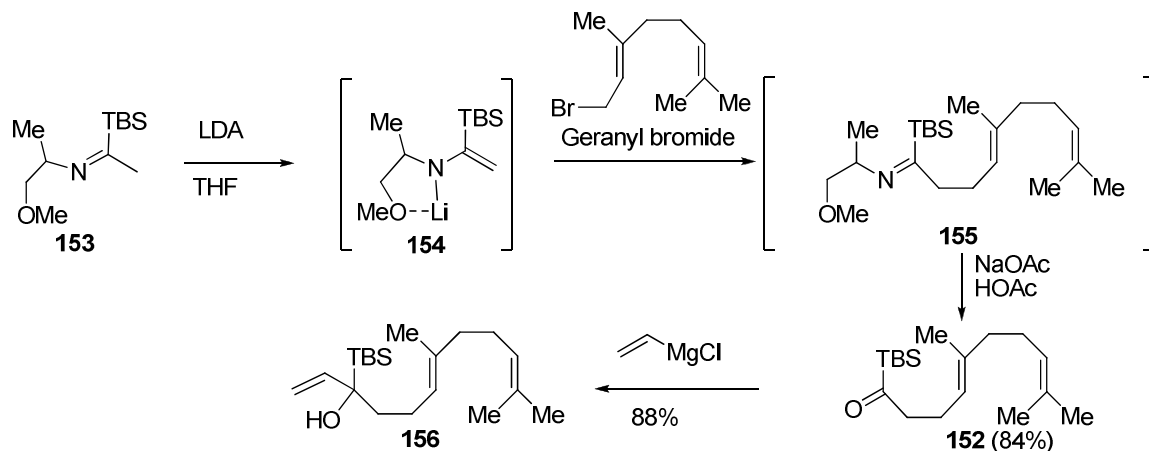
For the synthesis of squalene-like precursor **149**, we envisioned that the carbon skeleton could be assembled by alkylation of farnesyl allylic bromide **150** with geranyl homoenolate **151** prepared in situ by Brook rearrangement⁷⁶ of alkoxide from vinyl Grignard addition to geranyl acylsilane **152** (figure 9), sequential transformations developed by Kuwajima⁷⁷ and extended by Corey²⁰ for synthesis of enol silane with high level of regioselectivity.

Figure 9. Fragments of squalene-like substrate **149**.



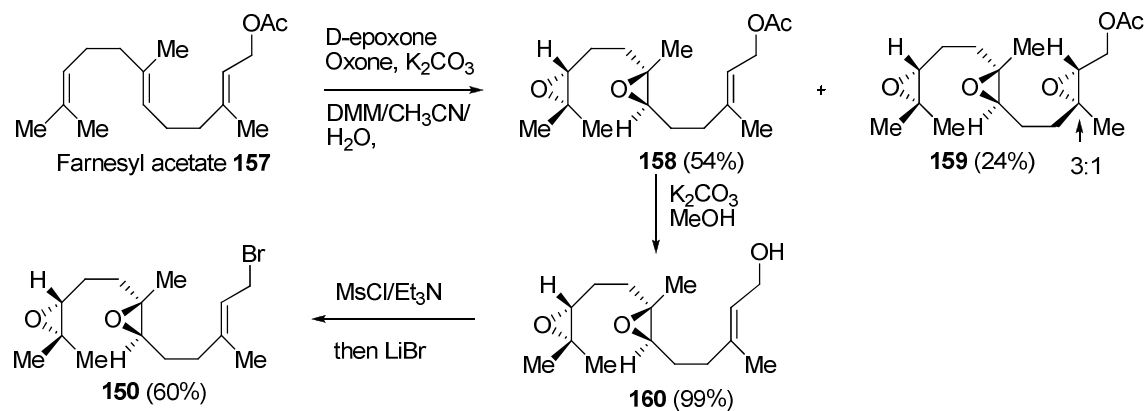
We started our syntheses with preparation of **151** and **152** from commercially available materials (scheme 37 and scheme 38). Specifically, deprotonation of known compound **153**⁷⁸ with freshly-prepared lithium diisopropylamide (LDA) in THF at -30 °C initially and then at 0 °C for 10 min produced the corresponding lithium azaenolate **154**, which was cooled to -30 °C again and treated with geranyl bromide to provide imine **155** (Scheme 36). Hydrolysis^{20a,b} in HOAc-NaOAc buffer afforded the acylsilane **152**, which underwent alkylation⁷⁷ with three equivalents of vinylmagnesium chloride in diethyl ether to afford tertiary alcohol **156** in excellent yield. No products resulting from Brook rearrangement were found by TLC or ¹H NMR after aqueous workup, consistent with results from Kuwajima's experiments⁷⁷.

Scheme 37. Synthesis of coupling substrate **156**.

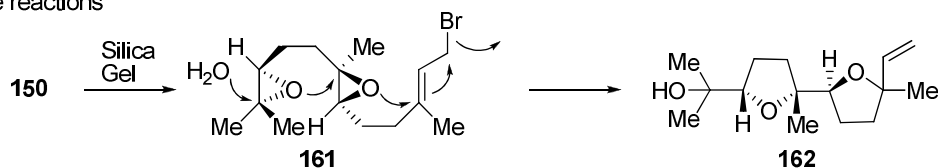


For the synthesis of **150** (scheme 38), double Shi epoxidation⁴¹ of *trans-trans* farnesyl acetate (**157**) afforded the desired diepoxide **158** with approximately 10:1 diastereoselectivity, along with starting material and triepoxide **159** with lower diastereoselectivity on the allylic alkene. Deacetylation of **158** with catalytic amount of potassium carbonate in methanol provided diepoxy alcohol **160**^{29a}, which was treated with methanesulfonyl chloride (MsCl) in the presence of

Scheme 38. Synthesis of farnesyl diepoxy bromide **150**.



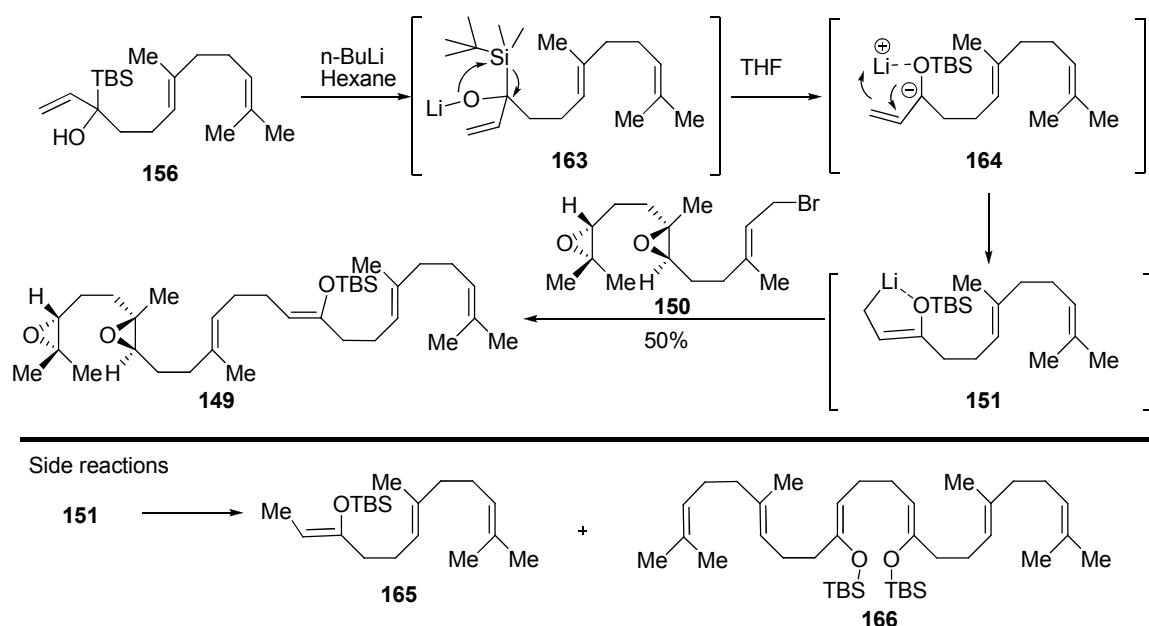
Side reactions



triethylamine at $-30\text{ }^{\circ}\text{C}$, followed by addition of THF solution of anhydrous lithium bromide, to produce diepoxy allylic bromide **150** in good yield. Particular caution must be exercised to the purification of **150** since silica gel can cause explosive tandem *exo*-cyclization reaction to generate bicyclic tetrahydrofuran **162** (scheme 38). The allylic bromide **150** is also sensitive to light, moisture (even with weak acid such as glassware) and oxygen, and therefore should be used as soon as possible or stored in the freezer ($-20\text{ }^{\circ}\text{C}$) under argon atmosphere. Shi epoxidation of *trans-trans* farnesol afforded mixtures of diepoxide (**160**) and triepoxide in approximate 1:1 ratio, so the acetate protective group of **157** was demonstrated to be a deactivating group for the adjacent alkene.

Synthesis of squalene-like **149** via coupling of **150** with **156** (or **151**) was performed by following Kuwajima's protocol⁷⁷ (Scheme 39). Deprotonation of the alcohol **156** by *n*-BuLi in hexane at $-78\text{ }^{\circ}\text{C}$ to lithium alkoxide **163** was followed by addition of THF to promote Brook rearrangement at $-78\text{ }^{\circ}\text{C}$ and delocalize the

Scheme 39. Synthesis of squalene-like substrate **149**.

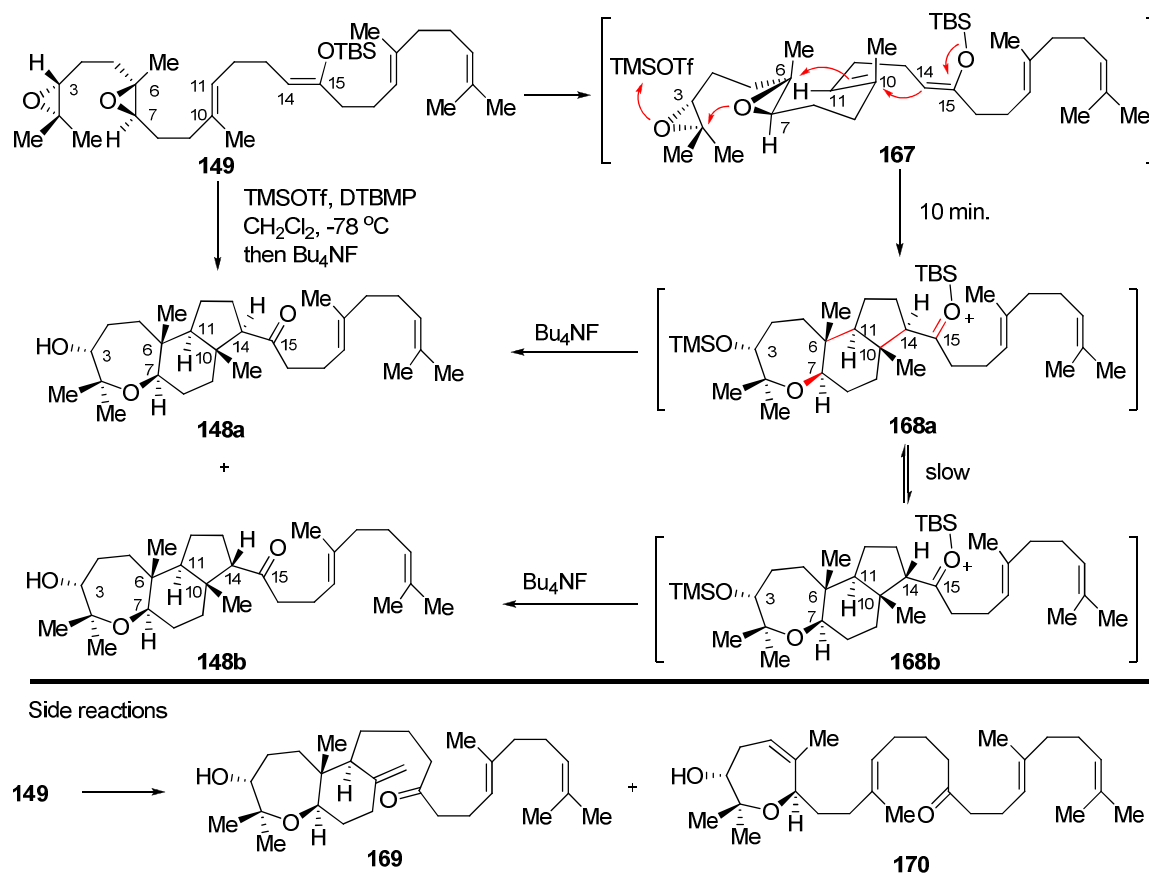


resulting anion **164** to generate chelated homoenolate **151**, which underwent alkylation with diepoxy allylic bromide **150** at $-30\text{ }^{\circ}\text{C}$ to provide the Z-coupled silyl enol ether **149** with squalene-like carbon skeleton. ^1H NMR and ^{13}C NMR analysis of both crude and chromatographed product demonstrated the absence of the isomeric *E*-tetrasubstituted enol ether. The stereoselective formation of **149** may be attributed to a chelated structure **151** analogous to chelated magnesium structures proposed by Kuwajima. Moderate yield of the alkylation may be due to poor electrophilicity of allylic bromide as compared with primary iodide (methyl iodide, alkylation occurred at $-78\text{ }^{\circ}\text{C}$), and therefore resulted in protonation and oxidative homocoupling of intermediate **151** to give side products **165** and **166**, respectively. In order to obtain a reasonable yield, stringent exclusion of oxygen and water from the reaction system was imperative to suppress these side reactions. Notably, compound **149** was also obtained in a one-pot reaction, but in lower yield, by following the Corey's protocol, in which intermediate **151** was generated *in situ* by addition of vinyl lithium to geranyl acylsilane **152** in diethyl ether at $-78\text{ }^{\circ}\text{C}$. The main drawback of this coupling method was that the strong nucleophilicity and basicity of vinyl lithium required the exact measurements of its amount, aging time and temperature for Brook rearrangement. Additionally, shorter shelf-life time of vinyl lithium solution required fresh preparation or titration prior to reaction.

1.3.3. First-stage biomimetic tricyclization

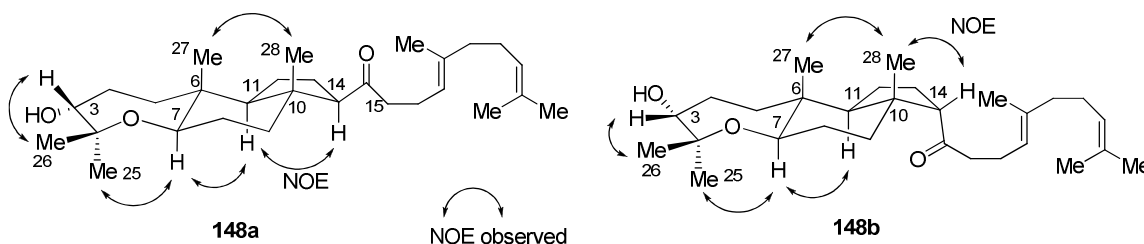
For the first stage of biomimetic tricyclization (Scheme 40), we found that 1.1 equivalents of trimethylsilyl triflate selectively activated the terminal epoxide of **149** and effectively promoted the regio- and stereoselective tandem cyclization to provide *trans-anti-trans*-fused tricyclic ketone **148a** as the major product, consistent with concerted *anti*-parallel addition and an expected chair-like conformation **167**. The best yield of **148a** (50%, single diastereomer) was achieved when the reaction was quenched with 1.1 equivalents of tetrabutylammonium fluoride at $-78\text{ }^{\circ}\text{C}$ within ten minutes of trimethylsilyl triflate

Scheme 40. First stage biomimetic tricyclization of **149**.



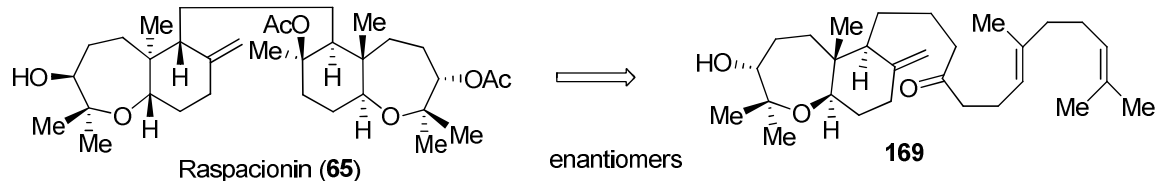
addition, whereas longer reaction times or aqueous quench resulted in the generation of the epimeric product at C14, **148b**, perhaps through silyloxonium ion intermediate **168a** and **168b**. Compound **148a** and **148b** were thoroughly characterized by ^1H NMR, ^{13}C NMR, ^1H - ^1H -COSY and NOESY spectroscopy (figure 10), as well as high resolution mass spectrometry.

Figure 10. NOESY NMR experiments of compounds **148a** and **148b**.



Bicyclic ether **169** and monocyclic ether **170** were also isolated as minor products resulted from partial (truncated) cyclization and *beta*-hydrogen elimination, processes that were well documented in polyalkene carbacyclization. In contrast, no partial cyclization products were isolated or detected in the oxacarbacyclization of diepoxy-en-yn **81**, probably because propargylic silane has a better orbital alignment with alkene than enol silane as well as more electron-richness and less steric hindrance. Interestingly, the cyclic part of the structure in **169** corresponds to the half of raspacionin (A and B rings) (figure 11), while the position of methyl substituents in acyclic part is also consistent with that of the other half of raspacionin, which may arouse interests in exploration of biomimetic synthesis of raspacionin.

Figure 11. Potential biomimetic synthesis of raspacionin from **149**.



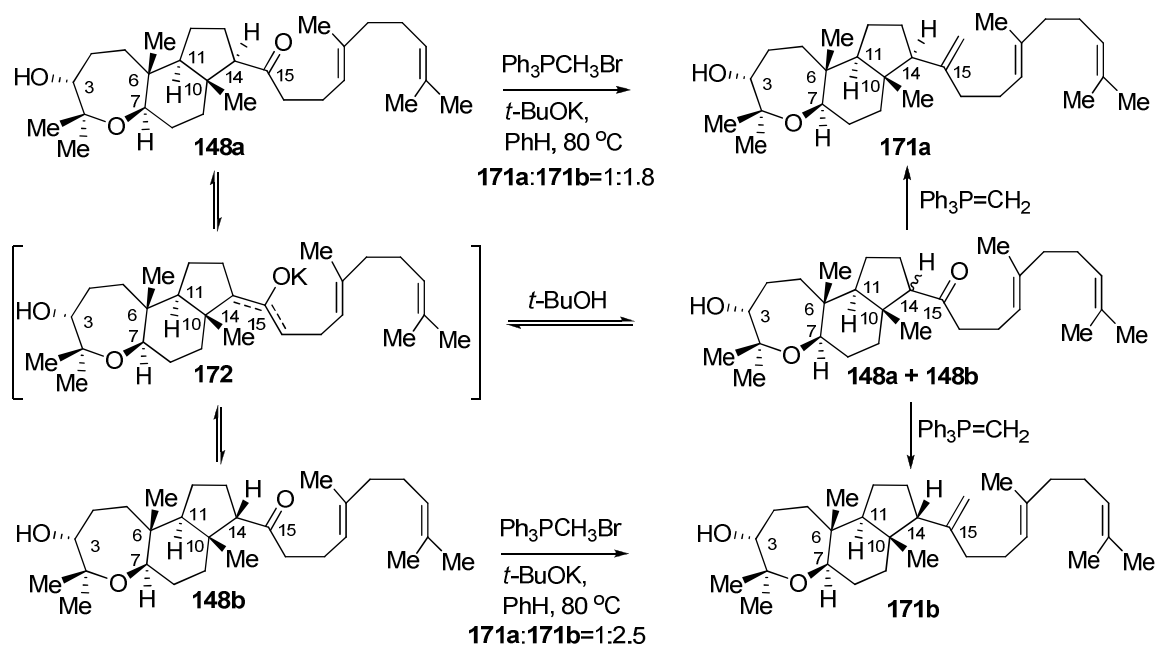
To our surprise, substrate **149** was unreactive with *tert*-butyldimethylsilyl triflate (TBSOTf) under a variety of conditions, in contrast with our previous observations with a simpler enolsilane-diepoxy substrate (Scheme 18). Other Lewis acids, including $\text{BF}_3\text{-Et}_2\text{O}$, AgClO_4 , TBSCl-AgClO_4 ⁷⁹, TBSCl-AgBF_4 ⁷⁹ and MeAlCl_2 ²⁰, resulted in lower yields of products or no reaction. These findings further demonstrated the importance of Lewis acid promoters, as well as nucleophilic terminators, to oxa-carbacyclization mimicking the biological production processes.

1.3.4. Second-stage biomimetic bicyclization

In order to explore the ultimate bicyclization of the hypothetical biogenesis of *ent*-abudinol B (**ent-64**) from the enantiomer of substrate **76** under abiological conditions, the conversion of **148** into **147** required methylenation of the C-15 ketone and double diastereoselective epoxidation of the trisubstituted alkenes of a triene intermediate. Unexpectedly, the olefination of the ketone in **148** presented serious challenges. Methylenation with Tebbe reagent (prepared *in situ* from Cp_2TiCl_2 and Me_3Al)⁸⁰, Petasis reagent (prepared *in situ* from Cp_2TiMe_2)⁸¹ or modified Julia tetrazole sulfone (1-*tert*-butyl-5-methanesulfonyl-1H-tetrazole)^{47c}, gave only trace amounts of desired olefination products **171** and

unidentified decomposition mixtures. After evaluating a variety of reagents for this transformation, we found that the classical Wittig reagent^{20c} prepared *in situ* from a refluxing benzene solution of methyltriphenylphosphine bromide ($\text{Ph}_3\text{PCH}_3\text{Br}$) and potassium *tert*-butoxide ($\text{KO-}t\text{-Bu}$) gave good yields of the disubstituted alkene product, albeit with some epimerization at C14 prior to methylenation (Scheme 41).

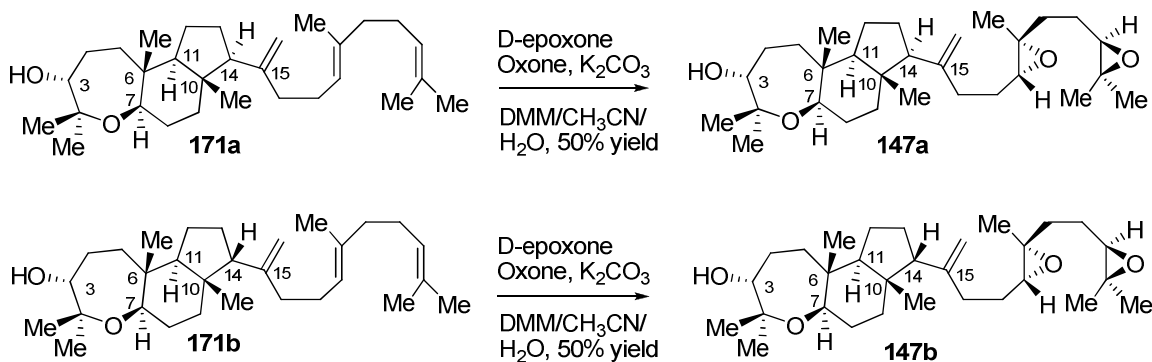
Scheme 41. Olefination of tricyclic ketone **148**.



Mechanistically, the presence of *tert*-butanol caused the dynamic equilibrium between enolate **172** and ketones **148**, while Wittig reagent drove the equilibrium to move past ketone mixtures (**148a** and **148b**) that were irreversibly converted to methylene **171**. Due to the steric hindrance of methyl substituents on C10, olefination of **148a** proceeded much slower to afford **171a** as a minor product. Regio- and enantioselective epoxidations of the two trisubstituted alkenes was then achieved in the presence of the disubstituted alkene by careful control of the

reaction temperature, concentration, amount of D-epoxone[®] and reaction time, to provide **147** (**147a** and **147b**) (scheme 42). To the best of our knowledge, this is the first example of epoxone-catalyzed regioselective epoxidation of trisubstituted alkenes in the presence of a disubstituted alkene.⁴¹

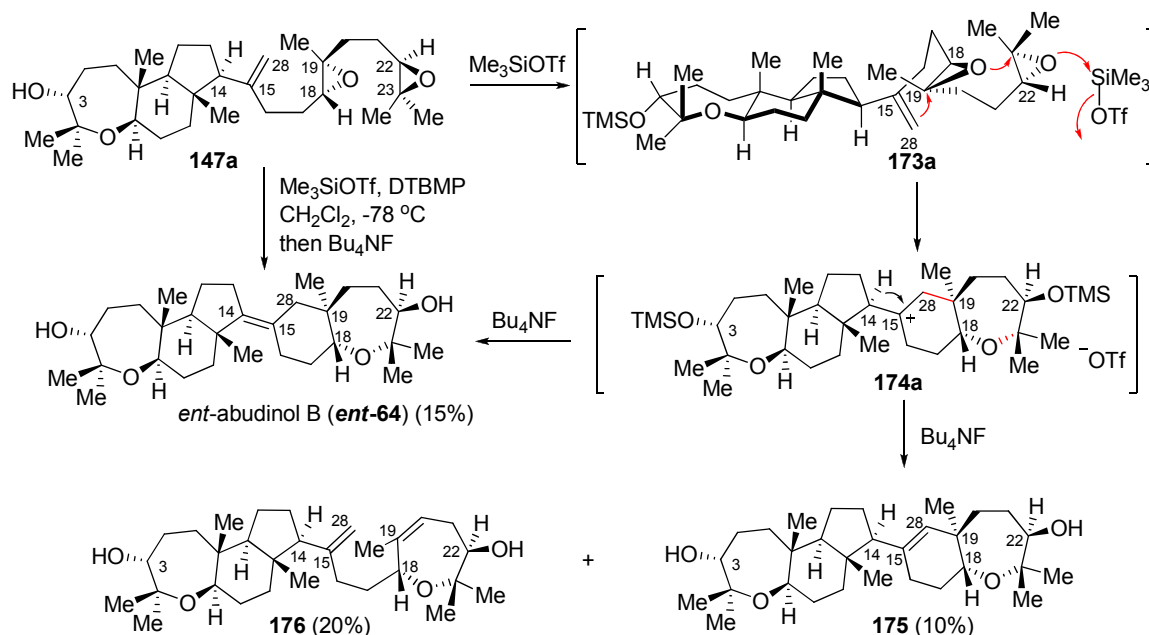
Scheme 42. Double Shi diastereoselective epoxidation of **148**.



A comment on the stereochemistry of **147** is warranted before describing our results on the ultimate bicyclization to abudinol B: although the relative stereochemistry at C14 is consistent with the lower energy conformation for the tandem cyclization process⁸² from **149** to **148a**, we were concerned that the C14 stereochemistry might not be consistent with a concerted cyclization mechanism terminating with cleavage of the C-H sigma bond at C14 resulting from orbital alignment with the C15-alkene, when in a favorable conformation^{82b,c} for cyclization onto the two epoxides. Thus we were pleased to observe that trimethylsilyl triflate-promoted reaction of **147a** did provide *ent*-abudinol B (*ent*-**64**) (scheme 43), albeit in modest yield accompanied by several byproducts including the trisubstituted alkene isomer **175** as well as the partial cyclization structure **176**. The spectroscopic properties of our synthetic product *ent*-**64** matched the reported literature data as well as direct comparison with another sample of *ent*-

64 generated in our first generation synthesis of *ent*-abudinol B, which in turn had been previously confirmed by X-ray diffractometry of the bis-silyl ether of *ent*-abudinol B.

Scheme 43. Bicyclization of **147a** to *ent*-abudinol B (**ent-64**).

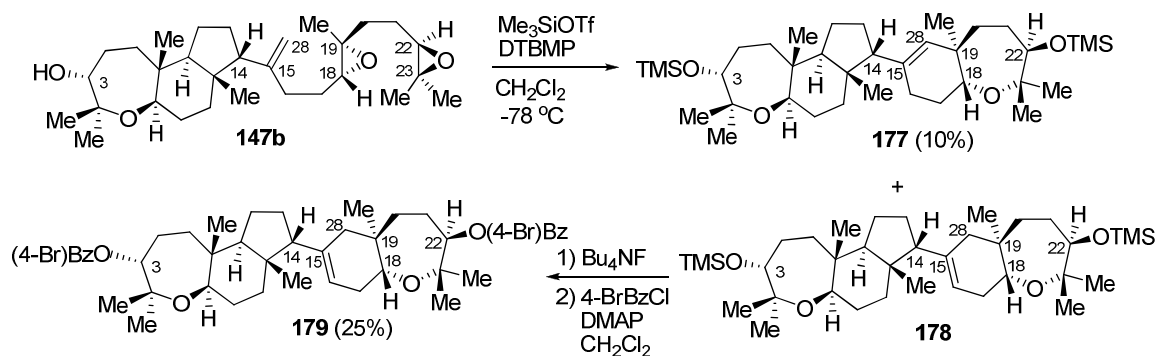


The partial cyclization⁸³ product **176**, resulting from beta-hydrogen elimination^{20c} from C20 after diepoxide cyclization, may arise due to the relatively low nucleophilicity expected for the C15-C28 disubstituted alkene. The mechanism for the tandem bicyclization process to *ent*-**64** and trisubstituted alkene isomer **175** is consistent with the intermediacy¹⁵ of a C15 carbenium ion or ion-pair, perhaps due to the relatively poor nucleophilicity of the 1,1-disubstituted alkene of **148a** which is also consistent with the generation of partial cyclization product **176** as a significant byproduct.

Interestingly, TMSOTf-promoted cascade oxa-carbacyclization of **147b** (with stereochemistry at C-14 corresponding to the initial tricyclization product **148b**)

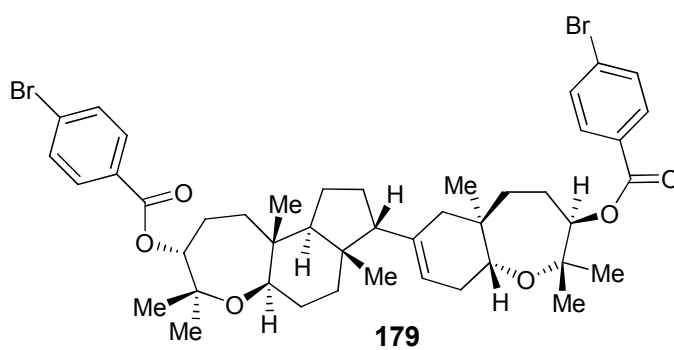
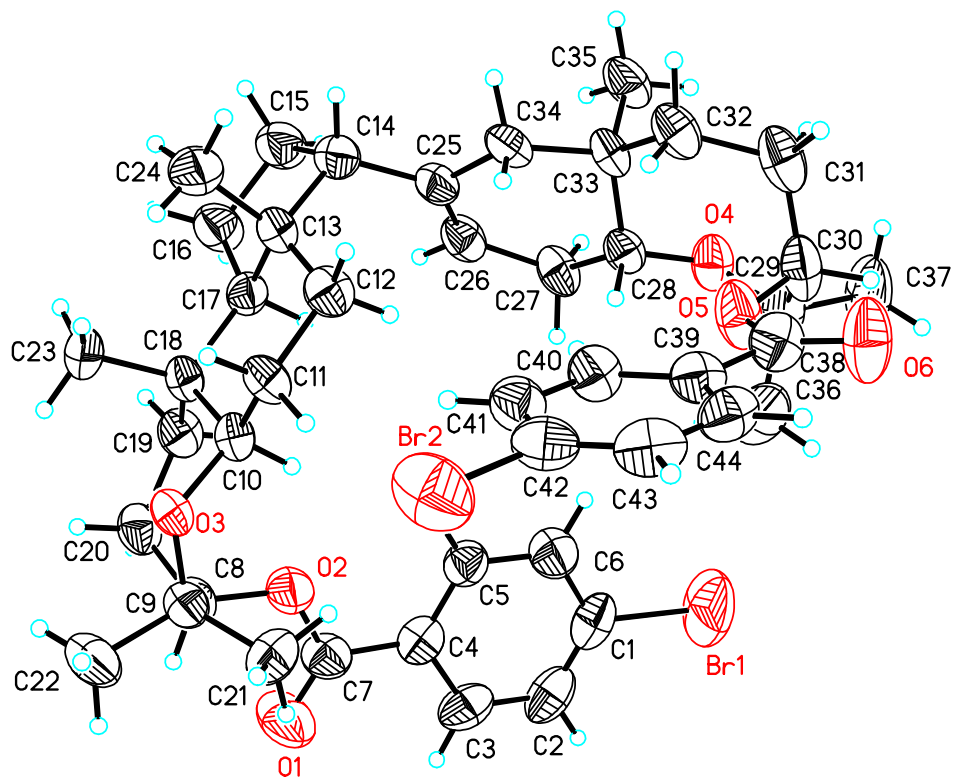
provided a mixture of trisubstituted alkenes **177** and **178** (scheme 44), consistent with bicyclization and *beta*-hydrogen elimination from C-16 and C-28, respectively. Similar carbenium ion intermediate as **174a** was speculated to involve in the cyclization of **147b**, supported by the isolation of the corresponding side products **177** and **178**, analogs of **175**.

Scheme 44. TMSOTf-promoted cyclization of diastereomeric **147b**.



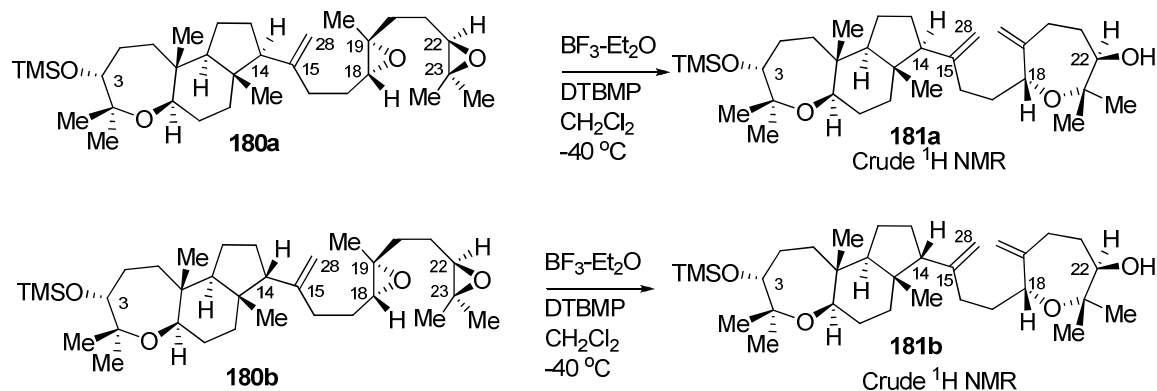
No trace of *ent*-abudinol B (**ent-64**) could be found in the crude product mixture or any of the isolated byproducts from the cyclization of **147b**, nor have we isolated a possible *Z*-tetrasubstituted alkene isomer of abudinol B. It still remains unclear that bicyclization of **147** proceeded in a concerted or stepwise mechanism.¹⁵ But these results have demonstrated the viability of oxabicyclization of diepoxide-alkene with certain Lewis acid promoters. The structure of **179** was unambiguously confirmed by X-ray diffractometry (figure 12), which also clarified the structural assignments for the key precursor compounds **147**, **148**, and **149**, and provided a lead structure for confidently assigning the structures of analogous compounds such as **175** and **177**.

Figure 12. Thermal ellipsoid diagram for pentacyclic product **179**.



In an effort to improve the final bicyclization of **147** by preventing the triflate anion from possible participation in the cyclization, we set out to protect the free alcohol with trimethylsilyl group (TMS) and performed the cyclization with $\text{BF}_3\text{-Et}_2\text{O}$ as the Lewis acid promoter (Scheme 45). However, mixtures of products resulted

Scheme 45. $\text{BF}_3\text{-Et}_2\text{O}$ promoted bicyclization of **180**.



from partial cyclization was found, in both cases, to be predominant, which was confirmed by crude ^1H NMR with four diagnostic resonances between 4.6 ppm and 5.1 ppm (singlet for 1,1-disubstituted alkene). The messy reaction indicated by TLC as well as the limited supply of the substrates **180** precluded further efforts on optimization of the reaction conditions.

In summary, a short and more biomimetic total synthesis of *ent*-abudinol B (*ent*-**64**) has been accomplished in 8 steps from commercially available *trans-trans*-farnesylacetate with 0.18% overall yield, following a synthetic strategy inspired by and closely mimicking the proposed biosynthetic pathway. This synthesis demonstrates the viability of tandem oxa- and carbacyclizations of structurally complex polyepoxide-alkene substrates. More significantly, the cyclization behavior of **147**, which is the enantiomer of a possible advanced biosynthetic

precursor to abudinol B, provides the first chemical evidence for the biosynthesis pathway proposed for abudinol B and other oxepane-containing triterpenoid marine natural products.

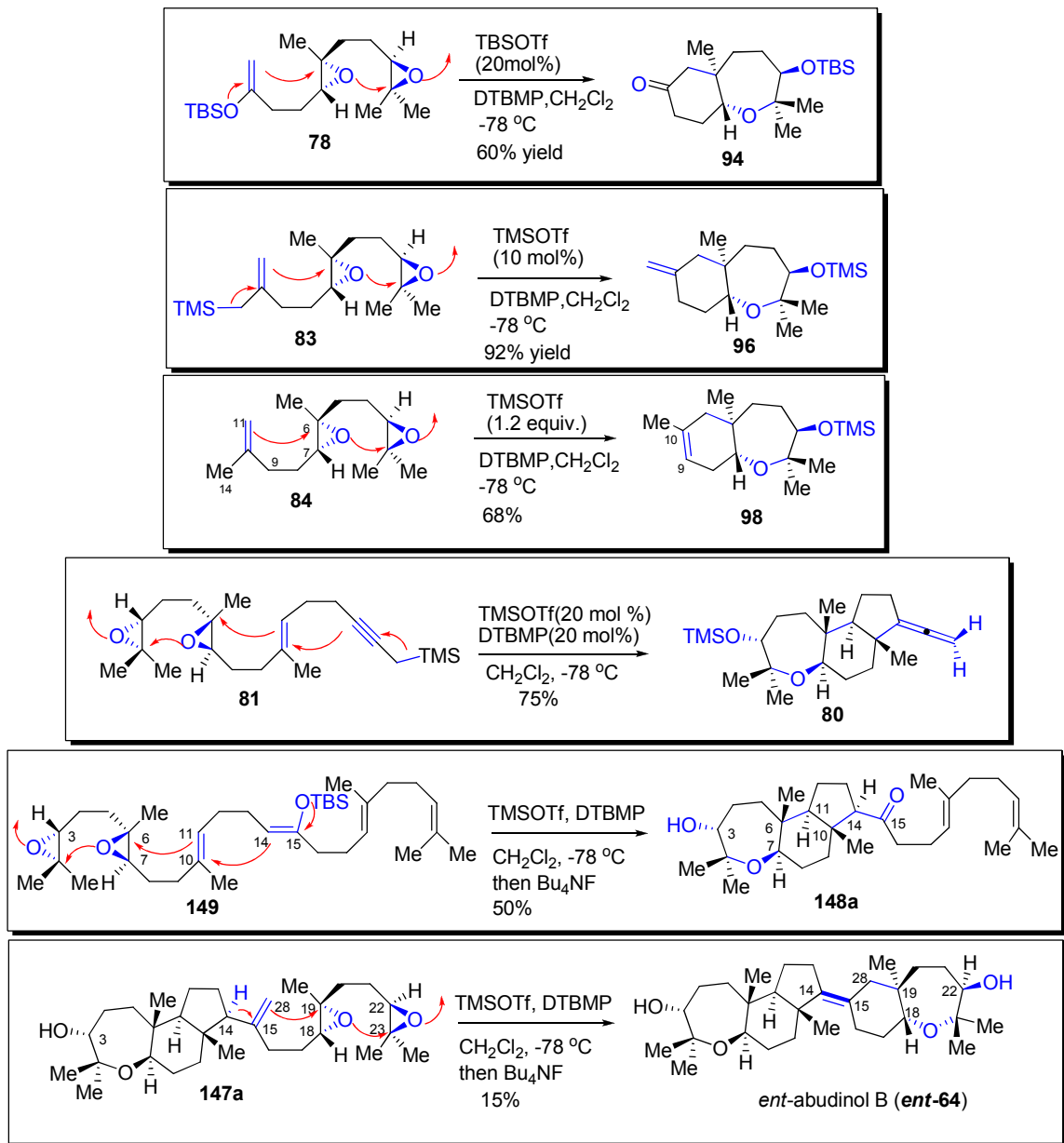
1.4. Conclusions

We have achieved the first biomimetic total synthesis of *ent*-durgamone (**ent-66**), *ent*-nakorone (**ent-67**), and *ent*-abudinol B (**ent-64**) via novel cascade cyclizations of diepoxides tethered to enolsilane and to ene-propargylsilane. Assembly of the tricyclic and bicyclic sectors for synthesis of *ent*-abudinol B was extensively explored to construct the tetrasubstituted alkene with the desired alkene geometry. Our synthesis clarified an ambiguous stereochemical assignment for abudinol B as well as for durgamone and nakorone, and provided valuable insights into the synthesis of the condensed oxepane-cycloalkane sectors of abudinol B. Cascade oxa-carbacyclizations of polyepoxide-alkene have been developed and could be applied to the efficient, potentially biomimetic syntheses of several structurally related terpenoid natural product structures.

A short, more biomimetic total synthesis of *ent*-abudinol B (**ent-64**) has also been accomplished from a squalene-like substrate **149**, following a synthetic strategy inspired by and closely mimicking the proposed biosynthetic pathway. This synthesis demonstrates the viability of tandem oxa- and carbacyclizations of structurally complex polyepoxide-alkene substrates. More significantly, the cyclization behavior of **147**, which is the enantiomer of a possible advanced

biosynthetic precursor to abudinol B, provides the first chemical evidence for the biosynthesis pathway proposed for abudinol B and other oxepane-containing triterpenoid marine natural products.

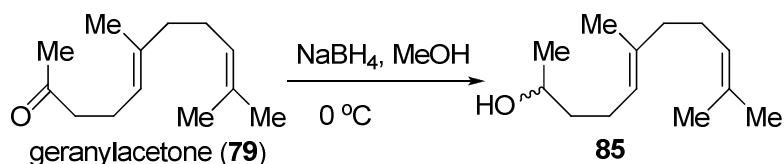
Oxa-carbocyclizations of polyepoxide-alkenes were extensively explored in this thesis, and the results were summarized below.



1.5. Experiments

General: ^1H and ^{13}C NMR spectra were recorded on an Inova-400 spectrometer (400 MHz for ^1H , 100 MHz for ^{13}C), or an Inova-600 spectrometer (600 MHz for ^1H , 150 MHz for ^{13}C). NMR spectra were recorded as solutions in deuterated chloroform (CDCl_3) with residual chloroform (7.27 ppm for ^1H NMR and 77.23 ppm for ^{13}C NMR) taken as the internal standard, and were reported in parts per million (ppm); or as specified in deuterated benzene (C_6D_6) (7.16 ppm for ^1H NMR, 128.2 ppm for ^{13}C NMR). Abbreviations for signal coupling are as follows: s, singlet; d, doublet; t, triplet; q, quartet; m, multiplet. IR spectra were collected on a Mattson Genesis II FT-IR spectrometer, with samples as neat films. Mass spectra (high resolution FAB) were recorded on a VG 70-S Nier Johanson Mass Spectrometer. Optical rotations were recorded at 23°C with a Perkin-Elmer Model 341 polarimeter. Melting point was recorded on FISHER-JOHNS melting point apparatus. Analytical thin layer chromatography (TLC) was performed on precoated glass backed plates purchased from Whatman (silica gel 60 F254; 0.25 mm thickness). Flash column chromatography was carried out with silica gel 60 (230-400 mesh ASTM) from EM Science. All reactions except as mentioned were conducted with anhydrous solvents in oven-dried or flame-dried and argon-charged glassware. All anhydrous solvents were dried over 3Å or 4Å molecular sieves. Trace water content was tested with Coulometric KF Titrator from Denver Instruments. Solvents used in workup, extraction and column chromatography were used as received from commercial suppliers without prior purification. All reagents were purchased from Sigma-Aldrich.

Reduction of geranylacetone (79)⁸⁴

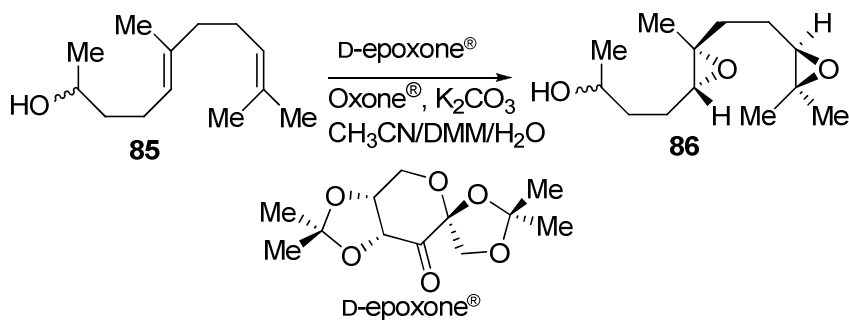


Geranylacetone (**79**, 4.00 g, 21.0 mmol) was dissolved in methanol (40 mL) and cooled to 0 °C. Sodium borohydride (0.78 g, 21 mmol) was added in three batches over 10 min. The reaction mixture was stirred at 0 °C for 30 min, and was then quenched slowly with saturated NH₄Cl (5 mL) at 0 °C, and diluted with Et₂O (60 mL). The organic layer was separated, and the aqueous layer was extracted with Et₂O (2 x 60 mL). The combined organic fractions were washed with brine (60 mL) and dried over anhydrous MgSO₄. Rotary evaporation of solvents gave the racemic secondary alcohol **85**, which was purified by flash column chromatography on silica gel to give pure **85** (3.70 g, 90%).

¹H NMR (600 MHz, CDCl₃) δ 5.12 (t, *J* = 7.2, 6.6 Hz, 1H), 5.06 (t, *J* = 7.2, 6.6 Hz, 1H), 3.78 (m, 1H), 2.05 (m, 4H), 1.96 (t, *J* = 7.8, 7.2 Hz, 2H), 1.65 (s, 3H), 1.60 (s, 3H), 1.57 (s, 3H), 1.47 (m, 2H), 1.37 (m, 1H), 1.17 (d, *J* = 6.6 Hz, 3H);

¹³C NMR (150 MHz, CDCl₃) δ 135.7, 131.5, 124.4, 124.1, 68.0, 39.8, 39.3, 26.8, 25.8, 24.5, 23.6, 17.8, 16.1.

Shi epoxidation of diene 85



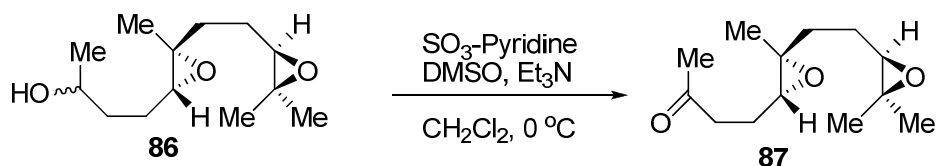
Diene **85** (3.70 g, 18.9 mmol), 1,2:4,5-di-*O*-isopropylidene-*D*-erythro-2,3-hexodiuro-2,6-pyranose (Shi catalyst: D-epoxone[®], 2.40 g, 9.40 mmol), tetrabutylammonium hydrogen sulfate (0.64 g, 1.9 mmol) and NaB₄O₇·10H₂O (0.05 M in aq. Na₂EDTA (4 × 10⁻⁴ M, 370 mL) were suspended with vigorous stirring in dimethoxymethane (DMM) : acetonitrile (AN, 2 : 1, 310 mL) and cooled to 0 °C. In a three-neck 2.0 L flask fitted with two addition funnels, one addition funnel was charged with an aqueous solution of K₂CO₃ (28.7 g, 208 mmol, in 200 mL H₂O), and the second addition funnel was charged with Oxone (32.0 g, 52.0 mmol) dissolved in aqueous Na₂EDTA (4 × 10⁻⁴ M, 200 mL). These solutions were added dropwise and simultaneously over 2 h from the two addition funnels. After the additions were complete, the reaction mixture was stirred for 20 min at 0 °C. The reaction was then diluted with water (200 mL) and Et₂O (300 mL) and transferred to a separatory funnel. The organic layer was collected and the aqueous layer was extracted with Et₂O (3 × 200 mL). The combined organic fractions were washed with brine (150 mL) and dried over anhydrous MgSO₄. Rotary evaporation of solvents gave the crude product **86**, which was purified by

short column on silica gel to give the mixture of alcohol diastereomers of **86** (4.09 g, 95% yield). These compounds were directly used in the next step.

$^1\text{H NMR}$ (600 MHz, CDCl_3) δ 3.83 (m, 1H), 2.75 (m, 1H), 2.67 (m, 1H), 1.80-1.50 (m, 9H), 1.28 (s, 3H), 1.25 (m, 6H), 1.19 (d, $J = 6$ Hz, 3H).

$^{13}\text{C NMR}$ (150 MHz, CDCl_3) δ 67.3, 63.9, 63.4, 60.6, 58.6, 36.0, 35.3, 25.1, 24.9, 24.8, 23.6, 18.7, 16.8.

Parikh-Doering oxidation of alcohol **86**



A 250 mL flame-dried flask with a magnetic stir bar was charged with compound **86** (3.65 g, 16.0 mmol), CH_2Cl_2 (80 mL), dry DMSO (13.0 mL, 190 mmol) and dry Et_3N (10.0 mL, 70.0 mmol). The reaction mixture was then cooled to $0\text{ }^\circ\text{C}$ using a water-ice bath. After stirring for 20 min, sulfur trioxide-pyridine complex (8.84 g, 55.0 mmol) was added in 10 batches over 20 min. The resulting mixture was stirred at $0\text{ }^\circ\text{C}$ for another 3 h before warming to room temperature. The reaction mixture was then diluted with Et_2O (80 mL) and quenched with saturated aq. NaHCO_3 (80 mL). The organic layer was separated, and the aqueous layer was extracted twice with Et_2O (2 x 80 mL). The combined organic fractions were washed with brine (50 mL), dried with anhydrous MgSO_4 and evaporated under reduced pressure (rotary evaporation) to afford the crude product **87**. Column

chromatography on Et₃N (2%) buffered silica gel using eluent of hexane : ethyl acetate (2 : 1) gave a clear oily product **8** (3.44 g, 95% yield, d.r.: 8 : 1 by ¹H NMR).

[α]_D = +24 (c 1.15, CHCl₃).

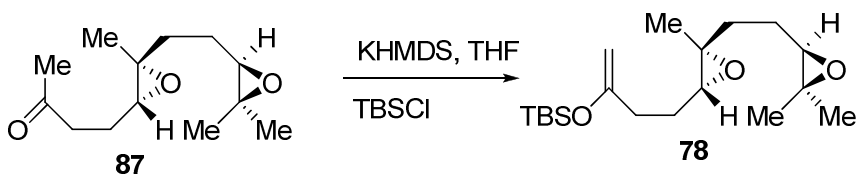
IR (neat, cm⁻¹) 2963, 2929, 1716, 1378, 1165.

¹H NMR (600 MHz, CDCl₃) δ 2.70 (dd, *J* = 7.6, 5.1 Hz, 1H), 2.63 (t, *J* = 6.0 Hz, 1H), 2.60-2.54 (m, 2H), 2.12 (s, 3H), 1.90-1.80 (m, 1H), 1.76-1.46 (m, 5H), 1.25 (s, 3H), 1.23 (s, 3H), 1.21 (s, 3H).

¹³C NMR (150 MHz, CDCl₃) δ 207.8, 63.9, 62.3, 60.9, 58.5, 40.3, 35.3, 30.1, 24.9, 24.6, 22.8, 18.8, 16.8.

HRMS (FAB) Calcd. for C₁₃H₂₃O₃ [(M+H⁺)] 227.1642, found 227.1640.

Kinetic enolization of ketone **87**⁴⁸



A 250 mL dry flask was charged with potassium bis(trimethylsilyl)amide (0.50 M in toluene, 48.0 mL, 24.0 mmol) and *tert*-butyldimethylsilyl chloride (4.90 g, 32.0 mmol) dissolved in THF (80 mL). The solution was cooled to -78 °C, then ketone **87** (3.62 g, 16.0 mmol) dissolved in toluene (50 mL) was added dropwise over 30 minutes. The reaction mixture was stirred for 90 minutes at the same temperature. Et₃N (6 mL) was added to quench the reaction, followed by addition

of saturated NaHCO₃ (50 mL). The reaction mixture was allowed to warm to room temperature and stirred for another 20 minutes. The organic layer was separated from the aqueous layer which was extracted with Et₂O (2 x 50 mL). The combined organic fractions were then washed with brine (50 mL), dried with anhydrous MgSO₄ and evaporated under reduced pressure (rotavap). Flash column chromatography on silica gel buffered with Et₃N (2%) using eluent of hexanes : ethyl acetate (10 : 1) gave silyl enol ether **78** (4.73 g, 87% yield).

[α]_D = +10 (c 0.29, CHCl₃).

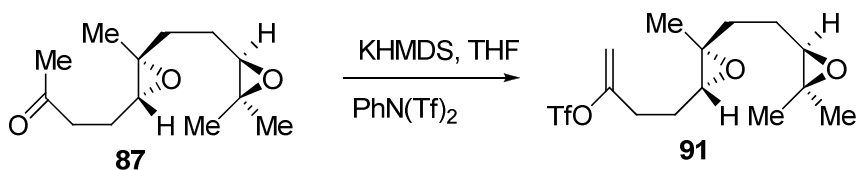
IR (neat, cm⁻¹) 2958, 2930, 2858, 1256, 839.

¹H NMR (400 MHz, CDCl₃) δ 4.01 (dd, *J* = 10.8, 0.6 Hz, 2H), 2.73 (t, *J* = 6.4 Hz, 1H), 2.67 (t, *J* = 6.4 Hz, 1H), 2.16-2.09 (m, 2H), 1.76-1.50 (m, 6H), 1.26 (s, 3H), 1.24 (s, 3H), 1.22 (s, 3H), 0.88 (s, 9H), 0.12 (s, 6H).

¹³C NMR (100 MHz, CDCl₃) δ 158.4, 90.4, 64.1, 63.2, 62.7, 60.5, 58.5, 35.4, 33.6, 26.3, 25.8, 25.0, 24.8(3), 18.8, 16.8, -4.6, -4.5.

HRMS (FAB) Calcd for C₁₉H₃₇O₃Si [(M+H⁺)] 341.2507, found 341.2504.

Trapping kinetic enolate of ketone **87** with Comins reagent⁴⁸



A 25 mL dry flask was charged with potassium bis(trimethylsilyl)amide (0.50 M in toluene, 4.8 mL, 2.4 mmol), then cooled to -78 °C. A THF (2 mL) solution of

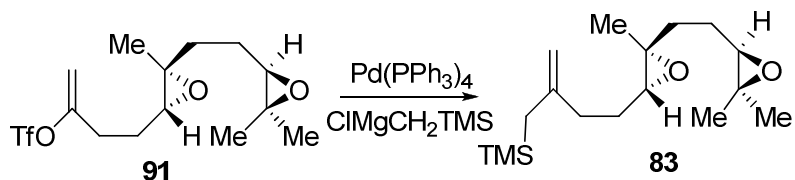
ketone **87** (0.36 g, 1.6 mmol) was added dropwise over 30 minutes to the cooled solution. After the addition was complete, the reaction mixture was stirred for 90 minutes at $-78\text{ }^{\circ}\text{C}$. Then, *N*-phenylbistrifluoromethanesulfonimide (PhNTf₂, comins' reagent, 1.15 g, 3.2 mmol) dissolved in THF (2 mL) was added dropwise over 15 minutes. The reaction mixture was stirred for another 1.5 hours at $-78\text{ }^{\circ}\text{C}$. Saturated NaHCO₃ (10 mL) was added at $-78\text{ }^{\circ}\text{C}$ to quench the reaction. The reaction mixture was allowed to warm to room temperature and stirred for another 20 minutes. The organic layer was separated from the aqueous layer which was extracted with Et₂O (2 x 10 mL). The combined organic fractions were then washed with brine (20 mL), dried with anhydrous MgSO₄ and evaporated under reduced pressure (rotavap). Flash column chromatography on silica gel using eluent of hexanes : ethyl acetate (10 : 1) gave silyl enol ether **91** (0.40 g, 70% yield).

IR (neat, cm⁻¹): 2966, 2930, 1671, 1416, 1212, 1141, 935, 898.

¹H NMR (400 MHz, CDCl₃) δ 5.15, (d, $J=3.2$ Hz, 1H), 5.03 (m, 1H), 2.77 (dd, $J = 7.6, 5.2$ Hz, 1H), 2.69 (m, 1H), 2.61-2.45 (m, 2H), 1.90-1.50 (m, 6H), 1.30 (s, 3H), 1.29 (s, 3H), 1.26 (s, 3H).

¹³C NMR (100 MHz, CDCl₃) δ 155.8, 118.7, 105.3, 63.9, 62.2, 61.6, 58.7, 35.2, 31.3, 25.7, 25.0, 24.7, 18.8, 16.9.

Nigishi Cross-coupling of **91** with Grignard reagent⁴⁸



To a dry 15 mL round bottom flask was charged with THF (1 mL) solution of enol triflate **91** (0.36 g, 1.06 mmol), then cooled to 0 °C. Tetrakis(triphenylphosphine) palladium (0.12 g, 0.11 mmol) was added to the cooled solution with stirring under argon atmosphere, resulting in a bright orange solution, to which was added (trimethylsilylmethyl)magnesium chloride (1.0 M in Et₂O, 1.2 mL, 1.2 mmol) at 0 °C. The reaction mixture was allowed to warm to room temperature slowly, while a precipitate was observed upon warming. After 30 minutes, saturated NH₄Cl (10 mL) was added to quench the reaction and the resulting mixture was transferred to a separatory funnel. Organic layer was collected and aqueous layer was extracted with Et₂O (10 mL). The organic fractions were combined and washed with brine (10 mL), dried with anhydrous Na₂SO₄ and evaporated under reduced pressure. Column chromatography on silica gel using eluent of EtOAc in hexane (5% to 20%) afforded allylic silane **76** (0.27 g, 0.9 mmol, 85%) as clear oil.

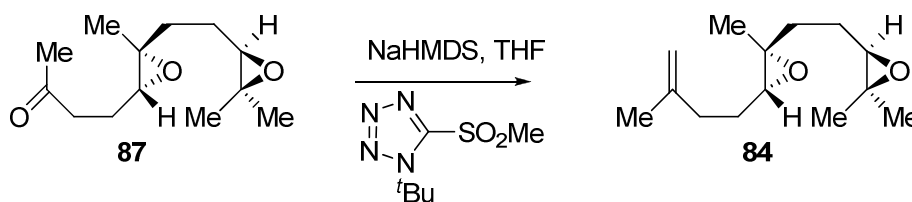
IR (neat, cm⁻¹) 3073, 2958, 2927, 1633, 1460, 1378, 1248, 855.

¹H NMR (400 MHz, CDCl₃) δ 4.62 (s, 1H), 4.55 (s, 1H), 2.75 (t, *J*=6.4 Hz, 1H), 2.71 (t, *J*=6.4 Hz, 1H), 2.18-2.09 (m, 2H), 1.81-1.50 (m, 6H), 1.31 (s, 3H), 1.28 (s, 3H), 1.26 (s, 3H), 0.02 (s, 9H).

^{13}C NMR (100 MHz, CDCl_3) δ 146.7, 107.6, 64.0, 63.1, 60.5, 58.6, 35.4, 35.1, 27.0, 25.0, 24.8, 18.8, 16.9, -1.15.

HRMS (FAB) Calcd for $\text{C}_{17}\text{H}_{32}\text{O}_2\text{Si}$ [$(\text{M}+\text{H}^+)$] 297.2244, found 297.2241.

Methylenation of ketone 87



1-tert-butyl-5-methanesulfonyl-1H-tetrazole was first synthesized by following the literature procedure^{47c} as follows: On refluxing water (27 mL) solution of NaN_3 (5.6 g, 82 mmol) was added *t*-Bu-NCS (10 g, 87 mmol) dissolved in *i*-PrOH (21 mL) over 30 minutes. After addition was complete, the mixture was refluxed for 16 h, then cooled down with an ice bath. Concentrated HCl (13 mL) was added carefully to the cooled mixture. Evaporated half of the water and stored at 0°C overnight, resulting in yellow solid that was filtered and washed with ice-cooled water, then dried under high vacuum for 48h. The pale yellow powder obtained above was diluted with 120 mL THF and added dropwise to a suspension of sodium hydride (NaH, 60%, 3.2 g, 82 mmol) in THF (40 mL) at 0°C. After 10 minutes stirring at 0°C, methyl iodide (MeI, 5.3 mL, 115 mmol.) was added via syringe. The mixture was allowed to warm up to room temperature and stirred overnight. Sat. NH_4Cl (60 mL) was added to the reaction mixture and diluted with CH_2Cl_2 (60 mL). The organic layer was then washed with brine, dried with MgSO_4 and evaporated. The crude solid thus obtained was diluted in EtOH (290

mL) at 0 °C, then $\text{Mo}_7\text{O}_{24}(\text{NH}_4)_6$ (6.34 g, 0.0845 equiv.) dissolved in H_2O_2 (30% in water, 63 mL) was added to the reaction mixture. After 4 hours, EtOH was evaporated almost completely. The mixture was then dissolved in CH_2Cl_2 and water. The organic layer was collected and washed with brine, dried with Na_2SO_4 , filtered and evaporated to dryness to give 1-*tert*-butyl-5-methanesulfonyl-1H-tetrazole (11.24 g).

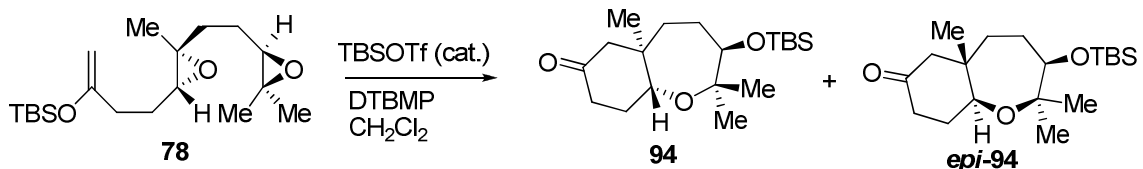
Julia olefination of ketone 87 with tetrazole: A 25 mL dry flask was charged with a THF (2 mL) solution of ketone **87** (0.36 g, 1.6 mmol) and 1-*tert*-butyl-5-methanesulfonyl-1H-tetrazole (0.38 g, 1.9 mmol) obtained above, then cooled to -78 °C. Sodium bis(trimethylsilyl)amide (1.0 M in THF, 2.1 mL, 2.1 mmol), was added dropwise over 30 minutes to the cooled solution. After the addition was complete, the reaction mixture was stirred for 60 minutes at -78 °C and allowed to warm slowly up to room temperature and stirred overnight. The reaction was quenched by adding a phosphate buffer solution (pH=7.0). Organic layer was collected and aqueous layer was extracted with Et_2O (10 mL). The organic fractions were combined and washed with brine (10 mL), dried with anhydrous Na_2SO_4 and evaporated under reduced pressure. Column chromatography on silica gel using eluent of EtOAc in hexane (5% to 20%) afforded diepoxy alkene **84** (0.32 g, 1.44 mmol, 90%) as a clear oil.

IR (neat, cm^{-1}) 3073, 2964, 2927, 1648, 1454, 1378, 1338, 1164, 887.

^1H NMR (400 MHz, CDCl_3) δ 4.73 (s, 1H), 4.70 (s, 1H), 2.74 (t, $J=6.0$ Hz, 1H), 2.70 (t, $J=6.4$ Hz, 1H), 2.22-2.09 (m, 2H), 1.81-1.50 (m, 6H), 1.73 (s, 3H), 1.29 (s, 3H), 1.27 (s, 3H), 1.25 (s, 3H).

^{13}C NMR (100 MHz, CDCl_3) δ 144.9, 110.6, 64.0, 63.0, 60.5, 58.6, 35.4, 34.6, 27.0, 25.0, 24.7, 22.6, 18.8, 16.8.

Cascade oxa-carbocyclization of diepoxy enolsilane **78**



General procedure A: A 500 mL flame-dried flask was charged with magnetic stir bar, diepoxy-enol silane **78** (1.70 g, 5.00 mmol), dry CH_2Cl_2 (200 mL) and di-2,6-*t*-butyl-4-methylpyridine (DTBMP, 0.21 g, 1.0 mmol) and cooled to $-78\text{ }^\circ\text{C}$. *tert*-Butyldimethylsilyl trifluoromethanesulfonate (TBSOTf) (0.23 mL, 1.0 mmol) was added dropwise via syringe under argon atmosphere. (The use of DTBMP with TBSOTf is essential for reproducibility of cyclization yields.) The reaction mixture was stirred at $-78\text{ }^\circ\text{C}$ for 2 hours. After the reaction was complete, Et_3N (1 mL) then was added at $-78\text{ }^\circ\text{C}$ and was stirred for another 15 minutes. Aqueous saturated NaHCO_3 (50 mL) was added to the reaction mixture at $-78\text{ }^\circ\text{C}$ and warmed to room temperature. The dichloromethane layer was separated and the aqueous layer was extracted with dichloromethane (2 x 50 mL). The combined dichloromethane fractions were washed with brine (80 mL), dried with anhydrous MgSO_4 and evaporated. Flash column chromatography on silica gel using eluent of EtOAc in hexane (5% to 10%) gave cyclization product **94** (1.02 g, 60% yield) as a white solid and *epi-94* (0.13 g, 7.5%).

Data for compound 94

m.p. = 113°C -115 °C. $[\alpha]_D = -2.2$ (c 0.32, CHCl₃).

IR (neat, cm⁻¹) 2948, 2895, 2858, 1720, 1462, 1251, 1086.

¹H NMR (400 MHz, CDCl₃) δ 3.66 (dd, $J = 11.2, 5.2$ Hz, 1H), 3.55 (d, $J = 9.6$ Hz, 1H), 2.30 (m, 1H), 2.21 (m, 1H), 2.10 (d, $J = 6.4$ Hz, 2H), 2.01-1.94 (m, 1H), 1.87-1.67 (m, 2H), 1.43 (m, 1H), 1.28 (m, 2H), 1.19 (s, 3H), 1.05 (s, 3H), 0.85 (s, 3H), 0.82 (s, 9H), 0.00 (s, 6H).

¹³C NMR (100 MHz, CDCl₃) δ 210.2, 80.4, 77.8, 72.6, 53.7, 43.3, 41.2, 39.7, 30.4, 29.7, 25.9, 24.7(3), 22.7, 18.0, 17.9, -3.9, -4.7.

HRMS (FAB) Calcd. for C₁₉H₃₇O₃Si [(M+H⁺)] 341.2507, found 341.2497.

Data for compound epi-94

IR (neat, cm⁻¹) 2950, 2887, 2857, 1721, 1464, 1250, 1090, 836.

¹H NMR (600 MHz, CDCl₃) δ 4.07 (dd, $J = 12.0, 5.4$ Hz, 1H), 3.72 (d, $J = 7.2$ Hz, 1H), 2.30 (ddd, $J = 14.4, 13.8, 6.6$ Hz, 1H), 2.21 (m, 1H), 2.15 (d, $J = 13.2$ Hz, 1H), 2.07 (dd, $J = 13.8, 2.4$ Hz, 1H), 1.92 (m, 2H), 1.88-1.80 (m, 1H), 1.74-1.66 (m, 1H), 1.62-1.54 (m, 1H), 1.19 (s, 3H), 1.09 (s, 3H), 0.94 (s, 9H), 0.88 (s, 3H), 0.032 (s, 3H), 0.017 (s, 3H).

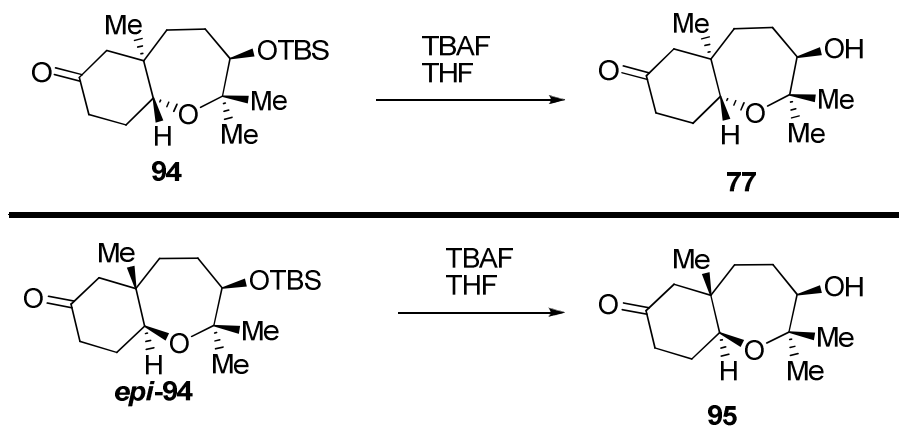
¹³C NMR (100 MHz, CDCl₃) δ 210.8, 789, 77.3, 73.1, 54.0, 41.8, 39.7, 36.1, 30.3, 29.0, 26.2, 26.0, 22.7, 18.4, 17.8, -4.3, -5.2.

Procedure B: The following conditions are generally utilized in our laboratory for the *endo*-selective tandem oxacyclization of polyepoxides. Specifically, the diepoxy enolsilane **78** (0.22 g, 0.65 mmol) was dissolved in dry CH₂Cl₂ (11 mL) with magnetic stirring under argon atmosphere. The solution was cooled to -40

°C, and freshly distilled BF₃-OEt₂ (0.1925 M in CH₂Cl₂, 3.4 mL, 0.65 mmol) was added dropwise over 10 minutes. After 30 minutes at -40 °C, the reaction mixture was quenched with saturated NaHCO₃ (5 mL), and followed by workup as described in procedure A. The crude ¹H NMR indicated the presence of **94** and desilylated product **77** (**94** : **77**= 1 : 1, 40% combined yield).

Procedure C: A 25 mL flame-dried flask was charged with magnetic stir bar, diepoxy enolsilane **78** (0.22 g, 0.65 mmol), dry CH₂Cl₂ (11.0 mL). The solution was cooled to -78 °C with stirring. Methylaluminum dichloride (1.00 M in hexanes, 0.66 mL, 0.66 mmol) was added dropwise via syringe under argon atmosphere. The reaction mixture was stirred for 1.5 hours at -78 °C, and monitored by TLC. When the reaction was complete, 1.0 N HCl (aqueous) was added at -78 °C, and the reaction mixture was warmed to room temperature and stirred for another 15 minutes. The reaction mixture was worked up as described in procedure A. The crude ¹H NMR indicated the presence of **94** and **77** favoring **94** (**94** : **77**= 4 : 1 , 60% combined yield).

Desilylation of bicyclic ketones **94** and *epi-94* and their X-ray crystal structures



Desilylation of **94:** Tetrabutylammonium fluoride (TBAF) (1.00 M in THF, 1.2 mL, 1.2 mmol) was added to the THF (50 mL) solution of bicyclic ketone **94** (0.23 g, 0.68 mmol). The reaction mixture was stirred at room temperature for 12 hours. Et₂O (30 mL) was then added to dilute the reaction, followed by addition of sat. NH₄Cl (25 mL). Organic layer was separated and the aqueous layer was extracted with Et₂O (2 x 30 mL). The organic fractions were washed with brine (50 mL), dried over MgSO₄ and evaporated. Column chromatography on silica gel afforded the product **77** (0.15 g, 99% yield) as a white crystal solid.

Exact same procedure as desilylation of **94** was executed for *epi-94* to afford **77** in 99% yield as white crystal.

Data for compound **77**

m.p. = 96°C -98 °C. $[\alpha]_D = -24$ ($c = 0.115$, CHCl₃).

IR(neat, cm⁻¹) 3463, 2972, 2942, 1704, 1078.

^1H NMR (400 MHz, CDCl_3) δ 4.06 (dd, $J = 11.6, 5.2$ Hz, 1H), 3.81 (d, $J = 7.6$ Hz, 1H), 2.42-1.67 (m, 10H), 1.29 (s, 3H), 1.13 (s, 3H), 0.90 (s, 3H).

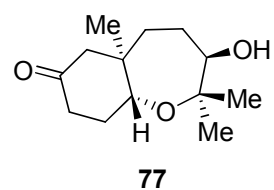
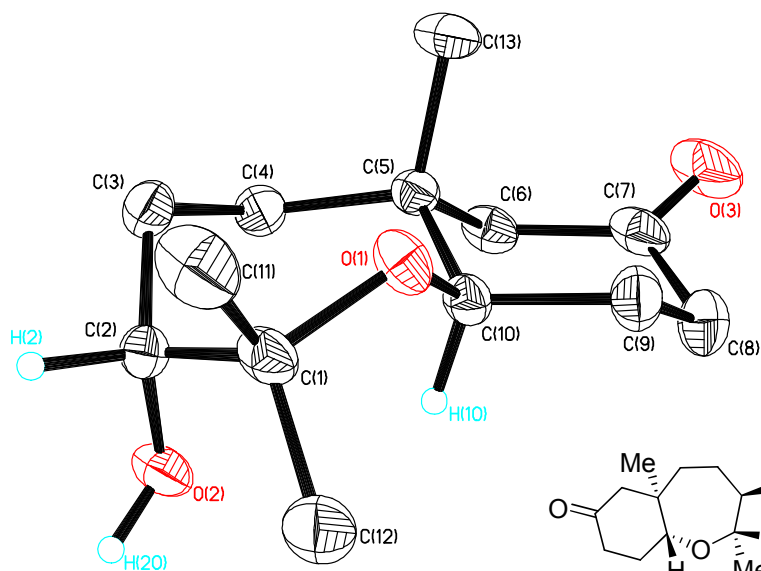
^{13}C NMR (100MHz, CDCl_3) δ 211.0, 78.2, 76.8, 73.3, 53.8, 41.9, 39.6, 35.9, 30.4, 29.2, 25.7, 21.6, 17.8.

HRMS (FAB) Calcd. for $\text{C}_{13}\text{H}_{23}\text{O}_3$ [$\text{M}+\text{H}^+$] 227.1642, found 227.1640.

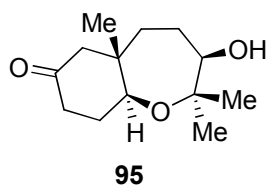
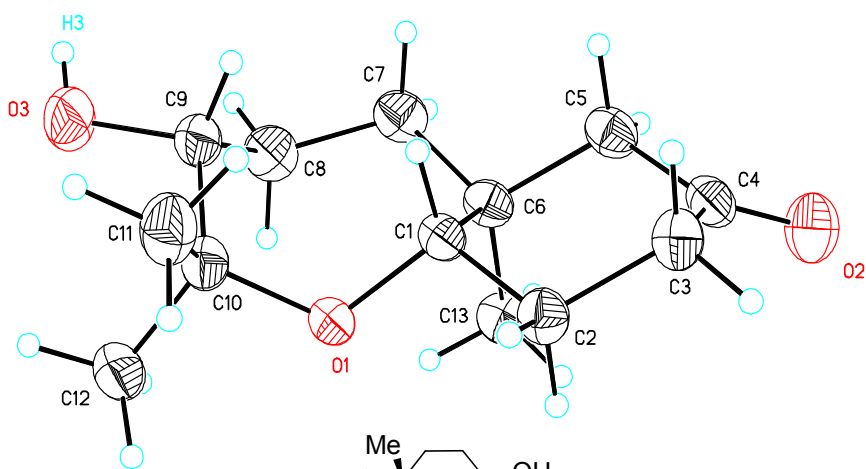
Data for compound 95

^1H NMR (400 MHz, C_6D_6) δ 3.16 (d, $J = 10.4$ Hz, 1H), 3.10 (dd, $J = 11.2, 5.0$ Hz, 1H), 2.01 (m, 1H), 1.95 (dd, $J=13.6, 2.8$ Hz, 1H), 1.84-1.68 (m, 2H), 1.66-1.54 (m, 2H), 1.47 (m, 1H), 1.13 (s, 3H), 1.08 (s, 3H), 1.16-0.94 (m, 2H), 0.77 (s, 3H).

X-Ray analysis: The structure of compounds **77**^{2b} and **95** was established by X-ray analysis. The thermal ellipsoid diagrams and data for compound **77** and **95** are provided below:



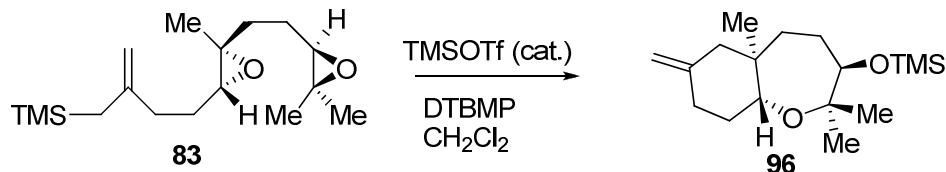
77



95

For the X-ray data of compound 77, see page 163-169; for the X-ray data of compound 95, see page 170-177.

Oxa-carbocyclization of diepoxy allylsilane 83



Following the general procedure A for oxa-carbocyclization of diepoxy enolsilane **78**, diepoxy allyl silane **83** (30 mg, 0.1 mmol) underwent TMSOTf (5.0 mg, 0.02 mmol) promoted oxacyclization in the presence of DTBMP (21 mg, 0.1 mmol) in CH₂Cl₂ (5 mL) at -78 °C to yield **96** (27 mg, 90%).

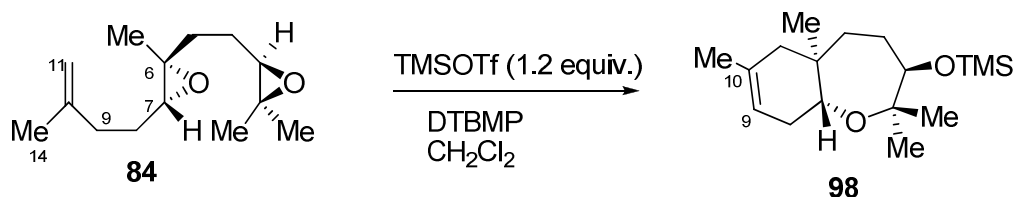
IR(neat, cm⁻¹) 3071, 2973, 2940, 2871, 1654, 1443, 1375, 1250, 1094, 1074, 862, 838.

¹H NMR (400 MHz, CDCl₃) δ 4.66 (s, 1H), 4.56 (s, 1H), 3.72 (d, *J*=7.2 Hz, 1H), 3.69 (dd, *J* = 12.0, 4.8 Hz, 1H), 2.21 (m, 1H), 2.00 (m, 1H), 1.95 (d, *J*=12.8 Hz, 2H), 1.90-1.72 (m, 2H), 1.57 (m, 2H), 1.37 (m, 1H), 1.16 (s, 3H), 1.11 (s, 3H), 1.03 (m, 1H), 0.82 (s, 3H), 0.11 (s, 9H).

¹³C NMR (100MHz, CDCl₃) δ 146.4, 108.8, 78.3, 77.7, 74.5, 48.7, 39.6, 36.5, 33.7, 31.6, 29.3, 26.6, 22.6, 17.3, 0.18.

HRMS (FAB) Calcd. for C₁₇H₃₃O₂Si₁ [(M+H⁺)] 297.2244, found 297.2238.

Oxa-carbocyclization of diepoxy alkene **84**



Following the general procedure A for oxa-carbocyclization of diepoxy enolsilane **78**, diepoxy alkene **84** (60 mg, 0.27 mmol) underwent TMSOTf (71 mg, 0.32 mmol) initiated oxacyclization in the presence of DTBMP (109 mg, 0.54 mmol) in CH₂Cl₂ (5 mL) at -78 °C to yield of **98** (51 mg, 65%).

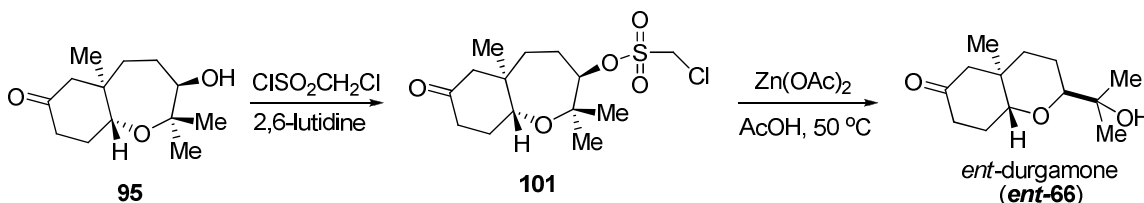
IR (neat, cm⁻¹): 2962, 2942, 1440, 1375, 1250, 1078, 837.

¹H NMR (400 MHz, CDCl₃) δ 5.04 (s, 1H), 3.76 (dd, *J*=12.4, 4.4 Hz, 1H), 3.73 (d, *J* = 7.2 Hz, 1H), 2.12-1.86 (m, 4H), 1.80-1.50 (m, 4H), 1.62 (s, 3H), 1.17 (s, 3H), 1.14 (s, 3H), 0.93 (s, 3H), 0.09 (s, 9H).

¹³C NMR (100 MHz, CDCl₃) δ 132.2, 130.3, 78.7, 77.8, 73.9, 39.3, 34.6, 30.7, 29.1, 27.5, 26.6, 23.5, 23.4, 19.8, 0.19.

HRMS (FAB) Calcd. for C₁₇H₃₃O₂Si₁ [(M+H⁺)] 297.2244, found 297.2252.

Ring-contraction of bicyclic alcohol **95** to furnish *ent*-durgamone (*ent*-**66**)

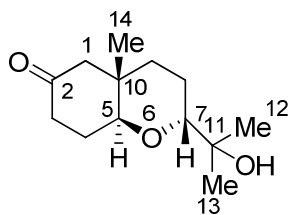


Bicyclic ketone **95** (60.0 mg, 0.27 mmol) was dissolved in dry CH_2Cl_2 (1.0 mL). 2,6-lutidine (0.12 mL, 1.06 mmol) was added to the solution and cooled to $0\text{ }^\circ\text{C}$ with ice-water bath. Chloromethanesulfonyl chloride (0.08 mL, 0.53 mmol) was added to the cooled solution. The reaction mixture was then allowed to warm to room temperature and continued stirring for 3 hours. The reaction mixture was diluted with ethyl acetate (5 mL) and washed with water (5 mL). The crude chloromethylsulfonate product (**101**) obtained after evaporation of organic solvents was dissolved in a mixture of acetic acid (3 mL) and water (3 mL). Zinc acetate (200 mg, 0.88 mmol, 1.30 mmol) was added and the resulting mixture was heated to $50\text{ }^\circ\text{C}$ for 3-4 hours. After the reaction was complete, Et_2O (5 mL) was added to dilute the reaction, which was then transferred to a separatory funnel. The organic layer was collected, and the aqueous layer was extracted with Et_2O (3 x 5 mL). The combined organic fractions were dried with anhydrous MgSO_4 and evaporated under reduced pressure. Flash column chromatography on silica gel (hexane: AcOEt = 1: 1) gave *ent*-durgamone (*ent*-**66**) (30.0 mg, 50% yield) as well as small amounts of starting material and acylated product.

Comparison of our synthetic *ent*-**66** with the published spectral data^{35a} showed mostly the expected similarities between our compound and the natural product,

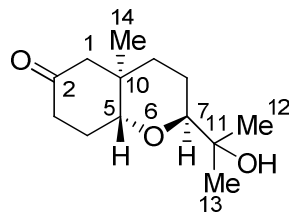
although the difference in magnitude of optical rotation is noted. Direct comparison is complicated by the absence of proton NMR data reported in ref 35a for methylene and methine hydrogens.

natural product **66** (ref. 35a)



durgamone (**66**)

our synthetic material (*ent*-**66**, this work)



ent-durgamone (*ent*-**66**)

$[\alpha]_D$ -28.5 (*c* 0.1, MeOH)

+14 (*c* 0.13, MeOH)

IR (neat, cm^{-1}):

O-H stretch not reported

3472

2972 (C-H stretches)

2947

2342

corresponding band not observed

1707 (C=O stretch)

1704

1459 (C-H methyl bend)

1382 (C-H methyl bend)

1095 (C-O stretch)

^1H NMR (C_6D_6 , δ):

H-7 3.74 (dd, $J = 11.5, 4.5$ Hz, 1H)

3.74 (dd, $J = 11.2, 4.8$ Hz, 1H)

H-5 3.27 (t, $J = 5.5$ Hz, 1H)

3.25 (t, $J = 5.6$ Hz, 1H)

CH or CH_2 not reported

2.10 (dt, $J = 14.8, 4.8, 2.4$ Hz, 1H)

not reported

1.98 (dd, $J = 13.8, 2.6$ Hz, 1H)

	<i>not reported</i>	1.78-1.65 (m, 2H)
	<i>not reported</i>	1.61-1.29 (m, 6H)
H-13	1.13 (s, 3H)	1.12 (s, 3H)
H-12	0.90 (s, 3H)	0.88 (s, 3H)
H-14	0.77 (s, 3H)	0.75 (s, 3H)

¹³C NMR (C₆D₆, δ): (100 MHz, C₆D₆, δ):

C-2	210.5	207.7
C-7	78.6	78.7
C-11	74.9	74.9
C-5	73.9	74.1
C-1	53.4	53.6
C-3	39.3	39.6
C-10	35.7	35.9
C-8	35.1	35.6
C-4	27.3	27.9, 27.7
C-13	26.9	27.5
C-9	19.3	19.7
C-14	18.4	18.6

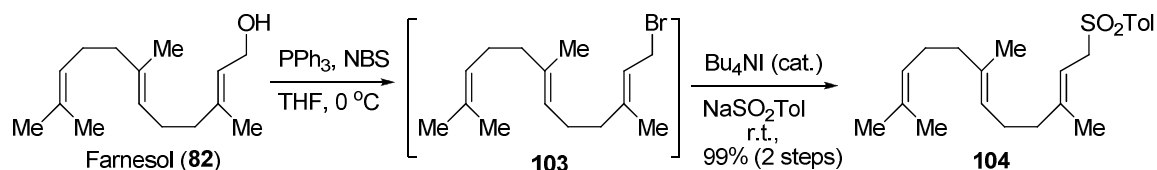
HRMS (EI) for (M⁺) C₁₃H₂₂O₃

found 226.1558, calcd. 226.1563

HRMS (FAB) for [(M+H⁺)] C₁₃H₂₃O₃

found 227.1642, calcd. 227.1642

Sulfonylation of farnesol 82



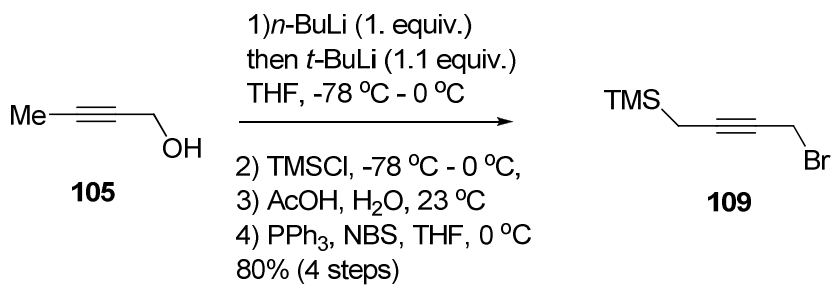
The known sulfonyl triene **104**^{51a} was prepared from *trans-trans*-farnesol (**82**) using a newer procedure.^{51b} Specifically, *trans-trans*-farnesol (**82**, 10.0 g, 43.0 mmol) and triphenylphosphine (14.7 g, 56.0 mmol) were dissolved in dry THF (200 mL) and then cooled to 0 °C with ice-water bath. *N*-Bromosuccinimide (NBS) (9.23 g, 51.6 mmol) was slowly added in ten batches over 20 minutes. The light yellow reaction mixture was stirred for 1.5 hours at 0 °C until complete conversion was achieved. Then, tetrabutylammonium iodide (1.60 g, 4.30 mmol) and *p*-toluenesulfinic acid sodium salt (NaSO₂Tol, 11.5 g, 64.5 mmol) were subsequently added. The brown suspension was warmed to room temperature and stirred overnight. The reaction was quenched with saturated aqueous sodium sulfite and transferred to a separatory funnel. Organic layer was collected and the aqueous layer was extracted with Et₂O (2 x 100 mL). The combined organic fractions were washed with saturated NaHCO₃ (100 mL), brine (100 mL), dried with anhydrous MgSO₄ and concentrated under reduced pressure. Purification by chromatography on silica gel using ethyl acetate: hexane (1 : 9) was performed to afford compound **104** (15.4 g, 99% yield).

IR (neat, cm⁻¹) 3024, 2965, 2921, 2856, 1919, 1662, 1597, 1444, 1346, 1302, 1149, 745.

^1H NMR (600 MHz, CDCl_3) δ 7.70 (d, $J = 7.8$ Hz, 2H), 7.28 (d, $J = 7.8$ Hz, 2H), 5.15 (t, $J = 8.4$ Hz, 2H), 5.03 (m, 2H), 3.75 (d, $J = 8.4$ Hz, 2H), 2.41 (s, 3H), 2.16 - 1.92 (m, 8H), 1.64 (s, 3H), 1.56 (s, 3H), 1.55 (s, 3H), 1.30 (s, 3H).

^{13}C NMR (100 MHz, CDCl_3) δ 146.4, 144.6, 136.0, 135.9, 131.6, 129.7, 128.7, 124.4, 123.6, 110.6, 56.3, 39.9, 26.9, 26.4, 25.9, 21.8, 17.9, 16.4, 16.2.

Preparation of propargylic bromide 109



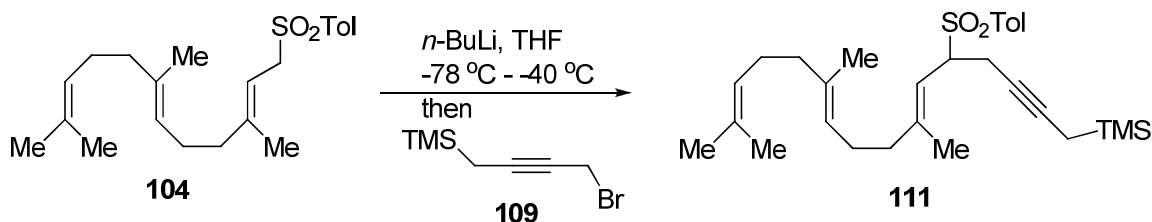
This known compound **109**^{52a} was more easily prepared by the following sequence^{52b} from 2-butyn-1-ol. Specifically, a 250 mL flame-dried flask charged with stir bar, 2-butyn-1-ol **105** (3.17 g, 45.3 mmol) and THF (100 mL) was cooled to -78 °C with acetone-dry ice bath for 20 minutes. *n*-BuLi (2.50 M in hexane, 18.1 mL, 45.3 mmol) then was added dropwise over 20 minutes, followed by slow addition of *t*-BuLi (1.70 M in pentane, 29.0 mL, 50.0 mmol) over 30 minutes. The reaction solution was allowed to warm to 0 °C over 2 hours and stirred at 0 °C for 20 minutes, and then cooled to -78 °C. Trimethylsilyl chloride (TMSCl, 11.5 mL, 90.5 mmol) was added slowly to the solution of the dianion intermediate. The reaction mixture was allowed to warm to room temperature and stirred overnight. A clear solution was turned into a yellowish suspension, which was checked by

TLC (ethyl acetate : hexane = 1 : 20) to ensure completion. Hydrolysis of the resulting crude *C*-silylpropargyl, *O*-silylether product to release the alcohol was conducted by adding water (40 mL) and acetic acid (2 mL) to the reaction mixture at room temperature and stirred for 2 hours. (Additional time was required when less water or acetic acid was used). The reaction progress was monitored by TLC (ethyl acetate : hexane = 1 : 4). After completion, Et₂O was added to dilute the reaction mixture, which was then transferred to a separatory funnel. The organic layer was collected and aqueous layer was extracted with Et₂O (3 x 40 mL). The combined organic fractions were washed with brine (50 mL), dried over anhydrous MgSO₄ and evaporated. Flash column chromatography on silica gel afforded the desired product 4-trimethylsilyl-2-butyne-1-ol (5.70 g, 89% yield), which matched the published spectral data.⁸⁵ The resulting alcohol (5.70 g, 40.0 mmol) was added to THF (100 mL) solution of PPh₃ (13.7 g, 52.2 mmol) and cooled to 0 °C. NBS (8.57 g, 48.2 mmol) was added in five portions over 20 minutes at 0 °C, and stirred for one hour at 0 °C. Hexane (100 mL) was then added to dilute the solution, which resulted in the precipitation of Ph₃PO. This solid was removed by filtration. Evaporating the solvent from the filtrate gave the crude product **109**. This compound was suitable for use in the next step, or could be further purified by hexane extraction (2 x 50 mL) of the desired product by filtering additional solid Ph₃PO, providing **109** after evaporation of solvents (7.38 g, 90% yield). Compound **109** partially decomposed in the presence of silica gel, as demonstrated by attempted thin layer chromatography.

^1H NMR (400 MHz, CDCl_3) δ 4.06 (dd, $J = 11.6, 5.2$ Hz, 1H), 3.81 (d, $J = 7.6$ Hz, 1H), 2.42-1.67 (m, 10H), 1.29 (s, 3H), 1.13 (s, 3H), 0.90 (s, 3H).

^{13}C NMR (100 MHz, CDCl_3) δ 87.1, 74.4, 32.2, 17.0, -1.82.

Alkylation of triene **104** with propargylic bromide **109**



Allylic sulfone **104** (9.10 g, 25.0 mmol) was dissolved in THF (110 mL) and cooled to -78°C under argon. $n\text{-BuLi}$ (2.5 M in hexane, 11.1 mL, 27.8 mmol) was added dropwise over 20 minutes via syringe. The solution was allowed to warm to -40°C over 1 hour, and then recooled to -78°C . The bromide **109** (4.60 g, 22.0 mmol) in THF (15 mL) was added slowly via syringe. Stirring was continued for 2 hours at -78°C , and then the reaction was allowed to warm to room temperature overnight. After the reaction was complete, Et_2O (100 mL) and water (100 mL) were added to dilute the reaction mixture, which was transferred to a separatory funnel for separation and collection of the organic fraction. The aqueous fraction was extracted with Et_2O (3 x 50 mL). The combined organic fractions were washed with brine (50 mL), dried with anhydrous MgSO_4 and evaporated. Flash column chromatography on silica gel (ethyl acetate : hexane = 1 : 4) afforded the product **111** as a clear oil (11.1 g, 92% yield).

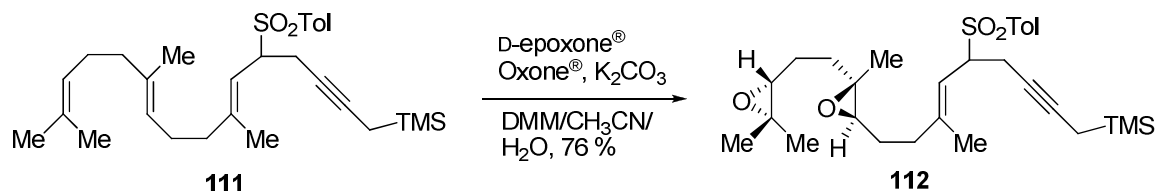
IR (neat, cm⁻¹) 2957, 2917, 2224, 1664, 1596, 1441, 1313, 1144, 849.

¹H NMR (400 MHz, CDCl₃) δ 7.68 (d, *J* = 8 Hz, 2H), 7.28 (d, *J* = 8 Hz, 2H), 5.07 (t, *J* = 6.4 Hz, 2H), 5.00 (d, *J* = 10.4 Hz, 1H), 3.87 (dt, *J* = 10.4, 3.2 Hz, 1H), 2.96 (m, 1H), 2.52 (m, 1H), 2.42 (s, 3H), 2.06 - 1.95 (m, 8H), 1.66 (s, 3H), 1.58 (s, 6H), 1.32 (t, *J* = 2.6 Hz, 2H), 1.29 (s, 3H), 0.00 (s, 9H).

¹³C NMR (100 MHz, CDCl₃) δ 146.3, 144.6, 135.7, 134.8, 131.6, 129.6, 129.5(2), 124.4, 123.7, 116.7(2), 80.4, 73.5, 64.1, 40.1, 39.9, 26.9, 26.5, 25.9, 21.8, 19.6, 17.9, 17.1, 16.2, 7.2, -2.0(3).

HRMS (FAB) Calcd. for C₂₉H₄₅O₂SSi [(M+H⁺)] 485.2904, found 485.2898.

Regio- and enantioselective diepoxidation of enyne 111



Trienyne **111** (3.50 g, 7.30 mmol), Shi catalyst (D-epoxone[®], 0.93 g, 3.63 mmol), tetrabutylammonium hydrogen sulfate (0.25 g, 0.72 mmol) and NaB₄O₇·10H₂O (0.05 M in Na₂EDTA [4x10⁻⁴ M], 109 mL) were suspended with vigorous stirring in DMM : acetonitrile (2 : 1, 109 mL) and cooled to 0 °C. From two separate addition funnels, solutions of K₂CO₃ (11 g, 80 mmol) dissolved in water (87 mL), and Oxone[®] (12.3 g, 20 mmol) dissolved in Na₂EDTA [4 x 10⁻⁴ M] (87 mL), were added dropwise and simultaneously over two hours. After the addition was

complete, the reaction mixture was stirred for 20 minutes at 0 °C. The reaction was diluted with water (100 mL) and Et₂O (100 mL), which was transferred to separatory funnel. Organic fractions were collected and the aqueous layer was extracted with Et₂O (3 x 100 mL). The combined organic fractions were washed with brine (100 mL) and dried over anhydrous MgSO₄. Evaporation of the solvents by rotary evaporation gave the crude products, which were a mixture of starting triene **111**, monoepoxide, and diepoxide **112** as judged by TLC. This crude mixture was then subjected to another cycle of enantioselective epoxidation as described above, including the same workup. Flash column chromatography on silica gel gave the product **112** as a mixture of sulfone diastereomers (2.86 g, 76% yield).

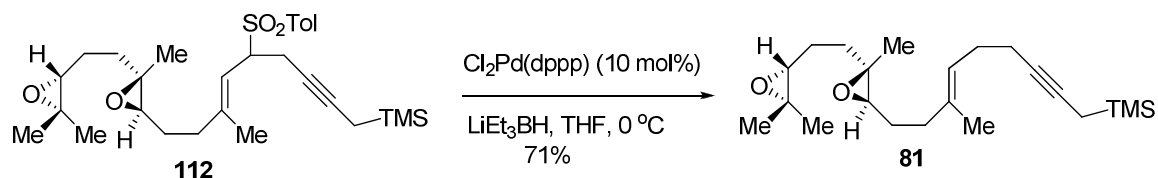
IR (neat, cm⁻¹) 2957, 2224, 1663, 1597, 1452, 1312, 1144, 852.

¹H NMR (400 MHz, CDCl₃) δ 7.67 (d, *J* = 8.4 Hz, 2H), 7.29 (d, *J* = 8 Hz, 2H), 5.03 (m, 1H), 3.87 (m, 1H), 2.93 (m, 1H), 2.70 (m, 2H), 2.55-2.47 (m, 1H), 2.42 (s, 3H), 2.16-2.03 (m, 2H), 1.80-1.56 (m, 8H), 1.37-1.25 (m, 12H), 0.00 (s, 9H).

¹³C NMR (100MHz, CDCl₃) δ 145.3, 134.8, 134.7, 129.6, 129.4, 129.4, 117.3, 117.1, 80.5, 73.3, 64.0, 63.3, 62.7, 60.5, 58.6, 36.6, 35.7, 27.2, 25.0, 21.8, 21.4, 19.7, 18.8, 16.4, 14.3, 7.1, -2.0(3).

HRMS(FAB): Calcd. for C₂₉H₄₅O₄SSi[(M+H⁺)] 517.2802, found 517.2791.

Palladium-catalyzed desulfonylation of **112**



Preparation of palladium catalyst ($\text{Cl}_2\text{Pd}(\text{dppp})$)⁸⁶: Anhydrous palladium dichloride (500 mg) was suspended in 12.5 mL of benzonitrile (12.5 mL) and the mixture was heated to 100 °C with stirring. After 20 minutes, the most PdCl_2 was dissolved in the solvent to give a red solution. This solution was filtered while is still warm and the filtrate was poured into 75 mL low-boiling petroleum ether (39-65 °C). A light yellow product was washed with additional petroleum ether. 1,3-Bis(diphenylphosphine)propane (dppp, 645 mg) was added once to a magnetically stirred suspension of yellow solid $\text{Cl}_2\text{Pd}(\text{PhCN})_2$ (600 mg) obtained above in 10 mL of anhydrous benzene. The solution immediately changes from a dark red color to pale yellow, and a yellow crystalline precipitate began to form. After the suspension has been stirred for 30 minutes, pentane (7 mL) was added to the reaction mixture, resulting in more precipitate. The yellow solid is then filtered under argon atmosphere and washed three times with pentane to give the desired palladium catalyst $\text{Cl}_2\text{Pd}(\text{dppp})$ (880 mg, 95%).

A 100 mL flame-dried flask was charged with sulfone-diepoxide **112** (2.10 g, 4.10 mmol), $\text{Cl}_2\text{Pd}(\text{dppp})$ (0.24 g, 0.41 mmol), and THF (50.0 mL). The suspension was cooled to 0 °C with vigorous stirring. Lithium triethylborohydride (Superhydride) (1.0 M in THF, 10.2 mL, 10.2 mmol) was added dropwise to the

suspension over 20 minutes. An initially heterogeneous reaction mixture became clear and homogeneous and then turned dark brown. The reaction proceeded for 30-60 minutes to reach 80 to 90% conversion, at which time Et₂O (30.0 mL) was added and followed by quenching with saturated aqueous NH₄Cl (30.0 mL). Longer reaction times resulted in partial reduction of epoxide. The reaction mixture was transferred to a separatory funnel. The organic layer was separated from the aqueous layer, which was extracted with Et₂O (2 x 30.0 mL). The combined organic fractions were washed with brine (50.0 mL), dried over anhydrous MgSO₄ and evaporated. Flash column chromatography on Et₃N (2%)-buffered silica gel (hexane: AcOEt = 4: 1) gave product **81** (0.94 g, 63% yield, 75% yield based on recovered starting material, > 20 : 1 dr) and starting sulfone **112** (0.32 g, 15% yield).

$[\alpha]_D = +7.5$ (*c* 1.0, CHCl₃).

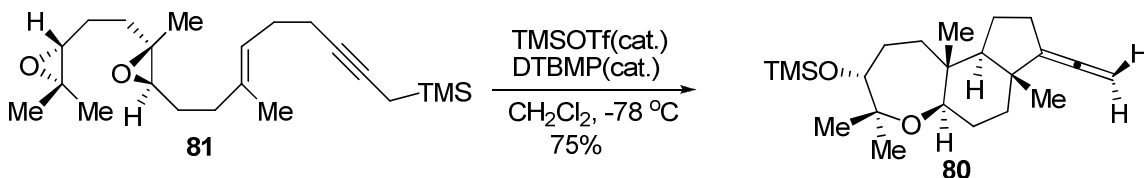
IR (neat, cm⁻¹) 2958, 2924, 2218, 1668, 1455, 1383, 1248, 850.

¹H NMR (400 MHz, CDCl₃) δ 5.23 (s, 1H), 2.72 (dd, *J* = 12.0, 6.0 Hz, 2H), 2.16 (s, 3H), 2.17-2.08 (m, 3H), 1.79-1.55 (m, 9H), 1.41 (s, 2H), 1.31 (s, 3H), 1.27 (s, 3H), 1.27 (s, 3H), 0.08 (s, 9H).

¹³C NMR (100MHz, CDCl₃) δ 135.2, 124.1, 78.7, 77.7, 64.0, 63.1, 60.5, 58.6, 36.5, 35.4, 28.3, 27.4, 25.0, 24.8, 19.5, 18.8, 16.9, 16.3, 7.1, -1.9(3).

HRMS (FAB) Calcd. for C₂₂H₃₉O₂Si [(M+H⁺)] 363.2714, found 363.2710.

Cascade oxa-carbocyclization of diepoxide-enyne **81**



A 250 mL flame-dried flask was charged with compound **81** (0.60 g, 1.70 mmol), CH₂Cl₂ (100 mL), and DTBMP (68.0 mg, 0.33 mmol) and then cooled to -78 °C. TMSOTf (0.06 mL, 0.33 mmol) was added dropwise with vigorous stirring at -78 °C. The reaction was usually complete within 1 hour. If not complete, more TMSOTf (0.03 mL, 0.16 mmol) was added to consume all starting material **81**. Et₃N (1.0 mL) was added to the reaction mixture and stirred for another 10 minutes before water (10 mL) was added to quench the reaction at -78 °C. The organic fractions were separated by decanting the organic layer from the frozen aqueous component when the reaction mixture was still cold. After this ice had melted upon warming to room temperature, the aqueous layer was extracted with CH₂Cl₂ (2 x 50 mL). The combined organic fractions were washed with brine (50 mL), dried with anhydrous MgSO₄ and evaporated. Flash column chromatography on silica gel (hexane: EtOAc = 30: 1) provided the desired tricyclic allene **80** (0.45 g, 75% yield).

[α]_D = -39 (c 1.55, CHCl₃).

IR (neat, cm⁻¹) 2954, 2879, 1960, 1443, 1250.

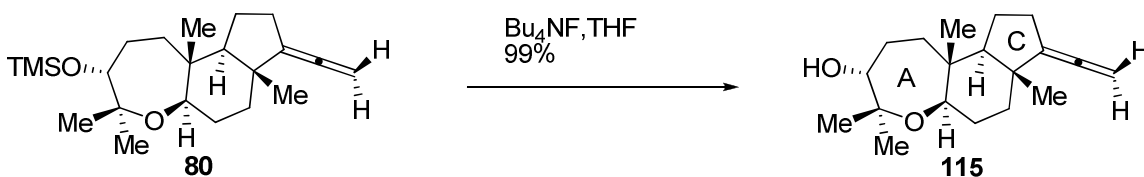
¹H NMR (400 MHz, CDCl₃) δ 4.62 (m, 1H), 4.57 (m, 1H), 3.62 (d, *J* = 6.8 Hz, 1H), 2.51 (dd, *J* = 11.6, 5.2 Hz, 1H), 2.49 (m, 1H), 2.33 (m, 1H), 1.87 (t, *J* = 13.6 Hz,

1H), 1.60-1.30 (m, 9H), 1.05 (m, 1H), 1.04 (s, 3H), 1.01 (s, 3H), 0.92 (s, 3H), 0.77 (s, 3H), 0.00 (s, 9H).

^{13}C NMR (100 MHz, CDCl_3) δ 200.2, 113.3, 78.5, 77.8, 76.9, 58.6(2), 44.3, 41.2, 35.4, 35.3, 29.1, 28.4, 27.6, 26.2, 22.9, 21.2, 20.9, 13.6, 0.2(3).

HRMS (FAB) Calcd. for $\text{C}_{22}\text{H}_{39}\text{O}_2\text{Si}$ [(M+H⁺)] 363.2714, found 363.2708.

Desilylation of allene **80** and X-ray crystal structure



Tetrabutylammonium fluoride (TBAF, 1.0 M in THF, 0.20 mL, 0.20 mmol) was added to a THF (5.0 mL) solution of tricyclic allene **80** (60.0 mg, 0.17 mmol). The resulting reaction mixture was stirred at room temperature for 1 hour. Et_2O (5.0 mL) was added to dilute the reaction mixture, followed by addition of sat. NH_4Cl (5 mL). Organic layer was separated, and aqueous layer was extracted with Et_2O twice (2 x 10 mL). The organic fractions was washed with brine (20 mL), dried over MgSO_4 and evaporated. Column chromatography on silica gel afforded the product **115** (59.4 mg, 99% yield).

m.p. =139-141 °C (decomposition).

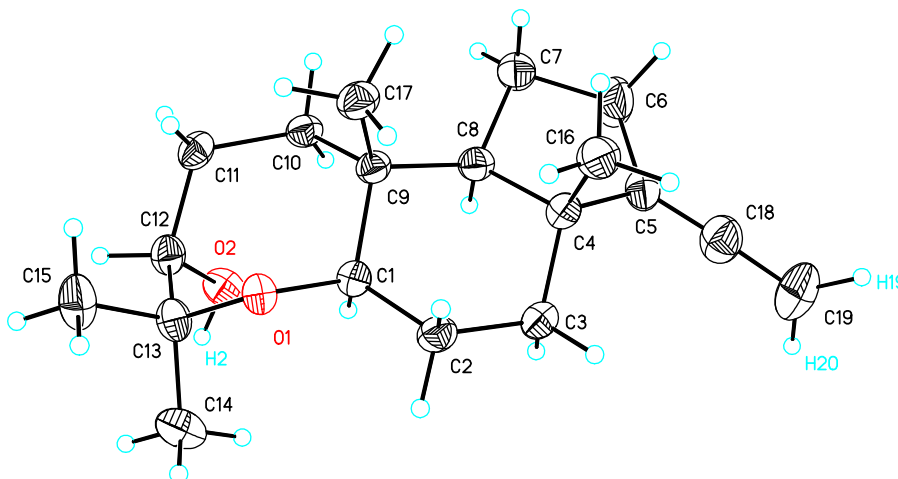
^1H NMR (400 MHz, CDCl_3) δ 4.67 (m, 1H), 4.63 (m, 1H), 3.80 (dd, J = 6.6, 3.6 Hz, 1H), 3.58 (dd, J = 11.4, 4.8 Hz, 1H), 2.57 (m, 1H), 2.38 (m, 1H), 2.02 (dt, J = 13.8,

2.4 Hz, 1H), 1.74-1.42 (m, 9 H), 1.26 (s, 3H), 1.13 (s, 3H), 1.01 (s, 3H), 0.87 (s, 3H).

^{13}C NMR (100 MHz, CDCl_3) δ 200.3, 113.0, 78.2, 77.8, 77.4, 76.8, 58.5(2), 44.2, 41.4, 35.2, 29.2, 28.5, 27.5, 25.6, 21.9, 21.1, 20.9, 13.4.

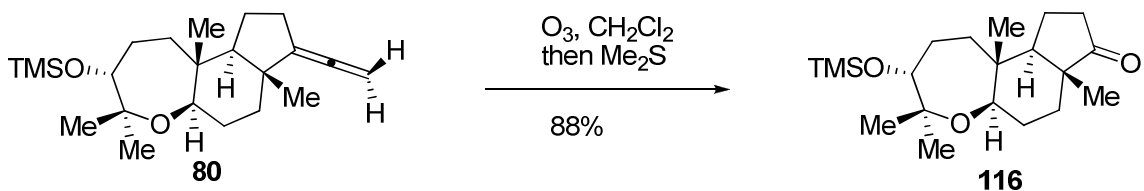
X-Ray analysis: The structure of **115** was substantiated by X-ray diffractometry.

The thermal ellipsoid diagram is shown for compound **115**:



For X-ray data of compound 115, see page 178-187.

Ozonolysis of allene 80



Procedure A: A solution of allene **80** (0.60 g, 1.7 mmol) in dry CH_2Cl_2 (20 mL) was cooled to $-78\text{ }^\circ\text{C}$, and an O_3 stream was passed through this solution for six minutes. Then Me_2S (2.0 mL) was added at $-78\text{ }^\circ\text{C}$, and the resulting reaction mixture was stirred and allowed to warm to room temperature overnight. Removal of the solvent and excess Me_2S under reduced pressure provided the crude ketone, which was purified by flash column chromatography on silica gel by using the eluent (ethyl acetate : hexane = 1 : 9) to afford the analytically pure crystalline product **116** (0.53 g, 88% yield).

m.p. = $98\text{--}101\text{ }^\circ\text{C}$. $[\alpha]_{\text{D}} = -57$ (c 0.69, CHCl_3).

IR (neat, cm^{-1}) 2939, 2869, 1740, 1250, 1096, 1049.

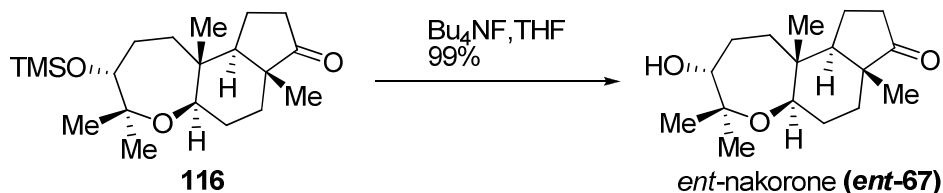
^1H NMR (400 MHz, CDCl_3) δ 3.63 (d, $J = 6.8$ Hz, 1H), 3.51 (dd, $J = 11, 5.4$ Hz, 1H), 2.37 (ddd, $J = 19.6, 8.8, 1.2$ Hz, 1H), 2.05 (dt, $J = 19.2, 9.2, 8.8$ Hz, 1H), 1.88 (dt, $J = 13.2, 1.2$ Hz, 1H), 1.75 (m, 1H), 1.66 (m, 2H), 1.55 (m, 1H), 1.47 (m, 4H), 1.18 (m, 2H), 1.05 (s, 3H), 1.02 (s, 3H), 0.90 (s, 3H), 0.83 (s, 3H), 0.00 (s, 9H).

^{13}C NMR (100 MHz, CDCl_3) δ 221.0, 78.6, 77.7, 76.8, 54.8, 47.9, 41.5, 36.3, 34.5, 30.6, 28.9, 27.4, 26.0, 22.8, 18.5, 16.2, 14.1, 0.18(3).

HRMS (FAB) Calcd. for $\text{C}_{20}\text{H}_{37}\text{O}_3\text{Si}$ $[(\text{M}+\text{H}^+)]$ 353.2507, found 353.2507.

Procedure B^{18f}: To a suspension of allene **80** (50 mg, 0.12 mmol) in mixture of acetonitrile (CH₃CN, 2 mL), tetrachloromethane (CCl₄, 2 mL) and water (3 mL) was added periodate (264 mg, 1.2 mmol) and ruthenium trichloride hydrate (4 mg) at room temperature. The reaction mixture was stirred vigorously for 15 hours at room temperature and diluted with diethyl ether. Similar workup was followed as procedure A to give ketone **116** and *ent*-**67** in about 40% combined yield.

Desilylation of tricyclic ketone 109 to furnish *ent*-nakorone (*ent*-67)



TBAF (1.0 M in THF, 1.2 mL, 1.2 mmol) was added to a solution of ketone **116** (0.35 g, 1.0 mmol) in THF (50 mL). The resulting reaction mixture was stirred at room temperature for 1 hour. Et₂O (30 mL) was added to dilute the reaction mixture, followed by addition of saturated aqueous NH₄Cl (25 mL) to quench the reaction. The organic layer was separated and aqueous layer was extracted with Et₂O (2 x 30 mL). The organic fractions were washed with brine (50 mL), dried over MgSO₄ and evaporated. Column chromatography afforded *ent*-nakorone (*ent*-**67**, 0.28 g, 99% yield).

[α]_D = -50° (c=0.25, MeOH).

IR(neat, cm⁻¹) 3427, 2973, 2935, 2867, 1725, 1452, 1376, 1090, 1058.

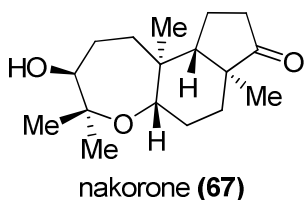
^1H NMR (400 MHz, C_6D_6) δ 3.52 (dd, $J=11.4, 5.0$ Hz, 1H), 3.34 (d, $J=6.4$ Hz, 1H), 2.08 (ddd, $J=19.2, 8.8, 1.6$ Hz, 1H), 1.89 (dt, $J=13.6, 2.8$ Hz, 1H), 1.77 (dd, $J=18.0, 8.8, 1.2$ Hz, 1H), 1.13-1.68 (m, 9H), 1.12 (s, 3H), 1.04 (s, 3H), 0.88 (s, 3H), 0.75 (s, 3H), 0.29 (s, 1H).

^{13}C NMR (100 MHz, C_6D_6) δ 218, 78.3, 77.5, 77.1, 54.7, 47.8, 41.9, 36.2, 34.5, 31.3, 29.4, 28.2, 25.9, 22.2, 18.7, 16.4, 14.5.

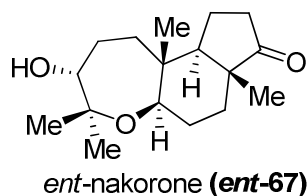
HRMS (FAB) Calcd. for $\text{C}_{17}\text{H}_{29}\text{O}_3$ $[(\text{M}+\text{H}^+)]$ 281.21112, found 281.21062.

Comparison of our synthetic *ent*-**67** with the published data (ref. 4) showed mostly the expected similarities between our compound and the natural product, although to our surprise, the optical rotations of both synthetic and naturally occurring compounds are reported to have the same sign (which should be opposite for antipodes), and the magnitude of the rotations are quite different. The original assignment of absolute stereochemistry in naturally occurring nakorone was made by CD/ORD measurement^{35a}, whereas our assignment of synthetic *ent*-**67** is based on the Flack absolute structure parameter of the crystal structure of compound **115**, with synthetic *ent*-**67** and **115** sharing **116** as the common parent precursor compound by straightforward reaction sequences.

Reported for natural product **67** (ref. 35a) our synthetic material (*ent*-**67**, this work)



$[\alpha]_{\text{D}}$ -210.0 (c 0.2, MeOH)



-50 (c 0.25, MeOH)

IR (neat, cm⁻¹):

<i>O-H stretch not reported</i>	3427
2950 (C-H stretches)	2973, 2935
2853 (C-H stretches)	2867
1737 (C=O stretch)	1725
<i>C-H methyl bends not reported</i>	1425, 1376
1085 (C-O stretch)	1090
1054 (C-O stretch)	1058

¹H NMR (C₆D₆, δ):

H-6	3.47 (dd, <i>J</i> = 11.3, 5.0 Hz)
H-3	3.28 (d, <i>J</i> = 4 Hz)
H-13 ^a	2.04 (dd, <i>J</i> = 18.9, 8.9 Hz)
H-12	1.82 (t, <i>J</i> = 14.0 Hz)
H-13 ^b	1.75 (dd, <i>J</i> = 18.9, 17.8 Hz)

CH or CH₂ not reported

H-15	1.07 (s, 3H)
H-16	1.00 (s, 3H)
H-17	0.85 (s, 3H)
H-18	0.72 (s, 3H)

H-O not reported

(400 MHz, C₆D₆, δ):

3.52 (dd, <i>J</i> = 11.4, 5.0 Hz, 1H)
3.34 (d, <i>J</i> = 6.4 Hz, 1H)
2.08 (ddd, <i>J</i> = 19.2, 8.8, 1.6 Hz, 1H)
1.89 (dt, <i>J</i> = 13.6, 2.8 Hz, 1H)
1.77 (ddd, <i>J</i> = 18.0, 8.8, 1.2 Hz, 1H)

1.68 - 1.13 (m, 10H)

1.12 (s, 3H)
1.04 (s, 3H)
0.88 (s, 3H)
0.75 (s, 3H)

0.29 (s, OH, 1H)

<u>^{13}C NMR (C_6D_6, δ):</u>	<u>(100 MHz, C_6D_6, δ):</u>
C-14 216.0	218
C-2 79.5	78.3
CH-O 76.8	77.5
CH-O 76.3	77.1
CH 54.3	54.7
4° C 49.5	47.8
4° C 42.0	41.9
CH_2 36.2	36.2
CH_2 33.8	34.5
CH_2 31.2	31.3
C-16 29.5	29.4
CH_2 27.2	28.2
CH_2 25.2	25.9
C-15 21.5	22.2
CH_2 18.2	18.7
C-18 15.0	16.4
C-17 13.3	14.5

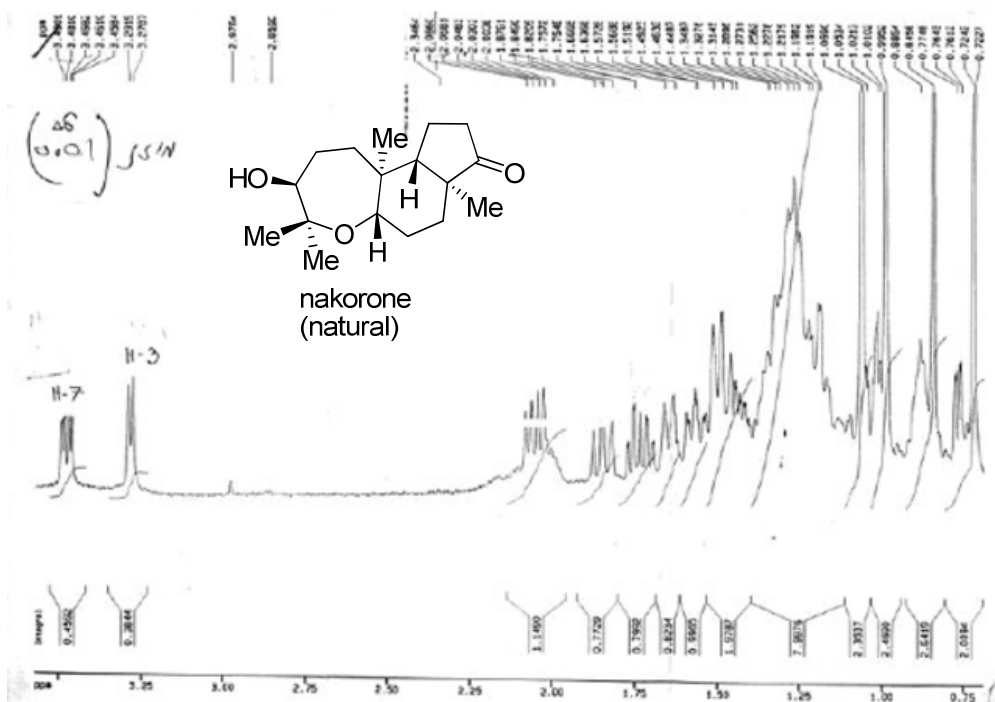
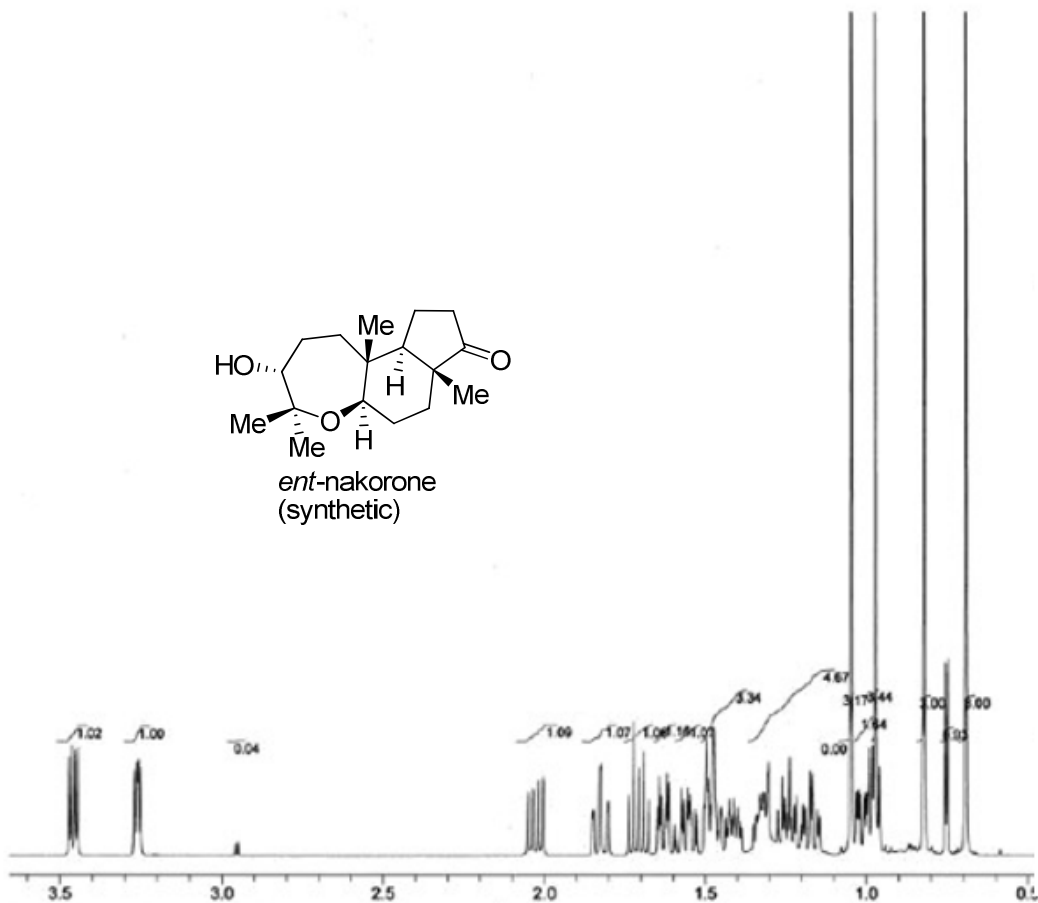
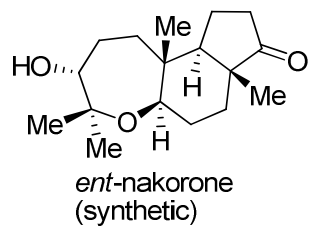
HRMS (EI) for (M^+) $\text{C}_{17}\text{H}_{28}\text{O}_3$

found 280.2036, calcd. 280.2031

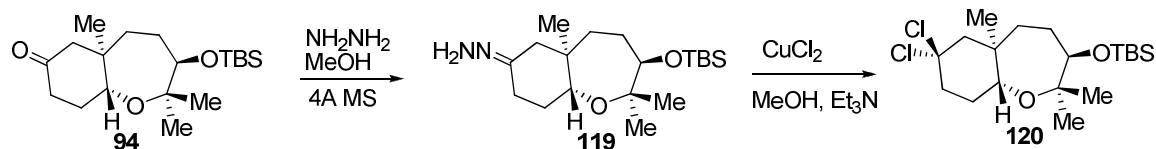
HRMS (FAB) for $[(\text{M}+\text{H}^+)]\text{C}_{17}\text{H}_{29}\text{O}_3$

found 281.2106, calcd. 281.2111.

^1H NMR spectra comparison is shown below



Gem-dichlorination of ketone 94



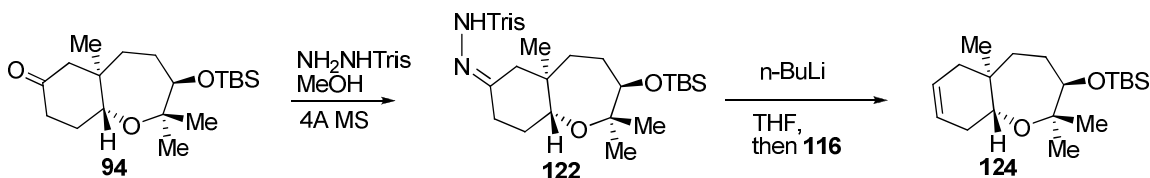
Finely powered molecular sieves (4 Å, 1.0 g) was dried in oven for 48 hours and cooled down under vacuum to room temperature. Methanol (2 mL) and hydrazine hydrate (18.8 mg, 0.59 mmol) were added successively to the flask with stirring. After 20 minutes, a methanol (2 mL) solution of ketone **94** (20 mg, 58 μmol) was added to the reaction mixture. After stirring for 2 hours, molecular sieves was removed by filtration and washed with diethyl ether (5 mL). The filtrate was concentrated with rotovap and the excess of hydrazine was removed under vacuum with gentle heating (30-35 °C) to give the crude product (**119**), which was used for next step without further purification. To another flask was charged with copper dichloride (47 mg, 0.35 mmol) and methanol (2 mL). Triethylamine was added at room temperature with stirring. After stirring for 10 minutes, the reaction mixture was cooled to 0 °C with ice-water bath and a methanol solution of hydrazone (**119**) obtained above was added dropwise over 10 minutes. The cooling bath was removed to allow warming up to room temperature over 1 hour. The reaction was quenched with 3.5% aqueous ammonia solution. The organic materials were extracted with diethyl ether, washed with brine, dried over Na_2SO_4 and evaporated. Chromatography on silica gel afforded the gem-dichloride product **120** contaminated by eliminated products.

IR (neat, cm^{-1}) 2950, 2929, 2856, 1463, 1442, 1379, 1360, 1254, 1091, 833.

^1H NMR (400 MHz, CDCl_3) δ 3.72 (dd, $J = 9.2, 4.8$ Hz, 1H), 3.69 (d, $J = 7.2$ Hz, 1H), 2.53 (m, 1H), 2.18 (m, 1H), 2.1-1.46 (m 8H), 1.14 (s, 3H), 1.13 (s, 3H), 1.08 (s, 3H), 0.92 (s, 9H), 0.01 (m, 6H).

^{13}C NMR (100 MHz, CDCl_3) δ 89.4, 79.2, 73.9, 70.7, 58.7, 46.8, 40.5, 36.7, 28.8, 28.6, 26.3, 26.2, 25.8, 23.2, 18.5, -4.2, -5.1.

Shapiro reaction of ketone **94**



Ketone **94** (20 mg, 59 μmol), trisylhydrazide (19.2 mg, 64.6 μmol) and THF (2 mL) were stirred at room temperature for 4 hours. The THF was evaporated under reduced pressure and the solid residue was dissolved in methanol/water (85: 15, 8 mL). Filtration gave the white solid **122** that was dried under vacuum overnight. To a THF (1.0 mL) solution of **122** (10 mg, 16 μmol) was added $n\text{-BuLi}$ (1.6 M, 4 μL , 6.5 μmol) dropwise over 30 min at -55 $^\circ\text{C}$. after stirring at -50 $^\circ\text{C}$ for minutes, another $n\text{-BuLi}$ (1.6 M, 4 μL , 6.5 μmol) was added dropwise at -50 $^\circ\text{C}$ and the reaction mixture was warmed up to room 0 $^\circ\text{C}$ over 30 minutes in order to form the vinyl lithium. Addition of ketone **116** (5.6 mg, 16 μmol) dissolved in THF (1 mL) to this vinyl lithium solution at -78 $^\circ\text{C}$ resulted in the protonation of vinyl lithium to give alkene **124** as indicated by ^1H NMR. Addition of TMEDA resulted in the same outcome.

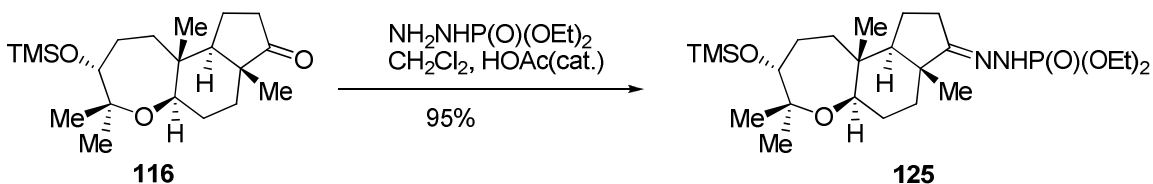
Data for compound 122

$^1\text{H NMR}$ (400 MHz, CDCl_3) δ 7.14 (s, 2H), 7.11 (s, br, 1H), 3.79 (dd, $J = 11.6, 5.2$ Hz, 1H), 3.69 (d, $J = 7.2$ Hz, 1H), 2.56 (m, 1H), 2.05 (dd, $J = 14.0, 2.8$ Hz, 1H), 1.94-1.60 (m, 6H), 1.24 (m, 21H), 1.14 (s, 3H), 1.06 (s, 3H), 0.92 (s, 3H), 0.87 (s, 3H), 0.00 (s, 9H).

Data for compound 124.

$^1\text{H NMR}$ (400 MHz, CDCl_3) δ 5.47 (m, 2H), 3.74 (dd, $J = 10.0, 6.8$ Hz, 1H), 3.63 (d, $J = 7.2$ Hz, 1H), 2.16 (m, 1H), 1.92-1.70 (m, 3H), 1.54 (m, 2H), 1.41 (s, 1H), 1.24-1.16 (m, 2H), 1.13 (s, 3H), 1.10 (s, 3H), 0.89 (s, 9H), 0.86 (s, 3H), 0.00 (s, 6H).

Hydrazidation of ketone 116



Phosphorylation of hydrazine¹: Hydrazine monohydrate (3.2 g, 100 mmol) was added dropwise with vigorous stirring to mixtures of carbon tetrachloride (60 mL), dichloromethane (100 mL) and powdered potassium bicarbonate (20.7 g, 150 mmol) and triethylbenzylammonium chloride (227 mg, 1 mmol) at room temperature. After stirring for 15 minutes, diethyl phosphite (13.8 g, 100 mmol) dissolved in dichloromethane was added dropwise to the reaction mixture at

¹ Zwierzak, A.; Sulewska, A. *Synthesis* **1976**, 835.

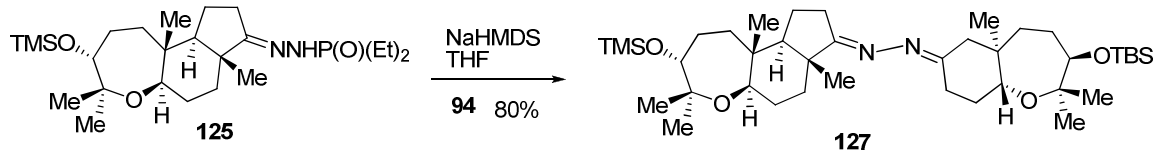
room temperature. After stirring 4 hours, filtration was undertaken to remove the K_2CO_3 . Solvents was evaporated and the residue was kept at 100 °C for 2 hours to give almost pure product diethylphosphorohydrazidate 15.0 g, 89 %).

Hydrazidation of ketone 116: A CH_2Cl_2 (1 mL) solution of ketone **116** (40 mg, 0.11 mmol) and a drop of acetic acid were added to stirring mixtures of diethylphosphorohydrazidate (21 mg, 0.13 mmol) obtained above and sodium bisulfate (400 mg) dissolved in CH_2Cl_2 (2 mL). The reaction mixture was stirred at room temperature for 3 days. Filtration through a celite pad and concentration of the filtrate gave the crude hydrazone **125**, which was used for the next step without further purification.

1H NMR (600 MHz, $CDCl_3$) δ 6.10 (d, $J = 25.2$ Hz, 1H), 4.04 (m, 4H), 3.63 (d, $J = 7.2$ Hz, 1H), 3.50 (dd, $J = 11.4, 48$ Hz, 1H), 2.21 (dd, $J = 17.4, 9.0$ Hz, 1H), 2.10 (ddd, $J = 18, 9.0$ Hz, 1H), 1.88 (t, $J = 13.8$ Hz, 1H), 1.71 (m, 2H), 1.60-1.40 (m, 6H), 1.25 (t, $J = 7.2$ Hz, 3H), 1.24 (t, $J = 6.6$ Hz, 3H), 1.20-1.00 (m, 2H), 1.05 (s, 3H), 1.01 (s, 3H), 0.89 (s, 3H), 0.79 (s, 3H), 0.00 (s, 9H).

^{13}C NMR (100 MHz, $CDCl_3$) δ 166.9, 78.6, 77.8, 77.7, 63.6, 63.6, 63.5, 57.0, 44.6, 41.1, 35.1, 33.4, 29.0, 27.9, 26.1, 25.3, 22.9, 20.0, 19.7, 16.4, 13.9, 0.20, 0.16.

Cross-coupling of hydrazone **125** with ketone **94** to bisazine **127**



To a dry 15 mL flask was charged with hydrazone **125** (112 mg, 0.23 mmol) and THF (8 mL). Sodium bis(trimethylsilyl)amide (1.0 M in THF, 0.43 mL, 0.43 mmol) was added to the hydrazone solution dropwise at room temperature. After stirring for 20 minutes, a THF (1 mL) solution of bicyclic ketone **94** (146 mg, 0.23 mmol) was added at room temperature. The resulting reaction mixture was stirred for 2 days. Saturated NaHCO₃ (10 mL) was added to quench the reaction and transferred to a separatory funnel. The organic materials were collected and the aqueous layer was extracted with diethyl ether (2x10 mL) twice. The combined organic fractions were dried with Na₂SO₄ and evaporated. Chromatography on silica gel using eluent mixture (5% to 25% of EtOAc in hexane) gave the bisazine **127** (136 mg, 86%)

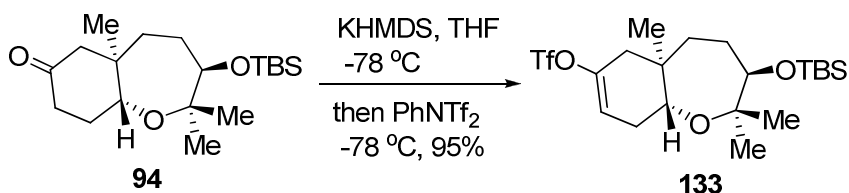
IR (neat, cm⁻¹) 2938, 2859, 1659, 1463, 1443, 1376, 1250, 1091, 1074, 837.

¹H NMR (600 MHz, CDCl₃) δ 3.85 (dd, *J* = 12.0, 5.4 Hz, 1H), 3.69 (d, *J* = 7.2 Hz, 1H), 3.68 (d, *J* = 7.2 Hz, 1H), 3.60 (dd, *J* = 12.0, 5.4 Hz, 1H), 2.86 (dd, *J* = 13.8, 2.4 Hz, 1H), 2.25 (m, 1H), 2.32 (m, 1H), 2.26 (m, 1H), 2.15 (m, 1H), 2.00-1.40 (m, 15H), 1.16 (s, 3H), 1.12 (s, 3H), 1.08 (s, 3H), 1.07 (s, 3H), 1.00 (s, 3H), 0.93 (s, 3H), 0.92 (s, 9H), 0.87 (s, 3H), 0.72 (s, 3H), 0.05 (s, 9H), 0.01 (s, 3H), 0.00 (s, 3H).

^{13}C NMR (100 MHz, CDCl_3) δ 176.7, 163.1, 78.8, 78.6, 77.8, 77.7, 76.9, 74.2, 56.3, 44.6, 41.2, 40.6, 40.5, 36.1, 35.1, 33.9, 33.2, 31.2, 29.1, 29.0, 28.0, 27.4, 26.3 (3C), 26.1, 25.5, 22.9, 22.8, 19.9, 19.4, 18.4, 17.7, 14.4, 13.9, 0.19, 0.18, -4.3, -5.1.

HRMS (FAB) Calcd. for $\text{C}_{39}\text{H}_{73}\text{O}_4\text{N}_2\text{Si}_2$ [(M+H⁺)] 689.5103, found 689.5108.

Kinetic formation of vinyl triflate from ketone 94



General procedure: A 25 mL flame-dried flask was charged with potassium bis(trimethylsilyl)amide (KHMDS) (0.50 M in toluene, 3.12 mL, 1.6 mmol), and then cooled to -78 °C. To this cooled solution was added ketone **94** (0.18 g, 0.53 mmol) in THF (5 mL) dropwise over 20 minutes via syringe. After the addition was complete, the solution was stirred for another 2 hours at -78 °C, then *N*-phenyl-bis-trifluoromethanesulfonimide (PhNTf_2 , 0.38 g, 1.05 mmol) in THF (2 mL) was added dropwise over 10 minutes. The reaction was complete within 2 hours at -78 °C with vigorous stirring. Then, saturated NaHCO_3 (5 mL) was added to quench the reaction and the reaction mixture was transferred to a separatory funnel. The organic layer was separated, and the aqueous layer was extracted with Et_2O (3 x 10 mL). The combined organic fractions were washed with brine (10 mL), dried with anhydrous MgSO_4 and evaporated under reduced pressure to

afford the crude product, which was flash column chromatographed on silica gel (hexane : EtOAc = 20 : 1) to give vinyl triflate **133** as a clear oil (0.24 g, 95%).

$[\alpha]_D = -1.2$ (c 1.2, CHCl₃).

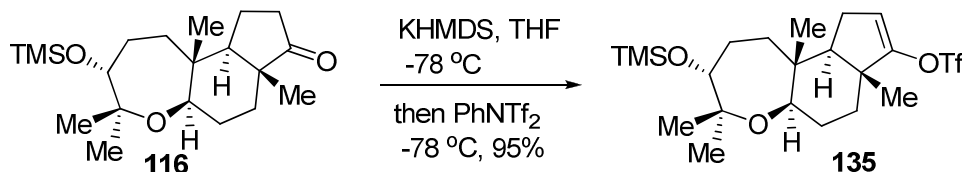
IR (neat, cm⁻¹) 2954, 2931, 2858, 1696, 1464, 1419, 1246, 1209, 1143.

¹H NMR (400 MHz, CDCl₃) δ 5.54 (ddd, *J* = 5.6, 2.4 Hz, 1H), 3.79 (dd, *J* = 9.8, 6.2 Hz, 1H), 2.65 (d, *J* = 7.2 Hz, 1H), 2.27-2.15 (m, 2H), 2.06 (d, *J* = 18.0 Hz, 1H), 2.03-1.94 (m, 1H), 1.89 (dd, *J* = 19.0, 13.4 Hz, 2H), 1.55 (m, 1H), 1.24 (dd, *J* = 12.4, 6.2 Hz, 1H), 1.27 (s, 3H), 1.08 (s, 3H), 0.95 (s, 3H), 0.90 (s, 9H), -0.03 (d, *J* = 2.4 Hz, 6H).

¹³C NMR (100 MHz, CDCl₃) δ 147.1, 116.1, 78.7, 77.5(2), 70.3, 42.6, 38.0, 35.7, 30.2, 29.2, 26.3, 26.1(3), 22.1, 18.3, 18.2, -4.2, -5.0.

HRMS (FAB) Calcd. for C₂₀H₃₆O₅F₃SSi [(M+H⁺)] 473.1999, found 473.1995.

Kinetic formation of vinyl triflate from ketone 116



Following the general procedure reported for compound **133**, vinyl triflate **135** was prepared) as a clear oil (0.33 g, 95%) from ketone **116** (0.25 g, 0.71 mmol), KHMDS (0.5 M in toluene, 4.30 mL, 2.13 mmol) and PhNTf₂ (0.51 g, 1.42 mmol

$[\alpha]_D = -11.1$ (c 1.7, CHCl₃).

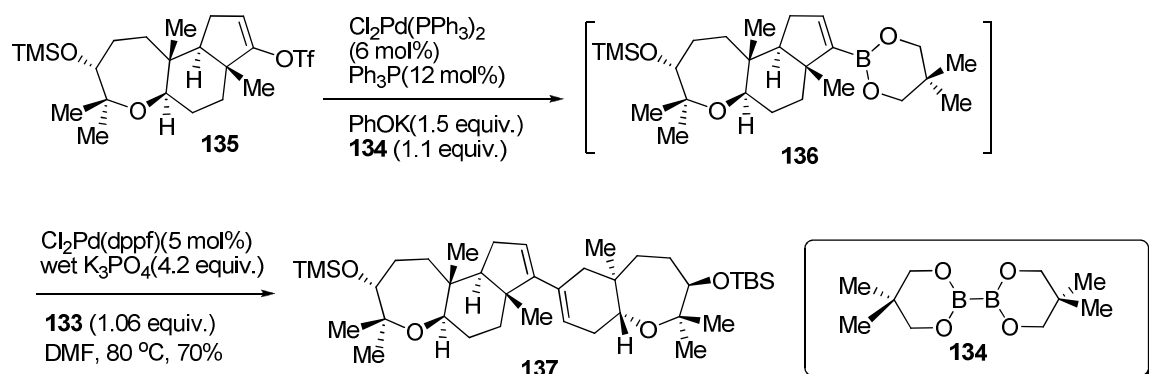
IR (neat, cm^{-1}) 2943, 2866, 1632, 1423, 1252, 1213, 1143.

^1H NMR (600 MHz, CDCl_3) δ 5.49 (t, $J = 2.4$ Hz, 1H), 3.63 (d, $J = 7.2$ Hz, 1H), 3.53 (t, $J = 8.0$ Hz, 1H), 2.04 (dd, $J = 8.1, 2.4$ Hz, 2H), 1.88 (dt, $J = 13.2, 1.2$ Hz, 1H), 1.51-1.36 (m, 8H), 1.04 (s, 3H), 1.00 (s, 3H), 0.99 (s, 3H), 0.83 (s, 3H), 0.00 (s, 9H).

^{13}C NMR (150 MHz, CDCl_3) 158.3, 114.9, 78.8, 77.7(2), 76.6, 57.1, 45.2, 40.4, 34.3, 32.3, 28.9, 27.8, 26.0, 25.7, 23.0, 17.7, 14.0, 0.20(3).

HRMS (FAB) Calcd. for $\text{C}_{21}\text{H}_{36}\text{O}_5\text{F}_3\text{SSi}$ [($\text{M}+\text{H}^+$)] 485.1999, found 485.1997.

Cross coupling of vinyl triflates **133** and **135**



A 15 mL flame-dried flask with stirring bar was charged with vinyl triflate **133** (48.4 mg, 0.10 mmol), $\text{Cl}_2\text{Pd(PPh}_3)_2$ (4.0 mg, 5.7 μmol), Ph_3P (3.0 mg, 11.5 μmol), potassium phenoxide (KOPh, 20.0 mg, 0.15 mmol), bis-(neopentylglycolato)diboron (**134**, 24.0 mg, 0.11 mmol) and toluene (4.0 mL, 6.8 ppm of H_2O) under argon atmosphere. The reaction mixture was degassed three times by the freeze-thaw method before it was heated to 50 $^\circ\text{C}$ and stirred for 3

hours at 50 °C under argon atmosphere. The corresponding alkenyl boronate was obtained in excellent yield (>90%) as judged by TLC. The reaction mixture was then cooled to room temperature. To this solution were added dppf (4.0 mg, 7.2 μmol), Cl₂Pd(dppf) (4.0 mg, 4.9 μmol), vinyl triflate **133** (50.0 mg, 0.106 mmol) in DMF (4.0 mL, 12.0 ppm of H₂O) and K₃PO₄ (wet) (90.0 mg, 0.424 mmol) sequentially. The resulting mixture was freeze-thaw degassed three times, before heating to 80 °C for 12 hours under argon. After it was complete as monitored by TLC, the reaction mixture was cooled to room temperature, diluted with Et₂O (20 mL), and transferred to a separatory funnel. The organic layer was collected and was washed with water (3 x 10 mL). The aqueous layer was extracted with Et₂O (2 x 10 mL). The combined organic fractions were dried over anhydrous MgSO₄ to afford the crude UV-active product, which was purified by preparative TLC to provide analytically pure diene **137** (46.1 mg, 70% yield).

[α]_D = -7.8 (c 0.78, CHCl₃).

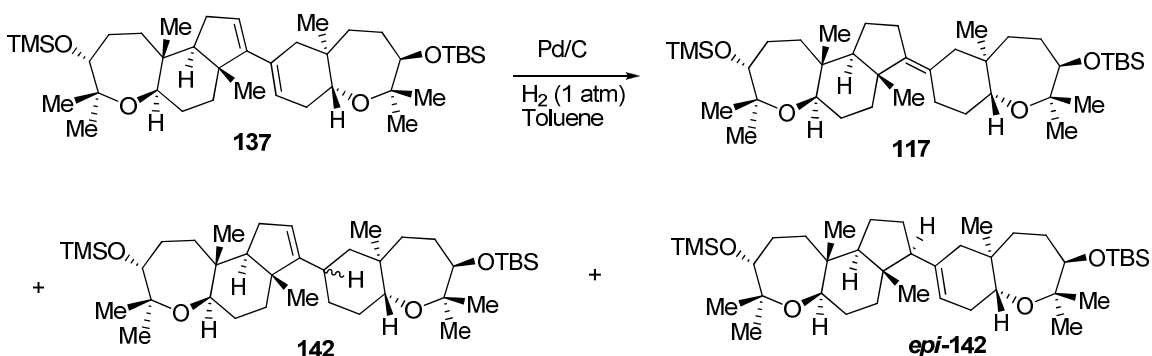
IR (neat, cm⁻¹) 3049, 2931, 2857, 2359, 2338, 2233, 1463, 1444, 1376, 1360, 1251, 1089, 1070, 1051, 999, 873, 837.

¹H NMR (400 MHz, CDCl₃) δ 5.61 (d, *J* = 3.2 Hz, 1H), 5.57 (s, 1H), 3.70 (dd, *J* = 12, 7.2 Hz, 1H), 3.68 (d, *J* = 6.4 Hz, 1H), 3.68 (d, *J* = 7.2 Hz, 1H), 3.59 (dd, *J* = 12, 4.6 Hz, 1H), 2.12 (dt, *J* = 17.6, 5.6 Hz, 1H), 1.96 (t, *J* = 10.8 Hz, 2H), 1.96 (s, 4H), 1.87 (t, *J* = 18, 13.2 Hz, 2H), 1.65-1.46 (m, 8H), 1.40 (t, *J* = 9.2, 8.8 Hz, 1H), 1.22-1.15 (m, 1H), 1.12 (s, 3H), 1.10 (s, 3H), 1.09 (s, 3H), 1.08 (s, 3H), 1.00 (s, 3H), 0.92 (s, 3H), 0.88 (s, 9H), 0.85 (s, 3H), 0.05 (s, 9H), 0.00 (s, 6H).

^{13}C NMR (100 MHz, CDCl_3) δ 154.5, 130.2, 124.9, 120.8, 78.5, 78.3, 77.9, 76.8, 77.5, 71.8, 60.2, 47.6, 43.4, 40.7, 36.7, 36.4, 35.8, 35.2, 32.7, 29.7, 29.1, 28.6, 27.6, 26.8, 26.2(3), 23.0, 22.0, 18.4, 18.3, 18.2(2), 14.0, 0.2(3), -4.1, -5.0.

HRMS (FAB) Calcd. for $\text{C}_{39}\text{H}_{71}\text{O}_4\text{Si}_2$ [(M+H⁺)] 659.4885, found 659.4877.

Palladium-catalyzed hydrogenation of diene **137** and X-ray crystal structure



A suspension of Pd-C (5 wt%, 8.0 mg, 3.7 μmol) in toluene (2.0 mL, 6.8 ppm of H₂O) was stirred for 1 hour at room temperature under 1 atm of H₂ pressure (balloon). Diene **137** (25.0 mg, 38 μmol) in toluene (1.0 mL) was then added to the precooled suspension (0 °C) and stirring was continued for 6-12 hours (monitored by TLC) at 0 °C under the same hydrogen pressure. If the reaction was too slow, up to 10-20 mol% additional Pd/C was added, which did not change the ratios or yields of products. The reaction mixture was filtered through Celite and washed with Et₂O (2 x 5 mL). The filtrate was collected. Removal of the solvents by rotary evaporation afforded mixtures of three isomers (23.8 mg, 95% combined yield), which were separated by preparative TLC to give desired

product **117** (7.5 mg, 30% yield), mp = 142-145 °C, trisubstituted alkene **142** (12.5 mg, 50% yield) and **epi-142** (2.5 mg, 10% yield).

Data for compound 117

$[\alpha]_D = +9.2$ (c 0.33, CHCl₃)

IR (neat, cm⁻¹) 2933, 2858, 1462, 1444, 1376, 1360, 1251, 1090, 1070, 1028.

¹H NMR (400 MHz, CDCl₃) δ 3.68 (d, *J* = 6.8 Hz, 2H), 3.65 (dd, *J* = 16.8, 5.2 Hz, 1H), 3.52 (dd, *J* = 12, 4.6 Hz, 1H), 2.68 (d, *J* = 10.8 Hz, 1H), 2.23 (m, 2H), 2.11 (m, 1H), 2.06 (d, *J* = 13.2, 2.4 Hz, 1H), 1.93 (m, 2H), 1.78 (t, *J* = 13.2, 12.8 Hz, 1H), 1.60-1.40 (m, 11H), 1.35-1.10 (m, 4H), 1.13 (s, 3H), 1.11 (s, 3H), 1.07 (s, 3H), 1.06 (s, 3H), 0.92 (s, 3H), 0.91 (s, 9H), 0.82 (s, 3H), 0.81 (s, 3H), 0.07 (s, 9H), 0.00 (s, 6H).

¹³C NMR (100 MHz, CDCl₃) δ 142.7, 125.0, 78.53, 78.50, 77.8, 77.4, 76.7, 75.3, 59.6, 45.6, 44.8, 41.1, 40.7, 37.3, 36.5, 35.6, 32.3, 30.2, 29.2, 29.1, 28.7, 28.3, 26.6, 26.3, 26.2(3), 23.0, 22.9, 20.7, 20.4, 18.4, 16.7, 13.9, 0.21(3), -4.19, -5.12.

HRMS (FAB) Calcd. for C₃₉H₇₃O₄Si₂ [(M+H⁺)] 661.5042, found 661.5038.

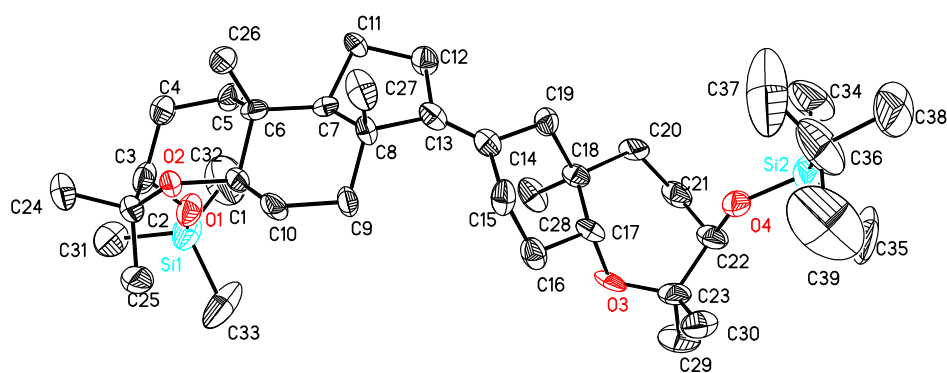
Data for compound 142

¹H NMR (600 MHz, CDCl₃) δ 5.20 (s, 1H), 3.70 (dd, *J* = 10.8, 6.6 Hz, 1H), 3.68 (d, *J* = 6.6 Hz, 1H), 3.63 (d, *J* = 16.8, 5.2 Hz, 1H), 3.55 (dd, *J* = 11.4, 4.2 Hz, 1H), 2.10 (m, 1H), 1.93-1.20 (m, 23H), 1.12 (s, 3H), 1.11 (s, 3H), 1.09 (s, 3H), 1.08 (s, 3H), 0.89 (s, 9H), 0.85 (s, 3H), 0.82 (s, 3H), 0.65 (s, 3H), 0.07 (s, 9H), 0.00 (s, 6H).

Data for compound epi-142

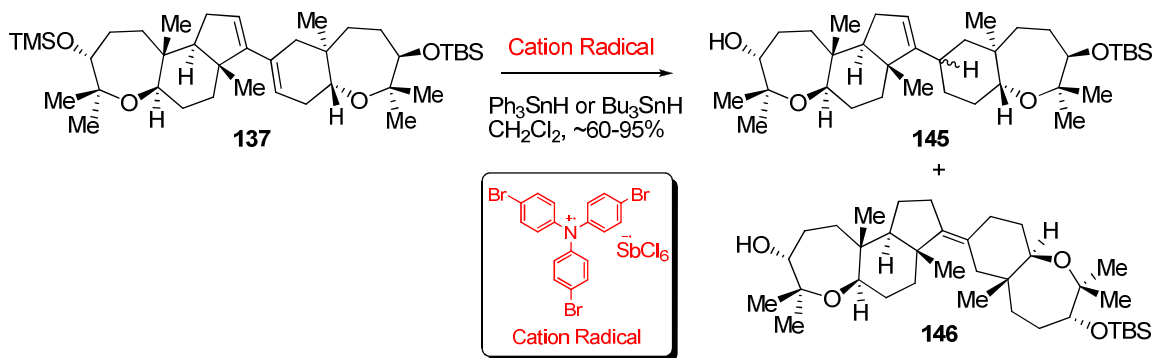
^1H NMR (600 MHz, CDCl_3) δ 5.32 (s, 1H), 3.69 (dd, $J=7.2, 4.2$ Hz, 2H), 3.57 (m, 2H), 1.98 (m, 5H), 1.71-1.20 (m, 19H), 1.14 (s, 3H), 1.11 (s, 3H), 1.09 (s, 3H), 1.08 (s, 3H), 0.93 (s, 9H), 0.90 (s, 3H), 0.89 (s, 3H), 83 (s, 3H), 0.07 (s, 9H), 0.00 (s, 6H).

X-ray data for compound 117: The structural skeleton and the alkene geometry of compound 117 were confirmed by X-ray analysis. The thermal ellipsoid diagram is provided below.



For X-ray data of compound 117, see page 188-205.

Hole transfer catalyst promoted hydrogenation of diene 137



To a CH₂Cl₂ (2 mL) solution of diene **137** (10 mg, 15.2 μmol) and tributyltin hydride (11 mg, 38 μmol) was added hole transfer catalyst [(p-BrPh)₃N⁺SbCl₆⁻, 24.8 mg, 30 μmol] under argon atmosphere at 0 °C. After completion of the reaction (about 1-2 minutes), the reaction was quenched with a saturated solution of potassium carbonate in methanol (2 mL). The reaction mixture was then transferred to a separatory funnel and the organic materials were collected, while the aqueous layer was extracted with diethyl ether twice (2x 5 mL). The combined organic fractions were washed with brine, dried with Na₂SO₄ and evaporated under reduced pressure (rotavap). The residue obtained was purified by column chromatography on silica gel to give the major product **145** (8.5 mg, 95%), along with a small amount of **146** (0.5 mg, 5%) that was subjected to desilylation to *epi*-abudinol B containing “wrong” alkene geometry.

Data for compound 145

¹H NMR (400 MHz, CDCl₃) δ 5.19 (dd, *J* = 4.4, 2.4 Hz, 1H), 3.84 (d, *J* = 8.8 Hz, 1H), 3.81 (dd, *J* = 10.4, 5.2 Hz, 1H), 3.74 (dd, *J* = 9.6, 6.4 Hz, 1H), 3.65 (d, *J* = 8.0

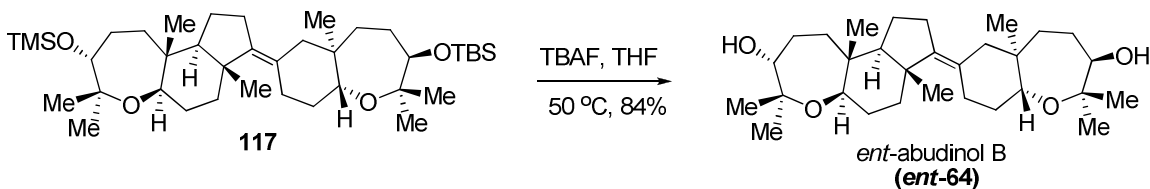
Hz, 1H), 2.18 (m, 1H), 2.10-1.4 (m, 23H), 1.17 (s, 3H), 1.15 (s, 3H), 1.12 (s, 3H), 1.04 (s, 3H), 1.00 (s, 3H), 0.95 (s, 3H), 0.92 (s, 9H), 0.81 (s, 3H), 0.00 (s, 6H).

Data for compound 146

^1H NMR (400 MHz, CDCl_3) δ 5.19 (m, 1H), 3.78 (d, $J = 7.2$ Hz, 1H), 3.68 (d, $J = 6.4$ Hz, 1H), 3.62 (dd, $J = 12.0, 4.8$ Hz, 1H), 3.51 (dd, $J = 12.4, 4.8$ Hz, 1H), 2.52 (dd, $J = 13.6, 2.4$ Hz, 1H), 2.10-1.4 (m, 23H), 1.14 (s, 3H), 1.11 (s, 3H), 1.07 (s, 3H), 1.00 (s, 3H), 0.92 (s, 9H), 0.89 (s, 3H), 0.87 (s, 3H), 0.78 (s, 3H), 0.00 (s, 6H).

^{13}C NMR (100 MHz, CDCl_3) δ 142.4, 124.4, 78.5, 78.1, 78.0, 77.4, 77.3, 75.1, 59.0, 44.8, 42.7, 41.3, 39.7, 37.7, 36.7, 35.4, 31.0, 30.6, 29.9, 29.2, 28.8, 28.1, 27.4, 27.1, 26.6, 26.3, 25.6, 23.0, 21.9, 20.9, 20.5, 18.3, 17.7, 13.8, -4.2, -5.1.

Global desilylation of diene 117 to furnish *ent*-abudinol B (*ent*-64)



To the THF (3.0 mL) solution of compound **117** (6.1 mg, 10 μmol) was added TBAF in THF (1.0 M in THF, 0.10 mL, 0.10 mmol) at room temperature under argon atmosphere. The resulting solution was then heated to 60 $^{\circ}\text{C}$ for 6-10 hours. Et_2O (5 mL) was added to dilute the reaction mixture, which was quenched by addition of saturated NH_4Cl (3 mL). The reaction mixture was

transferred to a separatory funnel. The organic layer was collected, and the aqueous layer was extracted with Et₂O (2 x 5 mL). The combined organic fractions were dried with anhydrous MgSO₄ and evaporated by rotavap. Flash column chromatography on silica gel by using eluent (hexane: ethyl acetate = 4 : 1) afforded *ent*-abudinol B (*ent*-**64**, 4.0 mg, 84% yield).

$[\alpha]_D = +23$ (*c* 0.05, MeOH).

IR (neat, cm⁻¹) 3460, 2970, 2930, 2868, 1446, 1376, 1359, 1076, 1036.

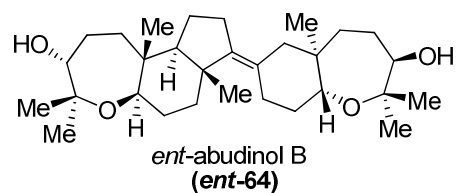
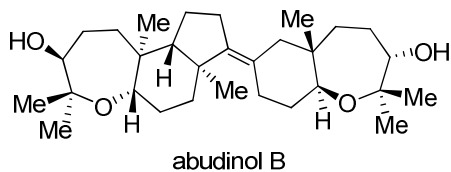
¹H NMR (400 MHz, C₆D₆) δ 3.77 (dd, *J*= 10.8, 5.2 Hz, 1H), 3.69 (dd, *J*=12, 4.8 Hz, 1H), 3.38 (d, *J*=6.8 Hz, 2H), 3.01 (s, OH), 2.74 (dt, *J*=9.2, 2.4 Hz, 1H), 2.36 (t, *J*=6.8 Hz, 2H), 2.19-2.31 (m, 1H), 2.10 (dt, *J*=9.6, 4.0 Hz, 1H), 1.89-2.01 (m, 2H), 1.28-1.89 (m, 14H), 1.21 (s, 3H), 1.20 (s, 3H), 1.09 (s, 3H), 1.08 (s, 3H), 1.07 (s, 3H), 1.02 (s, 3H), 1.01 (s, 3H), 0.91 (t, *J*=7.2, 6.8, 2H).

¹³C NMR(100MHz, C₆D₆) δ 142.6, 125.3, 77.7, 77.5, 77.0, 76.8, 76.6, 75.5, 59.7, 54.0, 45.5, 44.8, 41.3, 40.8, 37.4 36.6, 35.4, 32.5, 30.4, 29.3, 29.0, 28.1, 26.2, 25.7, 21.9, 21.7, 20.8, 20.4, 16.8, 14.1.

HRMS (FAB) Calcd. for C₃₀H₅₁O₄ [(M+H⁺)]475.37819, found 475.37809.

Comparison of our synthetic *ent*-**64** with the published spectral data (ref. ⁴) showed mostly the expected similarities between our compound and the natural product. Direct comparison is complicated by the absence of proton and carbon NMR data reported in ref. 4 for methylene and methine.

Reported for natural product **64** (ref. 4) our synthetic material (*ent*-**64**, this work)



$[\alpha]_D -5.0$ (*c* 0.05, MeOH)

+23 (*c* 0.05, MeOH)

IR (neat, cm^{-1}):

3484 (O-H stretches)

3460

2950 (C-H stretches)

2970, 2930, 2868

1446 (C-H stretches)

1446

not reported

1376 (C-H methyl bend)

1359 (C-H methyl bend)

1076 (C-O stretch)

1036 (C-O stretch)

1023 (C-O stretch)

1024

^1H NMR (C_6D_6 , δ):

H-7 3.75 (dd, $J = 10.5, 5.1$ Hz, 1H)

3.77 (dd, $J = 10.8, 5.2$ Hz, 1H)

H-18 3.66 (dd, $J = 11.9, 4.6$ Hz, 1H)

3.69 (dd, $J = 12.0, 4.8$ Hz, 1H)

H-3 3.36 (d, $J = 6.8$, 1H)

3.38 (d, $J = 6.8$, 1H)

H-23 3.36 (d, $J = 6.8$, 1H)

3.38 (d, $J = 6.8$, 1H)

H-O *not reported*

3.01 (s, OH) *chemical shift is variable*

CH or CH_2 *not reported*

2.74 (dt, $J = 9.2, 2.4$ Hz, 1H)

not reported

2.36 (t, $J = 6.8$ Hz, 2H)

not reported

2.31-2.19 (m, 1H)

<i>not reported</i>	2.10 (dt, $J = 9.6, 4.0$ Hz, 1H)
<i>not reported</i>	2.01-1.89 (m, 2H)
<i>not reported</i>	1.89-1.28 (m, 14H)
H-27 1.19 (s, 3H)	1.21 (s, 3H)
H-25 1.18 (s, 3H)	1.20 (s, 3H)
H-26 1.08 (s, 3H)	1.09 (s, 3H)
H-28 1.06 (s, 3H)	1.08 (s, 3H)
H-31 1.05 (s, 3H)	1.07 (s, 3H)
H-29 1.01 (s, 3H)	1.02 (s, 3H)
H-30 1.00 (s, 3H)	1.01 (s, 3H)
<i>not reported</i>	0.91 (t, $J = 7.2, 6.8$ Hz, 2H)
<u>^{13}C NMR ($\text{C}_6\text{D}_6, \delta$):</u>	<u>(100 MHz, $\text{C}_6\text{D}_6, \delta$):</u>
C-14 143.6 (C=C)	142.6
C-15 125.6 (C=C)	125.3
<i>C-2, 3, 7, 18, 23, 24 (C-O) not reported</i>	77.7, 77.5, 77.0, 76.8, 76.6, 75.5
<i>C-4, 5, 6, 8, 9, 10, 11, 12, 13, 16, 17, 19, 20, 21, 22 (C-H) not reported</i>	59.7, 54.0, 45.5, 44.8, 41.3, 40.8, 37.4, 36.6, 35.4, 32.5, 30.4, 28.1, 26.2, 25.7, 20.4
C-26 29.2 (Me)	29.3
C-28 28.9 (Me)	29.0
C-27 21.3 (Me)	21.9
C-25 21.2 (Me)	21.7
C-30 20.1 (Me)	20.8

C-31 18.4 (Me) 16.8

C-29 13.9 (Me) 14.1

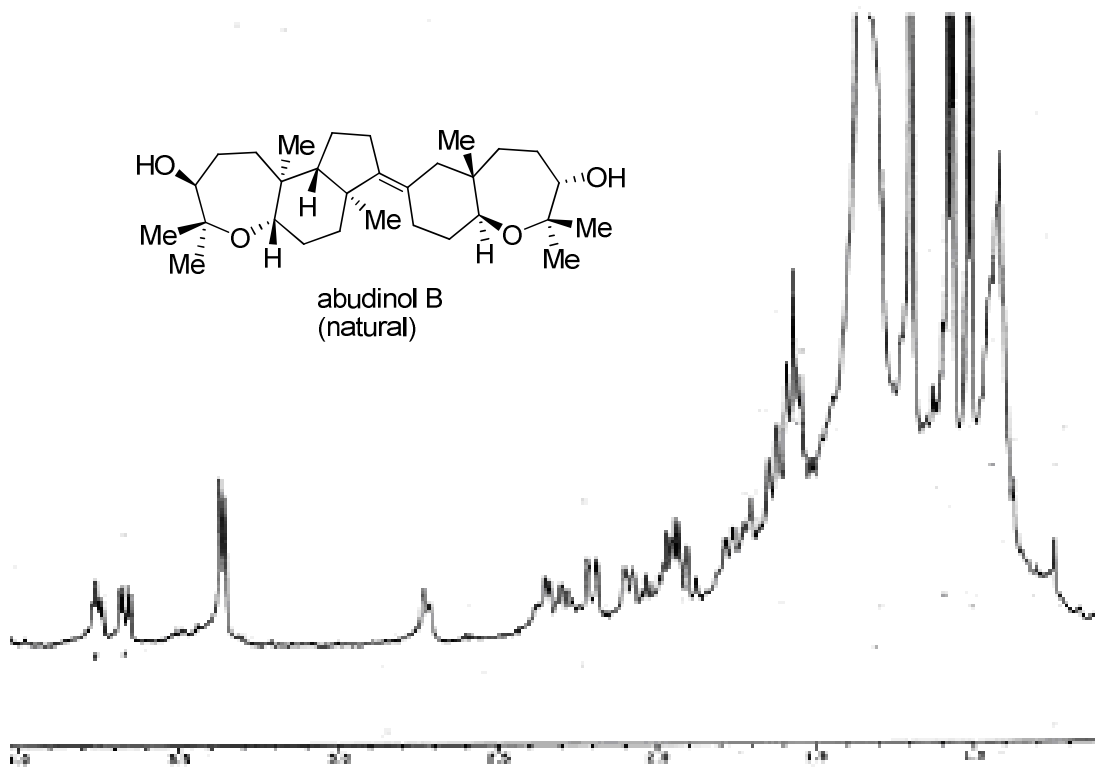
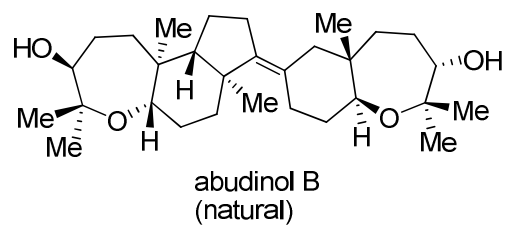
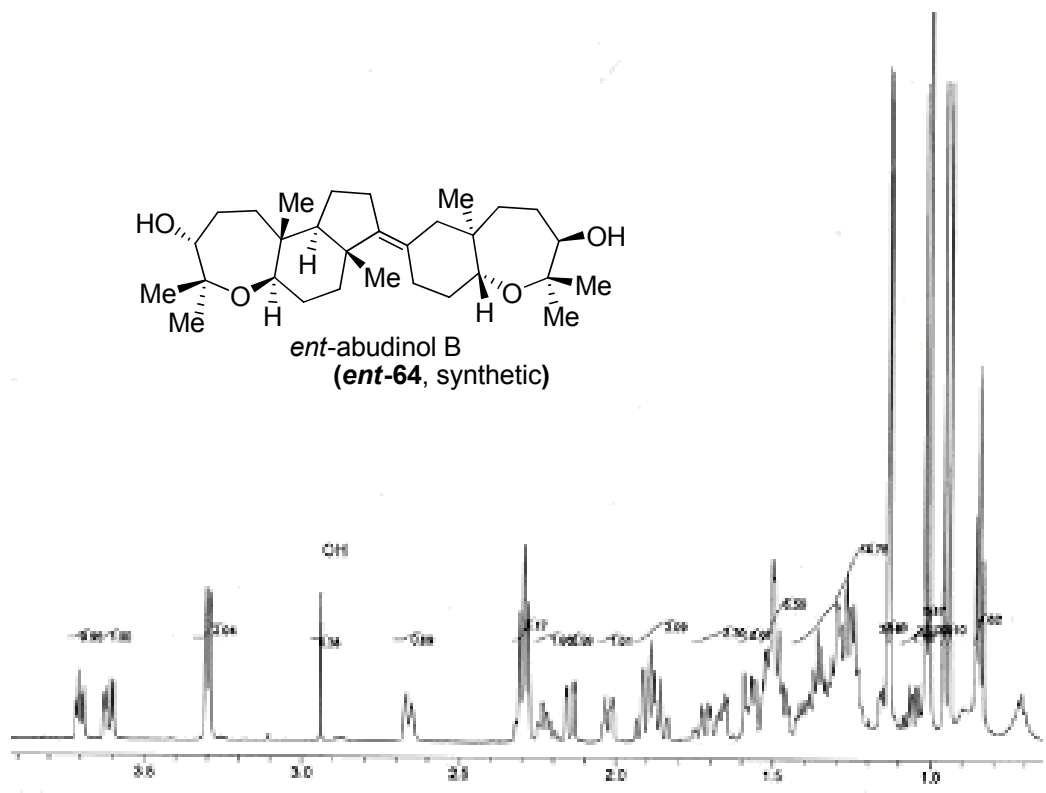
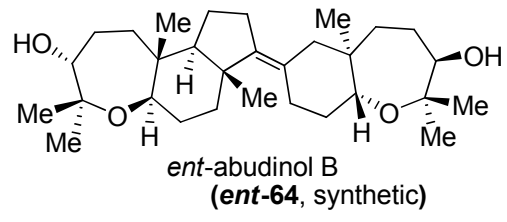
HRMS (EI) for $(M^+)C_{30}H_{50}O_4$

found 474.3702, calcd. 474.3696

HRMS (FAB⁺) for $[(M+H^+)] C_{30}H_{51}O_4$

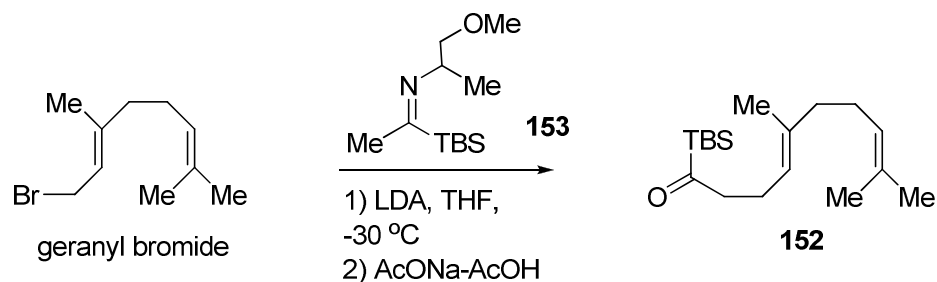
found 475.3781, calcd. 475.3782.

¹H NMR spectra comparison of natural abudinol B and synthetic ent-abudinol B (ent-64) is shown below



Biomimetic total synthesis of abudinol B from squalene-like precursor

Alkylation of imine **153** to acylsilane **152**^{20b}



To a 80 mL THF solution of diisopropyl amine (5.95 g, 8.24 mL, 58.8 mmol) was slowly added *n*-BuLi (2.5 M in hexane, 23.5 mL, 58.8 mmol) at -30 °C (acetonitrile-dry ice) and stirring continued for 30 min. To this LDA solution was added imine **153**⁷⁸ (12.0 g, 52.4 mmol) dropwise at -30 °C. The resulting yellow solution was allowed to warm to 0 °C over 30 min. The reaction solution then was cooled to -30 °C, and a 10 mL THF solution of geranyl bromide (7.60 g, 6.60 mL, 35.0 mmol) was added dropwise. The reaction mixture was allowed to warm up to -10 °C over 60 min and quenched with 40 mL of sat. NH₄Cl at -10 °C. The reaction mixture was then transferred to a separating funnel. The organic fractions were collected and aqueous fractions were extracted with Et₂O (2 x 80 mL). The combined organic fractions were washed with brine, dried over anhydrous MgSO₄, and evaporated under reduced pressure. The residue obtained was dissolved in pentane (80 mL) and treated with 80 mL of AcOH-NaOAc buffer (prepared by mixing 9.9 g of NaOAc, 21 mL of AcOH and 90 mL of

H₂O). The resulting reaction mixture was vigorously stirred for 3 hours at room temperature, diluted with 80 mL of H₂O and 80 mL of hexane, and transferred to a separating funnel. Organic fractions were collected and the aqueous fractions were extracted with hexane (2 x 80 mL). The combined organic solution was successively washed with sat. NaHCO₃, brine, dried over anhydrous MgSO₄ and concentrated. The residue was purified by column chromatography on silica gel to give acylsilane **152** as a colorless oil (8.63 g, 84%).

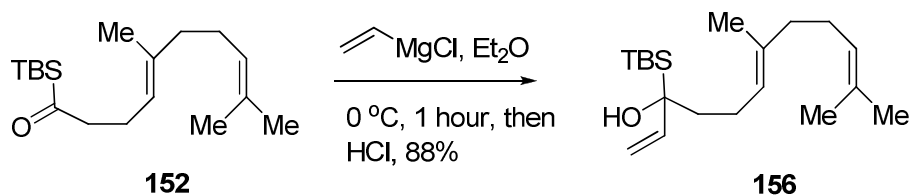
IR (neat, cm⁻¹) 2953.5, 2928.4, 2858.0, 1642.1, 1462.8, 1249.7, 836.9, 775.2.

¹H NMR (400 MHz, CDCl₃) δ 5.07 (m, 2H), 2.62 (t, *J*=7.2, 7.6 Hz, 2H), 2.19 (q, *J*=7.2, 7.6 Hz, 2H), 2.04 (t, *J*=8.0, 6.8 Hz, 2H), 1.95 (t, *J* = 8.4, 6.8 Hz, 2H), 1.68 (s, 3H), 1.60 (s, 6H), 0.93 (s, 9H), 0.18 (s, 6H).

¹³C NMR (100 MHz, CDCl₃) δ 247.6, 136.0, 131.6, 124.5, 123.3, 50.4, 39.9, 26.9, 26.6, 26.6, 26.6, 25.9, 20.8, 17.9, 16.7, 16.1, -6.8, -6.8.

HRMS (ESI): Calcd. for C₁₈H₃₅OSi[(M+H⁺)] 295.2452, found 295.2448.

Vinyl Grignard addition to acylsilane **152**⁷⁷



Acylsilane **152** (5.88 g, 20.0 mmol) was added dropwise to anhydrous Et₂O solution (100 mL) of vinyl magnesium chloride (37.5 mL, 1.6 M in THF, 60.0 mmol). The resulting reaction mixture was stirred for 1 hour at 0 °C and quenched with 1.0 N HCl (60 mL). Separation of organic layers from the aqueous layer was performed on a separating funnel. The aqueous phase was extracted with hexane (2 x100 mL). The combined extracts and organic fractions were washed with brine and dried over anhydrous MgSO₄. Removal of the solvents by rotary evaporation and column chromatography on silica gel gave the corresponding tertiary alcohol **156** (5.66 g, 87.9%) as clear oil.

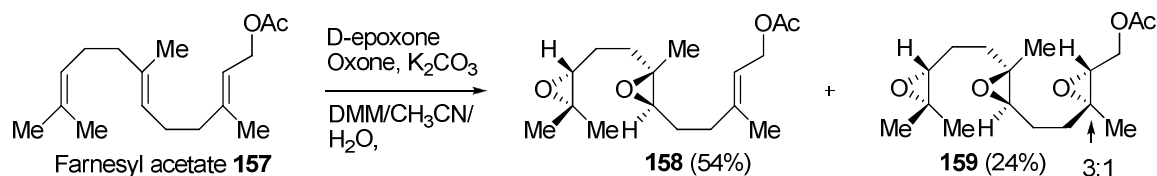
IR(neat, cm⁻¹): 3506.0, 3083.6, 2960.2, 2929.4, 2858.0, 1810.8, 1668.1, 1625.7, 1463.7, 1382.7, 1247.7, 902.5, 833.1, 769.5.

¹H NMR(400 MHz, CDCl₃) δ 5.95 (dd, *J*=10.8, 16.8 Hz, 1H), 5.15 (m, 1H), 5.08 (m, 2H), 5.03 (dd, *J*=15.8, 1.6 Hz, 1H), 2.10-2.02 (m, 3H), 2.00-1.95 (m, 3H), 1.95-1.80 (m, 2H), 1.68 (s, 3H), 1.60 (s, 3H), 1.58 (s, 3H), 1.42 (s, 1H), 0.95 (s, 9H), 0.00 (d, *J*=2.4 Hz, 6H).

¹³C NMR(100 MHz, CDCl₃) δ 143.8, 135.6, 131.7, 124.9, 124.4, 110.2, 74.3, 39.9, 37.4, 28.0, 28.0, 28.0, 26.7, 25.9, 21.4, 18.5, 17.9, 16.3, -7.5, -7.6.

HRMS (ESI): Calcd. for C₂₀H₃₉OSi[(M+H⁺)] 323.2765, found 323.2766.

Double Shi epoxidation of farnesyl acetate 157⁴¹



In a three-neck 3.0 L flask fitted with two addition funnels was charged with farnesyl acetate **157** (9.0 g, 34.1 mmol), 1,2:4,5-di-*O*-isopropylidene-D-*erythro*-2,3-hexodiuro-2,6-pyranose (D-epoxone, 4.38 g, 17.1 mmol, added in three batches over 90 min), tetrabutylammonium hydrogen sulfate (0.93 g, 2.70 mmol) and $NaB_4O_7 \cdot 10H_2O$ (0.05 M in aq. Na_2EDTA (4×10^{-4} M, 360 mL) and mixture of dimethoxymethane (DMM) and acetonitrile (2 : 1, 480 mL). The suspension was cooled to $-5^\circ C$ with salt-ice bath and vigorously stirred. One addition funnel was charged with an aqueous solution of K_2CO_3 (54.6 g, 246 mmol, in 465 mL H_2O), and the second addition funnel was charged with Oxone (57.9 g, 94.2 mmol) dissolved in aqueous Na_2EDTA (4×10^{-4} M, 465 mL). These solutions were added dropwise and simultaneously over 90 min from the two addition funnels. After the additions were complete, the reaction mixture was stirred for 10 min at $0^\circ C$. The reaction was then diluted with water (200 mL) and Et_2O (300 mL) and transferred to a separatory funnel. The organic layer was collected and the aqueous layer was extracted with Et_2O (3 x 200 mL). The combined organic fractions were washed with brine (150 mL) and dried over anhydrous $MgSO_4$. Rotary evaporation of solvents gave the crude product, which was purified by column chromatography on silica gel to give the diepoxy acetate **158** (5.40 g,

53.6%, d.r.: 10:1 based on ^1H NMR) and triepoxy acetate **159** (3.60 g, 24%, d.r.: 3:1 based on ^1H NMR)).

Data for compound 158

$[\alpha]_{\text{D}} +15.2$ (c 0.835, CHCl_3).

IR(neat, cm^{-1}): 2963.1, 2927.4, 1738.5, 1455.0, 1379.8, 1232.3, 1024.0

^1H NMR(400 MHz, CDCl_3) δ 5.37 (m, 1H), 4.58 (d, $J= 6.6$ Hz, 2H), 2.71 (q, $J= 6.0$, 6.4 Hz, 2H), 2.18 (m, 2H), 2.05 (s, 3H), 1.80-1.55 (m, 6H), 1.72 (s, 3H), 1.30 (s, 3H), 1.27(s, 3H), 1.26 (s, 3H).

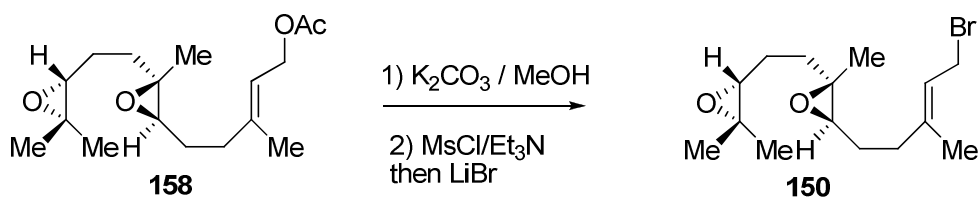
^{13}C NMR(100 MHz, CDCl_3) δ 171.3, 141.3, 119.1, 64.0, 62.9, 61.4, 60.5, 58.6, 36.3, 35.4, 27.0, 25.0, 24.9, 21.2, 18.8, 16.9, 16.6.

HRMS (ESI): Calcd. for $\text{C}_{17}\text{H}_{29}\text{O}_4[(\text{M}+\text{H}^+)]$ 297.2060, found 297.2057.

Data for compound 159

^1H NMR(400 MHz, CDCl_3) δ 4.28 (dd, $J=12$, 4.4 Hz, 1H), 4.00 (dd, $J=12$, 6.4 Hz, 1H), 2.98 (dd, $J= 6.8$, 4.0 Hz, 1H), 2.69 (m, 2H), 2.07 (s, 3H), 1.80-1.50 (m, 6H), 1.30 (s, 3H), 1.27 (s, 3H), 1.24 (s, 3H), 1.23 (s, 3H).

Bromination of diepoxy acetate 158



To a solution of farnesyl diepoxy acetate **158** (5.40 g, 18.3 mmol) in 20 mL of anhydrous MeOH was added powdered K_2CO_3 (252 mg, 1.83 mmol) at room temperature. After stirring for 30-60 min, solid NH_4Cl (120 mg, 2.19 mmol) was added to neutralize the reaction mixture. Et_2O (20 mL) was added to facilitate the precipitation of the salts, which was removed by filtration through a celite. Removal of solvents using rotary evaporation afforded crude diepoxy allylic alcohol, which passed through a very short column (100 mL of silica gel, eluents: 1:1 mixture of hexane: EtOAc) or was used for next step without further purification. To the solution of resulting alcohol obtained above in 60 mL of THF was added Et_3N (4.95 mL, 36.6 mmol) and MsCl (1.80 mL, 23.9 mmol), successively, at $-40\text{ }^\circ\text{C}$ (mesitylene-dry ice). After stirring 45 min at $-40\text{ }^\circ\text{C}$, the reaction mixture was allowed to warm up to $0\text{ }^\circ\text{C}$, and a solution of lithium bromide (LiBr, 6.38 g, 73.5 mmol, flame-dried under vacuum) in 14 mL of THF was added. After stirring for 1 hour at $0\text{ }^\circ\text{C}$, The reaction mixture was diluted with hexane (30 mL) and cold water(30 mL). The organic layer was collected and the aqueous layer was extracted with hexane (2 x 50 mL). The combined organic fractions were washed with brine (80 mL) and dried over anhydrous $MgSO_4$. Rotary evaporation of solvents gave the crude product **150**, which went through a

very short silica gel column and was used for the next step without further purification (3.44 g, 60%).

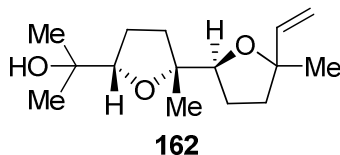
$[\alpha]_D = +7.3$ (c 1.1, CHCl_3).

IR (neat, cm^{-1}): 2961.2, 2925.5, 1656.6, 1456.0, 1379.8, 1250.6, 1202.4, 1121.4, 872.6.

^1H NMR (400 MHz, CDCl_3) δ 5.52 (m, 1H), 4.08 (d, $J=8$ Hz, 1H), 4.00 (d, $J=8$ Hz, 1H), 2.71 (q, $J=6.0, 5.2, 6.4$ Hz, 2H), 2.28-2.12 (m, 2H), 1.74 (s, 3H), 1.70-1.52 (m, 6H), 1.30 (s, 3H), 1.27 (s, 3H), 1.26 (s, 3H).

^{13}C NMR (100 MHz, CDCl_3) δ 142.6, 121.3, 64.0, 62.7, 60.5, 58.6, 41.0, 36.4, 35.3, 29.4, 26.9, 25.0, 24.7, 18.8, 16.9.

HRMS (ESI): Calcd. for $\text{C}_{15}\text{H}_{26}\text{O}_2\text{Br}[(\text{M}+\text{H}^+)]$ 317.1111, found 317.1109.

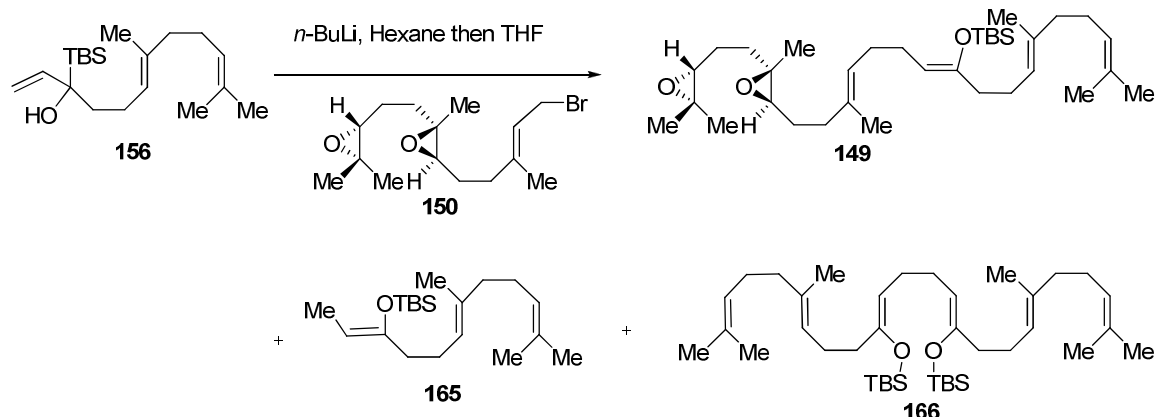


Data for compound 162

^1H NMR (600 MHz, CDCl_3) δ 5.83 (dd, $J = 16.8, 10.2$ Hz, 1H), 5.18 (d, $J=17.4$ Hz, 1H), 4.95 (d, $J=10.2$ Hz, 1H), 4.02 (t, $J = 7.2$ Hz, 1H), 3.82 (dd, $J = 7.8, 4.8$ Hz, 1H), 3.76 (s, 1H), 2.14 (m, 1H), 2.08 (m, 1H), 2.00-1.64 (m, 4H), 1.58 (m, 1H), 1.51 (m, 1H), 1.28 (s, 3H), 1.22 (s, 3H), 1.12 (s, 3H), 1.05 (s, 3H).

^{13}C NMR (150 MHz, CDCl_3) δ 143.6, 111.5, 85.9, 85.6, 84.4, 83.3, 72.0, 37.4, 31.6, 28.3, 28.0, 27.1, 26.5, 25.3, 24.7.

Brook rearrangement and alkylation of the resulting homoenolate with 150



To a hexane solution of $n\text{-BuLi}$ (3.52 mL, 8.80 mmol, 2.5 M in hexane) was added a hexane (8.0 mL) solution of allylic alcohol **156** (2.58 g, 8.00 mmol) at $-78\text{ }^{\circ}\text{C}$ and the solution was stirred for 20 min at this temperature. THF (32 mL) was then slowly added along the sidewall of the flask and the resulting light yellow solution was stirred for 1 hour at $-78\text{ }^{\circ}\text{C}$. A THF (30 mL) solution of allylic bromide **150** (3.06 g, 9.60 mmol) was then cannulated slowly to the reaction mixture, which was then allowed to warm up to $-40\text{ }^{\circ}\text{C}$ and stirred for another 3 hours at $-40\text{ }^{\circ}\text{C}$, and then was placed in the freezer for overnight at $-20\text{ }^{\circ}\text{C}$. The reaction was diluted with Et_2O (30 mL), quenched with H_2O (20 mL) at $-20\text{ }^{\circ}\text{C}$ and warmed up to room temperature. The organic fraction was collected and the aqueous layer was extracted with hexane (2 x 50 mL). The combined organic extracts were washed with brine (80 mL) and dried over anhydrous MgSO_4 . After rotary evaporation of solvents, the residue was purified by column chromatography on silica gel (gradient eluents from 1% to 10% of EtOAc in Hexane) gave the corresponding product **149** (2.23 g, 50%) as a colorless oil, along with **165** (128 mg, 5%) and **166** (411 mg, 8%).

Data for compound 149

$[\alpha]_D = +7.3$ (c 0.345, CHCl_3).

IR (neat, cm^{-1}): 2958.3, 2928.4, 2857.0, 1672.0, 1451.2, 1377.9, 1252.5, 1139.7, 836.9.

^1H NMR (400 MHz, CDCl_3) δ 5.15 (t, $J=6.8, 6.4$ Hz, 1H), 5.07 (m, 2H), 4.41 (t, $J=6.4$ Hz, 1H), 2.70 (m, 2H), 2.12 (q, $J=7.2, 7.6$ Hz, 4H), 2.07-1.90 (m, 12H), 1.80-1.70 (m, 1H), 1.65 (s, 3H), 1.59 (s, 3H), 1.58 (s, 6H), 1.56 (s, 3H), 1.29 (s, 3H), 1.25 (q, $J=2.8, 2.0$ Hz, 6H), 0.92 (s, 9H), 0.10 (s, 6H).

^{13}C NMR (100 MHz, CDCl_3) δ 150.5, 135.5, 134.2, 131.5, 125.4, 124.5, 123.9, 107.8, 64.1, 63.3, 60.5, 58.6, 39.9, 36.9, 36.5, 35.5, 28.6, 27.5, 26.9, 26.1, 26.1, 26.1, 25.9, 25.7, 25.1, 25.0, 24.9, 18.9, 18.5, 17.9, 16.9, 16.6, 16.2, -3.7, -3.7 .

HRMS (ESI): Calcd. for $\text{C}_{35}\text{H}_{63}\text{O}_3\text{Si}[(\text{M}+\text{H}^+)]$ 559.4541, found 559.4534.

Data for compound 165

IR (neat, cm^{-1}): 2958, 2929, 2858, 1677, 1462, 1446, 1381, 1330, 1254, 1191, 1045, 836.

^1H NMR (400 MHz, CDCl_3) δ 5.12 (m, 2H), 4.52 (ddd, $J = 12.8, 6.8, 6.0$ Hz, 1H), 2.20-1.88 (m, 8H), 1.69 (s, 3H), 1.61 (s, 6H), 0.98 (s, 9H), 0.91 (s, 3H), 0.15 (s, 6H).

^{13}C NMR (100 MHz, CDCl_3) δ 151.2, 135.5, 131.5, 124.6, 124.0, 102.0, 39.9, 36.9, 26.9, 26.3, 26.1 (3C), 26.0, 25.9, 17.9, 16.2, 11.0, -3.7, -3.7.

Data for compound 166

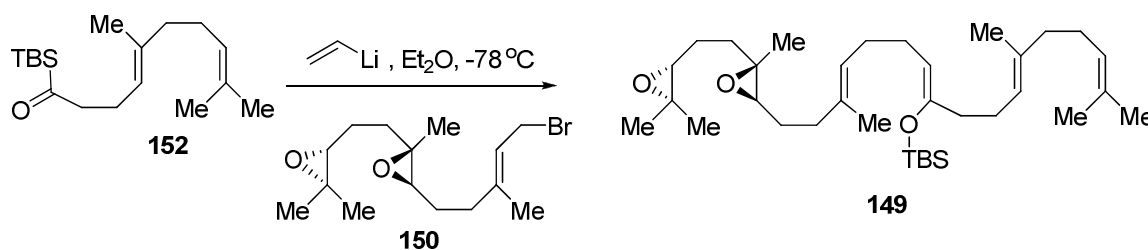
IR (neat, cm^{-1}): 2957, 2928, 2857, 1672, 1462, 1361, 1253, 1171, 836, 777.

^1H NMR (400 MHz, CDCl_3) δ 5.12 (m, 2H), 4.44 (t, $J = 6.8$ Hz, 1H), 2.20-1.88 (m, 8H), 1.69 (s, 3H), 1.61 (s, 6H), 1.29 (m, 4H), 0.97 (s, 9H), 0.14 (s, 6H).

^{13}C NMR (100 MHz, CDCl_3) δ 150.0, 135.5, 131.5, 124.6, 124.0, 108.5, 39.9, 36.9, 31.9, 29.9, 26.9, 26.3, 26.1 (6C), 25.9, 25.5, 22.8, 18.5, 17.9, 16.3, 14.3, -3.8 (4C).

Alternatively, the compound **149** was prepared in one-pot procedure from acylsilane **152** and allylic bromide **143** by following Corey's protocol.¹³

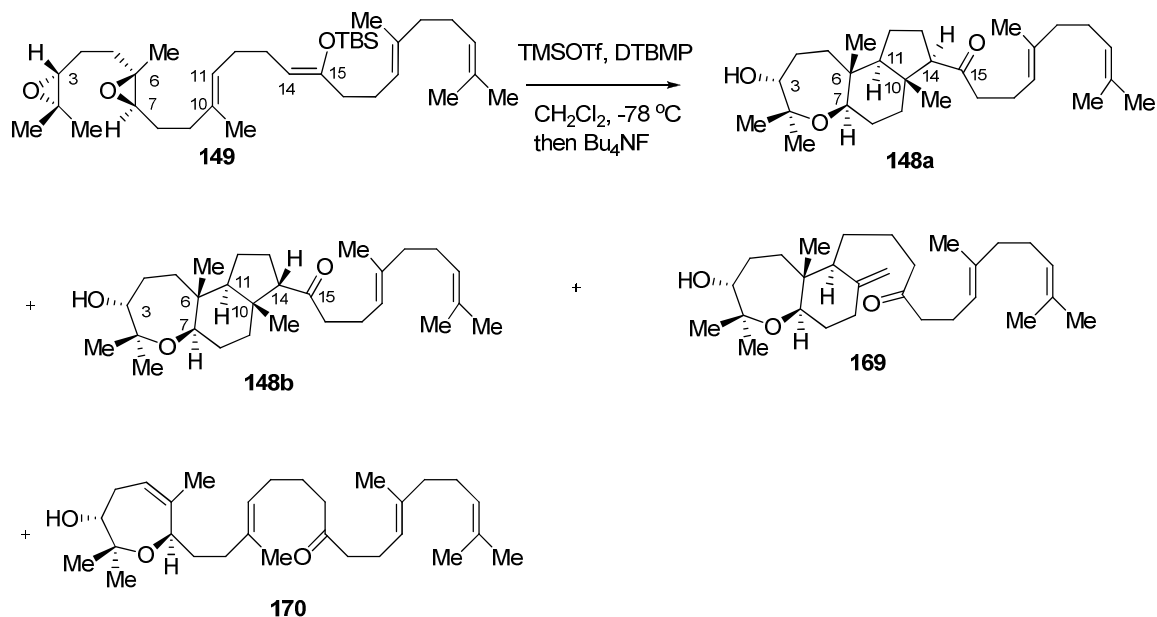
One-pot preparation of 142



To a diethyl ether (2 mL) solution of vinyl lithium (0.81 mL, 0.30 mmol, 0.37 M in THF, prepared from tetravinyltin and *n*-BuLi) was added an Et_2O (2 mL) solution of acylsilane **152** (58.8 mg, 0.20 mmol) at -78°C and the solution was stirred for 2 hours at this temperature. A THF (2 mL) solution of allylic bromide **150** (63.6 mg, 0.20 mmol) was then added slowly along the flask wall and the reaction mixture was stirred for another 3 hours at -40°C . The reaction was diluted with Et_2O (4 mL) and quenched with H_2O (4 mL) at -40°C . The organic fraction was collected and the aqueous layer was extracted with hexane (2 x 5 mL). The combined organic extracts were washed with brine (8 mL) and dried over anhydrous MgSO_4 . After rotary evaporation of solvents, the residue was purified

by column chromatography on silica gel (gradient eluents from 1% to 10% of EtOAc in Hexane) gave the corresponding product **149** (20 mg, 18%) as a colorless oil as well as recovery of allylic bromide **150** (32 mg).

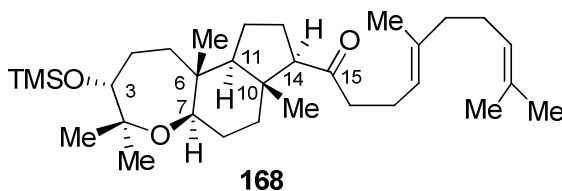
Cascade oxa-carbocyclization of diepoxy enol alkene 149



Procedure A: To a solution of diepoxy silyl enol ether **149** (2.20 g, 3.94 mmol) in CH₂Cl₂ (200 mL) was added 2,6-di-*tert*-butyl-4-methylpyridine (DTBMP, 88.8 mg, 0.433 mol) at -78 °C was added TMSOTf (0.783 mL, 4.33 mmol). After 10 min, TBAF (4.33 mL, 1.0 M in THF, 4.33 mmol) was added at -78 °C to reaction mixture. After 30 minutes, the reaction mixture was quenched with saturated NaHCO₃ (50 mL), diluted with hexane (50 mL) and water (50 mL) at -78 °C and warmed up to room temperature. The organic layer was collected and the aqueous layer was extracted with hexane (2 x 80 mL). The combined organic fractions were washed with brine (100 mL) and dried over anhydrous MgSO₄.

Rotary evaporation of solvents gave the crude product, which was shown to be the mixture of silylated products and free alcohols. The desired silylated product of **148a** could be isolated by two times of slow column chromatography on silica gel with gradient eluents. However, better separation could be achieved by desilylation. The mixtures obtained above were dissolved in THF (20 mL) and treated with TBAF (4.50 mL, 1.0 M in THF, 4.50 mmol) at room temperature. After 30 minutes, the reaction was quenched with saturated NH₄Cl (20 mL), and transferred to a separation funnel. The aqueous fraction was extracted with diethyl ether (2 x 50 mL) twice. The combined organic fractions were washed with brine (80 mL) and dried over anhydrous MgSO₄. Column chromatography on silica gel provided the three products: **148a** (875 mg, 50%), **169** (175 mg, 10%), **170** (210 mg, 12%).

Procedure B: To a solution of diepoxy **149** (1.40 g, 2.51 mmol) in CH₂Cl₂ (160 mL) was added 2,6-di-*tert*-butyl-4-methyl pyridine (DTBMP, 56.6 mg, 0.276 mmol) at -78 °C was added TMSOTf (0.498 mL, 2.76 mmol). After 60 min, Sat. NaHCO₃ (30 mL) was then added at -78 °C and reaction mixture was allowed to warm up to room temperature with vigorous stirring over 10 min. More water (100 mL) was added to the reaction mixture. Workup and purification were performed by following the procedure A to provide four major products: **148a** (223 mg, 20%), **148b** (223 mg, 20%), **169** (89 mg, 8%), **170** (111 mg, 10%).



Data for 168, silylated product of 148a

$[\alpha]_D$ -58 (c 0.13, CHCl₃).

IR(neat, cm⁻¹): 2959.3, 2937.1, 2857.0, 2728.8, 1707.7, 1446.4, 1376.9, 1250.6, 1099.2, 873.6, 839.9.

¹H NMR(400 MHz, CDCl₃) δ 5.08 (m, 2 H), 3.72 (d, $J=6.4$ Hz, 1H), 3.61 (dd, $J=11.6, 4.4$ Hz, 1H), 2.46 (t, $J=9.2$ Hz, 1H), 2.37 (t, $J=8.0$ Hz, 1H), 2.38 (m, 1H), 2.24 (m, 3H), 2.04 (m, 3H), 1.96 (m, 3H), 1.85 (m, 1H), 1.69 (s, 3H), 1.61 (s, 3H), 1.60 (s, 3H), 1.57-1.40 (m, 4H), 1.30-1.18 (m, 5H), 1.15 (s, 3H), 1.11 (s, 3H), 0.84 (s, 3H), 0.71 (s, 3H), 0.11(s, 9H).

¹³C NMR(100 MHz, CDCl₃) δ 211.5, 136.3, 131.6, 124.5, 123.2, 78.6, 77.8, 77.0, 64.2, 60.0, 44.4, 44.3, 41.2, 39.9, 38.2, 35.6, 29.1, 28.2, 26.9, 26.2, 25.9, 23.1, 22.9, 22.5, 20.4, 17.9, 16.2, 15.3, 13.2, 0.2, 0.2, 0.2.

HRMS (ESI): Calcd for C₃₂H₅₇O₃Si[(M+H⁺)] 517.4072, found 517.4066.

Data for compound 148a

$[\alpha]_D$ -28.5 (c 0.785, CHCl₃).

IR(neat, cm⁻¹): 3501.2, 2968.9, 2933.2, 1702.8, 1446.6, 1376.9, 1092.5.

¹H NMR(400 MHz, CDCl₃) δ 5.07 (m, 2 H), 3.82 (dd, $J=6.6, 3.8$ Hz, 1H), 3.59 (dd, $J=11.4, 4.6$ Hz, 1H), 2.42 (m, 1H), 2.34 (d, $J=8.0$ Hz, 1H), 2.35 (m, 1H), 2.24 (m, 3H), 2.03 (m, 3H), 1.96 (m, 3H), 1.86 (m, 1H), 1.68 (s, 3H), 1.60 (s, 3H), 1.59 (s, 3H), 1.65-1.40 (m, 8H), 1.35-1.20 (m, 2H), 1.28 (s, 3H), 1.14 (s, 3H), 0.87 (s, 3H), 0.71 (s, 3H).

^{13}C NMR(100 MHz, CDCl_3) δ 211.5, 136.3, 131.6, 124.4, 123.1, 78.2, 77.5, 77.3, 64.1, 59.8, 44.3, 44.3, 41.3, 39.9, 38.1, 35.3, 29.1, 28.3, 26.8, 25.9, 25.5, 23.1, 22.5, 22.0, 20.3, 17.9, 16.2, 15.3, 13.1.

HRMS (ESI): Calcd for $\text{C}_{29}\text{H}_{49}\text{O}_3$ [(M+H⁺)] 445.36762, found 445.36633.

Data for compound 148b

$[\alpha]_{\text{D}}=+31.5$ (c 1.465, CHCl_3).

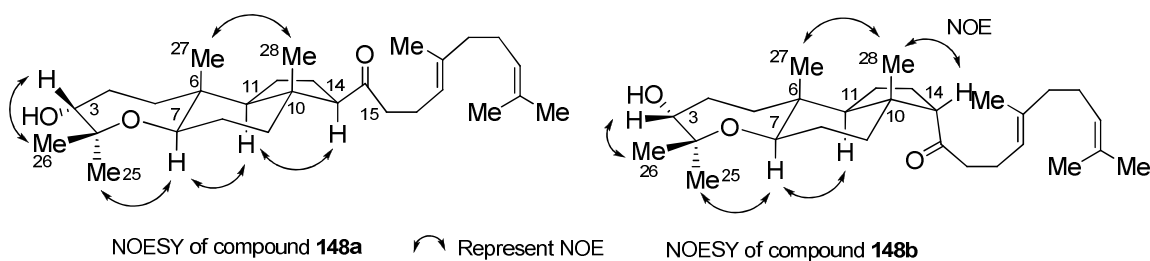
IR (neat, cm^{-1}): 3506.9, 2967.0, 2935.1, 1703.8, 1445.4, 1378.9, 1090.6.

^1H NMR (400 MHz, CDCl_3) δ 5.08 (m, 2 H), 3.77 (dd, $J=6.4, 2.4$ Hz, 1H), 3.47 (dd, $J=11.2, 4.8$ Hz, 1H), 2.63 (dd, $J=8.4, 2.8$ Hz, 1H), 2.50-2.10 (m, 5H), 2.04 (m, 3H), 1.97 (m, 3H), 1.88 (m, 1H), 1.68 (s, 3H), 1.61 (s, 3H), 1.60 (s, 3H), 1.8-1.40 (m, 8H), 1.25 (m, 1H), 1.23 (s, 3H), 1.11 (s, 3H), 1.05 (s, 3H), 0.85 (s, 3H).

^{13}C NMR (100 MHz, CDCl_3) δ 214.7, 136.3, 131.6, 124.4, 123.0, 78.2, 77.5, 77.2, 61.7, 53.5, 46.2, 45.9, 41.0, 39.9, 35.5, 33.9, 29.2, 28.3, 26.9, 25.9, 25.8, 24.6, 23.8, 22.4, 22.0, 21.9, 17.9, 16.2, 13.5.

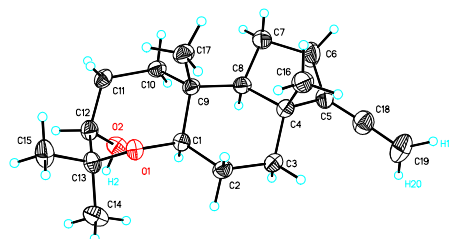
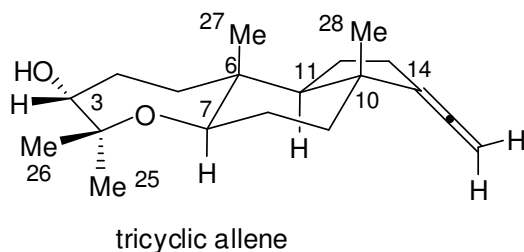
HRMS (ESI): Calcd for $\text{C}_{29}\text{H}_{49}\text{O}_3$ [(M+H⁺)] 445.36762, found 445.36815.

Noesy NMR experiments for stereochemistry confirmation of **148a** and **148b**:



NMR spectrum comparison of **148a** and **148b** with known compound tricyclic allene (X-ray)⁵.

For 2-D NMR spectra of 148a and 148b, see page 159-162.



Tricyclic allene	compound 148a	compound 148b
<u>$^1\text{H NMR}$ (400 MHz, δ)</u>	<u>$^1\text{H NMR}$ (400 MHz, δ)</u>	<u>$^1\text{H NMR}$ (400 MHz, δ)</u>
H-3:		
3.80(dd, $J=6.6, 3.6$ Hz, 1H)	3.82(dd, $J=6.6, 3.8$ Hz, 1H)	3.77(dd, $J=6.4, 2.4$ Hz, 1H)
H-7:		
3.58(dd, $J=11.4, 4.8$ Hz, 1H)	3.59(dd, $J=11.4, 4.6$ Hz, 1H)	3.47(dd, $J=11.2, 4.8$ Hz, 1H)
Me-25: 1.26 (s, 3H)	1.28 (s, 3H)	1.23 (s, 3H)
Me-26: 1.13 (s, 3H)	1.14 (s, 3H)	1.11 (s, 3H)
Me-27: 0.87 (s, 3H)	0.87 (s, 3H)	0.85 (s, 3H).
Me-28: 1.01 (s, 3H)	0.71 (s, 3H)	1.05 (s, 3H)
<u>$^{13}\text{C NMR}$ (100MHz, δ)</u>	<u>$^{13}\text{C NMR}$ (100MHz, δ)</u>	<u>$^{13}\text{C NMR}$ (100MHz, δ)</u>
C-2: 78.2	78.2	78.2
C-3: 76.8	77.3	77.2
C-7: 77.8	77.5	77.5
C-25: 21.9	22.0	22.0
C-26: 29.2	29.1	29.2
C-27: 13.4	13.1	13.5
C-28: 20.9	15.3	16.2

Data for compound 169

IR (neat, cm⁻¹): 3491.5, 3077.9, 2966.9, 293.2, 1709.6, 1644.0, 1443.5, 1377.0, 1082.8, 1060.7.

¹H NMR (400 MHz, CDCl₃) δ 5.07 (m, 2 H), 4.87(d, *J*=1.2 Hz, 1H), 4.58 (s, 1H), 3.81 (dd, *J*=6.8, 3.6 Hz, 1H), 3.68 (dd, *J*=11.8, 5.0 Hz, 1H), 2.41 (dd, *J*=15.2, 7.6 Hz, 2H), 2.39 (m, 3H), 2.26 (m, 4H), 2.05 (m, 3H), 1.97 (m, 5H), 1.68 (s, 3H), 1.62 (s, 3H), 1.61 (s, 3H), 1.60 (s, 3H), 1.80-1.44 (m, 2H), 1.44-1.18 (m, 2H), 1.27 (s, 3H), 1.11 (s, 3H), 0.69 (s, 3H).

¹³C NMR (100 MHz, CDCl₃) δ 211.3, 147.0, 136.5, 131.6, 124.4, 122.9, 107.7, 77.8, 77.1, 76.1, 52.5, 43.5, 43.5, 42.9, 39.9, 35.8, 34.0, 33.0, 29.3, 26.8, 26.3, 25.9, 24.3, 23.3, 22.7, 21.4, 17.9, 16.2, 12.3.

HRMS (ESI): Calcd. for C₂₉H₄₉O₃ [(M+H⁺)] 445.36762, found 445.36728.

Data for compound 170

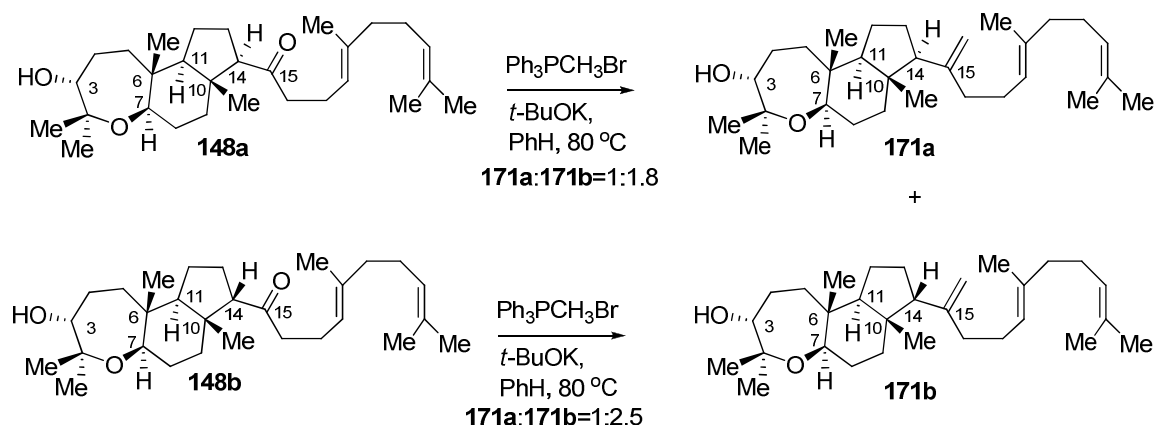
IR (neat, cm⁻¹): 3482.0, 2966.0, 2927.4, 2859.9, 1712.5, 1448.3, 1375.0, 1099.2, 1076.1.

¹H NMR (400 MHz, CDCl₃) δ 5.50 (m, 1 H), 5.14 (t, *J*=6.4 Hz, 1H), 5.07 (m, 2H), 3.96 (d, *J*=9.6 Hz, 1H), 3.41 (dd, *J*=11.0, 3.4 Hz, 1H), 2.41 (ddd, *J*=14, 7.6, 7.2 Hz, 5H), 2.25 (m, 3H), 2.18-1.82 (m, 10H), 1.72-1.58 (m, 3H), 1.68 (s, 3H), 1.64 (s, 3H), 1.61 (s, 3H), 1.61 (s, 3H), 1.60 (s, 3H), 1.26 (s, 3H), 1.16 (s, 3H).

^{13}C NMR(100 MHz, CDCl_3) δ 211.3, 136.5, 135.7, 135.7, 131.6, 124.4, 124.4, 122.9, 119.4, 76.8, 72.6, 71.9, 43.0, 42.5, 39.9, 36.5, 29.8, 27.6, 27.0, 26.8, 25.9, 25.6, 24.2, 24.1, 22.6, 20.1, 17.9, 16.3, 16.2.

HRMS (ESI): Calcd. for $\text{C}_{29}\text{H}_{49}\text{O}_3$ [(M+H⁺)] 445.36762, found 445.36841.

Wittig methylenation of ketone **148**^{20c}



General procedure: To a suspension solution of methyltriphenylphosphonium bromide (804 mg, 2.25 mmol) in benzene (15 mL) was added potassium *tert*-butoxide (1.0 M in THF, 2.25 mL, 2.25 mmol) at room temperature. The resulting mixture was heated to 90 °C (external temperature, refluxing) for 15 minutes. Then yellow solution was cooled down to 50 °C and the ketone **148** (100 mg, 0.225 mmol) in benzene (4 mL) was added. Refluxing was continued for 2-4 hours (checked by TLC). The reaction mixture then was cooled to room temperature and went through a short silica gel column (filtration to remove salt) under pressure and washed the column with diethyl ether. After evaporating the solvents, the residue was chromatographed on silica gel(hexane to 25% Et_2O in hexane) to give **171a** and **171b** (85 mg) as a colorless oil in 82 % yield.

The Wittig olefination seems to epimerize at the ketone α chiral center. Other methods that have been attempted without success included: Petasis, modified Julia (tetrazole sulfone), Tebbe reagent.

Data for compound 171a

$[\alpha]_D^{25} = +22.0$ (c 0.375, CHCl_3).

IR (neat, cm^{-1}): 3452.0, 3074.0, 2964.1, 2931.3, 2877.3, 1639.2, 1446.4, 1378.9, 1087.7, 889.0.

^1H NMR (400 MHz, CDCl_3): δ 5.10 (m, 2H), 4.88 (s, 1H), 4.61 (s, 1H), 3.80 (dd, $J=6.4, 3.2$ Hz, 1H), 3.45 (dd, $J=11.8, 4.6$ Hz, 1H), 2.25-1.80 (m, 12H), 1.80-1.38 (m, 9H), 1.68 (s, 3H), 1.61 (s, 3H), 1.60 (s, 3H), 1.25 (s, 3H), 1.23 (s, 3H), 1.01 (s, 3H), 0.88 (s, 3H).

^{13}C NMR (100 MHz, CDCl_3): δ 154.3, 135.3, 131.5, 124.6, 124.4, 109.3, 78.1, 77.8, 77.5, 56.3, 52.0, 44.9, 41.0, 39.9, 39.4, 35.6, 33.5, 29.3, 28.4, 28.4, 27.1, 26.9, 25.9, 25.7, 24.0, 22.0, 21.3, 17.9, 16.2, 13.2.

HRMS (ESI): Calcd. for $\text{C}_{30}\text{H}_{50}\text{O}_2$ $[(\text{M}+\text{H}^+)]$ 443.38836, found 443.38913.

Data for compound 171b

$[\alpha]_D^{25} = +8.2$ (c 0.305, CHCl_3).

IR (neat, cm^{-1}): 3450.0, 3077.9, 2966.0, 2931.3, 2877.3, 1639.2, 1446.4, 1378.9, 1091.5, 1054.9, 889.0.

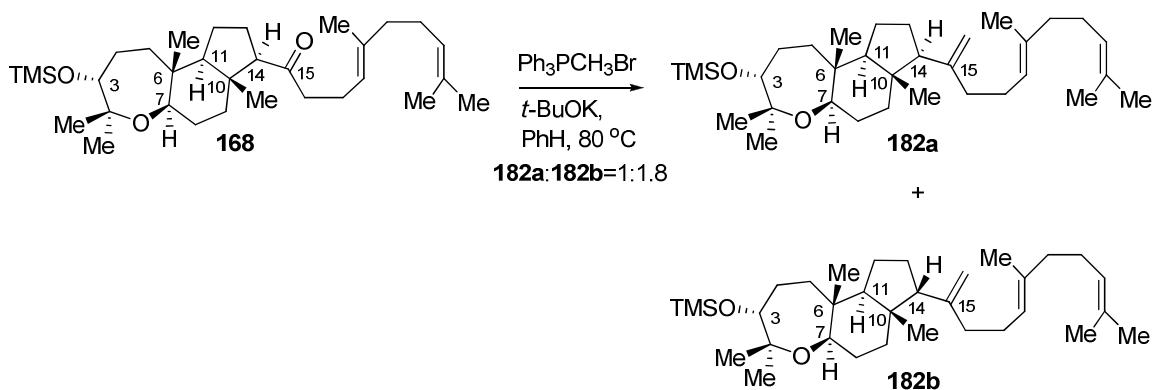
^1H NMR (400 MHz, CDCl_3): δ 5.10 (m, 2H), 4.90 (s, 1H), 4.74 (s, 1H), 3.82 (dd, $J=6.8, 3.6$ Hz, 1H), 3.56 (dd, $J=11.6, 4.8$ Hz, 1H), 2.25-1.80 (m, 12H), 1.80-1.20

(m, 9H), 1.69 (s, 3H), 1.61 (s, 3H), 1.60 (s, 3H), 1.27 (s, 3H), 1.14 (s, 3H), 0.88 (s, 3H), 0.69(s, 3H).

^{13}C NMR (100 MHz, CDCl_3) δ 149.3, 135.2, 131.5, 124.6, 124.4, 110.4, 78.2, 78.0, 77.5, 59.6, 56.9, 43.2, 41.3, 39.9, 37.9, 37.7, 35.2, 29.2, 28.5, 27.2, 26.9, 26.0, 25.9, 25.6, 22.0, 20.0, 17.9, 16.3, 14.4, 13.0.

HRMS (ESI): Calcd. for $\text{C}_{30}\text{H}_{50}\text{O}_2$ [(M+H⁺)] 443.38836, found 443.38844.

Wittig methylenation of ketone 168



Following the general procedure for Wittig methylenation of ketone **148**, ketone **168** was olefinated to provide mixtures of **182a** and **182b**, which were difficult to separate by column chromatography. Mixtures of **182a** and **182b** were used for the next Shi epoxidation for better separation.

Data for compound 182b

IR (neat, cm^{-1}): 3072, 2939, 2877, 1639, 1444, 1378, 1251, 1099, 873, 838.

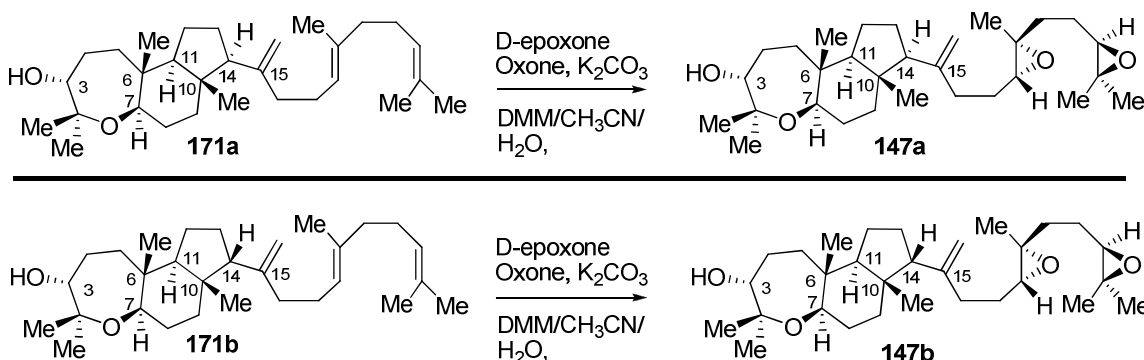
^1H NMR (400 MHz, CDCl_3): δ 5.10 (m, 2H), 4.88 (s, 1H), 4.61 (s, 1H), 3.70 (d, $J=7.2$ Hz, 1H), 3.73 (dd, $J=12.0, 4.4$ Hz, 1H), 2.20-1.80 (m, 12H), 1.80-1.38 (m,

9H), 1.69 (s, 3H), 1.61 (s, 6H), 1.13 (s, 3H), 1.10 (s, 3H), 0.99(s, 3H), 0.86 (s, 3H), 0.09 (s, 6H).

^{13}C NMR (100 MHz, CDCl_3): δ 154.6, 135.3, 131.5, 124.6, 124.4, 108.8, 78.4, 77.8, 77.1, 56.3, 52.1, 44.8, 40.6, 39.9, 39.4, 35.8, 33.5, 28.9, 28.4, 28.2, 27.1, 26.9, 26.2, 25.9, 23.9, 22.9, 21.3, 17.9, 16.2, 13.4, 0.22, 0.12.

HRMS (ESI): Calcd. for $\text{C}_{33}\text{H}_{59}\text{O}_2\text{Si}$ [(M+H⁺)] 515.42789, found 515.42837.

Regio- and stereoselective Shi epoxidation of triene 171



Triene **171a** (50.0 mg, 0.113 mmol), 1,2:4,5-di-*O*-isopropylidene-*D*-*erythro*-2,3-hexodiuro-2,6-pyranose (Shi catalyst, D-epoxone, 14.6 mg, 0.056 mmol), tetrabutylammonium hydrogen sulfate (3.80 mg, 0.011 mmol) and $\text{NaB}_4\text{O}_7 \cdot 10\text{H}_2\text{O}$ (0.05 M in aq. Na_2EDTA (4×10^{-4} M), 2.0 mL) were suspended with vigorous stirring in dimethoxymethane (DMM) : acetonitrile (2 : 1, 3.2 mL) and cooled to -10°C with ice-salt bath. In a three-neck 10 mL flask fitted with two addition funnels, one addition funnel was charged with an aqueous solution of K_2CO_3 (172 mg, 1.24 mmol, in 1.25 mL H_2O), and the second addition funnel was charged with Oxone (192 mg, 0.32 mmol) dissolved in aqueous Na_2EDTA (4×10^{-4} M, 1.25 mL). These solutions were added dropwise and simultaneously

over 90 min from the two addition funnels with the reaction temperature at -5°C . After the additions were complete, the reaction mixture was stirred for 10 min at 0°C . The reaction was then diluted with Et_2O (3.0 mL) and transferred to a separatory funnel. The organic layer was collected and the aqueous layer was extracted with Et_2O (2 x 5.0 mL). The combined organic fractions were washed with brine (10 mL) and dried over anhydrous MgSO_4 . Rotary evaporation of solvents gave the crude product, which was indicated by TLC to be the mixture of starting material triene, monoepoxide, diepoxide and triepoxide. The separation of the mixture by column chromatography on silica gel gave the diepoxide **147a** (20 mg, 37.4%), and monoepoxide (25 mg, with small amount of starting material) and triepoxide (4 mg). The mixture of starting material and monoepoxide was subjected to another epoxidation (second cycle, 0.5 equivalent of the first cycle) and workup as described for the first cycle. The second cycle gave the diepoxide **147a** (6.8 mg). Overall yield is 50%.

$[\alpha]_{\text{D}} = +30.5$ (c 0.31, CHCl_3)

IR (neat, cm^{-1}): 3482.8, 3074.0, 2961.2, 2934.1, 2877.3, 1640.2, 1454.1, 1378.9, 1251.6, 1089.6, 890.9.

^1H NMR (400 MHz, CDCl_3): δ 4.90 (s, 1H), 4.67 (s, 1H), 3.80 (dd, $J=6.6, 3.8$ Hz, 1H), 3.45 (dd, $J=11.6, 4.8$ Hz, 1H), 2.75 (t, $J=6.4$ Hz, 1H), 2.72 (t, $J=6.0$ Hz, 1H), 2.25-1.90 (m, 6H), 1.80-1.38 (m, 15H), 1.31 (s, 3H), 1.29 (s, 3H), 1.27 (s, 3H), 1.25 (s, 3H), 1.23 (s, 3H), 1.01 (s, 3H), 0.88 (s, 3H).

^{13}C NMR (100 MHz, CDCl_3): δ 153.3, 109.9, 78.1, 77.8, 77.4, 64.1, 63.1, 60.5, 58.7, 56.5, 52.1, 44.9, 41.0, 35.8, 35.7, 35.4, 33.5, 29.3, 28.3, 28.3, 27.8, 25.7, 25.1, 24.8, 24.0, 22.0, 21.3, 18.9, 16.9, 13.2

HRMS (ESI): Calcd. for $\text{C}_{30}\text{H}_{51}\text{O}_4[(\text{M}+\text{H}^+)]$ 475.37819, found 475.37933.

The same procedure as diepoxide **171a** was followed to obtain **147b**: **171b** (20 mg, 0.045 mmol), Shi ketone (D-epoxone, 5.8 mg, 0.023 mmol), Oxone (76.4 mg, 0.124 mmol), K_2CO_3 (68.3 mg, 0.495 mmol), Bu_4NHSO_4 (1.5 mg, 4.5 μmol), solvent (AN:DMM=1:2, 1.26 mL), Buffer ($\text{Na}_2\text{B}_4\text{O}_7$, 0.05 M in Na_2EDTA , 0.5 mL). Yield: 56% (12 mg of diepoxide **171b**).

$[\alpha]_{\text{D}}^{25} = +6.6$ (c 0.385, CHCl_3).

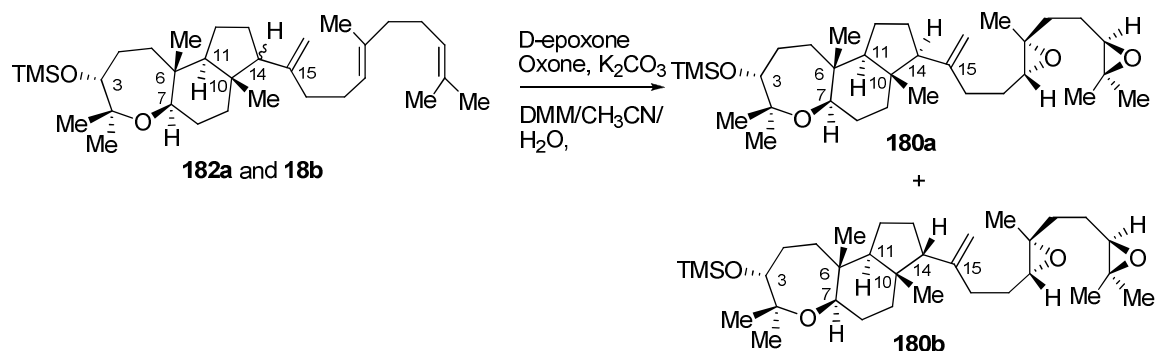
IR (neat, cm^{-1}): 3461.6, 3075.9, 2962.1, 2931.3, 2877.3, 1639.2, 1446.4, 1378.9, 1251.6, 1091.5, 892.9.

^1H NMR (400 MHz, CDCl_3) δ 4.92 (s, 1H), 4.77 (s, 1H), 3.81 (dd, $J=6.6, 3.2$ Hz, 1H), 3.56 (dd, $J=11.4, 5.0$ Hz, 1H), 2.73 (t, $J=5.4$ Hz, 1H), 2.72 (t, $J=5.6$ Hz, 1H), 2.13 (t, $J=7.6$ Hz, 2H), 2.02 (d, $J=10.8$ Hz, 1H), 2.02 (dd, $J=14, 9.2$ Hz, 1H), 1.85-1.40 (m, 16H), 1.36-1.20 (m, 2H), 1.31 (s, 3H), 1.29 (s, 3H), 1.27 (s, 3H), 1.27 (s, 3H), 1.14 (s, 3H), 0.88 (s, 3H), 0.70 (s, 3H).

^{13}C NMR (100 MHz, CDCl_3) δ 148.4, 111.1, 78.2, 77.9, 77.4, 64.1, 63.2, 60.6, 59.6, 56.7, 43.3, 41.3, 37.9, 35.5, 35.1, 34.4, 29.9, 29.2, 28.5, 27.7, 26.0, 25.6, 25.1, 24.8, 22.0, 20.0, 18.9, 17.0, 14.4, 13.0.

HRMS (ESI): Calcd. for $\text{C}_{30}\text{H}_{51}\text{O}_4[(\text{M}+\text{H}^+)]$ 475.37819, found 475.37857.

Regio- and stereoselective Shi epoxidation of triene 182



Shi epoxidation of mixture of **182a** and **182b** was carried out by following the procedure above for Shi epoxidation of **171** to yield **180a** and **180b**, respectively.

Data for compound 180a

IR (neat, cm⁻¹): 3081, 2958, 2939, 2875, 1639, 1444, 1378, 1249, 1097, 1064, 873, 838.

¹H NMR (400 MHz, CDCl₃) δ 4.84 (s, 1H), 4.70 (s, 1H), 3.64 (d, *J*=6.8 Hz, 1H), 3.50 (dd, *J*=11.6, 5.2 Hz, 1H), 2.65 (m, 2H), 2.12-1.30 (m, 22H), 1.23 (s, 3H), 1.20 (s, 3H), 1.19 (s, 3H), 1.18, (s, 3H), 1.02(s, 3H), 0.77 (s, 3H), 0.60 (s, 3H), 0.03 (s, 9H).

¹³C NMR (100 MHz, CDCl₃) δ 148.4, 110.9, 78.5, 77.9, 77.4, 64.1, 63.2, 59.7, 58.7, 43.3, 41.2, 38.0, 35.5, 35.4, 34.4, 29.1, 28.4, 27.8, 26.3, 26.1, 25.1, 24.8, 22.9, 20.1, 19.9, 18.9, 18.1, 17.0, 14.4, 13.1, 0.24 (3C).

HRMS (ESI): Calcd. for C₃₃H₅₉O₄Si[(M+H⁺)] 547.41772, found 547.41795.

Data for compound 180b

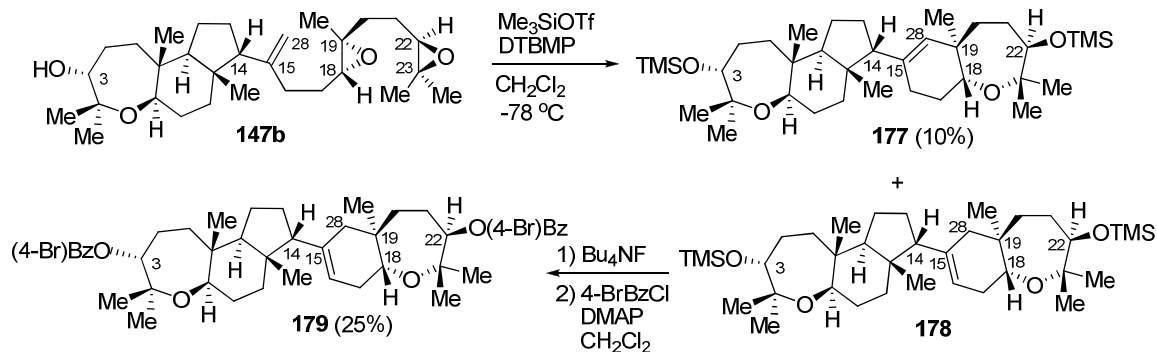
IR (neat, cm⁻¹): 3073, 2956, 2940, 2875, 1639, 1452, 1378, 1249, 1099, 873, 838.

^1H NMR (400 MHz, CDCl_3) δ 4.90 (s, 1H), 4.65 (s, 1H), 3.69 (d, J = 7.2 Hz, 1H), 3.54 (dd, J = 12.0, 4.4 Hz, 1H), 2.73 (m, 2H), 2.21 (m, 1H), 2.15-1.90 (m, 4H), 1.82-1.34 (m, 16H), 1.31 (s, 3H), 1.29 (s, 3H), 1.28 (s, 3H), 1.13 (s, 3H), 1.10 (s, 3H), 1.00 (s, 3H), 0.86 (s, 3H), 0.08 (s, 9H).

^{13}C NMR (100 MHz, CDCl_3) δ 153.9, 109.3, 78.4, 77.8, 77.0, 64.1, 63.2, 60.5, 58.6, 56.3, 52.0, 44.9, 40.6, 36.0, 35.8, 35.4, 33.5, 28.9, 28.5, 28.2, 27.9, 26.2, 25.1, 24.8, 23.9, 22.9, 21.3, 18.9, 16.9, 13.4, 0.13 (3C).

HRMS (ESI): Calcd. for $\text{C}_{33}\text{H}_{59}\text{O}_4\text{Si}[(\text{M}+\text{H}^+)]$ 547.41772, found 547.41782.

Cascade oxa-carbocyclization of diepoxy alkene 147b



To a solution of diepoxy alkene **149b** (25.6 mg, 54 μmol) in 2 mL of CH_2Cl_2 was added 2,6-di-*tert*-butyl-4-methyl pyridine (DTBMP, 17 mg, 81 μmol) at -78°C was added TMSOTf (14 μL , 81 μmol). Reaction mixture was stirred for another 30 min. Sat. NaHCO_3 was then added at -78°C . The reaction mixture was diluted with hexane (5 mL) and cold water (5 mL). The organic layer was collected and the aqueous layer was extracted with hexane (2 x 10 mL). The combined organic fractions were washed with brine (10 mL) and dried over anhydrous MgSO_4 . Rotary evaporation of solvents gave the crude product, which was purified with

silica gel column to give product **177** (6.3 mg, 20%) and impure **178** (10 mg, 30%). The impure **178** was desilylated with tetrabutylammonium fluoride in THF at room temperature for 1 hour, followed by esterification with 4-bromobenzoyl chloride in the presence of dimethylamino pyridine (DMAP) in dichloromethane at room temperature for 24 hours, to afford **179** (11.4 mg, 25%).

Data for compound 177

$[\alpha]_D^{25} = +28.0$ (c 0.145, CHCl₃).

IR (neat, cm⁻¹): 2935.1, 2875.4, 1442.5, 1378.9, 1249.7, 1093.4, 873.6, 838.9

¹H NMR (600 MHz, CDCl₃) δ 4.91 (s, 1H), 3.79 (dd, $J=12.6, 3.6$ Hz, 1H), 3.74(d, $J=4.8$ Hz, 1H), 3.70 (d, $J=6.6$ Hz, 1H), 3.52(dd, $J=11.7, 4.5$ Hz, 1H), 2.40-1.90 (m, 7H), 1.75 (m, 2H), 1.64-1.48 (m, H), 1.48-1.42 (m, 2H), 1.42-1.35 (m, 4H), 1.17 (s, 3H), 1.14 (s, 3H), 1.13 (s, 3H), 1.10 (s, 3H), 0.97 (s, 3H), 0.96 (s, 3H), 0.85 (s, 3H), 0.09 (s, 9H), 0.088 (s, 9H).

¹³C NMR (100 MHz, CDCl₃) δ 137.8, 132.6, 78.7, 78.4, 77.9, 77.9, 77.9, 77.5, 74.0, 56.3, 52.4, 45.1, 40.9, 39.6, 35.9, 34.8, 33.3, 29.9, 29.1, 28.3, 27.7, 27.4, 26.7, 26.3, 23.8, 23.4, 22.9, 21.3, 20.8, 13.3, 0.2 (6 C).

HRMS (ESI): Calcd. for C₃₆H₆₇O₄Si₂[(M+H⁺)] 619.45724, found 619.45697.

Data for compound 179

$[\alpha]_D^{25} = +9.0$ (c 0.25, CHCl₃).

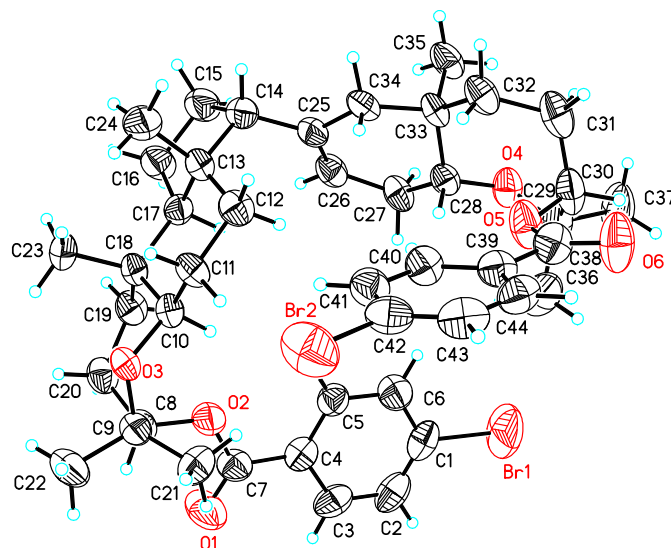
IR (neat, cm⁻¹): 2923.6, 2854.1, 1722.1, 1589.1, 1446.4, 1270.9, 1170.6, 1101.2, 1012.5, 756.0.

^1H NMR (600 MHz, CDCl_3) δ 7.91 (d, $J=7.8$ Hz, 4H), 7.58 (dd, $J=15.6$, 8.4 Hz, 4H), 5.21 (d, $J=7.2$ Hz, 1H), 5.19 (d, $J=7.8$ Hz, 1H), 5.18 (s, 1H), 3.88 (dd, $J=9.6$, 6.6 Hz, 1H), 3.51 (dd, $J=12.0$, 4.8 Hz, 1H), 2.22 (m, 1H), 2.11 (m, 3H), 2.18-1.92 (m, 8H), 1.82-1.71 (m, 2H), 1.64-1.42 (m, 8H), 1.38 (m, 2H), 1.33 (s, 3H), 1.32 (s, 3H), 1.30 (s, 3H), 1.28 (s, 3H), 1.01 (s, 3H), 0.96 (s, 3H), 0.96 (s, 3H), 0.94 (s, 9H).

^{13}C NMR (100 MHz, CDCl_3) δ 165.0, 164.9, 139.6, 132.1, 132.1, 131.1, 131.0, 129.5, 129.4, 128.5, 128.4, 119.4, 80.7, 80.5, 78.7, 78.0, 77.4, 73.1, 57.7, 53.9, 45.1, 41.1, 37.3, 37.2, 36.9, 33.7, 32.6, 29.9, 29.4, 29.2, 28.6, 27.5, 24.2, 23.8, 23.5, 22.4, 21.9, 21.6, 18.6, 13.4.

HRMS (ESI): Calcd. for $\text{C}_{44}\text{H}_{57}\text{O}_6$ $^{79}\text{Br}^{81}\text{Br}$ [(M+H⁺)] 841.24959, found 841.24898.

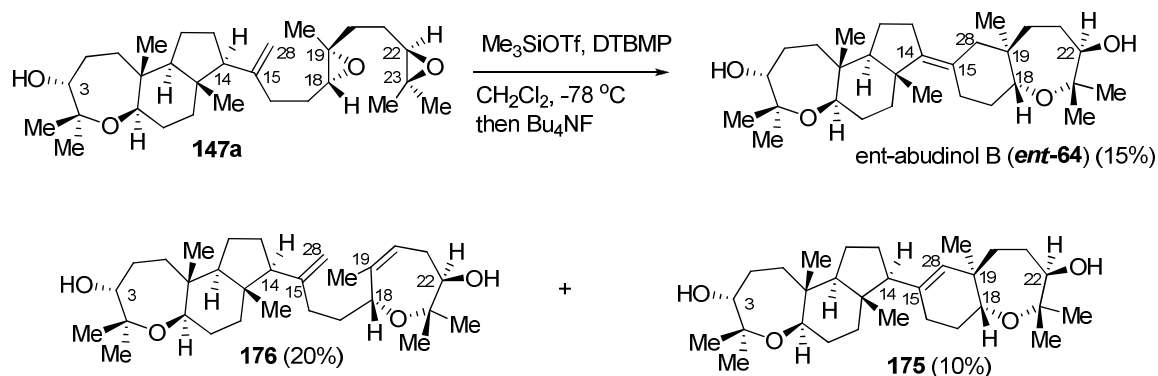
The structure of **179** was substantiated by X-Ray analysis: The thermal ellipsoid diagram was shown below:



For X-ray data of compound 179, see page 206-219.

Cascade oxa-carbocyclization of diepoxy alkene **147a** to furnish *ent*-

abudinol B



Diepoxy alkene **147a** (20 mg, 42 μmol) was dissolved in CH_2Cl_2 (4 mL), 2,6-di-*tert*-butyl-4-methylpyridine (DTBMP, 35 mg, 168 μmol) was added, and the solution was cooled to -78°C . TMSOTf (16 μL , 93 μmol) was added with stirring. After 60 min at -78°C , TBAF (1.0 M in THF, 186 μL , 186 μmol) was added at -78°C , and the reaction mixture was stirred at -78°C for another 30 min. Sat. NaHCO_3 was then added at -78°C . The reaction mixture was diluted with CH_2Cl_2 (5 mL) and cold water (5 mL) and warming to room temperature. The organic layer was collected and the aqueous layer was extracted with CH_2Cl_2 (2 x 10 mL). The combined organic fractions were washed with brine (20 mL) and dried over anhydrous MgSO_4 . Rotary evaporation of solvents gave the crude product, which was purified with silica gel column to give product *ent*-abudinol B (**ent-64**) (3.0 mg, 15%), compound **175** (2.0 mg, 10%) and compound **176** (4.0 mg, 20%). A small amount of an isomer attributed to be the 15-16 alkene isomer of **175** was observed but could not be purified to the extent required for unambiguous characterization.

Comparative characterization data for *ent*-abudinol B (**ent-64**):

Naturally occurring product 1st generation synthesis 2nd generation synthesis

$[\alpha]_D -5.0$ (c 0.05, MeOH) $+23$ (c 0.05, MeOH) $+20$ (c 0.05, MeOH)

IR (neat, cm⁻¹):

3484 (O-H stretches)	3460	3450
2950 (C-H stretches)	2970,2930	2971, 2931
<i>C-H stretches not reported</i>	2868	2871
1446 (C-H stretches)	1446	1456, 1447
	1376 (C-H methyl bend)	1376
	1359 (C-H methyl bend)	1361
	1076 (C-O stretch)	1076
	1036 (C-O stretch)	1056
1023(C-O stretch)	1024	1024

¹H NMR (500 MHz, C₆D₆, δ): (400 MHz, C₆D₆, δ): (600 MHz, C₆D₆, δ):

H-7:

3.75(dd, *J* =10.5, 5.1 Hz, 1H) 3.77(dd, *J* =10.8, 5.2 Hz, 1H) 3.77(dd, *J* =10.8, 5.2 Hz, 1H)

H-18:

3.66(dd, *J* =11.9, 4.6 Hz, 1H) 3.69(dd, *J* =12.0, 4.8 Hz, 1H) 3.68(dd, *J* =12.0, 4.8 Hz, 1H)

H-3: 3.36 (d, *J* =6.8, 1H) 3.38 (d, *J* =6.8, 1H) 3.36 (d, *J* =6.4, 1H)

H-23: 3.36 (d, *J* =6.8, 1H) 3.38 (d, *J* =6.8, 1H) 3.36 (d, *J* =6.4, 1H)

H-O not reported 3.01 (s, OH) 3.00 (s, OH)

CH or CH₂ not reported 2.74(dt, *J* =9.2, 2.4 Hz, 1H) 2.73 (dt, *J* =9.2, 2.4 Hz, 1H)

not reported 2.36(t, *J* =6.8 Hz, 2H) 2.34(m, 2H)

not reported 2.31-2.19(m, 1H) 2.22 (dd, *J* =13.2, 2.8 Hz, 1H)

not reported 2.10 (dt, *J* =9.6, 4.0 Hz, 1H) 2.09 (dt, *J* =9.6, 4.0 Hz, 1H)

not reported 2.01-1.89 (m, 2H) 2.01-1.89 (m, 2H)

<i>not reported</i>	1.89-1.28 (m, 14H)	1.89-1.28 (m, 14H)	
<i>not reported</i>	0.91(t, $J=7.2, 6.8, 2\text{H}$)		
H-27	1.19 (s, 3H) 1.21 (s, 3H)	1.20 (s, 3H)	
H-25	1.18 (s, 3H) 1.20 (s, 3H)	1.19 (s, 3H)	
H-26	1.08 (s, 3H) 1.09 (s, 3H)	1.09 (s, 3H)	
H-28	1.06 (s, 3H) 1.08 (s, 3H)	1.08 (s, 3H)	
H-31	1.05 (s, 3H) 1.07 (s, 3H)	1.08 (s, 3H)	
H-29	1.01 (s, 3H) 1.02 (s, 3H)	1.02 (s, 3H)	
H-30	1.00 (s, 3H) 1.01 (s, 3H)	1.01 (s, 3H)	
<u>^{13}C NMR ($\text{C}_6\text{D}_6, \delta$):</u>	<u>(100 MHz, $\text{C}_6\text{D}_6, \delta$):</u>	<u>(150 MHz, $\text{C}_6\text{D}_6, \delta$):</u>	
C-14	143.6 (C=C)	142.6	143.1
C-15	125.6 (C=C)	125.3	125.8
<i>C-2, 3, 7, 18, 23, 24</i>		77.7	78.3
<i>(C-O) not reported</i>		77.5	78.0
		77.0	77.5
		76.8	77.4
		76.6	77.2
		75.5	76.0
<i>C-4, 5, 6, 8, 9, 10 11, 12, 13,</i>		59.7	60.3
<i>16, 17, 19, 20, 21,22 (C-H)</i>		54.0 (impurity)	
<i>not reported</i>		45.5	46.1
		44.8	45.4

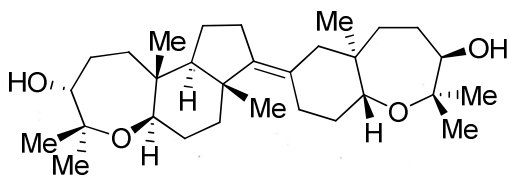
	41.3	41.8
	40.8	41.4
	37.4	37.9
	36.6	37.1
	35.4	35.9
	32.5	33.0
	30.4	31.0
	30.1(misassigned as impurity)	30.6
	28.1	28.6
	26.2	26.8
	25.7	26.2
	20.4	22.4
C-26 29.2 (Me)	29.3	29.8
C-28 28.9 (Me)	29.0	29.6
C-27 21.3 (Me)	21.9	22.2
C-25 21.2 (Me)	21.7	21.4
C-30 20.1 (Me)	20.8	20.9
C-31 18.4 (Me)	16.8	17.4
C-29 13.9 (Me)	14.1	14.5

HRMS (EI) for (M⁺) C₃₀H₅₀O₄

HRMS (ESI) for [(M+H⁺)] C₃₀H₅₁O₄

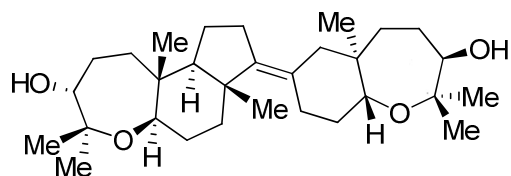
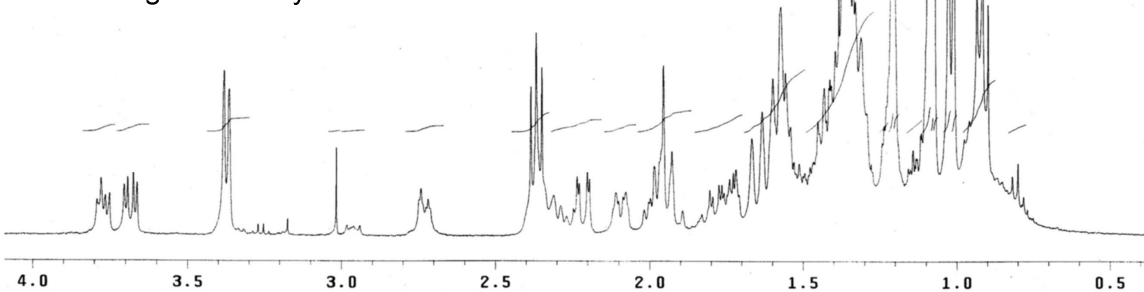
Calcd. 474.3696, found 474.3702. calcd. 475.3782. found 475.3782, 475.3799

¹H NMR spectra comparison of natural abudinol B and synthetic *ent*-abudinol B (1st and 2nd generations) is shown below.



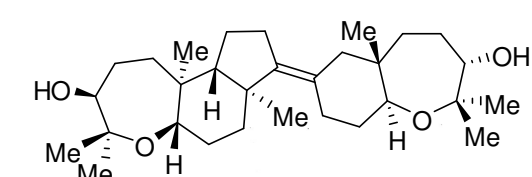
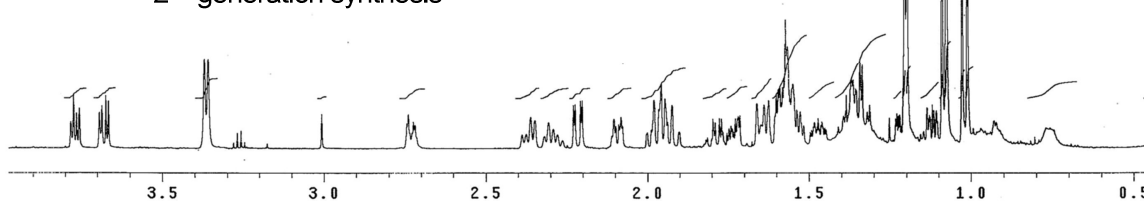
***ent*-abudinol B (ent-64)**

1st generation synthesis



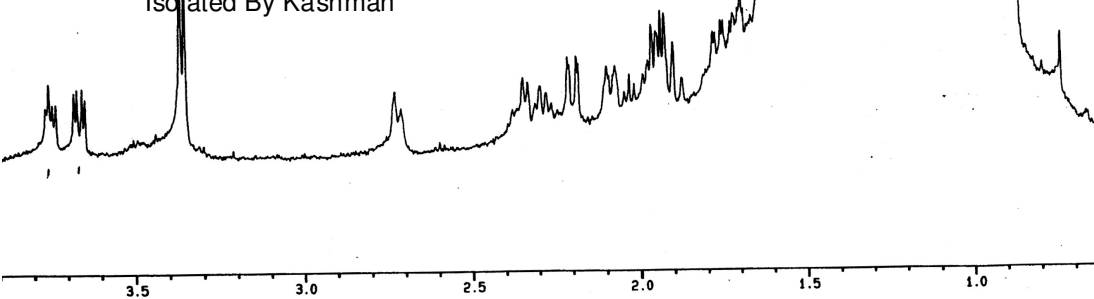
***ent*-abudinol B (ent-64)**

2nd generation synthesis



natural abudinol B

Isolated By Kashman



Data for compound 175

IR (neat, cm⁻¹): 3469.3, 2923.6, 2852.2, 1727.1, 1461.8, 1378.9, 1272.8, 1143.6, 1070.3.

¹H NMR (600 MHz, CDCl₃) δ 5.05 (s, 1H), 3.82 (s, br, 2H), 3.72 (dd, *J*=12.3, 3.9 Hz, 1H), 3.55(dd, *J*=12.0, 4.8 Hz, 1H), 3.36 (s, OH), 2.18-1.98 (m, 4H), 1.84 (m, 2H), 1.78 (m, 2H), 1.75-1.38 (m, 16H), 1.29 (s, 3H), 1.27 (s, 3H), 1.26 (s, 3H), 1.17 (s, 3H), 1.14(s, 3H), 0.96(s, 3H), 0.86 (s, 3H), 0.65 (s, 2H).

¹³C NMR (100 MHz, CDCl₃) δ 133.4, 133.0, 78.4, 78.2, 78.1, 74.9, 59.3, 57.8, 43.5, 41.3, 39.9, 37.8, 35.2, 34.7, 31.5, 29.9, 29.9, 29.2, 29.2, 28.5, 27.9, 26.1, 25.6, 24.8, 22.6, 22.0, 20.1, 20.1, 14.3, 13.0.

HRMS (ESI): Calcd. for C₃₀H₅₁O₄[(M+H⁺)] 475.3782, found 475.3785.

Data for compound 176

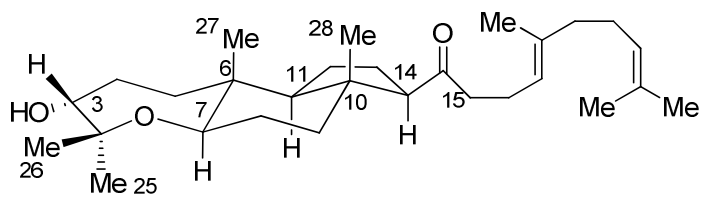
IR (neat, cm⁻¹): 3473.2, 2923.6, 2871.5, 2852.2, 1718.3, 1448.3, 1378.9, 1160.9, 1078.0, 1054.9, 914.1.

¹H NMR (600 MHz, CDCl₃) δ 5.43 (m, 1H), 4.86 (s, 1H), 4.71 (s, 1H), 3.92 (d, *J*=10.2 Hz, 1H), 3.74 (d, *J*=7.2 Hz, 1H), 3.82 (s, br, 2H), 3.49 (dd, *J*=11.7, 4.5 Hz, 1H), 3.32(dd, *J*=10.8, 3.6 Hz, 1H), 2.29 (s, 1H), 2.18-1.90 (m, 6H), 1.88-1.70 (m, 2H), 1.70-1.30 (m, 16H), 1.48 (s, 3H), 1.20 (s, 3H), 1.18 (s, 3H), 1.17 (s, 3H), 1.08 (s, 3H), 1.07(s, 3H), 0.81(s, 3H), 0.63 (s, 3H).

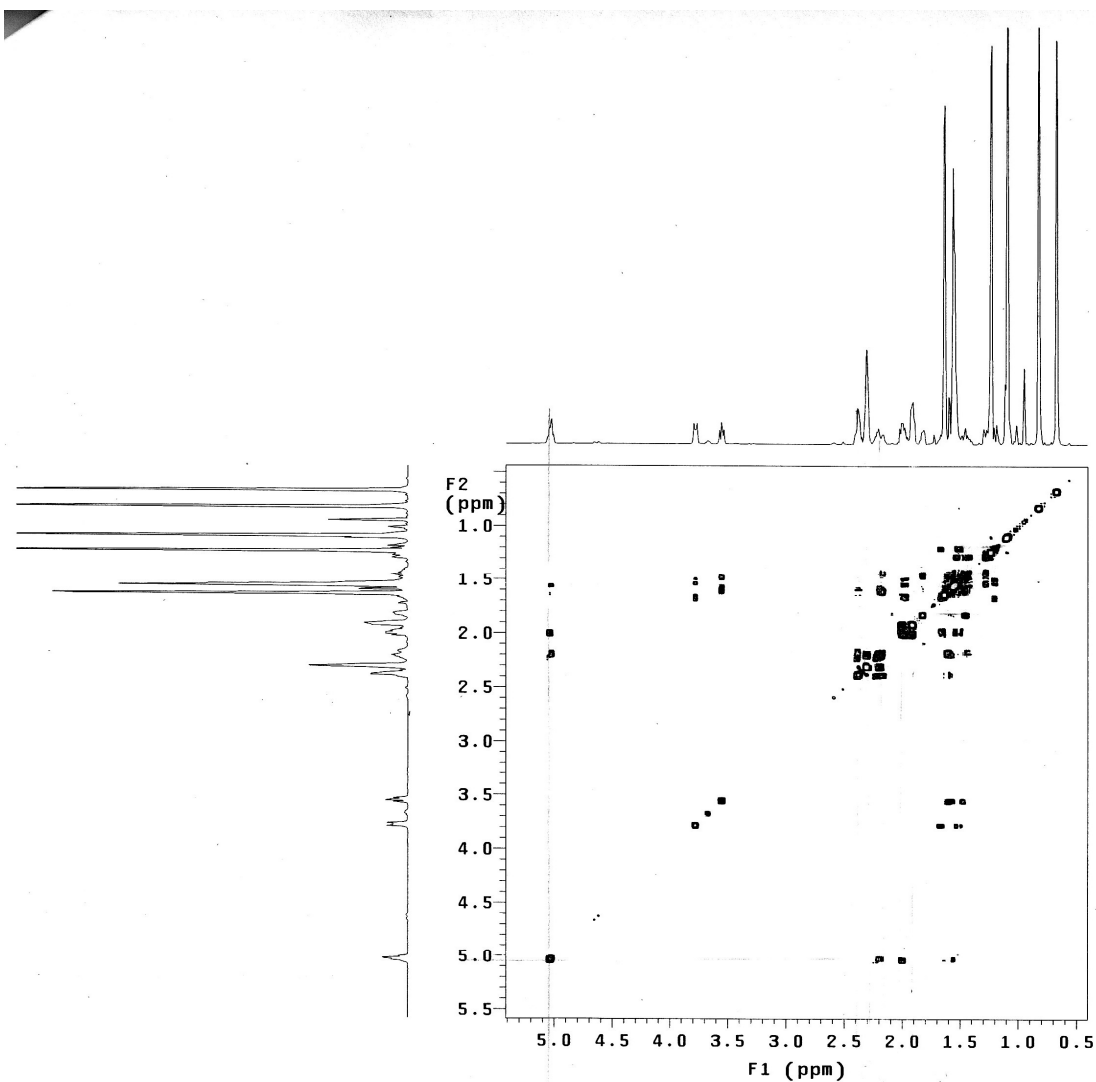
¹³C NMR (100 MHz, CDCl₃) δ 148.8, 135.8, 119.3, 110.8, 78.2, 78.0, 77.6, 76.7, 72.6, 71.9, 59.7, 56.9, 43.2, 41.3, 37.9, 35.2, 34.2, 29.9, 29.6, 29.2, 28.5, 27.0, 26.2, 25.6, 24.2, 22.0, 20.1, 20.0, 14.4, 13.0.

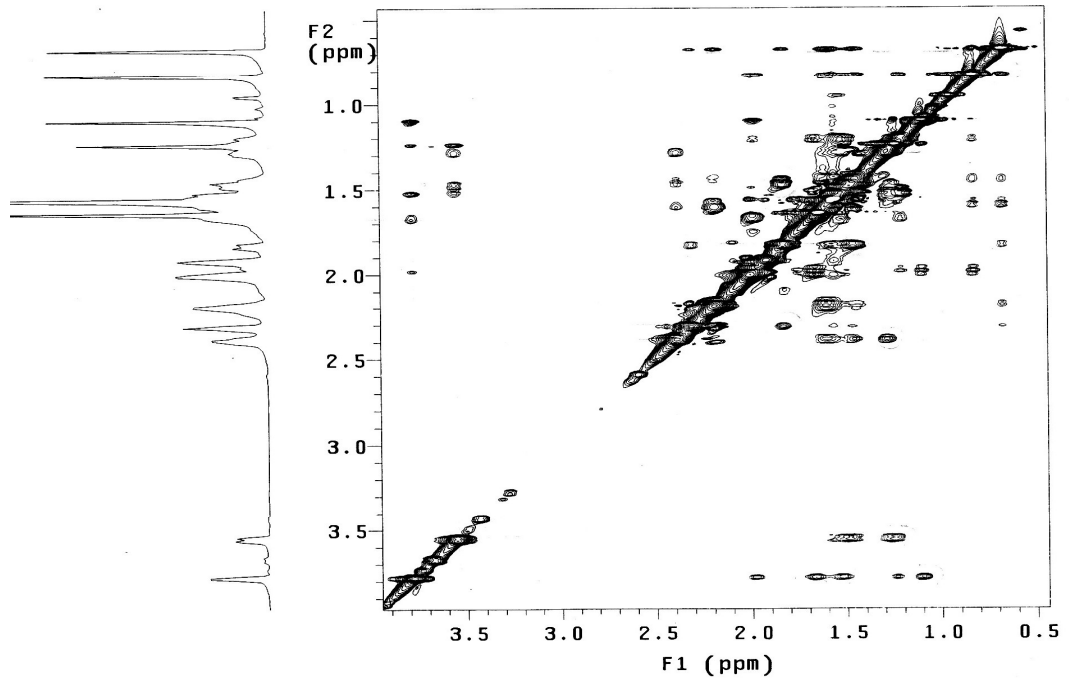
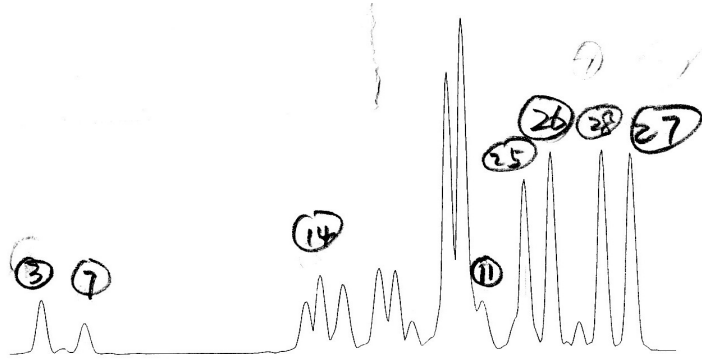
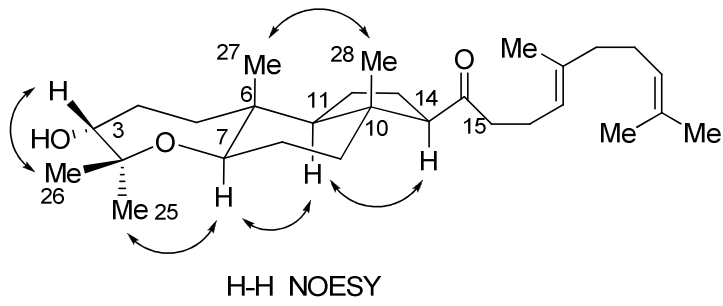
HRMS (ESI): Calcd. for C₃₀H₅₁O₄[(M+H⁺)] 475.3782, found 475.37874.

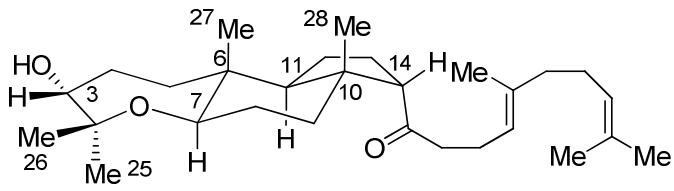
2-D NMR spectra for compounds 148a and 148b:



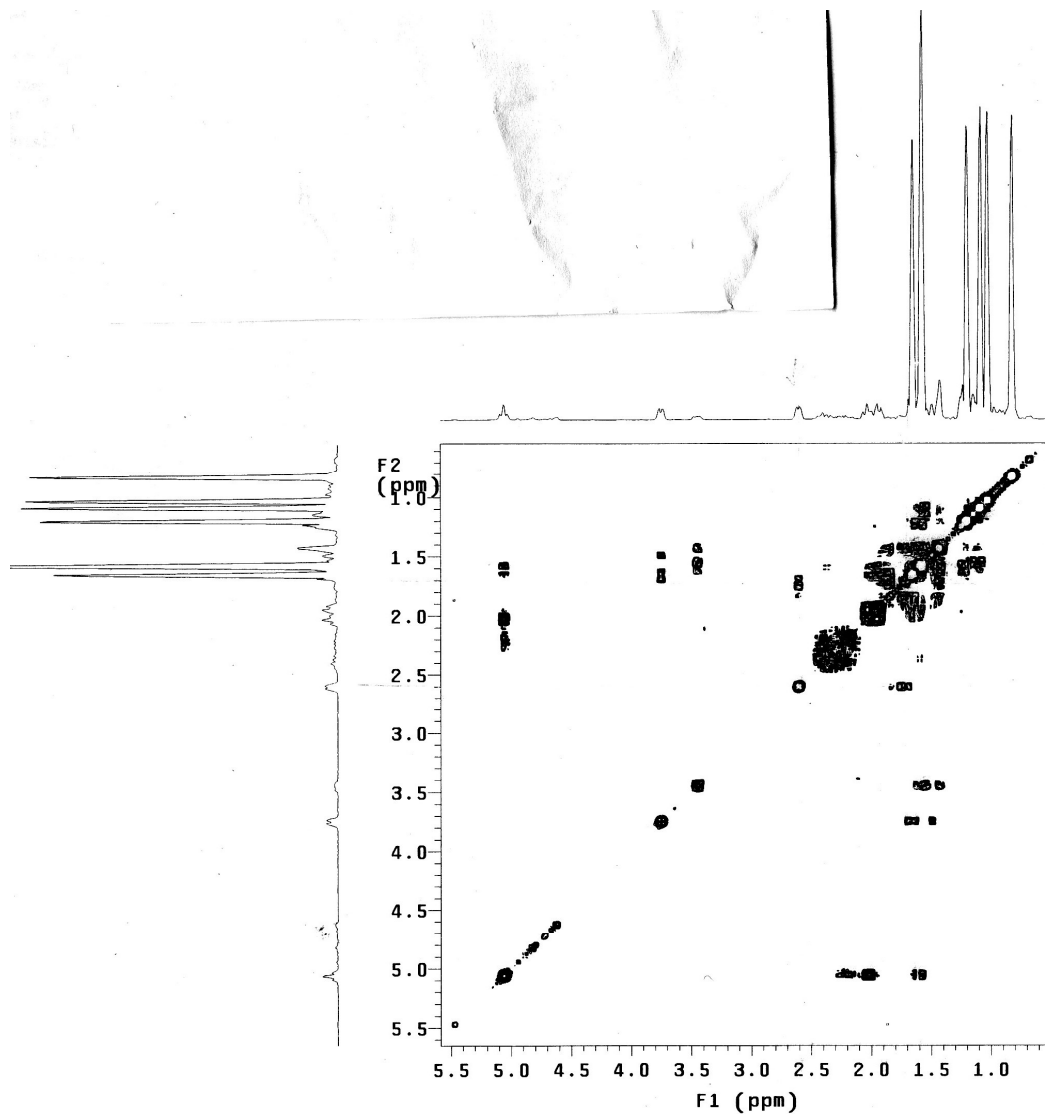
H-H COSY

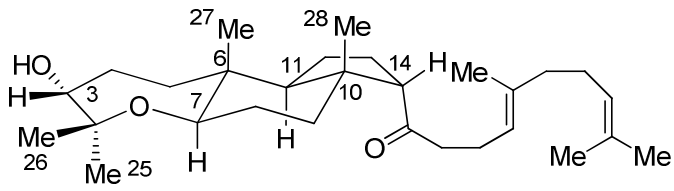




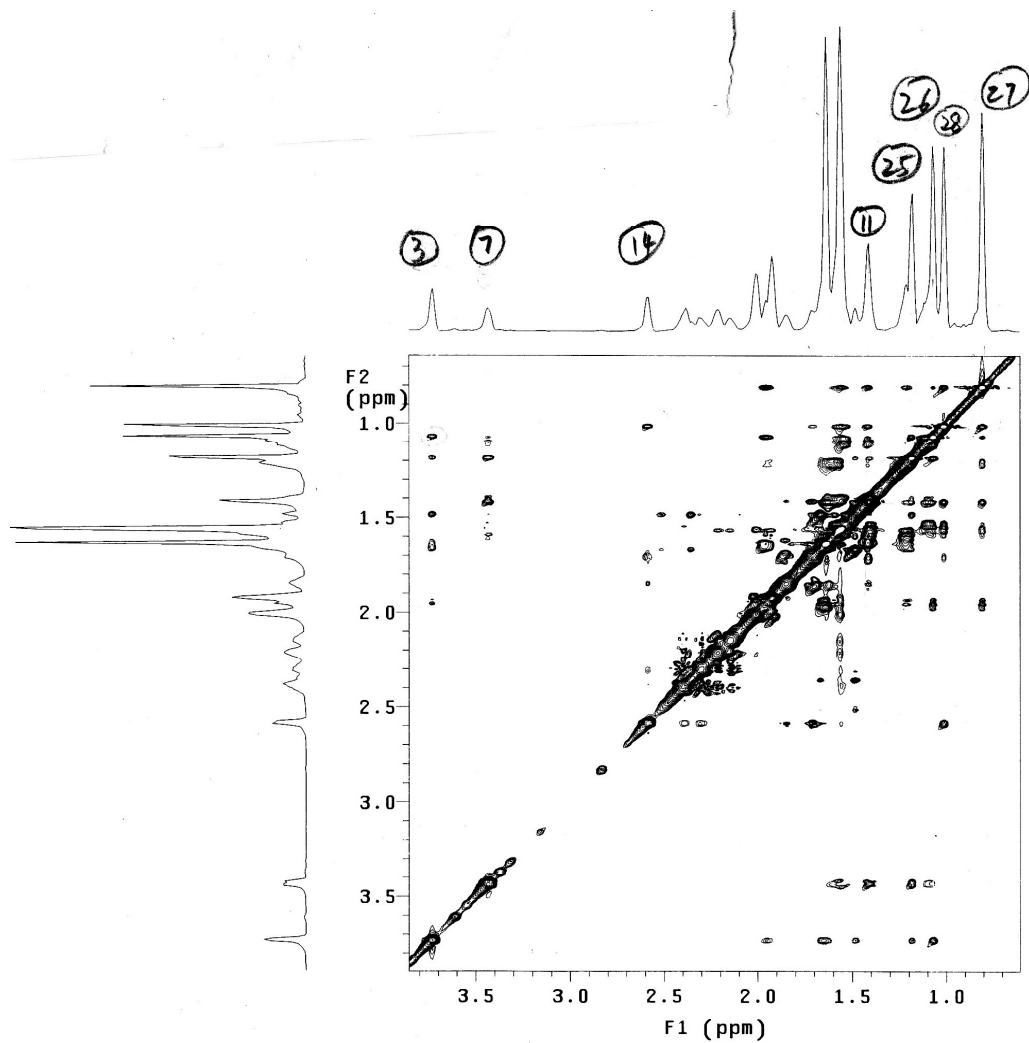


H-H COSY





H-H NOESY



X-Ray database in total synthesis of abudinol B

X-ray data for compound 77:

Table 1. Crystal data and structure refinement for compound 77.

Identification code	jcvs	
Empirical formula	C ₁₃ H ₂₂ O ₃	
Formula weight	226.31	
Temperature	173(2) K	
Wavelength	1.54178 Å	
Crystal system	Orthorhombic	
Space group	P2(1)2(1)2(1)	
Unit cell dimensions	a = 9.1824(4) Å	α = 90°.
	b = 10.6533(5) Å	β = 90°.
	c = 13.0707(6) Å	γ = 90°.
Volume	1278.61(10) Å ³	
Z	4	
Density (calculated)	1.176 Mg/m ³	
Absorption coefficient	0.655 mm ⁻¹	
F(000)	496	
Crystal size	0.23 x 0.08 x 0.08 mm ³	
Theta range for data collection	5.36 to 66.47°.	
Index ranges	-10 ≤ h ≤ 10, -10 ≤ k ≤ 11, -13 ≤ l ≤ 15	
Reflections collected	5713	
Independent reflections	2129 [R(int) = 0.0348]	
Completeness to theta = 66.47°	96.1 %	
Absorption correction	Semi-empirical from equivalents	
Max. and min. transmission	1.000 and 0.783724	
Refinement method	Full-matrix least-squares on F ²	
Data / restraints / parameters	2129 / 0 / 233	
Goodness-of-fit on F ²	1.064	
Final R indices [I > 2σ(I)]	R1 = 0.0377, wR2 = 0.0876	
R indices (all data)	R1 = 0.0503, wR2 = 0.1045	
Absolute structure parameter	0.1(3)	
Largest diff. peak and hole	0.184 and -0.224 e.Å ⁻³	

Table 2. Atomic coordinates ($\times 10^4$) and equivalent isotropic displacement parameters ($\text{\AA}^2 \times 10^3$) for compound **77**. $U(\text{eq})$ is defined as one third of the trace of the orthogonalized U^{ij} tensor.

	x	y	z	$U(\text{eq})$
C(1)	3371(2)	10644(2)	6408(2)	27(1)
C(2)	3810(2)	9384(2)	6919(2)	26(1)
C(3)	2715(3)	8932(2)	7716(2)	28(1)
C(4)	1425(2)	8214(2)	7280(2)	26(1)
C(5)	266(2)	8962(2)	6697(2)	22(1)
C(6)	-717(2)	8015(2)	6138(2)	27(1)
C(7)	-1799(3)	8635(2)	5443(2)	32(1)
C(8)	-1172(3)	9543(3)	4683(2)	38(1)
C(9)	-134(3)	10464(3)	5198(2)	32(1)
C(10)	984(2)	9818(2)	5880(2)	22(1)
C(11)	3859(3)	11721(3)	7087(3)	41(1)
C(12)	4023(3)	10779(3)	5347(2)	39(1)
C(13)	-652(3)	9729(3)	7448(2)	31(1)
O(1)	1808(2)	10792(1)	6363(1)	27(1)
O(2)	4023(2)	8392(2)	6200(1)	30(1)
O(3)	-3102(2)	8425(2)	5492(2)	50(1)

Table 3. Bond lengths [Å] and angles [°]
for compound **77**

C(1)-O(1)	1.445(3)	C(11)-C(1)-C(2)	108.9(2)
C(1)-C(12)	1.517(3)	O(2)-C(2)-C(3)	107.83(19)
C(1)-C(11)	1.519(3)	O(2)-C(2)-C(1)	113.08(18)
C(1)-C(2)	1.553(3)	C(3)-C(2)-C(1)	113.30(19)
C(2)-O(2)	1.428(3)	C(4)-C(3)-C(2)	114.6(2)
C(2)-C(3)	1.525(3)	C(3)-C(4)-C(5)	117.7(2)
C(3)-C(4)	1.521(3)	C(13)-C(5)-C(4)	110.02(19)
C(4)-C(5)	1.532(3)	C(13)-C(5)-C(6)	109.41(19)
C(5)-C(13)	1.529(3)	C(4)-C(5)-C(6)	107.59(18)
C(5)-C(6)	1.538(3)	C(13)-C(5)-C(10)	111.17(19)
C(5)-C(10)	1.552(3)	C(4)-C(5)-C(10)	110.64(18)
C(6)-C(7)	1.500(3)	C(6)-C(5)-C(10)	107.93(18)
C(7)-O(3)	1.219(3)	C(7)-C(6)-C(5)	112.80(19)
C(7)-C(8)	1.501(4)	O(3)-C(7)-C(6)	122.5(2)
C(8)-C(9)	1.525(4)	O(3)-C(7)-C(8)	122.0(2)
C(9)-C(10)	1.524(3)	C(6)-C(7)-C(8)	115.5(2)
C(10)-O(1)	1.430(3)	C(7)-C(8)-C(9)	111.2(2)
O(1)-C(1)-C(12)	110.14(19)	C(10)-C(9)-C(8)	112.9(2)
O(1)-C(1)-C(11)	103.59(19)	O(1)-C(10)-C(9)	106.68(19)
C(12)-C(1)-C(11)	110.2(2)	O(1)-C(10)-C(5)	110.36(16)
O(1)-C(1)-C(2)	111.70(19)	C(9)-C(10)-C(5)	112.49(19)
C(12)-C(1)-C(2)	111.9(2)	C(10)-O(1)-C(1)	117.70(17)

Symmetry transformations used
to generate equivalent atoms:

Table 4. Anisotropic displacement parameters ($\text{\AA}^2 \times 10^3$) for compound **77**. The anisotropic displacement factor exponent takes the form: $-2\pi^2 [h^2 a^{*2} U^{11} + \dots + 2 h k a^* b^* U^{12}]$

	U11	U22	U33	U23	U13	U12
C(1)	16(1)	32(1)	32(1)	-5(1)	1(1)	-4(1)
C(2)	20(1)	35(1)	23(1)	-5(1)	-3(1)	0(1)
C(3)	30(1)	30(1)	24(1)	2(1)	-3(1)	1(1)
C(4)	26(1)	29(1)	25(1)	5(1)	2(1)	0(1)
C(5)	20(1)	23(1)	22(1)	-2(1)	1(1)	-1(1)
C(6)	20(1)	26(1)	33(1)	-5(1)	4(1)	-5(1)
C(7)	19(1)	41(2)	36(1)	-17(1)	0(1)	-2(1)
C(8)	29(1)	51(2)	34(2)	1(1)	-10(1)	3(1)
C(9)	27(1)	37(2)	32(1)	6(1)	-4(1)	2(1)
C(10)	17(1)	26(1)	25(1)	-2(1)	-1(1)	-1(1)
C(11)	29(2)	36(2)	58(2)	-17(1)	-2(1)	-9(1)
C(12)	29(1)	48(2)	40(2)	11(1)	7(1)	-6(1)
C(13)	27(1)	35(2)	32(2)	-10(1)	9(1)	0(1)
O(1)	18(1)	24(1)	39(1)	-2(1)	-1(1)	-3(1)
O(2)	21(1)	34(1)	36(1)	-11(1)	4(1)	1(1)
O(3)	16(1)	76(1)	59(1)	-20(1)	2(1)	-4(1)

Table 5. Hydrogen coordinates ($\times 10^4$) and isotropic displacement parameters ($\text{\AA}^2 \times 10^3$) for compound **77**.

	x	y	z	U(eq)
H(2)	4840(30)	9540(20)	7279(18)	32(7)
H(3A)	2440(30)	9640(20)	8131(18)	32(7)
H(3B)	3260(30)	8320(30)	8211(19)	43(7)
H(4A)	980(30)	7770(20)	7860(20)	36(7)
H(4B)	1850(30)	7530(20)	6786(16)	30(6)
H(6A)	-1240(30)	7490(20)	6642(19)	37(7)
H(6B)	-80(30)	7450(20)	5679(17)	32(6)
H(8A)	-2020(30)	10040(30)	4290(20)	65(9)
H(8B)	-620(30)	9040(30)	4170(20)	52(9)
H(9A)	-700(30)	11080(20)	5635(19)	35(7)
H(9B)	400(30)	10950(20)	4640(20)	41(7)
H(10)	1640(20)	9250(20)	5441(16)	17(5)
H(11A)	3550(30)	11610(30)	7820(20)	54(9)
H(11B)	3500(30)	12550(30)	6780(20)	53(9)
H(11C)	4980(30)	11800(30)	7136(19)	50(8)
H(12A)	3670(30)	10090(30)	4800(20)	54(8)
H(12B)	3770(30)	11560(30)	5050(20)	44(8)
H(12C)	5140(30)	10690(20)	5360(20)	46(8)
H(13A)	-1080(30)	9190(20)	8010(20)	32(7)
H(13B)	-80(30)	10310(30)	7850(20)	46(8)
H(13C)	-1470(30)	10190(30)	7108(19)	50(8)
H(2O)	4940(40)	8430(40)	5980(30)	83(12)

Table 6. Torsion angles [°] for compound **77**.

O(1)-C(1)-C(2)-O(2)	93.0(2)
C(12)-C(1)-C(2)-O(2)	-31.0(3)
C(11)-C(1)-C(2)-O(2)	-153.1(2)
O(1)-C(1)-C(2)-C(3)	-30.0(3)
C(12)-C(1)-C(2)-C(3)	-154.1(2)
C(11)-C(1)-C(2)-C(3)	83.8(2)
O(2)-C(2)-C(3)-C(4)	-42.4(3)
C(1)-C(2)-C(3)-C(4)	83.6(2)
C(2)-C(3)-C(4)-C(5)	-72.7(3)
C(3)-C(4)-C(5)-C(13)	-73.3(3)
C(3)-C(4)-C(5)-C(6)	167.6(2)
C(3)-C(4)-C(5)-C(10)	50.0(3)
C(13)-C(5)-C(6)-C(7)	67.0(3)
C(4)-C(5)-C(6)-C(7)	-173.55(19)
C(10)-C(5)-C(6)-C(7)	-54.1(2)
C(5)-C(6)-C(7)-O(3)	-126.6(3)
C(5)-C(6)-C(7)-C(8)	53.1(3)
O(3)-C(7)-C(8)-C(9)	130.8(3)
C(6)-C(7)-C(8)-C(9)	-48.8(3)
C(7)-C(8)-C(9)-C(10)	49.2(3)
C(8)-C(9)-C(10)-O(1)	-176.08(19)
C(8)-C(9)-C(10)-C(5)	-54.9(3)
C(13)-C(5)-C(10)-O(1)	54.8(2)
C(4)-C(5)-C(10)-O(1)	-67.8(2)
C(6)-C(5)-C(10)-O(1)	174.78(17)
C(13)-C(5)-C(10)-C(9)	-64.2(2)
C(4)-C(5)-C(10)-C(9)	173.2(2)
C(6)-C(5)-C(10)-C(9)	55.8(2)
C(9)-C(10)-O(1)-C(1)	-135.84(19)
C(5)-C(10)-O(1)-C(1)	101.7(2)
C(12)-C(1)-O(1)-C(10)	70.0(3)
C(11)-C(1)-O(1)-C(10)	-172.1(2)
C(2)-C(1)-O(1)-C(10)	-55.0(2)

Symmetry transformations used to generate equivalent atoms:

Table 7. Hydrogen bonds for compound **77** [\AA and $^\circ$].

D-H...A	d(D-H)	d(H...A)	d(D...A)	$\angle(\text{DHA})$
O(2)-H(2O)...O(3)#1	0.89(4)	1.91(4)	2.797(2)	177(4)

Symmetry transformations used to generate equivalent atoms:

#1 $x+1,y,z$

X-ray data for compound 95:

Table 8. Crystal data and structure refinement for compound **95**.

Identification code	T105OH_0m	
Empirical formula	C13 H22 O3	
Formula weight	226.31	
Temperature	173(2) K	
Wavelength	1.54178 Å	
Crystal system	Monoclinic	
Space group	P2(1)/n	
Unit cell dimensions	a = 7.2507(4) Å	$\alpha = 90^\circ$.
	b = 15.5937(9) Å	$\beta = 99.195(2)^\circ$.
	c = 11.8296(7) Å	$\gamma = 90^\circ$.
Volume	1320.33(13) Å ³	
Z	4	
Density (calculated)	1.138 Mg/m ³	
Absorption coefficient	0.635 mm ⁻¹	
F(000)	496	
Crystal size	0.45 x 0.30 x 0.17 mm ³	
Theta range for data collection	8.27 to 66.02°.	
Index ranges	-8<=h<=7, -17<=k<=18, -12<=l<=13	
Reflections collected	7336	
Independent reflections	2022 [R(int) = 0.0221]	
Completeness to theta = 66.02°	87.9 %	
Absorption correction	Semi-empirical from equivalents	
Refinement method	Full-matrix least-squares on F ²	
Data / restraints / parameters	2022 / 0 / 149	
Goodness-of-fit on F ²	1.052	
Final R indices [I>2sigma(I)]	R1 = 0.0360, wR2 = 0.0925	
R indices (all data)	R1 = 0.0383, wR2 = 0.0945	
Largest diff. peak and hole	0.238 and -0.186 e.Å ⁻³	

Table 9. Atomic coordinates ($\times 10^4$) and equivalent isotropic displacement parameters ($\text{\AA}^2 \times 10^3$) for **95**. $U(\text{eq})$ is defined as one third of the trace of the orthogonalized U^{ij} tensor.

	x	y	z	$U(\text{eq})$
C(1)	66(2)	8886(1)	3480(1)	25(1)
C(2)	-1552(2)	9518(1)	3381(1)	29(1)
C(3)	-2171(2)	9823(1)	2146(1)	33(1)
C(4)	-524(2)	10142(1)	1646(1)	32(1)
C(5)	1101(2)	9532(1)	1744(1)	32(1)
C(6)	1774(2)	9232(1)	2989(1)	28(1)
C(7)	3201(2)	8507(1)	2937(1)	34(1)
C(8)	3805(2)	7986(1)	4033(1)	38(1)
C(9)	2274(2)	7393(1)	4332(1)	34(1)
C(10)	909(2)	7825(1)	5033(1)	31(1)
C(11)	-926(2)	7334(1)	4899(1)	41(1)
C(12)	1748(2)	7900(1)	6293(1)	41(1)
C(13)	2687(2)	9986(1)	3702(1)	36(1)
O(1)	584(1)	8707(1)	4679(1)	28(1)
O(2)	-523(2)	10843(1)	1189(1)	46(1)
O(3)	3012(2)	6663(1)	4981(1)	48(1)

Table 10. Bond lengths [\AA] and angles [$^\circ$] for **95**.

C(1)-O(1)	1.4353(14)	C(12)-H(12C)	0.9800
C(1)-C(2)	1.5223(17)	C(13)-H(13A)	0.9800
C(1)-C(6)	1.5464(16)	C(13)-H(13B)	0.9800
C(1)-H(1)	1.0000	C(13)-H(13C)	0.9800
C(2)-C(3)	1.5338(18)	O(3)-H(3)	0.8400
C(2)-H(2A)	0.9900		
C(2)-H(2B)	0.9900	O(1)-C(1)-C(2)	106.19(9)
C(3)-C(4)	1.4994(19)	O(1)-C(1)-C(6)	109.84(10)
C(3)-H(3A)	0.9900	C(2)-C(1)-C(6)	113.52(10)
C(3)-H(3B)	0.9900	O(1)-C(1)-H(1)	109.1
C(4)-O(2)	1.2192(16)	C(2)-C(1)-H(1)	109.1
C(4)-C(5)	1.5038(19)	C(6)-C(1)-H(1)	109.1
C(5)-C(6)	1.5486(18)	C(1)-C(2)-C(3)	112.22(10)
C(5)-H(5A)	0.9900	C(1)-C(2)-H(2A)	109.2
C(5)-H(5B)	0.9900	C(3)-C(2)-H(2A)	109.2
C(6)-C(13)	1.5341(19)	C(1)-C(2)-H(2B)	109.2
C(6)-C(7)	1.5405(18)	C(3)-C(2)-H(2B)	109.2
C(7)-C(8)	1.533(2)	H(2A)-C(2)-H(2B)	107.9
C(7)-H(7A)	0.9900	C(4)-C(3)-C(2)	110.40(11)
C(7)-H(7B)	0.9900	C(4)-C(3)-H(3A)	109.6
C(8)-C(9)	1.529(2)	C(2)-C(3)-H(3A)	109.6
C(8)-H(8A)	0.9900	C(4)-C(3)-H(3B)	109.6
C(8)-H(8B)	0.9900	C(2)-C(3)-H(3B)	109.6
C(9)-O(3)	1.4286(16)	H(3A)-C(3)-H(3B)	108.1
C(9)-C(10)	1.5433(18)	O(2)-C(4)-C(3)	121.94(13)
C(9)-H(9)	1.0000	O(2)-C(4)-C(5)	122.99(13)
C(10)-O(1)	1.4456(15)	C(3)-C(4)-C(5)	115.07(11)
C(10)-C(11)	1.5209(19)	C(4)-C(5)-C(6)	112.84(10)
C(10)-C(12)	1.5224(19)	C(4)-C(5)-H(5A)	109.0
C(11)-H(11A)	0.9800	C(6)-C(5)-H(5A)	109.0
C(11)-H(11B)	0.9800	C(4)-C(5)-H(5B)	109.0
C(11)-H(11C)	0.9800	C(6)-C(5)-H(5B)	109.0
C(12)-H(12A)	0.9800	H(5A)-C(5)-H(5B)	107.8
C(12)-H(12B)	0.9800	C(13)-C(6)-C(7)	110.54(11)

C(13)-C(6)-C(1)	111.25(10)	C(11)-C(10)-C(12)	110.32(11)
C(7)-C(6)-C(1)	110.04(10)	O(1)-C(10)-C(9)	110.36(10)
C(13)-C(6)-C(5)	109.49(11)	C(11)-C(10)-C(9)	110.48(11)
C(7)-C(6)-C(5)	107.16(10)	C(12)-C(10)-C(9)	111.66(11)
C(1)-C(6)-C(5)	108.23(10)	C(10)-C(11)-H(11A)	109.5
C(8)-C(7)-C(6)	117.25(11)	C(10)-C(11)-H(11B)	109.5
C(8)-C(7)-H(7A)	108.0	H(11A)-C(11)-H(11B)	109.5
C(6)-C(7)-H(7A)	108.0	C(10)-C(11)-H(11C)	109.5
C(8)-C(7)-H(7B)	108.0	H(11A)-C(11)-H(11C)	109.5
C(6)-C(7)-H(7B)	108.0	H(11B)-C(11)-H(11C)	109.5
H(7A)-C(7)-H(7B)	107.2	C(10)-C(12)-H(12A)	109.5
C(9)-C(8)-C(7)	113.38(11)	C(10)-C(12)-H(12B)	109.5
C(9)-C(8)-H(8A)	108.9	H(12A)-C(12)-H(12B)	109.5
C(7)-C(8)-H(8A)	108.9	C(10)-C(12)-H(12C)	109.5
C(9)-C(8)-H(8B)	108.9	H(12A)-C(12)-H(12C)	109.5
C(7)-C(8)-H(8B)	108.9	H(12B)-C(12)-H(12C)	109.5
H(8A)-C(8)-H(8B)	107.7	C(6)-C(13)-H(13A)	109.5
O(3)-C(9)-C(8)	112.51(11)	C(6)-C(13)-H(13B)	109.5
O(3)-C(9)-C(10)	106.08(10)	H(13A)-C(13)-H(13B)	109.5
C(8)-C(9)-C(10)	114.36(11)	C(6)-C(13)-H(13C)	109.5
O(3)-C(9)-H(9)	107.9	H(13A)-C(13)-H(13C)	109.5
C(8)-C(9)-H(9)	107.9	H(13B)-C(13)-H(13C)	109.5
C(10)-C(9)-H(9)	107.9	C(1)-O(1)-C(10)	118.45(9)
O(1)-C(10)-C(11)	110.44(10)	C(9)-O(3)-H(3)	109.5
O(1)-C(10)-C(12)	103.38(11)		

Symmetry transformations used to generate equivalent atoms:

Table 11. Anisotropic displacement parameters ($\text{\AA}^2 \times 10^3$) for **95**. The anisotropic displacement factor exponent takes the form: $-2\pi^2 [h^2 a^{*2} U^{11} + \dots + 2 h k a^* b^* U^{12}]$

	U11	U22	U33	U23	U13	U12
C(1)	27(1)	27(1)	22(1)	-1(1)	4(1)	-2(1)
C(2)	27(1)	31(1)	29(1)	3(1)	7(1)	0(1)
C(3)	30(1)	33(1)	34(1)	4(1)	3(1)	1(1)
C(4)	40(1)	32(1)	23(1)	1(1)	1(1)	-5(1)
C(5)	34(1)	37(1)	27(1)	0(1)	9(1)	-5(1)
C(6)	26(1)	32(1)	26(1)	-2(1)	6(1)	-3(1)
C(7)	29(1)	42(1)	33(1)	-1(1)	10(1)	2(1)
C(8)	29(1)	46(1)	39(1)	0(1)	7(1)	10(1)
C(9)	38(1)	33(1)	29(1)	3(1)	4(1)	9(1)
C(10)	36(1)	30(1)	29(1)	4(1)	6(1)	5(1)
C(11)	43(1)	38(1)	44(1)	9(1)	12(1)	-1(1)
C(12)	52(1)	43(1)	30(1)	5(1)	6(1)	11(1)
C(13)	33(1)	40(1)	35(1)	-4(1)	6(1)	-9(1)
O(1)	34(1)	29(1)	22(1)	1(1)	5(1)	4(1)
O(2)	57(1)	37(1)	46(1)	13(1)	11(1)	-3(1)
O(3)	61(1)	44(1)	43(1)	10(1)	15(1)	26(1)

Table 12. Hydrogen coordinates ($\times 10^4$) and isotropic displacement parameters ($\text{\AA}^2 \times 10^3$) for **95**.

	x	y	z	U(eq)
H(1)	-376	8345	3071	30
H(2A)	-1171	10021	3875	35
H(2B)	-2623	9242	3661	35
H(3A)	-2770	9343	1677	39
H(3B)	-3100	10289	2135	39
H(5A)	2150	9817	1451	39
H(5B)	734	9025	1257	39
H(7A)	2669	8105	2324	41
H(7B)	4335	8762	2706	41
H(8A)	4910	7637	3939	45
H(8B)	4182	8386	4678	45
H(9)	1533	7183	3599	40
H(11A)	-1759	7604	5370	62
H(11B)	-684	6739	5146	62
H(11C)	-1517	7343	4093	62
H(12A)	2964	8188	6365	62
H(12B)	1912	7327	6632	62
H(12C)	909	8236	6694	62
H(13A)	3160	9790	4482	54
H(13B)	1760	10440	3729	54
H(13C)	3724	10210	3351	54
H(3)	3686	6379	4602	73

Table 13. Torsion angles [°] for **95**.

O(1)-C(1)-C(2)-C(3)	175.80(10)
C(6)-C(1)-C(2)-C(3)	55.01(14)
C(1)-C(2)-C(3)-C(4)	-51.54(14)
C(2)-C(3)-C(4)-O(2)	-128.50(14)
C(2)-C(3)-C(4)-C(5)	51.95(15)
O(2)-C(4)-C(5)-C(6)	126.43(14)
C(3)-C(4)-C(5)-C(6)	-54.03(15)
O(1)-C(1)-C(6)-C(13)	-52.10(13)
C(2)-C(1)-C(6)-C(13)	66.61(14)
O(1)-C(1)-C(6)-C(7)	70.76(12)
C(2)-C(1)-C(6)-C(7)	-170.53(11)
O(1)-C(1)-C(6)-C(5)	-172.44(9)
C(2)-C(1)-C(6)-C(5)	-53.73(13)
C(4)-C(5)-C(6)-C(13)	-69.26(13)
C(4)-C(5)-C(6)-C(7)	170.82(11)
C(4)-C(5)-C(6)-C(1)	52.18(14)
C(13)-C(6)-C(7)-C(8)	71.91(15)
C(1)-C(6)-C(7)-C(8)	-51.37(15)
C(5)-C(6)-C(7)-C(8)	-168.84(12)
C(6)-C(7)-C(8)-C(9)	71.07(16)
C(7)-C(8)-C(9)-O(3)	153.14(11)
C(7)-C(8)-C(9)-C(10)	-85.74(15)
O(3)-C(9)-C(10)-O(1)	160.12(11)
C(8)-C(9)-C(10)-O(1)	35.51(15)
O(3)-C(9)-C(10)-C(11)	-77.45(13)
C(8)-C(9)-C(10)-C(11)	157.94(12)
O(3)-C(9)-C(10)-C(12)	45.72(15)
C(8)-C(9)-C(10)-C(12)	-78.88(14)
C(2)-C(1)-O(1)-C(10)	134.59(10)
C(6)-C(1)-O(1)-C(10)	-102.27(12)
C(11)-C(10)-O(1)-C(1)	-71.74(13)
C(12)-C(10)-O(1)-C(1)	170.25(10)
C(9)-C(10)-O(1)-C(1)	50.71(14)

Table 14. Hydrogen bonds for **95** [Å and °].

D-H...A	d(D-H)	d(H...A)	d(D...A)	<(DHA)
O(3)-H(3)...O(2)#1	0.84	1.94	2.7695(14)	171.7

Symmetry transformations used to generate equivalent atoms:

#1 $-x+1/2, y-1/2, -z+1/2$

X-ray data for compound 115:

Table 15. Crystal data and structure refinement for **115**.

Identification code	T104_0m
Empirical formula	C19 H30 O2
Formula weight	290.43
Temperature	173(2) K
Wavelength	1.54178 Å
Crystal system	Orthorhombic
Space group	P2(1)2(1)2(1)
Unit cell dimensions	a = 7.1883(5) Å α = 90°. b = 9.8601(7) Å β = 90°. c = 23.4975(16) Å γ = 90°.
Volume	1665.4(2) Å ³
Z	4
Density (calculated)	1.158 Mg/m ³
Absorption coefficient	0.561 mm ⁻¹
F(000)	640
Crystal size	0.73 x 0.53 x 0.10 mm ³
Theta range for data collection	8.37 to 65.97°.
Index ranges	-7<=h<=7, -10<=k<=9, -27<=l<=24
Reflections collected	6645
Independent reflections	2524 [R(int) = 0.0201]
Completeness to theta = 65.97°	90.0 %
Absorption correction	Semi-empirical from equivalents
Refinement method	Full-matrix least-squares on F ²
Data / restraints / parameters	2524 / 0 / 203
Goodness-of-fit on F ²	1.083
Final R indices [I>2sigma(I)]	R1 = 0.0322, wR2 = 0.0761
R indices (all data)	R1 = 0.0344, wR2 = 0.0774
Absolute structure parameter	0.0(2)
Largest diff. peak and hole	0.160 and -0.134 e.Å ⁻³

Table 16. Atomic coordinates ($\times 10^4$) and equivalent isotropic displacement parameters ($\text{\AA}^2 \times 10^3$) for **115**. $U(\text{eq})$ is defined as one third of the trace of the orthogonalized U^{ij} tensor.

	x	y	z	U(eq)
C(1)	-1110(2)	-5342(2)	-1681(1)	23(1)
C(2)	358(2)	-6056(2)	-1320(1)	27(1)
C(3)	564(2)	-5438(2)	-725(1)	27(1)
C(4)	-1304(2)	-5418(2)	-421(1)	27(1)
C(5)	-1417(3)	-4519(2)	112(1)	33(1)
C(6)	-3350(3)	-3881(3)	138(1)	53(1)
C(7)	-4343(3)	-4340(2)	-411(1)	35(1)
C(8)	-2721(2)	-4677(2)	-806(1)	25(1)
C(9)	-3063(2)	-5273(2)	-1404(1)	23(1)
C(10)	-4301(2)	-4259(2)	-1730(1)	26(1)
C(11)	-4439(2)	-4414(2)	-2380(1)	28(1)
C(12)	-2667(2)	-4086(2)	-2705(1)	29(1)
C(13)	-1251(2)	-5265(2)	-2732(1)	28(1)
C(14)	702(3)	-4754(2)	-2867(1)	39(1)
C(15)	-1883(3)	-6285(2)	-3182(1)	40(1)
C(16)	-1869(3)	-6854(2)	-228(1)	37(1)
C(17)	-4030(2)	-6665(2)	-1409(1)	30(1)
C(18)	-98(3)	-4426(2)	489(1)	42(1)
C(19)	1264(3)	-4351(2)	847(1)	51(1)
O(1)	-1196(2)	-6061(1)	-2213(1)	25(1)
O(2)	-1941(2)	-2863(1)	-2461(1)	32(1)

Table 17. Bond lengths [Å] and angles [°] for **115**.

C(1)-O(1)	1.4388(18)	C(13)-O(1)	1.4501(18)
C(1)-C(2)	1.525(2)	C(13)-C(14)	1.525(3)
C(1)-C(9)	1.549(2)	C(13)-C(15)	1.529(2)
C(1)-H(1)	1.0000	C(14)-H(14A)	0.9800
C(2)-C(3)	1.534(2)	C(14)-H(14B)	0.9800
C(2)-H(2A)	0.9900	C(14)-H(14C)	0.9800
C(2)-H(2B)	0.9900	C(15)-H(15A)	0.9800
C(3)-C(4)	1.521(2)	C(15)-H(15B)	0.9800
C(3)-H(3A)	0.9900	C(15)-H(15C)	0.9800
C(3)-H(3B)	0.9900	C(16)-H(16A)	0.9800
C(4)-C(5)	1.535(2)	C(16)-H(16B)	0.9800
C(4)-C(16)	1.541(2)	C(16)-H(16C)	0.9800
C(4)-C(8)	1.547(2)	C(17)-H(17A)	0.9800
C(5)-C(18)	1.301(3)	C(17)-H(17B)	0.9800
C(5)-C(6)	1.527(3)	C(17)-H(17C)	0.9800
C(6)-C(7)	1.544(3)	C(18)-C(19)	1.292(3)
C(6)-H(6A)	0.9900	C(19)-H(19)	1.00(2)
C(6)-H(6B)	0.9900	C(19)-H(20)	1.04(3)
C(7)-C(8)	1.527(2)	O(2)-H(2)	0.8400
C(7)-H(7A)	0.9900		
C(7)-H(7B)	0.9900	O(1)-C(1)-C(2)	106.59(12)
C(8)-C(9)	1.543(2)	O(1)-C(1)-C(9)	110.35(12)
C(8)-H(8)	1.0000	C(2)-C(1)-C(9)	114.44(13)
C(9)-C(17)	1.539(2)	O(1)-C(1)-H(1)	108.4
C(9)-C(10)	1.543(2)	C(2)-C(1)-H(1)	108.4
C(10)-C(11)	1.537(2)	C(9)-C(1)-H(1)	108.4
C(10)-H(10A)	0.9900	C(1)-C(2)-C(3)	113.00(13)
C(10)-H(10B)	0.9900	C(1)-C(2)-H(2A)	109.0
C(11)-C(12)	1.521(2)	C(3)-C(2)-H(2A)	109.0
C(11)-H(11A)	0.9900	C(1)-C(2)-H(2B)	109.0
C(11)-H(11B)	0.9900	C(3)-C(2)-H(2B)	109.0
C(12)-O(2)	1.434(2)	H(2A)-C(2)-H(2B)	107.8
C(12)-C(13)	1.547(2)	C(4)-C(3)-C(2)	110.41(13)
C(12)-H(12)	1.0000	C(4)-C(3)-H(3A)	109.6

C(2)-C(3)-H(3A)	109.6	C(10)-C(9)-C(1)	110.03(12)
C(4)-C(3)-H(3B)	109.6	C(11)-C(10)-C(9)	117.77(13)
C(2)-C(3)-H(3B)	109.6	C(11)-C(10)-H(10A)	107.9
H(3A)-C(3)-H(3B)	108.1	C(9)-C(10)-H(10A)	107.9
C(3)-C(4)-C(5)	115.90(14)	C(11)-C(10)-H(10B)	107.9
C(3)-C(4)-C(16)	111.03(14)	C(9)-C(10)-H(10B)	107.9
C(5)-C(4)-C(16)	106.07(13)	H(10A)-C(10)-H(10B)	107.2
C(3)-C(4)-C(8)	108.20(13)	C(12)-C(11)-C(10)	115.09(14)
C(5)-C(4)-C(8)	99.76(13)	C(12)-C(11)-H(11A)	108.5
C(16)-C(4)-C(8)	115.65(14)	C(10)-C(11)-H(11A)	108.5
C(18)-C(5)-C(6)	127.31(16)	C(12)-C(11)-H(11B)	108.5
C(18)-C(5)-C(4)	123.87(16)	C(10)-C(11)-H(11B)	108.5
C(6)-C(5)-C(4)	108.64(14)	H(11A)-C(11)-H(11B)	107.5
C(5)-C(6)-C(7)	105.41(15)	O(2)-C(12)-C(11)	106.42(13)
C(5)-C(6)-H(6A)	110.7	O(2)-C(12)-C(13)	114.12(14)
C(7)-C(6)-H(6A)	110.7	C(11)-C(12)-C(13)	114.30(14)
C(5)-C(6)-H(6B)	110.7	O(2)-C(12)-H(12)	107.2
C(7)-C(6)-H(6B)	110.7	C(11)-C(12)-H(12)	107.2
H(6A)-C(6)-H(6B)	108.8	C(13)-C(12)-H(12)	107.2
C(8)-C(7)-C(6)	102.66(14)	O(1)-C(13)-C(14)	109.20(13)
C(8)-C(7)-H(7A)	111.2	O(1)-C(13)-C(15)	103.50(12)
C(6)-C(7)-H(7A)	111.2	C(14)-C(13)-C(15)	110.29(15)
C(8)-C(7)-H(7B)	111.2	O(1)-C(13)-C(12)	113.03(13)
C(6)-C(7)-H(7B)	111.2	C(14)-C(13)-C(12)	111.47(14)
H(7A)-C(7)-H(7B)	109.1	C(15)-C(13)-C(12)	109.06(14)
C(7)-C(8)-C(9)	120.99(14)	C(13)-C(14)-H(14A)	109.5
C(7)-C(8)-C(4)	104.45(13)	C(13)-C(14)-H(14B)	109.5
C(9)-C(8)-C(4)	117.24(13)	H(14A)-C(14)-H(14B)	109.5
C(7)-C(8)-H(8)	104.0	C(13)-C(14)-H(14C)	109.5
C(9)-C(8)-H(8)	104.0	H(14A)-C(14)-H(14C)	109.5
C(4)-C(8)-H(8)	104.0	H(14B)-C(14)-H(14C)	109.5
C(17)-C(9)-C(8)	114.76(13)	C(13)-C(15)-H(15A)	109.5
C(17)-C(9)-C(10)	108.30(13)	C(13)-C(15)-H(15B)	109.5
C(8)-C(9)-C(10)	107.26(12)	H(15A)-C(15)-H(15B)	109.5
C(17)-C(9)-C(1)	111.56(13)	C(13)-C(15)-H(15C)	109.5
C(8)-C(9)-C(1)	104.77(13)	H(15A)-C(15)-H(15C)	109.5

H(15B)-C(15)-H(15C)	109.5	C(9)-C(17)-H(17C)	109.5
C(4)-C(16)-H(16A)	109.5	H(17A)-C(17)-H(17C)	109.5
C(4)-C(16)-H(16B)	109.5	H(17B)-C(17)-H(17C)	109.5
H(16A)-C(16)-H(16B)	109.5	C(19)-C(18)-C(5)	177.4(2)
C(4)-C(16)-H(16C)	109.5	C(18)-C(19)-H(19)	121.7(15)
H(16A)-C(16)-H(16C)	109.5	C(18)-C(19)-H(20)	118.6(15)
H(16B)-C(16)-H(16C)	109.5	H(19)-C(19)-H(20)	120(2)
C(9)-C(17)-H(17A)	109.5	C(1)-O(1)-C(13)	117.70(11)
C(9)-C(17)-H(17B)	109.5	C(12)-O(2)-H(2)	109.5
H(17A)-C(17)-H(17B)	109.5		

Symmetry transformations used to generate equivalent atoms:

Table 18. Anisotropic displacement parameters ($\text{\AA}^2 \times 10^3$) for **115**. The anisotropic displacement factor exponent takes the form: $-2\pi^2 [h^2 a^{*2} U^{11} + \dots + 2 h k a^* b^* U^{12}]$

	U ¹¹	U ²²	U ³³	U ²³	U ¹³	U ¹²
C(1)	24(1)	21(1)	23(1)	-1(1)	-1(1)	0(1)
C(2)	22(1)	29(1)	30(1)	1(1)	-1(1)	3(1)
C(3)	24(1)	28(1)	29(1)	1(1)	-4(1)	0(1)
C(4)	24(1)	32(1)	25(1)	2(1)	-3(1)	-1(1)
C(5)	35(1)	41(1)	24(1)	1(1)	-1(1)	2(1)
C(6)	45(1)	86(2)	28(1)	-11(1)	-2(1)	21(1)
C(7)	28(1)	48(1)	30(1)	1(1)	2(1)	7(1)
C(8)	23(1)	26(1)	27(1)	1(1)	0(1)	-1(1)
C(9)	20(1)	23(1)	25(1)	2(1)	-2(1)	-2(1)
C(10)	20(1)	27(1)	29(1)	2(1)	0(1)	1(1)
C(11)	26(1)	30(1)	29(1)	4(1)	-7(1)	2(1)
C(12)	32(1)	30(1)	25(1)	3(1)	-3(1)	2(1)
C(13)	36(1)	27(1)	22(1)	4(1)	0(1)	1(1)
C(14)	37(1)	36(1)	43(1)	8(1)	12(1)	6(1)
C(15)	54(1)	40(1)	27(1)	-6(1)	-5(1)	8(1)
C(16)	32(1)	40(1)	38(1)	13(1)	-2(1)	-3(1)
C(17)	26(1)	30(1)	34(1)	4(1)	-3(1)	-6(1)
C(18)	44(1)	45(1)	35(1)	-9(1)	-3(1)	7(1)
C(19)	56(2)	50(1)	49(1)	-10(1)	-21(1)	8(1)
O(1)	30(1)	24(1)	22(1)	-1(1)	-1(1)	1(1)
O(2)	37(1)	24(1)	36(1)	3(1)	6(1)	-3(1)

Table 19. Hydrogen coordinates ($\times 10^4$) and isotropic displacement parameters ($\text{\AA}^2 \times 10^3$) for **115**.

	x	y	z	U(eq)
H(1)	-678	-4396	-1758	27
H(2A)	1571	-6007	-1519	33
H(2B)	20	-7025	-1283	33
H(3A)	1465	-5978	-500	32
H(3B)	1049	-4502	-757	32
H(6A)	-3259	-2880	154	64
H(6B)	-4033	-4201	479	64
H(7A)	-5131	-5147	-342	42
H(7B)	-5122	-3604	-570	42
H(8)	-2127	-3778	-883	30
H(10A)	-5574	-4321	-1572	31
H(10B)	-3837	-3333	-1648	31
H(11A)	-4803	-5359	-2467	34
H(11B)	-5444	-3814	-2520	34
H(12)	-3036	-3871	-3106	34
H(14A)	1542	-5529	-2914	58
H(14B)	1146	-4181	-2554	58
H(14C)	674	-4224	-3220	58
H(15A)	-3134	-6611	-3088	60
H(15B)	-1018	-7052	-3191	60
H(15C)	-1905	-5844	-3556	60
H(16A)	-1076	-7138	90	55
H(16B)	-1719	-7488	-546	55
H(16C)	-3172	-6848	-105	55
H(17A)	-3119	-7375	-1322	45
H(17B)	-4568	-6831	-1786	45
H(17C)	-5020	-6677	-1122	45
H(2)	-1126	-2536	-2678	49
H(19)	1350(40)	-4970(20)	1180(10)	66(7)
H(20)	2250(40)	-3600(30)	791(11)	83(8)

Table 20. Torsion angles [°] for **115**.

O(1)-C(1)-C(2)-C(3)	-177.74(13)
C(9)-C(1)-C(2)-C(3)	-55.46(18)
C(1)-C(2)-C(3)-C(4)	55.24(18)
C(2)-C(3)-C(4)-C(5)	-165.30(14)
C(2)-C(3)-C(4)-C(16)	73.61(16)
C(2)-C(3)-C(4)-C(8)	-54.32(17)
C(3)-C(4)-C(5)-C(18)	-40.8(2)
C(16)-C(4)-C(5)-C(18)	83.0(2)
C(8)-C(4)-C(5)-C(18)	-156.60(19)
C(3)-C(4)-C(5)-C(6)	143.87(16)
C(16)-C(4)-C(5)-C(6)	-92.42(18)
C(8)-C(4)-C(5)-C(6)	28.03(18)
C(18)-C(5)-C(6)-C(7)	-178.9(2)
C(4)-C(5)-C(6)-C(7)	-3.8(2)
C(5)-C(6)-C(7)-C(8)	-22.7(2)
C(6)-C(7)-C(8)-C(9)	176.15(16)
C(6)-C(7)-C(8)-C(4)	41.22(19)
C(3)-C(4)-C(8)-C(7)	-164.06(14)
C(5)-C(4)-C(8)-C(7)	-42.51(16)
C(16)-C(4)-C(8)-C(7)	70.70(18)
C(3)-C(4)-C(8)-C(9)	59.00(18)
C(5)-C(4)-C(8)-C(9)	-179.46(13)
C(16)-C(4)-C(8)-C(9)	-66.24(19)
C(7)-C(8)-C(9)-C(17)	-62.2(2)
C(4)-C(8)-C(9)-C(17)	67.31(19)
C(7)-C(8)-C(9)-C(10)	58.13(19)
C(4)-C(8)-C(9)-C(10)	-172.33(13)
C(7)-C(8)-C(9)-C(1)	175.06(15)
C(4)-C(8)-C(9)-C(1)	-55.39(17)
O(1)-C(1)-C(9)-C(17)	47.15(16)
C(2)-C(1)-C(9)-C(17)	-73.05(16)
O(1)-C(1)-C(9)-C(8)	171.90(11)
C(2)-C(1)-C(9)-C(8)	51.70(17)
O(1)-C(1)-C(9)-C(10)	-73.08(16)

C(2)-C(1)-C(9)-C(10)	166.71(13)
C(17)-C(9)-C(10)-C(11)	-71.13(18)
C(8)-C(9)-C(10)-C(11)	164.48(14)
C(1)-C(9)-C(10)-C(11)	51.06(19)
C(9)-C(10)-C(11)-C(12)	-68.57(19)
C(10)-C(11)-C(12)-O(2)	-44.03(18)
C(10)-C(11)-C(12)-C(13)	82.88(18)
O(2)-C(12)-C(13)-O(1)	86.53(16)
C(11)-C(12)-C(13)-O(1)	-36.29(19)
O(2)-C(12)-C(13)-C(14)	-36.92(19)
C(11)-C(12)-C(13)-C(14)	-159.74(14)
O(2)-C(12)-C(13)-C(15)	-158.93(14)
C(11)-C(12)-C(13)-C(15)	78.24(17)
C(6)-C(5)-C(18)-C(19)	-162(5)
C(4)-C(5)-C(18)-C(19)	24(5)
C(2)-C(1)-O(1)-C(13)	-135.27(14)
C(9)-C(1)-O(1)-C(13)	99.91(15)
C(14)-C(13)-O(1)-C(1)	78.00(17)
C(15)-C(13)-O(1)-C(1)	-164.53(14)
C(12)-C(13)-O(1)-C(1)	-46.70(18)

Symmetry transformations used to generate equivalent atoms:

Table 21. Hydrogen bonds for **115** [\AA and $^\circ$].

D-H...A	d(D-H)	d(H...A)	d(D...A)	$\angle(\text{DHA})$
O(2)-H(2)...O(1)#1	0.84	2.23	2.9706(16)	147.3

Symmetry transformations used to generate equivalent atoms:

#1 $-x, y+1/2, -z-1/2$

X-ray data for compound 117

Table 22. Crystal data and structure refinement for **117**.

Identification code	T106s	
Empirical formula	C ₃₉ H ₇₂ O ₄ Si ₂	
Formula weight	661.15	
Temperature	173(2) K	
Wavelength	0.71073 Å	
Crystal system	Monoclinic	
Space group	P2(1)	
Unit cell dimensions	a = 13.008(2) Å	α = 90°.
	b = 7.6273(11) Å	β = 106.982(3)°.
	c = 22.235(3) Å	γ = 90°.
Volume	2109.9(5) Å ³	
Z	2	
Density (calculated)	1.041 Mg/m ³	
Absorption coefficient	0.118 mm ⁻¹	
F(000)	732	
Crystal size	0.21 x 0.13 x 0.08 mm ³	
Theta range for data collection	1.64 to 24.41°.	
Index ranges	-15 ≤ h ≤ 15, -8 ≤ k ≤ 8, -25 ≤ l ≤ 25	
Reflections collected	23220	
Independent reflections	6956 [R(int) = 0.0669]	
Completeness to theta = 24.41°	100.0 %	
Absorption correction	Semi-empirical from equivalents	
Refinement method	Full-matrix least-squares on F ²	
Data / restraints / parameters	6956 / 1 / 406	
Goodness-of-fit on F ²	1.051	
Final R indices [I > 2σ(I)]	R1 = 0.0887, wR2 = 0.2032	
R indices (all data)	R1 = 0.1065, wR2 = 0.2156	
Absolute structure parameter	-0.1(3)	
Largest diff. peak and hole	1.183 and -0.672 e.Å ⁻³	

Table 23. Atomic coordinates ($\times 10^4$) and equivalent isotropic displacement parameters ($\text{\AA}^2 \times 10^3$) for **117**. $U(\text{eq})$ is defined as one third of the trace of the orthogonalized U_{ij} tensor.

	x	y	z	U(eq)
C(1)	1679(4)	1592(7)	3426(2)	34(1)
C(2)	750(4)	2130(7)	4229(2)	40(1)
C(3)	1499(5)	826(8)	4683(3)	47(1)
C(4)	1519(5)	-1028(7)	4416(3)	46(1)
C(5)	2225(4)	-1293(7)	3986(2)	39(1)
C(6)	1868(4)	-401(7)	3335(2)	34(1)
C(7)	2791(4)	-506(6)	3042(2)	30(1)
C(8)	2723(4)	596(7)	2438(2)	33(1)
C(9)	2567(4)	2513(7)	2596(3)	40(1)
C(10)	1603(4)	2693(7)	2859(2)	37(1)
C(11)	3194(4)	-2297(7)	2898(3)	38(1)
C(12)	4052(4)	-1799(7)	2589(3)	41(1)
C(13)	3796(4)	32(7)	2323(2)	34(1)
C(14)	4393(4)	895(7)	2029(2)	37(1)
C(15)	4177(4)	2672(8)	1715(3)	43(1)
C(16)	5115(4)	3905(7)	1970(3)	42(1)
C(17)	6164(4)	3140(6)	1924(2)	33(1)
C(18)	6415(4)	1347(7)	2221(2)	34(1)
C(19)	5430(4)	141(7)	1949(2)	37(1)
C(20)	7364(4)	495(7)	2050(3)	40(1)
C(21)	8384(4)	1594(8)	2145(3)	45(1)
C(22)	8278(4)	3128(7)	1699(3)	44(1)
C(23)	7762(5)	4757(7)	1892(3)	47(1)
C(24)	-403(5)	1852(9)	4234(3)	59(2)
C(25)	1107(6)	4019(8)	4397(3)	67(2)
C(26)	837(4)	-1324(8)	2940(3)	48(1)
C(27)	1835(4)	76(9)	1839(3)	50(2)
C(28)	6647(5)	1462(9)	2940(2)	49(1)
C(29)	8646(5)	5735(9)	2379(3)	64(2)
C(30)	7253(5)	5946(8)	1328(3)	57(2)

C(31)	2607(6)	1670(10)	6196(3)	67(2)
C(32)	4318(8)	-243(15)	5797(5)	112(3)
C(33)	4108(8)	3734(14)	5637(4)	108(4)
C(34)	8863(8)	-342(12)	700(5)	108(3)
C(35)	9358(11)	3530(20)	503(6)	195(8)
C(36)	7174(9)	1897(17)	-193(4)	116(4)
C(37)	6332(9)	570(30)	-112(5)	242(12)
C(38)	7609(9)	1148(15)	-749(4)	124(4)
C(39)	6779(17)	3860(20)	-333(6)	283(14)
O(1)	2572(3)	1469(6)	4899(2)	52(1)
O(2)	693(2)	1796(5)	3581(2)	38(1)
O(3)	7007(3)	4340(5)	2217(2)	44(1)
O(4)	7708(3)	2595(5)	1070(2)	42(1)
Si(1)	3378(1)	1613(3)	5621(1)	61(1)
Si(2)	8257(2)	1961(3)	531(1)	75(1)

Table 24. Bond lengths [\AA] and angles [$^\circ$] for **117**.

C(1)-O(2)	1.431(5)	C(12)-H(12A)	0.9900
C(1)-C(10)	1.494(7)	C(12)-H(12B)	0.9900
C(1)-C(6)	1.562(7)	C(13)-C(14)	1.327(7)
C(1)-H(1)	1.0000	C(14)-C(15)	1.512(7)
C(2)-O(2)	1.442(6)	C(14)-C(19)	1.524(7)
C(2)-C(24)	1.518(7)	C(15)-C(16)	1.514(8)
C(2)-C(25)	1.526(8)	C(15)-H(15A)	0.9900
C(2)-C(3)	1.544(8)	C(15)-H(15B)	0.9900
C(3)-O(1)	1.424(7)	C(16)-C(17)	1.514(7)
C(3)-C(4)	1.537(8)	C(16)-H(16A)	0.9900
C(3)-H(3)	1.0000	C(16)-H(16B)	0.9900
C(4)-C(5)	1.521(7)	C(17)-O(3)	1.431(6)
C(4)-H(4A)	0.9900	C(17)-C(18)	1.513(7)
C(4)-H(4B)	0.9900	C(17)-H(17)	1.0000
C(5)-C(6)	1.542(7)	C(18)-C(20)	1.538(7)
C(5)-H(5A)	0.9900	C(18)-C(28)	1.541(7)
C(5)-H(5B)	0.9900	C(18)-C(19)	1.550(7)
C(6)-C(7)	1.528(7)	C(19)-H(19A)	0.9900
C(6)-C(26)	1.542(7)	C(19)-H(19B)	0.9900
C(7)-C(11)	1.530(7)	C(20)-C(21)	1.531(7)
C(7)-C(8)	1.563(7)	C(20)-H(20A)	0.9900
C(7)-H(7)	1.0000	C(20)-H(20B)	0.9900
C(8)-C(9)	1.531(7)	C(21)-C(22)	1.514(8)
C(8)-C(27)	1.538(7)	C(21)-H(21A)	0.9900
C(8)-C(13)	1.552(7)	C(21)-H(21B)	0.9900
C(9)-C(10)	1.537(6)	C(22)-O(4)	1.438(6)
C(9)-H(9A)	0.9900	C(22)-C(23)	1.532(8)
C(9)-H(9B)	0.9900	C(22)-H(22)	1.0000
C(10)-H(10A)	0.9900	C(23)-O(3)	1.413(7)
C(10)-H(10B)	0.9900	C(23)-C(29)	1.525(8)
C(11)-C(12)	1.519(7)	C(23)-C(30)	1.532(8)
C(11)-H(11A)	0.9900	C(24)-H(24A)	0.9800
C(11)-H(11B)	0.9900	C(24)-H(24B)	0.9800
C(12)-C(13)	1.515(7)	C(24)-H(24C)	0.9800

C(25)-H(25A)	0.9800	C(35)-H(35B)	0.9800
C(25)-H(25B)	0.9800	C(35)-H(35C)	0.9800
C(25)-H(25C)	0.9800	C(36)-C(37)	1.540(18)
C(26)-H(26A)	0.9800	C(36)-C(39)	1.582(17)
C(26)-H(26B)	0.9800	C(36)-C(38)	1.608(12)
C(26)-H(26C)	0.9800	C(36)-Si(2)	1.804(10)
C(27)-H(27A)	0.9800	C(37)-H(37A)	0.9800
C(27)-H(27B)	0.9800	C(37)-H(37B)	0.9800
C(27)-H(27C)	0.9800	C(37)-H(37C)	0.9800
C(28)-H(28A)	0.9800	C(38)-H(38A)	0.9800
C(28)-H(28B)	0.9800	C(38)-H(38B)	0.9800
C(28)-H(28C)	0.9800	C(38)-H(38C)	0.9800
C(29)-H(29A)	0.9800	C(39)-H(39A)	0.9800
C(29)-H(29B)	0.9800	C(39)-H(39B)	0.9800
C(29)-H(29C)	0.9800	C(39)-H(39C)	0.9800
C(30)-H(30A)	0.9800	O(1)-Si(1)	1.645(4)
C(30)-H(30B)	0.9800	O(4)-Si(2)	1.637(4)
C(30)-H(30C)	0.9800		
C(31)-Si(1)	1.841(6)	O(2)-C(1)-C(10)	107.4(4)
C(31)-H(31A)	0.9800	O(2)-C(1)-C(6)	108.9(4)
C(31)-H(31B)	0.9800	C(10)-C(1)-C(6)	114.3(4)
C(31)-H(31C)	0.9800	O(2)-C(1)-H(1)	108.7
C(32)-Si(1)	1.836(10)	C(10)-C(1)-H(1)	108.7
C(32)-H(32A)	0.9800	C(6)-C(1)-H(1)	108.7
C(32)-H(32B)	0.9800	O(2)-C(2)-C(24)	102.7(4)
C(32)-H(32C)	0.9800	O(2)-C(2)-C(25)	109.5(4)
C(33)-Si(1)	1.871(9)	C(24)-C(2)-C(25)	111.1(5)
C(33)-H(33A)	0.9800	O(2)-C(2)-C(3)	112.2(4)
C(33)-H(33B)	0.9800	C(24)-C(2)-C(3)	109.9(5)
C(33)-H(33C)	0.9800	C(25)-C(2)-C(3)	111.1(5)
C(34)-Si(2)	1.917(9)	O(1)-C(3)-C(4)	108.7(5)
C(34)-H(34A)	0.9800	O(1)-C(3)-C(2)	111.6(5)
C(34)-H(34B)	0.9800	C(4)-C(3)-C(2)	114.8(5)
C(34)-H(34C)	0.9800	O(1)-C(3)-H(3)	107.1
C(35)-Si(2)	1.879(9)	C(4)-C(3)-H(3)	107.1
C(35)-H(35A)	0.9800	C(2)-C(3)-H(3)	107.1

C(5)-C(4)-C(3)	116.5(4)	C(1)-C(10)-C(9)	114.3(4)
C(5)-C(4)-H(4A)	108.2	C(1)-C(10)-H(10A)	108.7
C(3)-C(4)-H(4A)	108.2	C(9)-C(10)-H(10A)	108.7
C(5)-C(4)-H(4B)	108.2	C(1)-C(10)-H(10B)	108.7
C(3)-C(4)-H(4B)	108.2	C(9)-C(10)-H(10B)	108.7
H(4A)-C(4)-H(4B)	107.3	H(10A)-C(10)-H(10B)	107.6
C(4)-C(5)-C(6)	117.3(4)	C(12)-C(11)-C(7)	102.3(4)
C(4)-C(5)-H(5A)	108.0	C(12)-C(11)-H(11A)	111.3
C(6)-C(5)-H(5A)	108.0	C(7)-C(11)-H(11A)	111.3
C(4)-C(5)-H(5B)	108.0	C(12)-C(11)-H(11B)	111.3
C(6)-C(5)-H(5B)	108.0	C(7)-C(11)-H(11B)	111.3
H(5A)-C(5)-H(5B)	107.2	H(11A)-C(11)-H(11B)	109.2
C(7)-C(6)-C(5)	108.6(4)	C(13)-C(12)-C(11)	107.5(4)
C(7)-C(6)-C(26)	113.2(4)	C(13)-C(12)-H(12A)	110.2
C(5)-C(6)-C(26)	107.9(4)	C(11)-C(12)-H(12A)	110.2
C(7)-C(6)-C(1)	106.2(4)	C(13)-C(12)-H(12B)	110.2
C(5)-C(6)-C(1)	108.9(4)	C(11)-C(12)-H(12B)	110.2
C(26)-C(6)-C(1)	112.0(4)	H(12A)-C(12)-H(12B)	108.5
C(6)-C(7)-C(11)	119.7(4)	C(14)-C(13)-C(12)	123.8(4)
C(6)-C(7)-C(8)	118.9(4)	C(14)-C(13)-C(8)	128.9(5)
C(11)-C(7)-C(8)	103.8(4)	C(12)-C(13)-C(8)	107.3(4)
C(6)-C(7)-H(7)	104.2	C(13)-C(14)-C(15)	128.0(5)
C(11)-C(7)-H(7)	104.2	C(13)-C(14)-C(19)	122.4(5)
C(8)-C(7)-H(7)	104.2	C(15)-C(14)-C(19)	109.6(4)
C(9)-C(8)-C(27)	109.2(5)	C(14)-C(15)-C(16)	111.3(4)
C(9)-C(8)-C(13)	119.2(4)	C(14)-C(15)-H(15A)	109.4
C(27)-C(8)-C(13)	105.7(4)	C(16)-C(15)-H(15A)	109.4
C(9)-C(8)-C(7)	107.2(4)	C(14)-C(15)-H(15B)	109.4
C(27)-C(8)-C(7)	116.4(4)	C(16)-C(15)-H(15B)	109.4
C(13)-C(8)-C(7)	99.4(4)	H(15A)-C(15)-H(15B)	108.0
C(8)-C(9)-C(10)	110.5(4)	C(15)-C(16)-C(17)	112.3(4)
C(8)-C(9)-H(9A)	109.6	C(15)-C(16)-H(16A)	109.1
C(10)-C(9)-H(9A)	109.6	C(17)-C(16)-H(16A)	109.1
C(8)-C(9)-H(9B)	109.6	C(15)-C(16)-H(16B)	109.1
C(10)-C(9)-H(9B)	109.6	C(17)-C(16)-H(16B)	109.1
H(9A)-C(9)-H(9B)	108.1	H(16A)-C(16)-H(16B)	107.9

O(3)-C(17)-C(18)	109.9(4)	O(3)-C(23)-C(29)	103.9(5)
O(3)-C(17)-C(16)	108.0(4)	O(3)-C(23)-C(22)	112.8(4)
C(18)-C(17)-C(16)	113.8(4)	C(29)-C(23)-C(22)	107.1(5)
O(3)-C(17)-H(17)	108.3	O(3)-C(23)-C(30)	110.6(5)
C(18)-C(17)-H(17)	108.3	C(29)-C(23)-C(30)	110.3(5)
C(16)-C(17)-H(17)	108.3	C(22)-C(23)-C(30)	111.7(5)
C(17)-C(18)-C(20)	111.1(4)	C(2)-C(24)-H(24A)	110.1
C(17)-C(18)-C(28)	110.7(4)	C(2)-C(24)-H(24B)	108.8
C(20)-C(18)-C(28)	110.7(4)	H(24A)-C(24)-H(24B)	109.5
C(17)-C(18)-C(19)	108.5(4)	C(2)-C(24)-H(24C)	109.5
C(20)-C(18)-C(19)	106.5(4)	H(24A)-C(24)-H(24C)	109.5
C(28)-C(18)-C(19)	109.2(4)	H(24B)-C(24)-H(24C)	109.5
C(14)-C(19)-C(18)	112.9(4)	C(2)-C(25)-H(25A)	110.0
C(14)-C(19)-H(19A)	109.0	C(2)-C(25)-H(25B)	110.0
C(18)-C(19)-H(19A)	109.0	H(25A)-C(25)-H(25B)	109.5
C(14)-C(19)-H(19B)	109.0	C(2)-C(25)-H(25C)	108.4
C(18)-C(19)-H(19B)	109.0	H(25A)-C(25)-H(25C)	109.5
H(19A)-C(19)-H(19B)	107.8	H(25B)-C(25)-H(25C)	109.5
C(21)-C(20)-C(18)	117.4(4)	C(6)-C(26)-H(26A)	109.5
C(21)-C(20)-H(20A)	107.9	C(6)-C(26)-H(26B)	109.7
C(18)-C(20)-H(20A)	107.9	H(26A)-C(26)-H(26B)	109.5
C(21)-C(20)-H(20B)	107.9	C(6)-C(26)-H(26C)	109.2
C(18)-C(20)-H(20B)	107.9	H(26A)-C(26)-H(26C)	109.5
H(20A)-C(20)-H(20B)	107.2	H(26B)-C(26)-H(26C)	109.5
C(22)-C(21)-C(20)	115.1(4)	C(8)-C(27)-H(27A)	109.8
C(22)-C(21)-H(21A)	108.5	C(8)-C(27)-H(27B)	109.6
C(20)-C(21)-H(21A)	108.5	H(27A)-C(27)-H(27B)	109.5
C(22)-C(21)-H(21B)	108.5	C(8)-C(27)-H(27C)	109.0
C(20)-C(21)-H(21B)	108.5	H(27A)-C(27)-H(27C)	109.5
H(21A)-C(21)-H(21B)	107.5	H(27B)-C(27)-H(27C)	109.5
O(4)-C(22)-C(21)	109.9(4)	C(18)-C(28)-H(28A)	110.0
O(4)-C(22)-C(23)	111.0(4)	C(18)-C(28)-H(28B)	109.3
C(21)-C(22)-C(23)	114.0(5)	H(28A)-C(28)-H(28B)	109.5
O(4)-C(22)-H(22)	107.2	C(18)-C(28)-H(28C)	109.1
C(21)-C(22)-H(22)	107.2	H(28A)-C(28)-H(28C)	109.5
C(23)-C(22)-H(22)	107.2	H(28B)-C(28)-H(28C)	109.5

C(23)-C(29)-H(29A)	109.2	Si(2)-C(35)-H(35A)	107.9
C(23)-C(29)-H(29B)	109.6	Si(2)-C(35)-H(35B)	109.5
H(29A)-C(29)-H(29B)	109.5	H(35A)-C(35)-H(35B)	109.5
C(23)-C(29)-H(29C)	109.6	Si(2)-C(35)-H(35C)	110.9
H(29A)-C(29)-H(29C)	109.5	H(35A)-C(35)-H(35C)	109.5
H(29B)-C(29)-H(29C)	109.5	H(35B)-C(35)-H(35C)	109.5
C(23)-C(30)-H(30A)	109.8	C(37)-C(36)-C(39)	116.3(13)
C(23)-C(30)-H(30B)	109.0	C(37)-C(36)-C(38)	106.2(9)
H(30A)-C(30)-H(30B)	109.5	C(39)-C(36)-C(38)	110.6(10)
C(23)-C(30)-H(30C)	109.6	C(37)-C(36)-Si(2)	108.0(8)
H(30A)-C(30)-H(30C)	109.5	C(39)-C(36)-Si(2)	105.9(9)
H(30B)-C(30)-H(30C)	109.5	C(38)-C(36)-Si(2)	109.7(7)
Si(1)-C(31)-H(31A)	109.3	C(36)-C(37)-H(37A)	109.6
Si(1)-C(31)-H(31B)	110.1	C(36)-C(37)-H(37B)	110.1
H(31A)-C(31)-H(31B)	109.5	H(37A)-C(37)-H(37B)	109.5
Si(1)-C(31)-H(31C)	109.0	C(36)-C(37)-H(37C)	108.7
H(31A)-C(31)-H(31C)	109.5	H(37A)-C(37)-H(37C)	109.5
H(31B)-C(31)-H(31C)	109.5	H(37B)-C(37)-H(37C)	109.5
Si(1)-C(32)-H(32A)	110.5	C(36)-C(38)-H(38A)	109.0
Si(1)-C(32)-H(32B)	109.5	C(36)-C(38)-H(38B)	111.3
H(32A)-C(32)-H(32B)	109.5	H(38A)-C(38)-H(38B)	109.5
Si(1)-C(32)-H(32C)	108.4	C(36)-C(38)-H(38C)	108.1
H(32A)-C(32)-H(32C)	109.5	H(38A)-C(38)-H(38C)	109.5
H(32B)-C(32)-H(32C)	109.5	H(38B)-C(38)-H(38C)	109.5
Si(1)-C(33)-H(33A)	108.5	C(36)-C(39)-H(39A)	109.5
Si(1)-C(33)-H(33B)	110.0	C(36)-C(39)-H(39B)	109.5
H(33A)-C(33)-H(33B)	109.5	H(39A)-C(39)-H(39B)	109.5
Si(1)-C(33)-H(33C)	109.9	C(36)-C(39)-H(39C)	109.4
H(33A)-C(33)-H(33C)	109.5	H(39A)-C(39)-H(39C)	109.5
H(33B)-C(33)-H(33C)	109.5	H(39B)-C(39)-H(39C)	109.5
Si(2)-C(34)-H(34A)	109.5	C(3)-O(1)-Si(1)	129.4(3)
Si(2)-C(34)-H(34B)	109.8	C(1)-O(2)-C(2)	118.2(4)
H(34A)-C(34)-H(34B)	109.5	C(23)-O(3)-C(17)	117.8(4)
Si(2)-C(34)-H(34C)	109.2	C(22)-O(4)-Si(2)	125.7(3)
H(34A)-C(34)-H(34C)	109.5	O(1)-Si(1)-C(32)	110.6(4)
H(34B)-C(34)-H(34C)	109.5	O(1)-Si(1)-C(31)	111.0(3)

C(32)-Si(1)-C(31)	109.5(4)	O(4)-Si(2)-C(35)	109.7(4)
O(1)-Si(1)-C(33)	104.6(3)	C(36)-Si(2)-C(35)	113.0(6)
C(32)-Si(1)-C(33)	111.1(5)	O(4)-Si(2)-C(34)	111.7(3)
C(31)-Si(1)-C(33)	110.0(4)	C(36)-Si(2)-C(34)	108.6(5)
O(4)-Si(2)-C(36)	105.5(3)	C(35)-Si(2)-C(34)	108.4(6)

Symmetry transformations used to generate equivalent atoms:

Table 25. Anisotropic displacement parameters ($\text{\AA}^2 \times 10^3$) for **117**. The anisotropic displacement factor exponent takes the form: $-2\pi^2 [h^2 a^{*2} U^{11} + \dots + 2 h k a^* b^* U^{12}]$

	U11	U22	U33	U23	U13	U12
C(1)	33(3)	28(3)	43(3)	-2(2)	16(2)	1(2)
C(2)	48(3)	37(3)	40(3)	-8(2)	22(2)	-3(3)
C(3)	48(3)	60(4)	40(3)	-6(3)	24(3)	-16(3)
C(4)	46(3)	46(3)	51(4)	11(3)	20(3)	-9(3)
C(5)	40(3)	33(3)	49(3)	5(2)	20(3)	-6(2)
C(6)	26(2)	34(3)	40(3)	-2(2)	8(2)	-5(2)
C(7)	32(3)	25(2)	31(3)	1(2)	7(2)	-1(2)
C(8)	31(3)	38(3)	32(3)	2(2)	12(2)	5(2)
C(9)	42(3)	37(3)	47(3)	5(2)	24(3)	8(2)
C(10)	40(3)	31(3)	42(3)	5(2)	14(2)	12(2)
C(11)	35(3)	35(3)	48(3)	-5(2)	18(2)	5(2)
C(12)	39(3)	39(3)	47(3)	-1(2)	15(2)	9(2)
C(13)	39(3)	36(3)	28(3)	1(2)	11(2)	11(2)
C(14)	38(3)	39(3)	33(3)	-3(2)	7(2)	7(2)
C(15)	40(3)	55(3)	39(3)	11(3)	21(2)	14(3)
C(16)	52(3)	37(3)	41(3)	10(2)	19(3)	18(3)
C(17)	41(3)	27(3)	29(3)	-12(2)	8(2)	3(2)
C(18)	36(3)	34(3)	31(2)	-5(2)	8(2)	3(2)
C(19)	42(3)	30(3)	40(3)	-1(2)	16(2)	7(2)
C(20)	43(3)	36(3)	41(3)	6(2)	12(2)	10(3)
C(21)	30(3)	49(3)	57(3)	-15(3)	12(2)	8(3)
C(22)	33(3)	46(3)	53(3)	-11(3)	10(3)	-3(2)
C(23)	51(3)	30(3)	56(4)	-11(3)	11(3)	-10(3)
C(24)	58(4)	64(4)	69(4)	-12(4)	40(3)	3(3)
C(25)	95(5)	50(4)	69(5)	-19(3)	45(4)	-6(4)
C(26)	39(3)	47(3)	61(4)	-18(3)	21(3)	-7(3)
C(27)	38(3)	69(4)	39(3)	-8(3)	5(2)	8(3)
C(28)	54(3)	57(4)	34(3)	0(3)	9(2)	18(3)
C(29)	58(4)	58(4)	69(4)	-20(3)	5(3)	-10(3)
C(30)	65(4)	41(3)	66(4)	-9(3)	22(3)	-11(3)
C(31)	89(5)	70(4)	43(3)	-9(3)	20(3)	-25(4)

C(32)	98(7)	135(9)	99(7)	5(6)	20(5)	34(7)
C(33)	113(7)	155(9)	51(5)	4(5)	16(4)	-79(7)
C(34)	136(8)	86(6)	109(7)	-10(5)	48(6)	46(6)
C(35)	215(12)	262(16)	176(12)	-142(11)	164(11)	-187(13)
C(36)	141(8)	147(9)	60(5)	-7(6)	30(5)	46(8)
C(37)	100(8)	550(40)	87(7)	-120(13)	39(6)	-163(14)
C(38)	176(10)	153(10)	56(5)	-36(6)	54(6)	-63(8)
C(39)	470(30)	231(19)	88(9)	46(10)	-14(13)	260(20)
O(1)	50(2)	68(3)	40(2)	-3(2)	19(2)	-12(2)
O(2)	36(2)	39(2)	45(2)	-11(2)	20(2)	-4(2)
O(3)	49(2)	35(2)	46(2)	-19(2)	12(2)	2(2)
O(4)	42(2)	38(2)	44(2)	-10(2)	13(2)	-11(2)
Si(1)	59(1)	88(1)	38(1)	2(1)	15(1)	-14(1)
Si(2)	82(1)	89(2)	68(1)	-37(1)	44(1)	-45(1)

Table 26. Hydrogen coordinates ($\times 10^4$) and isotropic displacement parameters ($\text{\AA}^2 \times 10^3$) for **117**.

	x	y	z	U(eq)
H(1)	2282	2043	3784	40
H(3)	1230	714	5059	57
H(4A)	1761	-1853	4773	55
H(4B)	774	-1355	4180	55
H(5A)	2281	-2569	3919	47
H(5B)	2956	-867	4209	47
H(7)	3418	6	3369	35
H(9A)	2445	3237	2212	48
H(9B)	3225	2945	2910	48
H(10A)	1535	3937	2968	44
H(10B)	941	2368	2525	44
H(11A)	3503	-2980	3288	46
H(11B)	2610	-2984	2609	46
H(12A)	4771	-1823	2902	50
H(12B)	4049	-2637	2249	50
H(15A)	3523	3183	1787	51
H(15B)	4044	2532	1256	51
H(16A)	5182	4173	2415	50
H(16B)	4971	5019	1731	50
H(17)	6123	3042	1469	39
H(19A)	5337	-50	1496	44
H(19B)	5569	-1013	2161	44
H(20A)	7562	-590	2302	48
H(20B)	7111	143	1602	48
H(21A)	8604	2046	2581	55
H(21B)	8966	819	2098	55
H(22)	9021	3464	1699	53
H(24A)	-898	2454	3876	88
H(24B)	-487	2328	4627	88
H(24C)	-565	595	4210	88
H(25A)	1814	4216	4336	100

H(25B)	1144	4257	4836	100
H(25C)	579	4804	4121	100
H(26A)	516	-647	2557	71
H(26B)	323	-1417	3184	71
H(26C)	1020	-2501	2827	71
H(27A)	1139	509	1864	75
H(27B)	1809	-1203	1797	75
H(27C)	1996	597	1474	75
H(28A)	6897	325	3133	74
H(28B)	5988	1798	3040	74
H(28C)	7203	2349	3105	74
H(29A)	8321	6650	2574	97
H(29B)	9140	6273	2174	97
H(29C)	9043	4914	2703	97
H(30A)	6583	5421	1068	85
H(30B)	7756	6080	1078	85
H(30C)	7101	7099	1477	85
H(31A)	2184	2752	6140	101
H(31B)	3097	1628	6625	101
H(31C)	2124	657	6126	101
H(32A)	3929	-1353	5686	169
H(32B)	4710	-244	6246	169
H(32C)	4826	-108	5551	169
H(33A)	4514	3670	5329	162
H(33B)	4605	3934	6057	162
H(33C)	3592	4702	5527	162
H(34A)	9145	-514	1155	162
H(34B)	9446	-479	507	162
H(34C)	8302	-1214	524	162
H(35A)	9052	4710	441	293
H(35B)	9630	3222	149	293
H(35C)	9948	3486	895	293
H(37A)	5716	559	-492	363
H(37B)	6089	892	251	363
H(37C)	6661	-596	-45	363
H(38A)	7921	-17	-631	186

H(38B)	8154	1925	-830	186
H(38C)	6998	1054	-1130	186
H(39A)	6618	4093	-784	425
H(39B)	7344	4658	-99	425
H(39C)	6130	4038	-202	425

Table 27. Torsion angles [°] for **117**.

O(2)-C(2)-C(3)-O(1)	91.2(5)
C(24)-C(2)-C(3)-O(1)	-155.2(4)
C(25)-C(2)-C(3)-O(1)	-31.8(6)
O(2)-C(2)-C(3)-C(4)	-33.1(6)
C(24)-C(2)-C(3)-C(4)	80.6(5)
C(25)-C(2)-C(3)-C(4)	-156.0(5)
O(1)-C(3)-C(4)-C(5)	-45.0(6)
C(2)-C(3)-C(4)-C(5)	80.7(6)
C(3)-C(4)-C(5)-C(6)	-69.1(6)
C(4)-C(5)-C(6)-C(7)	168.2(4)
C(4)-C(5)-C(6)-C(26)	-68.8(6)
C(4)-C(5)-C(6)-C(1)	53.0(6)
O(2)-C(1)-C(6)-C(7)	168.6(4)
C(10)-C(1)-C(6)-C(7)	48.5(5)
O(2)-C(1)-C(6)-C(5)	-74.7(5)
C(10)-C(1)-C(6)-C(5)	165.2(4)
O(2)-C(1)-C(6)-C(26)	44.6(5)
C(10)-C(1)-C(6)-C(26)	-75.6(5)
C(5)-C(6)-C(7)-C(11)	62.2(6)
C(26)-C(6)-C(7)-C(11)	-57.6(6)
C(1)-C(6)-C(7)-C(11)	179.1(4)
C(5)-C(6)-C(7)-C(8)	-168.9(4)
C(26)-C(6)-C(7)-C(8)	71.4(6)
C(1)-C(6)-C(7)-C(8)	-51.9(5)
C(6)-C(7)-C(8)-C(9)	56.3(6)
C(11)-C(7)-C(8)-C(9)	-167.7(4)
C(6)-C(7)-C(8)-C(27)	-66.1(6)
C(11)-C(7)-C(8)-C(27)	69.8(5)
C(6)-C(7)-C(8)-C(13)	-179.0(4)
C(11)-C(7)-C(8)-C(13)	-43.0(5)
C(27)-C(8)-C(9)-C(10)	73.5(5)
C(13)-C(8)-C(9)-C(10)	-165.1(4)
C(7)-C(8)-C(9)-C(10)	-53.4(5)
O(2)-C(1)-C(10)-C(9)	-175.4(4)

C(6)-C(1)-C(10)-C(9)	-54.5(6)
C(8)-C(9)-C(10)-C(1)	56.8(6)
C(6)-C(7)-C(11)-C(12)	177.3(4)
C(8)-C(7)-C(11)-C(12)	41.8(5)
C(7)-C(11)-C(12)-C(13)	-23.4(5)
C(11)-C(12)-C(13)-C(14)	178.8(5)
C(11)-C(12)-C(13)-C(8)	-3.6(5)
C(9)-C(8)-C(13)-C(14)	-38.5(8)
C(27)-C(8)-C(13)-C(14)	84.7(7)
C(7)-C(8)-C(13)-C(14)	-154.3(5)
C(9)-C(8)-C(13)-C(12)	144.1(5)
C(27)-C(8)-C(13)-C(12)	-92.7(5)
C(7)-C(8)-C(13)-C(12)	28.3(5)
C(12)-C(13)-C(14)-C(15)	176.2(5)
C(8)-C(13)-C(14)-C(15)	-0.9(9)
C(12)-C(13)-C(14)-C(19)	-2.2(8)
C(8)-C(13)-C(14)-C(19)	-179.3(5)
C(13)-C(14)-C(15)-C(16)	125.3(6)
C(19)-C(14)-C(15)-C(16)	-56.2(5)
C(14)-C(15)-C(16)-C(17)	54.3(6)
C(15)-C(16)-C(17)-O(3)	-175.8(4)
C(15)-C(16)-C(17)-C(18)	-53.4(5)
O(3)-C(17)-C(18)-C(20)	-69.7(5)
C(16)-C(17)-C(18)-C(20)	169.0(4)
O(3)-C(17)-C(18)-C(28)	53.7(5)
C(16)-C(17)-C(18)-C(28)	-67.6(5)
O(3)-C(17)-C(18)-C(19)	173.5(4)
C(16)-C(17)-C(18)-C(19)	52.2(5)
C(13)-C(14)-C(19)-C(18)	-123.5(5)
C(15)-C(14)-C(19)-C(18)	57.9(5)
C(17)-C(18)-C(19)-C(14)	-55.1(5)
C(20)-C(18)-C(19)-C(14)	-174.8(4)
C(28)-C(18)-C(19)-C(14)	65.6(5)
C(17)-C(18)-C(20)-C(21)	49.9(6)
C(28)-C(18)-C(20)-C(21)	-73.4(6)
C(19)-C(18)-C(20)-C(21)	168.0(4)

C(18)-C(20)-C(21)-C(22)	-69.2(6)
C(20)-C(21)-C(22)-O(4)	-43.9(6)
C(20)-C(21)-C(22)-C(23)	81.5(6)
O(4)-C(22)-C(23)-O(3)	93.8(5)
C(21)-C(22)-C(23)-O(3)	-31.0(6)
O(4)-C(22)-C(23)-C(29)	-152.6(5)
C(21)-C(22)-C(23)-C(29)	82.7(6)
O(4)-C(22)-C(23)-C(30)	-31.7(6)
C(21)-C(22)-C(23)-C(30)	-156.4(4)
C(4)-C(3)-O(1)-Si(1)	-102.4(5)
C(2)-C(3)-O(1)-Si(1)	130.1(4)
C(10)-C(1)-O(2)-C(2)	-133.0(4)
C(6)-C(1)-O(2)-C(2)	102.7(5)
C(24)-C(2)-O(2)-C(1)	-167.6(4)
C(25)-C(2)-O(2)-C(1)	74.2(6)
C(3)-C(2)-O(2)-C(1)	-49.6(6)
C(29)-C(23)-O(3)-C(17)	-169.1(4)
C(22)-C(23)-O(3)-C(17)	-53.4(6)
C(30)-C(23)-O(3)-C(17)	72.6(5)
C(18)-C(17)-O(3)-C(23)	102.1(5)
C(16)-C(17)-O(3)-C(23)	-133.3(4)
C(21)-C(22)-O(4)-Si(2)	-95.7(5)
C(23)-C(22)-O(4)-Si(2)	137.2(4)
C(3)-O(1)-Si(1)-C(32)	98.7(6)
C(3)-O(1)-Si(1)-C(31)	-23.1(6)
C(3)-O(1)-Si(1)-C(33)	-141.7(6)
C(22)-O(4)-Si(2)-C(36)	-168.6(6)
C(22)-O(4)-Si(2)-C(35)	-46.6(7)
C(22)-O(4)-Si(2)-C(34)	73.6(5)
C(37)-C(36)-Si(2)-O(4)	-60.4(10)
C(39)-C(36)-Si(2)-O(4)	64.8(11)
C(38)-C(36)-Si(2)-O(4)	-175.8(7)
C(37)-C(36)-Si(2)-C(35)	179.8(10)
C(39)-C(36)-Si(2)-C(35)	-55.0(11)
C(38)-C(36)-Si(2)-C(35)	64.4(10)
C(37)-C(36)-Si(2)-C(34)	59.4(10)

C(39)-C(36)-Si(2)-C(34)	-175.4(10)
C(38)-C(36)-Si(2)-C(34)	-56.0(9)

Symmetry transformations used to generate equivalent atoms:

X-ray data for compound 179

Table 28. Crystal data and structure refinement for **179**.

Identification code	Tong112907SQ
Empirical formula	C44 H56 Br2 O6
Formula weight	840.71
Temperature	200(2) K
Wavelength	1.54178 Å
Crystal system	Orthorhombic
Space group	P2(1)2(1)2(1)
Unit cell dimensions	a = 8.8790(4) Å $\alpha = 90^\circ$. b = 20.7162(7) Å $\beta = 90^\circ$. c = 24.1069(8) Å $\gamma = 90^\circ$.
Volume	4434.2(3) Å ³
Z	4
Density (calculated)	1.259 Mg/m ³
Absorption coefficient	2.654 mm ⁻¹
F(000)	1752
Crystal size	0.48 x 0.32 x 0.22 mm ³
Theta range for data collection	8.34 to 66.70°.
Index ranges	-8<=h<=9, -21<=k<=23, -24<=l<=24
Reflections collected	17742
Independent reflections	6314 [R(int) = 0.0407]
Completeness to theta = 66.70°	88.0 %
Absorption correction	Semi-empirical from equivalents
Max. and min. transmission	0.5929 and 0.3624
Refinement method	Full-matrix least-squares on F ²
Data / restraints / parameters	6314 / 0 / 476
Goodness-of-fit on F ²	1.048
Final R indices [I>2sigma(I)]	R1 = 0.0491, wR2 = 0.1342
R indices (all data)	R1 = 0.0579, wR2 = 0.1401
Absolute structure parameter	0.05(2)
Largest diff. peak and hole	0.581 and -0.467 e.Å ⁻³

Table 29. Atomic coordinates ($\times 10^4$) and equivalent isotropic displacement parameters ($\text{\AA}^2 \times 10^3$) for **179**. $U(\text{eq})$ is defined as one third of the trace of the orthogonalized U^{ij} tensor.

	x	y	z	U(eq)
Br(1)	8263(1)	11135(1)	3643(1)	120(1)
Br(2)	6930(1)	6352(1)	1331(1)	89(1)
C(1)	7412(6)	11044(3)	2930(2)	62(1)
C(2)	7931(6)	11408(2)	2506(2)	63(1)
C(3)	7346(5)	11339(2)	1987(2)	59(1)
C(4)	6164(5)	10903(2)	1893(2)	48(1)
C(5)	5634(6)	10534(2)	2333(2)	50(1)
C(6)	6253(6)	10607(2)	2856(2)	61(1)
C(7)	5564(6)	10855(2)	1328(2)	52(1)
C(8)	3942(6)	10248(2)	722(2)	52(1)
C(9)	4381(5)	9561(2)	544(2)	48(1)
C(10)	2745(5)	9086(2)	1254(2)	39(1)
C(11)	2725(5)	8385(2)	1446(2)	43(1)
C(12)	2052(6)	8294(2)	2023(2)	47(1)
C(13)	482(5)	8578(2)	2063(2)	47(1)
C(14)	-200(5)	8680(2)	2663(2)	49(1)
C(15)	-1385(6)	9222(3)	2572(2)	61(1)
C(16)	-966(6)	9569(3)	2030(2)	57(1)
C(17)	570(5)	9282(2)	1865(2)	42(1)
C(18)	1196(5)	9412(2)	1274(2)	39(1)
C(19)	1385(5)	10149(2)	1219(2)	47(1)
C(20)	2285(5)	10401(2)	716(2)	50(1)
C(21)	5952(6)	9377(3)	760(3)	69(2)
C(22)	4403(7)	9540(3)	-90(2)	68(1)
C(23)	171(5)	9180(2)	810(2)	53(1)
C(24)	-640(7)	8136(3)	1754(2)	67(2)
C(25)	950(5)	8803(2)	3115(2)	46(1)
C(26)	1521(6)	9378(2)	3227(2)	49(1)
C(27)	2761(6)	9496(2)	3642(2)	49(1)
C(28)	3511(5)	8882(2)	3855(2)	41(1)

C(29)	5823(6)	8795(3)	4410(2)	66(2)
C(30)	5823(7)	8057(3)	4379(2)	63(1)
C(31)	4365(7)	7724(3)	4573(2)	65(1)
C(32)	3091(6)	7715(2)	4142(2)	53(1)
C(33)	2338(5)	8350(2)	3971(2)	43(1)
C(34)	1490(5)	8218(2)	3426(2)	47(1)
C(35)	1241(6)	8569(3)	4426(2)	55(1)
C(36)	6912(7)	9104(3)	4007(3)	82(2)
C(37)	6189(8)	8980(4)	5015(2)	90(2)
C(38)	7043(6)	7371(2)	3715(2)	54(1)
C(39)	7003(6)	7154(2)	3134(2)	49(1)
C(40)	5984(5)	7393(2)	2745(2)	49(1)
C(41)	5945(6)	7158(2)	2212(2)	57(1)
C(42)	6962(6)	6676(2)	2062(2)	59(1)
C(43)	7955(6)	6422(2)	2431(2)	60(1)
C(44)	8000(6)	6662(2)	2969(2)	55(1)
O(1)	5933(6)	11198(2)	954(2)	90(1)
O(2)	4550(4)	10378(2)	1274(1)	59(1)
O(3)	3299(3)	9084(1)	692(1)	42(1)
O(4)	4311(4)	9057(2)	4336(1)	52(1)
O(5)	6069(4)	7846(2)	3810(1)	63(1)
O(6)	7869(5)	7151(2)	4067(2)	79(1)

Table 30. Bond lengths [Å] and angles [°] for **179**.

Br(1)-C(1)	1.887(5)	C(25)-C(34)	1.503(6)
Br(2)-C(42)	1.887(5)	C(26)-C(27)	1.508(7)
C(1)-C(2)	1.351(8)	C(27)-C(28)	1.524(6)
C(1)-C(6)	1.383(8)	C(28)-O(4)	1.410(5)
C(2)-C(3)	1.362(7)	C(28)-C(33)	1.542(6)
C(3)-C(4)	1.404(6)	C(29)-O(4)	1.459(6)
C(4)-C(5)	1.389(6)	C(29)-C(36)	1.513(9)
C(4)-C(7)	1.464(7)	C(29)-C(30)	1.531(8)
C(5)-C(6)	1.384(7)	C(29)-C(37)	1.542(7)
C(7)-O(1)	1.195(6)	C(30)-O(5)	1.456(6)
C(7)-O(2)	1.343(5)	C(30)-C(31)	1.540(9)
C(8)-O(2)	1.462(6)	C(31)-C(32)	1.537(7)
C(8)-C(20)	1.504(7)	C(32)-C(33)	1.533(6)
C(8)-C(9)	1.537(7)	C(33)-C(35)	1.535(6)
C(9)-O(3)	1.424(5)	C(33)-C(34)	1.540(6)
C(9)-C(22)	1.527(7)	C(38)-O(6)	1.210(6)
C(9)-C(21)	1.537(7)	C(38)-O(5)	1.332(5)
C(10)-O(3)	1.442(5)	C(38)-C(39)	1.471(7)
C(10)-C(11)	1.523(5)	C(39)-C(40)	1.394(6)
C(10)-C(18)	1.533(6)	C(39)-C(44)	1.407(6)
C(11)-C(12)	1.525(6)	C(40)-C(41)	1.377(7)
C(12)-C(13)	1.516(7)	C(41)-C(42)	1.393(7)
C(13)-C(17)	1.537(6)	C(42)-C(43)	1.357(7)
C(13)-C(24)	1.544(7)	C(43)-C(44)	1.390(7)
C(13)-C(14)	1.582(6)		
C(14)-C(25)	1.516(6)	C(2)-C(1)-C(6)	121.4(5)
C(14)-C(15)	1.554(7)	C(2)-C(1)-Br(1)	119.8(4)
C(15)-C(16)	1.538(7)	C(6)-C(1)-Br(1)	118.7(4)
C(16)-C(17)	1.540(6)	C(1)-C(2)-C(3)	120.5(5)
C(17)-C(18)	1.551(6)	C(2)-C(3)-C(4)	120.0(5)
C(18)-C(23)	1.521(6)	C(5)-C(4)-C(3)	118.9(4)
C(18)-C(19)	1.542(6)	C(5)-C(4)-C(7)	123.3(4)
C(19)-C(20)	1.544(6)	C(3)-C(4)-C(7)	117.7(4)
C(25)-C(26)	1.323(6)	C(6)-C(5)-C(4)	120.2(5)

C(5)-C(6)-C(1)	118.9(5)	C(10)-C(18)-C(17)	105.9(3)
O(1)-C(7)-O(2)	123.2(5)	C(19)-C(18)-C(17)	106.8(3)
O(1)-C(7)-C(4)	124.2(4)	C(18)-C(19)-C(20)	117.3(4)
O(2)-C(7)-C(4)	112.6(4)	C(8)-C(20)-C(19)	115.4(4)
O(2)-C(8)-C(20)	109.3(4)	C(26)-C(25)-C(34)	120.2(4)
O(2)-C(8)-C(9)	109.3(4)	C(26)-C(25)-C(14)	123.8(4)
C(20)-C(8)-C(9)	116.1(4)	C(34)-C(25)-C(14)	115.9(4)
O(3)-C(9)-C(22)	103.8(4)	C(25)-C(26)-C(27)	124.1(4)
O(3)-C(9)-C(21)	110.8(4)	C(26)-C(27)-C(28)	114.1(3)
C(22)-C(9)-C(21)	108.7(5)	O(4)-C(28)-C(27)	106.4(3)
O(3)-C(9)-C(8)	113.7(4)	O(4)-C(28)-C(33)	112.0(3)
C(22)-C(9)-C(8)	108.0(4)	C(27)-C(28)-C(33)	111.3(4)
C(21)-C(9)-C(8)	111.4(4)	O(4)-C(29)-C(36)	110.6(4)
O(3)-C(10)-C(11)	106.7(3)	O(4)-C(29)-C(30)	111.5(5)
O(3)-C(10)-C(18)	109.7(3)	C(36)-C(29)-C(30)	113.0(5)
C(11)-C(10)-C(18)	113.5(3)	O(4)-C(29)-C(37)	102.5(4)
C(10)-C(11)-C(12)	113.6(3)	C(36)-C(29)-C(37)	111.5(5)
C(13)-C(12)-C(11)	111.7(4)	C(30)-C(29)-C(37)	107.1(5)
C(12)-C(13)-C(17)	107.6(4)	O(5)-C(30)-C(29)	110.2(4)
C(12)-C(13)-C(24)	109.4(4)	O(5)-C(30)-C(31)	106.2(4)
C(17)-C(13)-C(24)	116.5(4)	C(29)-C(30)-C(31)	115.6(4)
C(12)-C(13)-C(14)	117.5(4)	C(32)-C(31)-C(30)	114.8(4)
C(17)-C(13)-C(14)	100.1(4)	C(31)-C(32)-C(33)	119.4(4)
C(24)-C(13)-C(14)	105.8(4)	C(35)-C(33)-C(32)	109.8(4)
C(25)-C(14)-C(15)	115.8(4)	C(35)-C(33)-C(34)	110.6(4)
C(25)-C(14)-C(13)	115.0(4)	C(32)-C(33)-C(34)	106.8(3)
C(15)-C(14)-C(13)	103.2(4)	C(35)-C(33)-C(28)	110.3(4)
C(16)-C(15)-C(14)	107.0(4)	C(32)-C(33)-C(28)	111.6(4)
C(15)-C(16)-C(17)	104.7(4)	C(34)-C(33)-C(28)	107.6(3)
C(13)-C(17)-C(16)	103.9(4)	C(25)-C(34)-C(33)	115.9(4)
C(13)-C(17)-C(18)	117.9(3)	O(6)-C(38)-O(5)	123.5(4)
C(16)-C(17)-C(18)	119.2(4)	O(6)-C(38)-C(39)	124.6(4)
C(23)-C(18)-C(10)	112.0(3)	O(5)-C(38)-C(39)	112.0(4)
C(23)-C(18)-C(19)	108.3(3)	C(40)-C(39)-C(44)	118.4(4)
C(10)-C(18)-C(19)	109.6(3)	C(40)-C(39)-C(38)	123.2(4)
C(23)-C(18)-C(17)	114.0(4)	C(44)-C(39)-C(38)	118.3(4)

C(41)-C(40)-C(39)	121.2(4)
C(40)-C(41)-C(42)	118.7(5)
C(43)-C(42)-C(41)	122.0(5)
C(43)-C(42)-Br(2)	118.9(4)
C(41)-C(42)-Br(2)	119.1(4)
C(42)-C(43)-C(44)	119.4(5)
C(43)-C(44)-C(39)	120.4(5)
C(7)-O(2)-C(8)	118.1(3)
C(9)-O(3)-C(10)	117.6(3)
C(28)-O(4)-C(29)	117.9(3)
C(38)-O(5)-C(30)	118.8(4)

Symmetry transformations used to
generate equivalent atoms:

Table 31. Anisotropic displacement parameters ($\text{\AA}^2 \times 10^3$) for **179**. The anisotropic displacement factor exponent takes the form: $-2\pi^2 [h^2 a^{*2} U^{11} + \dots + 2 h k a^* b^* U^{12}]$

	U11	U22	U33	U23	U13	U12
Br(1)	123(1)	145(1)	91(1)	-18(1)	-51(1)	-26(1)
Br(2)	121(1)	77(1)	69(1)	-20(1)	16(1)	-7(1)
C(1)	52(3)	62(3)	71(3)	-16(3)	-19(3)	4(2)
C(2)	52(3)	44(2)	92(4)	-18(3)	-19(3)	-4(2)
C(3)	47(3)	43(2)	87(4)	0(2)	-3(3)	-5(2)
C(4)	51(3)	32(2)	60(3)	-4(2)	-3(2)	2(2)
C(5)	49(3)	51(3)	51(3)	-3(2)	-5(2)	-4(2)
C(6)	64(3)	61(3)	58(3)	2(2)	-4(3)	-1(2)
C(7)	61(3)	41(2)	56(3)	-1(2)	2(3)	-11(2)
C(8)	61(3)	53(3)	43(3)	10(2)	-7(2)	-9(2)
C(9)	46(3)	57(3)	41(3)	8(2)	0(2)	3(2)
C(10)	45(2)	37(2)	34(2)	-1(2)	-4(2)	5(2)
C(11)	55(3)	38(2)	36(2)	2(2)	7(2)	9(2)
C(12)	55(3)	35(2)	51(3)	7(2)	0(2)	4(2)
C(13)	51(3)	56(3)	34(2)	8(2)	-5(2)	-5(2)
C(14)	42(3)	57(3)	49(3)	8(2)	2(2)	-1(2)
C(15)	46(3)	79(3)	59(3)	14(3)	8(2)	6(2)
C(16)	51(3)	71(3)	49(3)	9(2)	7(2)	14(2)
C(17)	35(2)	51(2)	39(2)	-2(2)	1(2)	4(2)
C(18)	43(2)	40(2)	32(2)	3(2)	-4(2)	5(2)
C(19)	55(3)	40(2)	47(3)	6(2)	-5(2)	11(2)
C(20)	61(3)	40(2)	50(3)	12(2)	-9(2)	2(2)
C(21)	42(3)	90(4)	75(4)	4(3)	-7(3)	4(3)
C(22)	81(4)	81(4)	43(3)	5(2)	12(3)	-7(3)
C(23)	47(3)	65(3)	47(3)	4(2)	-16(2)	-3(2)
C(24)	76(4)	64(3)	60(3)	6(2)	-3(3)	-30(3)
C(25)	46(3)	58(3)	33(2)	7(2)	7(2)	1(2)
C(26)	56(3)	46(2)	44(3)	9(2)	1(2)	13(2)
C(27)	72(3)	40(2)	33(2)	-1(2)	-1(2)	2(2)
C(28)	48(3)	42(2)	32(2)	-2(2)	4(2)	5(2)
C(29)	66(4)	80(4)	51(3)	-10(2)	-18(3)	21(3)

C(30)	67(4)	82(3)	39(3)	-4(2)	-9(2)	27(3)
C(31)	94(4)	58(3)	43(3)	10(2)	-5(3)	25(3)
C(32)	71(3)	42(2)	45(3)	8(2)	3(2)	9(2)
C(33)	56(3)	45(2)	28(2)	7(2)	-3(2)	7(2)
C(34)	53(3)	50(2)	38(2)	10(2)	8(2)	-1(2)
C(35)	63(3)	69(3)	34(3)	4(2)	12(2)	10(2)
C(36)	60(4)	94(4)	91(4)	-9(3)	-6(3)	-3(3)
C(37)	88(5)	130(6)	52(3)	-34(3)	-29(3)	26(4)
C(38)	56(3)	42(2)	65(3)	0(2)	-1(3)	9(2)
C(39)	51(3)	37(2)	59(3)	3(2)	3(2)	4(2)
C(40)	53(3)	43(2)	52(3)	-1(2)	1(2)	7(2)
C(41)	60(3)	52(3)	58(3)	9(2)	1(2)	-1(2)
C(42)	61(3)	48(2)	66(3)	-1(2)	10(3)	-7(2)
C(43)	63(3)	39(2)	77(3)	-10(2)	15(3)	0(2)
C(44)	46(3)	42(2)	78(3)	7(2)	0(3)	6(2)
O(1)	125(4)	81(3)	64(3)	13(2)	1(2)	-52(3)
O(2)	66(2)	59(2)	51(2)	10(2)	-4(2)	-24(2)
O(3)	50(2)	48(2)	29(2)	-2(1)	1(1)	1(1)
O(4)	55(2)	57(2)	42(2)	-6(1)	-10(2)	13(2)
O(5)	72(2)	72(2)	45(2)	1(2)	-4(2)	37(2)
O(6)	92(3)	80(2)	64(2)	-12(2)	-26(2)	43(2)

Table 32. Hydrogen coordinates ($\times 10^4$) and isotropic displacement parameters ($\text{\AA}^2 \times 10^3$) for **179**.

	x	y	z	U(eq)
H(2)	8708	11714	2570	75
H(3)	7739	11586	1688	71
H(5)	4845	10232	2274	60
H(6)	5887	10360	3159	73
H(8)	4443	10554	459	63
H(10)	3461	9335	1492	46
H(11A)	3769	8218	1446	52
H(11B)	2137	8126	1177	52
H(12A)	2009	7827	2110	56
H(12B)	2711	8504	2301	56
H(14)	-759	8278	2763	59
H(15A)	-2408	9034	2545	73
H(15B)	-1368	9529	2887	73
H(16A)	-887	10040	2089	68
H(16B)	-1729	9485	1739	68
H(17)	1310	9492	2120	50
H(19A)	1882	10309	1560	57
H(19B)	368	10345	1206	57
H(20A)	1840	10217	375	60
H(20B)	2164	10876	697	60
H(21A)	5883	9259	1153	104
H(21B)	6635	9746	718	104
H(21C)	6340	9010	547	104
H(22A)	4666	9103	-213	103
H(22B)	5152	9847	-229	103
H(22C)	3406	9655	-233	103
H(23A)	551	9340	453	79
H(23B)	-851	9345	871	79
H(23C)	152	8707	805	79
H(24A)	-244	8035	1384	100

H(24B)	-1610	8357	1717	100
H(24C)	-778	7735	1964	100
H(26)	1125	9740	3033	58
H(27A)	2339	9735	3962	58
H(27B)	3537	9773	3469	58
H(28)	4239	8723	3569	49
H(30)	6674	7893	4611	75
H(31A)	4605	7274	4678	78
H(31B)	3997	7947	4910	78
H(32A)	2291	7426	4285	63
H(32B)	3494	7511	3802	63
H(34A)	2161	7967	3178	56
H(34B)	608	7943	3510	56
H(35A)	1786	8618	4776	83
H(35B)	445	8245	4470	83
H(35C)	791	8983	4320	83
H(36A)	6541	9046	3627	123
H(36B)	7903	8900	4043	123
H(36C)	6997	9566	4089	123
H(37A)	6067	9447	5062	136
H(37B)	7230	8859	5100	136
H(37C)	5503	8753	5266	136
H(40)	5302	7725	2851	59
H(41)	5239	7320	1950	68
H(43)	8612	6083	2322	72
H(44)	8706	6493	3227	66

Table 33. Torsion angles [°] for **179**.

C(6)-C(1)-C(2)-C(3)	-1.8(8)
Br(1)-C(1)-C(2)-C(3)	178.8(4)
C(1)-C(2)-C(3)-C(4)	2.0(7)
C(2)-C(3)-C(4)-C(5)	-1.6(7)
C(2)-C(3)-C(4)-C(7)	179.1(4)
C(3)-C(4)-C(5)-C(6)	1.0(7)
C(7)-C(4)-C(5)-C(6)	-179.8(5)
C(4)-C(5)-C(6)-C(1)	-0.7(8)
C(2)-C(1)-C(6)-C(5)	1.1(8)
Br(1)-C(1)-C(6)-C(5)	-179.5(4)
C(5)-C(4)-C(7)-O(1)	174.7(5)
C(3)-C(4)-C(7)-O(1)	-6.1(8)
C(5)-C(4)-C(7)-O(2)	-5.8(7)
C(3)-C(4)-C(7)-O(2)	173.5(4)
O(2)-C(8)-C(9)-O(3)	91.0(4)
C(20)-C(8)-C(9)-O(3)	-33.2(5)
O(2)-C(8)-C(9)-C(22)	-154.3(4)
C(20)-C(8)-C(9)-C(22)	81.5(5)
O(2)-C(8)-C(9)-C(21)	-35.0(5)
C(20)-C(8)-C(9)-C(21)	-159.2(4)
O(3)-C(10)-C(11)-C(12)	-175.6(4)
C(18)-C(10)-C(11)-C(12)	-54.7(5)
C(10)-C(11)-C(12)-C(13)	55.1(5)
C(11)-C(12)-C(13)-C(17)	-53.0(5)
C(11)-C(12)-C(13)-C(24)	74.4(4)
C(11)-C(12)-C(13)-C(14)	-165.0(4)
C(12)-C(13)-C(14)-C(25)	28.9(6)
C(17)-C(13)-C(14)-C(25)	-87.1(4)
C(24)-C(13)-C(14)-C(25)	151.5(4)
C(12)-C(13)-C(14)-C(15)	156.0(4)
C(17)-C(13)-C(14)-C(15)	39.9(4)
C(24)-C(13)-C(14)-C(15)	-81.5(5)
C(25)-C(14)-C(15)-C(16)	106.4(5)
C(13)-C(14)-C(15)-C(16)	-20.1(5)

C(14)-C(15)-C(16)-C(17)	-7.7(6)
C(12)-C(13)-C(17)-C(16)	-168.8(4)
C(24)-C(13)-C(17)-C(16)	68.0(5)
C(14)-C(13)-C(17)-C(16)	-45.5(4)
C(12)-C(13)-C(17)-C(18)	56.8(5)
C(24)-C(13)-C(17)-C(18)	-66.4(6)
C(14)-C(13)-C(17)-C(18)	-179.9(4)
C(15)-C(16)-C(17)-C(13)	33.7(5)
C(15)-C(16)-C(17)-C(18)	167.4(4)
O(3)-C(10)-C(18)-C(23)	45.2(4)
C(11)-C(10)-C(18)-C(23)	-74.1(4)
O(3)-C(10)-C(18)-C(19)	-75.1(4)
C(11)-C(10)-C(18)-C(19)	165.7(3)
O(3)-C(10)-C(18)-C(17)	170.0(3)
C(11)-C(10)-C(18)-C(17)	50.8(4)
C(13)-C(17)-C(18)-C(23)	68.9(5)
C(16)-C(17)-C(18)-C(23)	-58.5(5)
C(13)-C(17)-C(18)-C(10)	-54.7(5)
C(16)-C(17)-C(18)-C(10)	177.9(4)
C(13)-C(17)-C(18)-C(19)	-171.5(4)
C(16)-C(17)-C(18)-C(19)	61.1(5)
C(23)-C(18)-C(19)-C(20)	-68.7(5)
C(10)-C(18)-C(19)-C(20)	53.8(5)
C(17)-C(18)-C(19)-C(20)	168.1(4)
O(2)-C(8)-C(20)-C(19)	-44.9(5)
C(9)-C(8)-C(20)-C(19)	79.2(5)
C(18)-C(19)-C(20)-C(8)	-68.1(6)
C(15)-C(14)-C(25)-C(26)	-36.0(6)
C(13)-C(14)-C(25)-C(26)	84.3(6)
C(15)-C(14)-C(25)-C(34)	146.9(4)
C(13)-C(14)-C(25)-C(34)	-92.8(5)
C(34)-C(25)-C(26)-C(27)	2.5(7)
C(14)-C(25)-C(26)-C(27)	-174.5(4)
C(25)-C(26)-C(27)-C(28)	10.3(7)
C(26)-C(27)-C(28)-O(4)	-164.0(4)
C(26)-C(27)-C(28)-C(33)	-41.7(5)

O(4)-C(29)-C(30)-O(5)	90.6(5)
C(36)-C(29)-C(30)-O(5)	-34.8(6)
C(37)-C(29)-C(30)-O(5)	-158.1(5)
O(4)-C(29)-C(30)-C(31)	-29.8(6)
C(36)-C(29)-C(30)-C(31)	-155.1(4)
C(37)-C(29)-C(30)-C(31)	81.6(6)
O(5)-C(30)-C(31)-C(32)	-42.0(5)
C(29)-C(30)-C(31)-C(32)	80.5(5)
C(30)-C(31)-C(32)-C(33)	-67.2(6)
C(31)-C(32)-C(33)-C(35)	-76.9(6)
C(31)-C(32)-C(33)-C(34)	163.1(4)
C(31)-C(32)-C(33)-C(28)	45.8(6)
O(4)-C(28)-C(33)-C(35)	56.9(4)
C(27)-C(28)-C(33)-C(35)	-62.0(4)
O(4)-C(28)-C(33)-C(32)	-65.4(4)
C(27)-C(28)-C(33)-C(32)	175.6(3)
O(4)-C(28)-C(33)-C(34)	177.7(3)
C(27)-C(28)-C(33)-C(34)	58.7(4)
C(26)-C(25)-C(34)-C(33)	17.4(6)
C(14)-C(25)-C(34)-C(33)	-165.4(4)
C(35)-C(33)-C(34)-C(25)	73.5(5)
C(32)-C(33)-C(34)-C(25)	-167.1(4)
C(28)-C(33)-C(34)-C(25)	-47.1(5)
O(6)-C(38)-C(39)-C(40)	176.5(5)
O(5)-C(38)-C(39)-C(40)	-4.3(7)
O(6)-C(38)-C(39)-C(44)	-0.6(7)
O(5)-C(38)-C(39)-C(44)	178.6(4)
C(44)-C(39)-C(40)-C(41)	-0.1(7)
C(38)-C(39)-C(40)-C(41)	-177.3(4)
C(39)-C(40)-C(41)-C(42)	-0.7(7)
C(40)-C(41)-C(42)-C(43)	1.9(7)
C(40)-C(41)-C(42)-Br(2)	-179.6(4)
C(41)-C(42)-C(43)-C(44)	-2.2(7)
Br(2)-C(42)-C(43)-C(44)	179.3(4)
C(42)-C(43)-C(44)-C(39)	1.4(7)
C(40)-C(39)-C(44)-C(43)	-0.2(7)

C(38)-C(39)-C(44)-C(43)	177.0(4)
O(1)-C(7)-O(2)-C(8)	3.8(7)
C(4)-C(7)-O(2)-C(8)	-175.7(4)
C(20)-C(8)-O(2)-C(7)	-114.5(5)
C(9)-C(8)-O(2)-C(7)	117.4(4)
C(22)-C(9)-O(3)-C(10)	-165.6(4)
C(21)-C(9)-O(3)-C(10)	77.9(5)
C(8)-C(9)-O(3)-C(10)	-48.5(5)
C(11)-C(10)-O(3)-C(9)	-136.2(4)
C(18)-C(10)-O(3)-C(9)	100.4(4)
C(27)-C(28)-O(4)-C(29)	-137.1(4)
C(33)-C(28)-O(4)-C(29)	101.1(5)
C(36)-C(29)-O(4)-C(28)	71.4(5)
C(30)-C(29)-O(4)-C(28)	-55.3(5)
C(37)-C(29)-O(4)-C(28)	-169.5(5)
O(6)-C(38)-O(5)-C(30)	-8.8(8)
C(39)-C(38)-O(5)-C(30)	171.9(4)
C(29)-C(30)-O(5)-C(38)	135.0(5)
C(31)-C(30)-O(5)-C(38)	-99.1(5)

Symmetry transformations used to generate equivalent atoms:

1.6 References

1. (a) Nicolaou, K. C.; Sorensen, E. J. *Classics in Total Synthesis*; VCH Publishers: Weinheim, Germany, **1996**. (b) Nicolaou, K. C.; Snyder, S. A. *Classics in Total Synthesis II*; VCH Publishers: Weinheim, Germany, **2003**. (c) Nicolaou, K. C.; Vourloumis, D.; Winssinger, N.; Baran, P. S. *Angew. Chem. Int. Ed.* **2000**, *39*, 44.
2. Corey, E. J.; Cheng, X.-M. *The Logic of Chemical Synthesis* Publisher: John Wiley & Sons, Inc, **1995**.
3. *Strategies and Tactics in Organic Synthesis* ed.: Harmata, M. **2004**, Publisher: Elsevier.
4. (a) de la Torre, M. C.; Sierra, M. A. *Angew. Chem. Int. Ed.* **2004**, *43*, 160. (b) Heathcock, C. H. *Angew. Chem. Int. Ed.* **1992**, *31*, 665.
5. (a) Robinson, R. *J. Chem. Soc.* **1917**, *111*, 762. (b) Robinson, R. *J. Chem. Soc.* **1917**, *111*, 876.
6. van Tamelen, E. E. *Fortschr. Chem. Org. Naturst.* **1961**, *19*, 242.
7. Skyler, D.; Heathcock, C. H. *Org. Lett.* **2001**, *3*, 4323.
8. Heathcock, C. H. *Proc. Natl. Acad. Sci.* **1996**, *93*, 14323.
9. (a) Abe, I.; Rohmer, M.; Prestwich, G. D. *Chem. Rev.* **1993**, *93*, 2189. (b) Yoder, R. A.; Johnston, J. N. *Chem. Rev.* **2005**, *105*, 4730.
10. (a) Harrison, D. M. *Nat. Prod. Rep.* **1985**, *2*, 525. (b) Bloch, K. *Science*, **1965**, *150*, 19. (c) Wendt, K. U.; Schulz, G. E.; Corey, E. J.; Liu, D. R. *Angew. Chem. Int. Ed.* **2000**, *39*, 2812.

11. (a) Feil, C.; Sussmuth, R.; Jung, G.; Poralla, K. *Eur. J. Biochem.* **1996**, *242*, 51. (b) Corey, E. J.; Cheng, H.; Baker, C. H.; Matsuda, S. P. T.; Li, D.; Song, X. *J. Am. Chem. Soc.* **1997**, *119*, 1289. (c) Corey, E. J.; Cheng, H.; Baker, H. C.; Matsuda, S. P. T.; Li, D.; Song, X. *J. Am. Chem. Soc.* **1997**, *119*, 1277.
12. (a) Wendt, K. U.; Poralla, K.; Schulz, G. E. *Science* **1997**, *277*, 1811. (b) Wendt, K. U.; Lenhart, A.; Schulz, G. E. *J. Mol. Biol.* **1999**, *286*, 175. (c) Reinert, D. J.; Balliano, G.; Schulz, G. E. *Chem. Biol.* **2004**, *11*, 121.
13. (a) Rajamani, R.; Gao, J. *J. Am. Chem. Soc.* **2003**, *125*, 12768. (b) Corey, E. J.; Staas, D. D. *J. Am. Chem. Soc.* **1998**, *120*, 3526.
14. Eschenmoser, A.; Arigoni, D. *Helv. Chim. Acta.* **2005**, *88*, 3011.
15. Stork, G.; Burgstahler, A. W. *J. Am. Chem. Soc.* **1955**, *77*, 5068.
16. (a) Eschenmoser, A.; Ruzicka, L.; Jeger, O.; Arigoni, D. *Helv. Chim. Acta.* **1955**, *38*, 1890. (b) Gamboni, G.; Schinz, H.; Eschenmoser, A. *Helv. Chim. Acta.* **1954**, *37*, 964.
17. (a) Goldsmith, D. J.; Philips, C. F. *J. Am. Chem. Soc.* **1969**, *91*, 5862. (b) Goldsmith, D. J. *J. Am. Chem. Soc.* **1962**, *84*, 3913.

18. (a) Johnson, W. S.; Chenera, B.; Tham, F. S.; Kullnig, R. K. *J. Am. Chem. Soc.* **1993**, *115*, 493. (b) Johnson, W. S.; Fletcher, V. R.; Chenera, B.; Bartlett, W. R.; Tham, F. S.; Kullnig, R. K. *J. Am. Chem. Soc.* **1993**, *115*, 497. (c) Johnson, W. S.; Buchanan, R. A.; Bartlett, W. R.; Tham, F. S.; Kullnig, R. K. *J. Am. Chem. Soc.* **1993**, *115*, 504. (d) Johnson, W. S.; Plummer, M. S.; Reddy, S. P.; Bartlett, W. R. *J. Am. Chem. Soc.* **1993**, *115*, 515. (e) Fish, P. V.; Johnson, W. S. *J. Org. Chem.* **1994**, *59*, 2324. (f) Fish, P. V.; Johnson, W. S.; Jones, G. S.; Tham, F. S.; Kullnig, R. K. *J. Org. Chem.* **1994**, *59*, 6150.
19. van Tamelen, E. E.; Leiden, T. M. *J. Am. Chem. Soc.* **1982**, *104*, 2061.
20. (a) Corey, E. J.; Lin, S. *J. Am. Chem. Soc.* **1996**, *118*, 8765. (b) Corey, E. J.; Luo, G.; Lin, L. S. *J. Am. Chem. Soc.* **1997**, *119*, 9927. (c) Zhang, J.; Corey, E. J. *Org. Lett.* **2001**, *3*, 3215. (d) Mi, Y.; Schreiber, J. V.; Corey, E. J. *J. Am. Chem. Soc.* **2002**, *124*, 11290. (e) Corey, E. J.; Luo, G.; Lin, L. S. *Angew. Chem. Int. Ed.* **1998**, *37*, 1126.
21. (a) Murata, M.; Yasumoto, T. *Nat. Prod. Rep.* **2000**, *17*, 293. (b) Deranas, A. H.; Norte, M.; Fernandez, J. J. *Toxicon* **2001**, *39*, 1101. (c) Nakata, T. *Chem. Rev.* **2005**, *105*, 4314. (d) Inoue, M. *Chem. Rev.* **2005**, *105*, 4379.
22. (a) Poli, M. A.; Mende, T. J.; Baden, D. G. *Mol. Pharmacol.* **1986**, *30*, 129. (b) Lasker, R.; Smith, F. G. W. *U. S. Fish Wildl. Serv. Fish Bull.* **1954**, 55. (c) Poli, M. A.; Musser, S. M.; Dickey, R. W.; Eilers, P. P.; Hall, S. *Toxicon* **2000**, *38*, 981.

23. (a) Fujiwara, K.; Murai, A. *Bull. Chem. Soc. Jpn.* **2004**, *77*, 2129. (b) Kadota, I.; Yamamoto, Y. *Acc. Chem. Res.* **2005**, *38*, 423. (c) Sasaki, M.; Fuwa, H. *Synlett* **2004**, *11*, 1851.
24. (a) Nakanishi, K. *Toxicon* **1985**, *23*, 473. (b) Shimizu, Y. *Natural Toxins: Animal, Plant, and Microbial* ed. by Harris, J. B.; Clarendon Press, Oxford **1986**, 123. (c) Lee, M. S.; Repeta, D. J.; Nakanishi, K.; Zagorski, M. G. *J. Am. Chem. Soc.* **1986**, *108*, 7855. (d) Chou, H.-N.; Shimizu, Y. *J. Am. Chem. Soc.*, **1987**, *109*, 2184. (e) Lee, M. S.; Qin, Q.-W.; Nakanishi, K.; Zagorski, M. G. *J. Am. Chem. Soc.* **1989**, *111*, 6234.
25. Cane, D. E.; Celmer, W. D.; Westley, J. W. *J. Am. Chem. Soc.* **1983**, *105*, 3954.
26. Gallimore, A. R.; Spencer, J. B. *Angew. Chem. Int. Ed.* **2006**, *45*, 4406.
27. (a) Valentine, J. C.; McDonald, F. E. *Synlett* **2006**, *12*, 1816. (b) McDonald, F. E.; Tong, R.; Valentine, J. C.; Bravo, F. *Pure Appl. Chem.* **2007**, *79*, 281. (c) Hayashi, N.; Fujiwara, K.; Murai, A. *Tetrahedron* **1997**, *53*, 12425.
28. Vilotijevic, I.; Jamison, T. F. *Science* **2007**, *317*, 1189.
29. (a) McDonald, F. E.; Bravo, F.; Wang, X.; Wei, X.; Toganoh, M.; Rodríguez, J. R.; Do, B.; Neiwert, W. A.; Hardcastle, K. I. *J. Org. Chem.* **2002**, *67*, 2515. (b) Valentine, J. C.; McDonald, F. E.; Neiwert, W. A.; Hardcastle, K. I. *J. Am. Chem. Soc.* **2005**, *127*, 4586, and references therein.

30. Wan, S.; Gunaydin, H.; Houk, K. N.; Floreancig, P. E. *J. Am. Chem. Soc.* **2007**, *129*, 7915.
31. (a) Baldwin, J. E.; Thomas, R.C.; Kruse, L. I.; Silberman, L. *J. Org. Chem.* **1977**, *42*, 3846. (b) Baldwin, J. E.; Cutting, J.; Dupont, W.; Kruse, L. I.; Silberman, L.; Thomas, R.C. *J. Chem. Soc., Chem. Commun.* **1976**, 736. (c) Baldwin, J. E. *J. Chem. Soc., Chem. Commun.* **1976**, 738.
32. Zakarian, A.; Batch, A.; Holton, R. A. *J. Am. Chem. Soc.* **2003**, *125*, 7822.
33. Kashman, Y.; Rudi, A. *Phytochem. Rev.* **2004**, *3*, 309.
34. Fernández, J.; Souto, M.; Norte, M. *Nat. Prod. Rep.*, **2000**, *17*, 235
35. (a) Rudi, A.; Yosief, T.; Schleyer, M.; Kashman, Y. *Tetrahedron* **1999**, *55*, 5555; (b) Rudi, A.; Stein, Z.; Goldberg, I.; Yosief, T.; Schleyer, M. and Kashman, Y. *Tetrahedron Lett.* **1998**, *39*, 1445. (c) Rudi, A.; Aknin, M.; Gaydou, E.; Kashman, Y. *J. Nat. Prod.* **1997**, *60*, 700. (d) Ciavatta, M. L.; Scognamiglio, G.; Trivellone, E.; Bisogno, T.; Cimino, G. *Tetrahedron* **2002**, *58*, 4943, and references therein.
36. Ciavatta, M. L.; Scognamiglio, G.; Trivellone, E.; Bisogno, T.; Cimino, G. *Tetrahedron* **2002**, *58*, 4943; and references therein.
37. (a) Rudi, A.; Kashman, Y.; Benayahu, Y.; Schleyer, M. *J. Nat. Prod.* **1994**, *57*, 1416. (b) Rudi, A.; Goldberg, I.; Stein, Z.; Kashman, Y.; Benayahu, Y.; Schleyer, M.; Garcia-Gravalos, M. D. *J. Nat. Prod.* **1995**, *58*, 1702. (c) Rudi, A.; Aknin, M.; Gayhou, E. M.; Kashman, Y. *J. Nat. Prod.* **1997**, *60*, 700.
38. Caspi, E. *Acc. Chem. Res.* **1980**, *13*, 97, and references cited therein.

39. Tong, R.; Valentine, J. C.; McDonald, F. E.; Cao, R.; Fang, X.; Hardcastle, K. I. *J. Am. Chem. Soc.* **2007**, 129, 1050.
40. (a) Hori, N.; Nagasawa, K.; Shimizu, T.; Nakata, T. *Tetrahedron Lett.* **1999**, 40, 2145. (b) Nakata, T.; Nomura, S.; Matsukura, H. *Tetrahedron Lett.* **1996**, 37, 213. For examples of mechanistically similar ring contractions, see (c) Hayashi, N.; Fujiwara, K.; Murai, A. *Synlett* **1997**, 793.
41. (a) Wang, X.; Tu, Y.; Frohn, M.; Zhang, J.; Shi, Y. *J. Am. Chem. Soc.* **1997**, 119, 11224. (b) Shi, Y. *Acc. Chem. Res.* **2004**, 37, 488. (c) Zhao, M.-X.; Shi, Y. *J. Org. Chem.* **2006**, 71, 5377.
42. Lipshutz, B. H.; Harvey, D. F. *Synth. Commun.* **1982**, 12, 267.
43. Scott, W. J.; McMurry, J. E. *Acc. Chem. Res.* **1988**, 21, 47.
44. (a) Corey, E. J.; Sodeoka, M. *Tetrahedron Lett.* **1991**, 32, 7005. (b) Corey, E. J.; Roberts, B. E. *Tetrahedron Lett.* **1997**, 38, 8921
45. Comins, D. L.; Dehgehani, A. *Tetrahedron Lett.* **1992**, 33, 6299.
46. Negishi, E.; Luo, F.-T.; Rand, C. L. *Tetrahedron Lett.* **1982**, 23, 27.
47. (a) Baudin, J. B.; Hareau, G.; Julia, S. A.; Ruel, O. *Tetrahedron Lett.* **1991**, 32, 1175. (b) Blakemore, P. R. *J. Chem. Soc., Perkin Trans. 1* **2002**, 2563. (c) Aissa, C. *J. Org. Chem.* **2006**, 71, 360.
48. Valentine, J. C. Ph. D. *Dissertation, Emory University*, **2005**.
49. Tong, R.; McDonald, F. E.; Fang, X.; Hardcastle, K.I. *Synthesis* **2007**, 2337.
50. Morimoto, Y.; Nishikawa, Y.; Ueba, C.; Tanaka, T. *Angew. Chem. Int. Ed.* **2006**, 45, 810.

51. (a) Grieco, P. A.; Masaki, Y. *J. Org. Chem.* **1974**, *39*, 2135. (b) Murakami, T.; Furusawa, K. *Synthesis* **2002**, 479.
52. (a) Klaver, W. J.; Hiemstra, H.; Speckamp, W. N. *Tetrahedron* **1988**, *44*, 6729. (b) Despo, A. D.; Chiu, S. K.; Flood, T.; Petersen, P. E. *J. Am. Chem. Soc.* **1980**, *102*, 5120. (c) Chiu, S. K.; Peterson, P. E. *Tetrahedron Lett.* **1980**, *21*, 4047. (d) Tietze, L. F.; Wiinsch, J. R.; Noltemeyer, M. *Tetrahedron* **1992**, *48*, 2081.
53. Noma, H.; Tanaka, H.; Noguchi, H.; Shibuya, M.; Ebizuka, Y.; Abe, I. *Tetrahedron Lett.* **2004**, *45*, 8299.
54. (a) Hutchins, R. O.; Learn, K. *J. Org. Chem.* **1982**, *47*, 4382. (b) Mohri, M.; Kinoshita, H.; Inomata, K.; Kotake, H. *Chem. Lett.* **1985**, 451. (c) Orita, A.; Watanabe, A.; Tsuehiya, H.; Otera, J. *Tetrahedron* **1999**, *55*, 2889.
55. (a) Suzuki, T.; Sato, O.; Hirma, M. *Tetrahedron Lett.* **1990**, *31*, 4747. (b) Fagnou, K.; Lautens, M. *Org. Lett.* **2000**, *2*, 2319. (c) Evans, P. A.; Leahy, D. K. *J. Am. Chem. Soc.* **2002**, *124*, 7882. (d) Takeuchi, R.; Kashio, M. *J. Am. Chem. Soc.* **1998**, *120*, 8647. (e) Trost, B. M.; Lautens, M. *J. Am. Chem. Soc.* **1987**, *109*, 1469.
56. Trost, B. M.; Toste, F. D. *Tetrahedron Lett.* **1999**, *40*, 7739; and references therein.
57. (a) Crandall, J. K.; Conover, W. W. *J. Chem. Soc., Chem. Commun.* **1973**, 340. (b) Kobertz, W. R.; Bertozzi, C. R.; Bednarski, M. D. *Tetrahedron Lett.* **1992**, *33*, 737.

58. Carlsen, P. H. J.; Katsuki, T.; Martin, V. S.; Sharpless, K. B. *J. Org. Chem.* **1981**, *46*, 3936.
59. (a) McMurry, J. E. *Chem. Rev.* **1989**, *89*, 1513. (b) Sabelle, S.; Hydrio, J.; Leclerc, E.; Mioskowski, C.; Renard, P.-Y. *Tetrahedron Lett.* **2002**, *43*, 3645. (c) Hirao, T. *Synlett*, **1999**, 175. (d) Mukaiyama, T.; Kagayama, A.; Shiina, I. *Chem. Lett.* **1998**, 1107. (e) Chisholm, M. H.; Klang, J. A. *J. Am. Chem. Soc.* **1989**, *111*, 2324.
60. (a) Pospisil, J.; Pospisil, T.; Marko, I. E. *Org. Lett.* **2005**, *7*, 2373. (b) Healy, M. P.; Parsons, A. F.; Rawlinson, J. G. T. *Org. Lett.* **2005**, *7*, 1597. (c) Takeda, T.; Sasaki, R.; Fujiwara, T. *J. Org. Chem.* **1998**, *63*, 7286.
61. Takeda, T.; Sasaki, R.; Yamauchi, S.; Fujiwara, T. *Tetrahedron* **1997**, *53*, 557.
62. (a) Tormakangas, O. P.; Toivola, R. J.; Karvinen, E. K.; Koskinen, A. M. P. *Tetrahedron* **2002**, *58*, 2175. (b) Siemeling, U.; Neumann, B.; Stammer, H.-G. *J. Org. Chem.* **1997**, *62*, 3407. (c) Adlington, R. M.; Barrett, A. G. M. *Acc. Chem. Res.* **1983**, *16*, 55. (d) Chamberlin, A. R.; Stemke, J. E.; Bond, F. T. *J. Org. Chem.* **1978**, *43*, 147.
63. (a) Ollivier, J.; Dorizon, P.; Piras, P. P.; de Meijere, A.; Salaun, J. *Inorg. Chim. Acta* **1994**, *222*, 37. (b) Chau, A.; Paquin, J.-F.; Lautens, M. *J. Org. Chem.* **2006**, *71*, 1924.

64. (a) Barton, D. H. R.; Willis, B. J. *J. Chem. Soc., Chem. Commun.* **1970**, 1225. (b) Barton, D. H. R.; Smith, E. H.; Willis, B. J. *J. Chem. Soc., Chem. Commun.* **1970**, 1226. (c) Hoogesteger, F. J.; Havenith, R. W. A.; Zwikker, J. W.; Jenneskens, L. W.; Kooijman, H.; Veldman, N.; Spek, A. L. *J. Org. Chem.* **1995**, *60*, 4375.
65. Zwierzak, A.; Sulewska, A. *Synthesis* **1976**, 835.
66. Buters, J.; Wassenaar, S.; Kellogg, R. M. *J. Org. Chem.* **1972**, *37*, 4045.
67. (a) Miyaura, T.; Suzuki, A. *Chem. Rev.* **1995**, *95*, 2457. (b) Corbet, J.-P.; Mignani, G. *Chem. Rev.* **2006**, *106*, 2651. (c) Chemler, S. R.; Trauner, D.; Danishefsky, S. J. *Angew. Chem. Int. Ed.* **2001**, *40*, 4544. (d) *Topics in Organometallic Chemistry 19: Metal catalyzed cascade Reactions* Volume editor: Muller, T. J. J.; Publisher: Springer, **2006**.
68. Takagi, J.; Takahashi, K.; Ishiyama, T.; Miyaura, N. *J. Am. Chem. Soc.* **2002**, *124*, 8001.
69. (a) Montiel-Smith, S.; Quintero-Cartes, L.; Sandoval-Ramirez, J. *Tetrahedron Lett.* **1995**, *36*, 8359. (b) Lee, J.-T.; Alper, H. *J. Org. Chem.* **1990**, *55*, 1854. (c) Shibasaki, M.; Sodeoka, M. *Tetrahedron Lett.* **1985**, *26*, 3491. (d) Maye, J. P.; Negishi, E.-I. *J. Chem. Soc., Chem. Commun.* **1993**, 1830. (e) Reger, D. L.; Habib, M. M.; Fauth, D. J. *J. Org. Chem.* **1980**, *45*, 3860. (f) Cramer, R. *Acc. Chem. Res.* **1968**, *1*, 186.
70. (a) Cota, J. G.; Meilan, M. C.; Mourino, A.; Castedo, L. *J. Org. Chem.* **1988**, *53*, 6094. (b) Thery, N.; Szymoniak, J.; Moise, C. *Tetrahedron Lett.* **1999**, *40*, 3155.

71. (a) Young, J. F.; Osborn, J. A.; Jardine, F. H.; Wilkinson, G. *Chem. Commun.* **1965**, 131. (b) Osborn, J. A.; Jardine, F. H.; Young, J. F.; Wilkinson, G. *J. Chem. Soc. A* **1966**, 1711. (c) Hornfeldt, A.-B.; Gronowitz, J. S.; Gronowitz, S. *Acta Chem. Scand.* **1968**, 22, 2725.
72. Posner, G. H.; Switzer, C. *J. Am. Chem. Soc.* **1986**, 108, 1239.
73. Takahashi, A.; Kirio, Y.; Sodeoka, M.; Sasai, H.; Shibasaki, M. *J. Am. Chem. Soc.* **1989**, 111, 643.
74. (a) Nelson, S. G.; Bungard, C. J.; Wang, K. *J. Am. Chem. Soc.* **2003**, 125, 13000. (b) Hubert, A. J.; Reimlinger, H. *Synthesis* **1969**, 97. (c) Hubert, A. J.; Reimlinger, H. *Synthesis* **1970**, 405. (d) Brown, A. C. *J. Chem. Soc., Chem. Comm.* **1975**, 222.
75. (a) Mirafzal, G. A.; Liu, J.; Bauld, N. L. *J. Am. Chem. Soc.* **1993**, 115, 6072. (b) Mirafzal, G. A.; Bauld, N. L. *J. Am. Chem. Soc.* **1993**, 114, 5457. (c) Bauld, N. L. *Tetrahedron* **1989**, 45, 5307.
76. Brook, A. G. *Acc. Chem. Res.* **1974**, 7, 77.
77. (a) Kato, M.; Mori, A.; Oshino, H.; Enda, J.; Kobayashi, K.; Kuwajima, I. *J. Am. Chem. Soc.* **1984**, 106, 1773. (b) Enda, J.; Kuwajima, I. *J. Am. Chem. Soc.* **1985**, 107, 5495
78. Nowick, J. S.; Danheiser, R. L.; *Tetrahedron* **1988**, 44, 4133.
79. Dilman, A. D.; Ioffe, S. L. *Chem. Rev.* **2003**, 103, 733.
80. (a) Tebbe, F. N.; Parshall, G. W.; Reddy, G. S. *J. Am. Chem. Soc.* **1978**, 100, 3611. (b) Pine, S. H.; Kim, G.; Lee, V. *Org. Synth.* **1990**, 69, 72.

81. (a) Petasis, N. A.; Bzowej, E. I. *J. Am. Chem. Soc.* **1990**, *112*, 6392. (b) Payack, J. F.; Hughes, D. L.; Cai, D.; Cottrell, I. F.; Verhoeven, T. R. *Org. Synth.* **2002**, *79*, 19.
82. (a) Abe, I.; Rohmer, M. *J. Chem. Soc., Perkin Trans. 1* **1994**, 783. (b) Corey, E. J.; Virgil, S. C.; Sarshar, S. *J. Am. Chem. Soc.* **1991**, *113*, 8171. (c) Corey, E. J.; Virgil, S. C. *J. Am. Chem. Soc.* **1991**, *113*, 4025.
83. (a) Corey, E. J.; Burk, R. M.; *Tetrahedron Lett.* **1987**, *28*, 6413. (b) Corey, E. J.; Reid, J. G.; Myers, A. G.; Hahl, R. W. *J. Am. Chem. Soc.* **1987**, *109*, 918.
84. Zheng, Y.F.; Oehlshchlager, A. C.; Georgopapadakou, N. H.; Hartman, P. G.; Scheliga, P. *J. Am. Chem. Soc.* **1995**, *117*, 670.
85. Mastalerz, H. *J. Org. Chem.* **1984**, *49*, 4092.
86. (a) Stefen, W. L.; Palenik, G.J. *Inorg. Chem.* **1976**, *15*, 2432. (b) Doyle, J. R.; Slade, P. E.; Jonassen, H. B. *Inorg. Synth.* **1960**, *6*, 216.

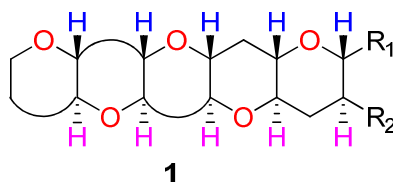
Chapter 2

Biomimetic Synthesis of Fused Polypyranans

2.1. Introduction and Background

Polycyclic ether marine natural products¹ with the characteristic characteristic “ladder-like” *trans-syn-trans*-fused structure have attracted the attention of many scientists in various research fields because of their potent bioactivities and unique, challenging molecular architectures. The structure-activity relationship (SAR) of polycyclic ethers has been focused on by many research groups². However, most of the natural polycyclic ethers are scarce in amount, which caused limitations in their biological studies. Thus, the chemical synthesis of polycyclic ethers would offer alternative ways to supply these compounds. For instance, total syntheses of brevetoxin B³ (1995/Nicolaou, 2004/Nakata, 2005/Kadota/Yamamoto), brevetoxin A⁴ (1998/Nicolaou), ciguatoxin CTX3C⁵ (2001/Hirama), gambierol⁶ (2002/Sasaki, 2002/Kadota/Yamamoto and 2005/Rainier) and gymnocin A⁷ (2003/Sasaki) were achieved. These landmark achievements were made possible by development of many efficient synthetic methodologies⁸, which will be briefly reviewed in this section for synthesis of polypyranans.

Figure 1. Representative core structure of polycyclic ethers.

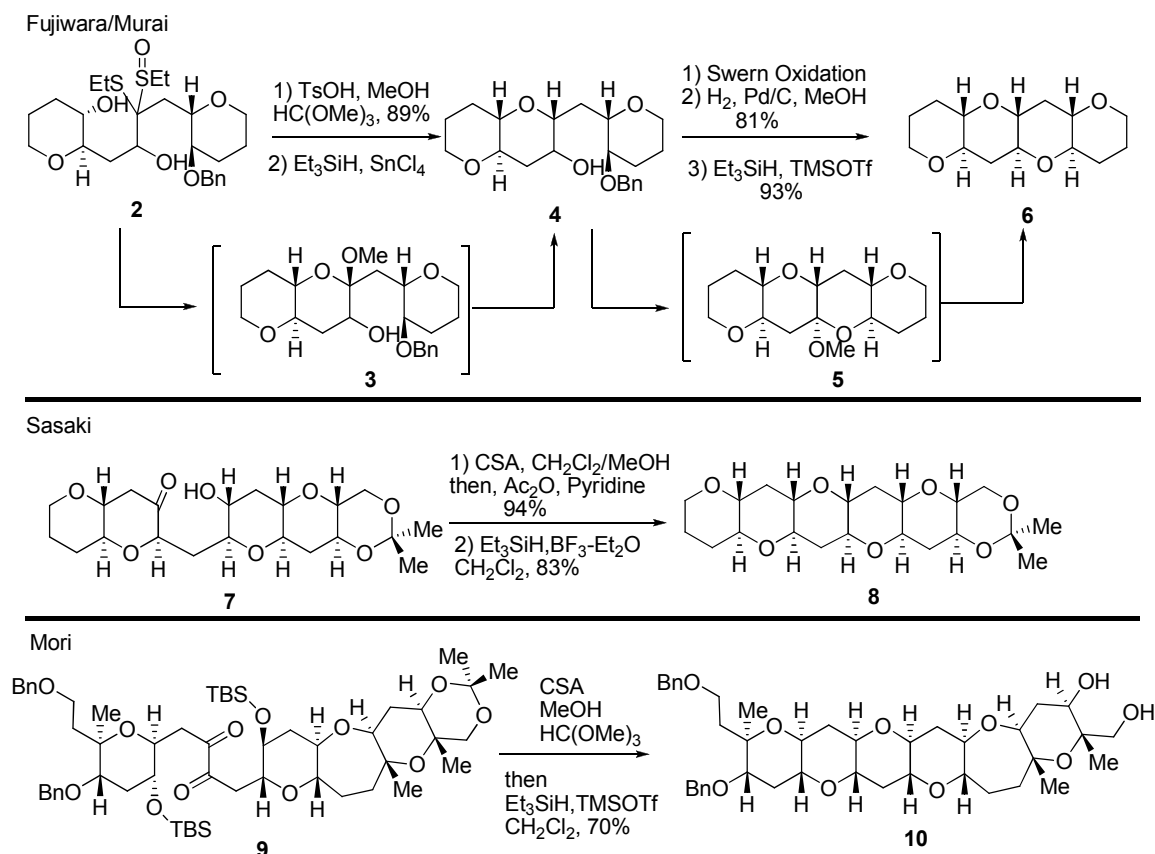


The existing methods for closure of cyclic ethers were roughly categorized into two classes based on construction of fused polypyrans: reductive etherification and *endo*-selective cyclization of epoxides.

2.1.1. Reductive etherification

The hydroxyl dithioacetal cyclization strategy⁹, one of the earliest and most powerful approaches, was developed by Nicolaou in 1986 for the specific synthesis of medium-sized rings of brevetoxins. Further exploration of this cyclization strategy was undertaken by Fujiwara and Murai¹⁰ to establish an efficient synthetic method for construction of the *trans*-fused polypyrans (Scheme1). S-oxido dithioacetal **2**, easily prepared from condensation of aldehyde and lithiated S-oxido dithioacetal underwent stereoselective acid-promoted cyclization to provide the desired polypyrans **4** after reductive etherification of hemiketal **3**. Tetracyclic pyran **6** could be synthesized in three steps from **4** in high yields. A formal total synthesis of hemibrevetoxin B was achieved by assembly of the B and C rings using this strategy. As seen in the conversion of tricyclic ether **4** to the tetracyclic ether **6**, the most widely used and successful method for the construction of *trans*-fused polypyrans in total synthesis of marine natural products is arguably the ketal formation followed by stereoselective reductive etherification. Bronsted acid is usually used to promote the formation of ketal that was subsequently subjected to reductive cleavage of C-O bond. For instance, in 1998, Sasaki¹¹ reported exposure of substrates as complex as **7** to acidic methanol followed by acetylation, gave hemiacetal,

Scheme 1. Reductive etherification for synthesis of polycyclic pyrans.



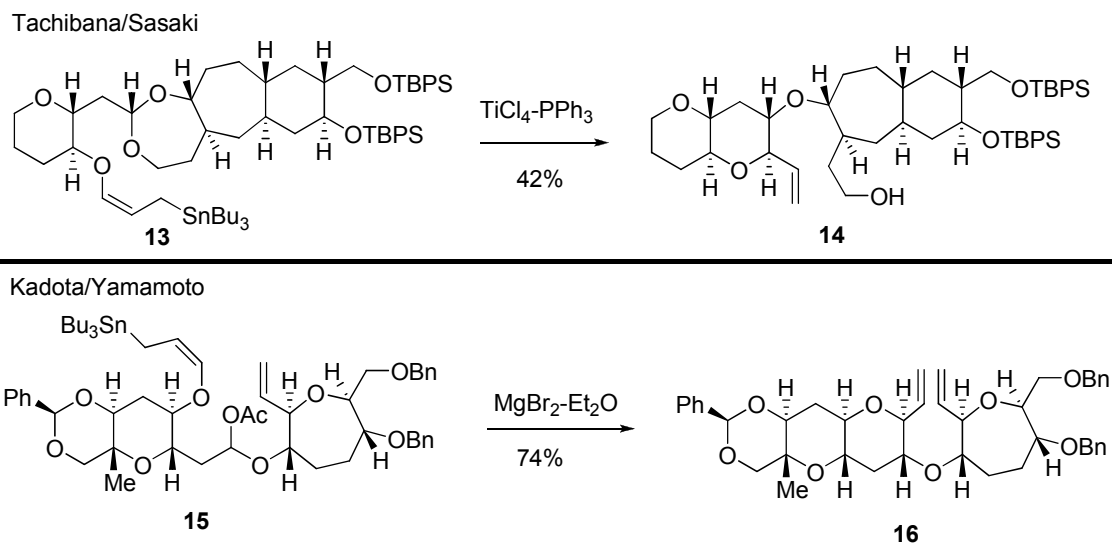
which underwent reductive etherification with triethylsilane in the presence of Lewis acid BF₃·OEt₂ to provide pentacyclic ether **8** in excellent yield. The stereochemical outcome of the reduction of hemiacetal can be explained by nucleophilic hydride attack from less congested face, consistent with the Cieplak effect¹² that favors the axial addition to cyclohexene-like substrates. Application of this synthetic method combined with the powerful Suzuki cross-coupling and regio- and stereoselective hydroboration of enol ether led to total syntheses of ciguatoxin (2002/Sasaki), gambierol (2002/Sasaki), gymnocin A (2003/Sasaki) and CTX3C (2004/Sasaki). Elegant extension of this method was also achieved by three independent groups¹³ (Fujiwara/Murai, Nakata, and Mori) by developing

a bidirectional cyclization to construct the two cyclic ether rings at a time. 1,2-Diketone **9**, easily prepared from oxidation of the corresponding alkyne with $\text{RuO}_2/\text{NaIO}_4$, underwent stereoselective double ketalization and stereoselective reductive etherification to yield hexacyclic ether **10** that was used for total synthesis of yessotoxin (2003/Mori)¹⁴.

In 1997, Tachibana and co-workers developed a strategy^{15a,b} for the synthesis of *trans-syn-trans* fused polycyclic ethers using the intramolecular allylation of chiral acetals with γ -alkoxyallylstannane. However, the allylation reaction usually gave diastereomers with moderate stereoselectivity and yields, which varied with the reactivity of the acetals and the allylstannane by model studies. In 1998, Sasaki and Tachibana explored the use of less reactive γ -alkoxyallylsilane^{15c,d} for allylation of acetal **13** in order to improve the stereoselectivity and yields (Scheme 2). $\text{TiCl}_4\text{-PPh}_3$ induced the intramolecular allylation to produce the tetracyclic ether **14** as a major product with right stereochemistry. The moderate yield and poor stereoselectivity remains unsolved. On the other hand, in 2001 Kadota and Yamamoto developed a stereoselective allylation^{8b} of α -acetoxy ethers with γ -alkoxyallylstannane for synthesis of *trans*-fused polycyclic ethers. Treatment of the mixed acetal **15** with $\text{MgBr}_2\text{-Et}_2\text{O}$ induced the intramolecular cyclization to afford the **16** as single diastereomer in 74% yield, which is an excellent substrate for olefin ring closing metathesis. The stereochemical outcome of the cyclization was not affected by the chirality of α -acetoxy ethers probably due to the formation of oxonium cation intermediate. The efficiency and

powerfulness was demonstrated by the total synthesis of gambierol (2002/Kadota/Yamamoto).

Scheme 2. Intramolecular allylation of acetals.



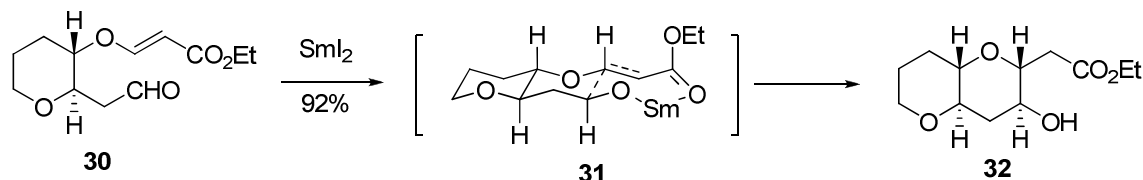
Reductive etherification with reliable control of the newly formed stereocenters in the desired fashion has been shown to be a highly general and powerful method for the assembly of complex polypyran. Combination of reductive etherification with other C-C bond formation methods^{1c,d} (Suzuki coupling/hydroboration, S-oxido dithioacetal-aldehyde coupling, and acetylide-triflate coupling) provided many efficient and practical methods for construction of complex polycyclic ether natural products, and still become a major strategy for designing new synthetic routes of complex polycyclic ether natural products.

Before moving on to *endo*-selective cyclization of epoxide, a stereoselective SmI_2 -promoted reductive etherification developed by Nakata attracted my attention because it efficiently constructs the cyclic pyran by formation of C-C bond with correctly setting both of newly formed stereocenters (Scheme 3). Treatment of **30** with SmI_2 induced the reductive cyclization to produce the

desired bipyran **32** in 92% yield via presumably a chair-like transition state **31**. Polypyran units could be efficiently achieved by iterative use of this reductive cyclization.

Scheme 3. Reductive etherification of carbonyl and unsaturated ester.

Nakata



Many efficient and powerful synthetic methods for the synthesis of polypyrans could not be covered here, including Clark¹⁷, McDonald¹⁸, Rainier¹⁹ and West²⁰, because of the limited space here. Readers who are interested in these topics are strongly recommended to consult the related references.

2.1.2. *Endo*-selective cyclization of epoxide

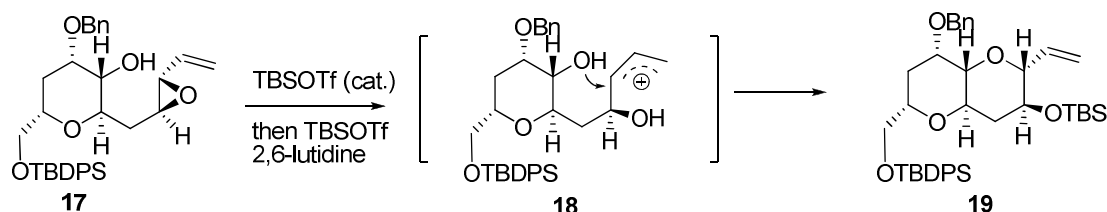
Most marine natural polycyclic ethers are produced by marine dinoflagellates via a sequential chemical processes that are still unknown. Cascade cyclization of polyepoxide has been proposed as a key process²¹ that involves successive epoxide opening in *endo* selectivity. Inspired by this elegant hypothesis, many synthetic chemists have developed a number of important reactions and methodologies^{8a} for construction of *trans*-fused polypyran using epoxide opening/ring closure strategy.

A main problem encountered in the epoxide opening is to control the ring opening mode in favoring the *endo* products that was normally disfavored in

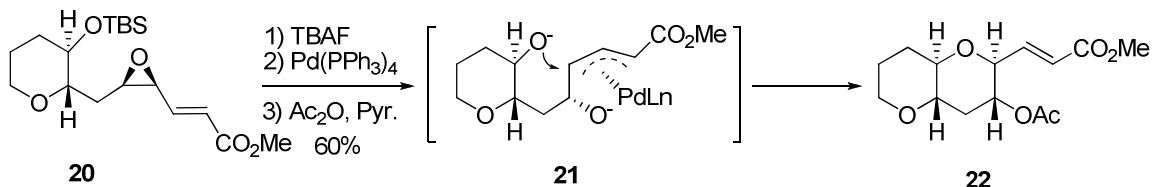
accordance with Baldwin's rule.²² In order to suppress the potential *exo*-mode opening, new synthetic methods are eagerly sought and efforts based on the hypothetical biosynthesis are well rewarded (scheme 4). Among the most powerful and widely used methods is hydroxy-vinylepoxyde cyclization developed by Nicolaou²³ in 1980s. In order to achieve *endo*-selective epoxide opening, vinyl group was introduced by Nicolaou and placed on the *endo*-site carbon to stabilize the developing cation by π -electron donation (such as in **18**).

Scheme 4. *Endo*-selective cyclizations of epoxide.

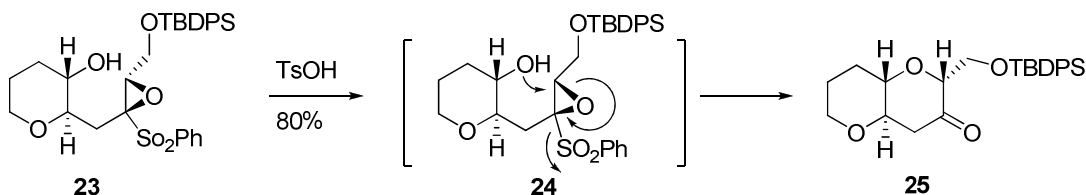
Nicolaou



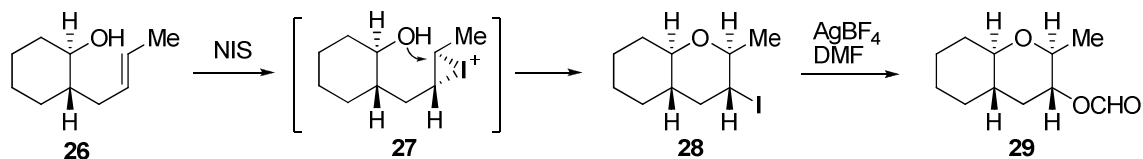
Hirama



Mori



Bartlett



Endo product **19** with *trans*-fusion was obtained exclusively from cyclization of hydroxy vinyl epoxide **17**. Subsequently, Hirama²⁴ reported a mechanistically related method using palladium *endo*-activation of epoxide, in which π -allyl palladium intermediate (**21**) was proposed. However, only *cis*-epoxide such as **20** yielded the *trans*-product (**22**). In addition, alkoxide from desilylation with fluoride ion was necessary to obtain favorable reactivity and stereoselectivity.

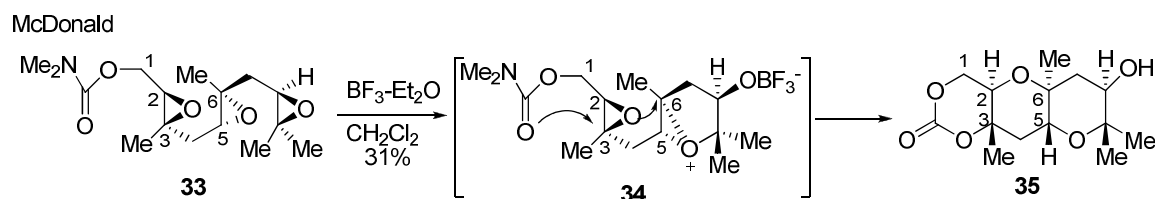
In 1996, Mori²⁵ established a unique method for *endo*-selective cyclization of epoxides based on a complementary idea to π -electron stabilization. The electron-withdrawing sulfone group was expected to destabilize the potentially developing cation on the *exo*-site carbon and thus favor epoxide opening at the *endo*-site. Moreover, sulfone acting as good leaving group was released to drive the cyclization complete. Iterative use of this method by Mori led to an efficient total synthesis of hemibrevetoxin B.

Although it has not been demonstrated in the total synthesis, iodo-etherification of hydroxy alkene is worthy of comments. As epoxides are relatively reactive and usually could not be carried forward for many steps, alkene is much stable toward many acidic and basic conditions. In 1986, Bartlett²⁶ found that activation of alkene **26** with NIS or iodine gave iodopyran (**28**) exclusively (Scheme 4), which was transformed into dehalogenated pyran **29** when treated with silver salt (AgBF_4) in DMF. In addition, products resulted from *exo* epoxide opening in some cases could be transformed into the *endo*-products when exposed to silver salt in DMF.

2.1.3. Biomimetic oxacyclization of skipped polyepoxide

Traditional approaches^{1c,d,8} (including mentioned above) to the syntheses of polypyran have been based on construction of each cyclic ether one at a time, whereas the proposed biosynthesis is potentially more efficient, namely polyoxacyclization of a polyepoxide to furnish the basic backbone in one single step. We have previously reported the chemical demonstration²⁷ of this biogenetic hypothesis, by Lewis acid-promoted *endo*-selective and stereospecific tandem cyclizations of polyepoxides to form *trans*-fused polyoxepane and polypyran structures, including the oxacyclization of triepoxide **33** to tricyclic product **35** (Scheme 5)²⁸.

Scheme 5. Biomimetic oxacyclization of skipped polyepoxide.



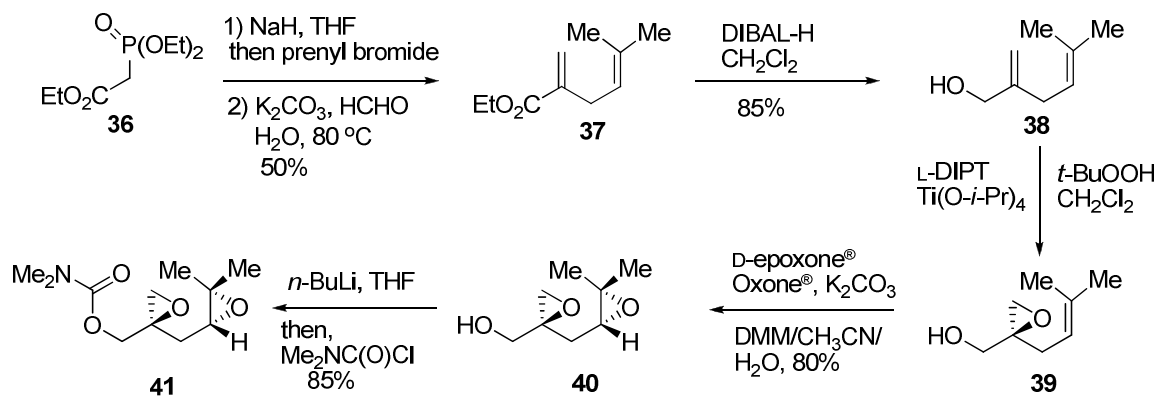
This cascade cyclization process has involved nucleophilic addition at the more substituted carbon of each epoxide via oxonium ion intermediate such as **34**, but we note that such methyl substituents are not always present at all ring junctions in fused polypyran natural products. In addition, the role of substituents on C-3 on the regioselectivity of oxacyclization of skipped polyepoxide has not been extensively explored. Herein we undertake our studies of Lewis acid-mediated tandem oxacyclizations of skipped polyepoxides containing an internal 2,3-disubstituted epoxide and/or 5,6-disubstituted epoxide, leading to polypyran.

2.2. Results and Discussion

2.2.1. Oxacyclization with internal disubstituted epoxide

In order to focus the question of compatibility of an internal disubstituted epoxide, we elected to prepare triepoxide substrate **48** (scheme 7), as well as diepoxide **41** as a model system (scheme 6). Alkylation of triethyl phosphonoacetate **36** with prenyl bromide, and subsequent olefination with formaldehyde provided dienyl ester **37**²⁹, which was reduced to the allylic alcohol **38** with diisobutyl aluminum hydride (DIBAL-H) at -78 °C. Sharpless asymmetric epoxidation^{30a} of alcohol **38** and subsequent Shi diastereoselective epoxidation^{30b} gave diepoxide **40**, which was converted to the *O*-carbamate derivative **41** bearing the anticipated nucleophilic terminating group for tandem oxacyclization²⁸.

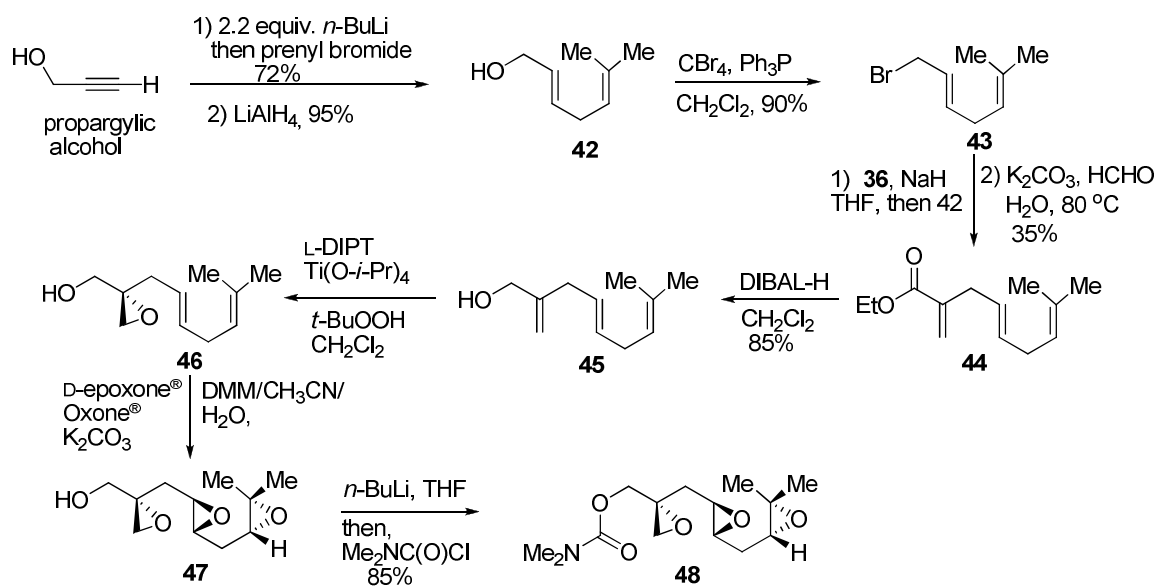
Scheme 6. Synthesis of model substrate **41**.



A similar sequence from the known dienyl bromide **43**³¹ was utilized for the preparation of triepoxide substrate **48** (Scheme 7). Specifically, lithiated propargylic alcohol was alkylated with prenyl bromide and hydroxyl-directed reduction³² of the resulting enyne with LAH provided *trans*-alkene **42** as a single

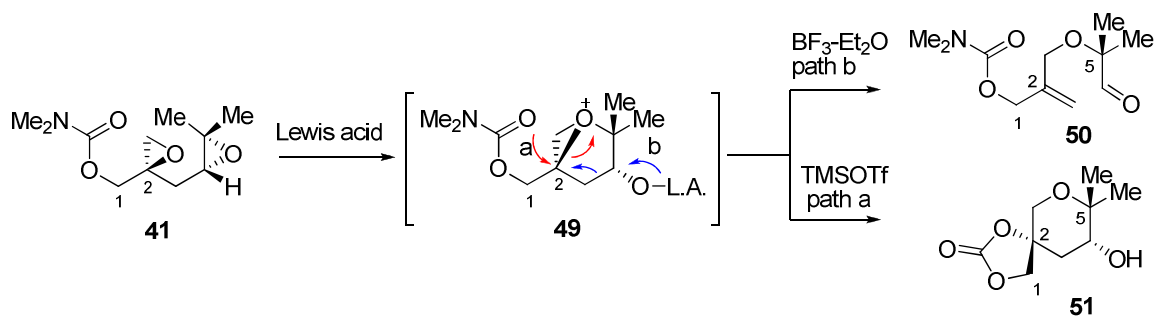
isomer. Bromination of allylic alcohol **42** was performed under mild condition to produce light sensitive allylic bromide **43**, which underwent alkylation with triethyl phosphonoacetate **36** and subsequent olefination with formaldehyde to provide trienyl ester **44**. DIBAL-H reduction of **44** was followed by Sharpless asymmetric epoxidation to produce dienyl epoxy alcohol **46** with comparable yield as **42**. Triepoxide **48** was obtained by double Shi epoxidation of hydroxy epoxy alkene **46** and *O*-carbamate formation under identical conditions used in scheme 6.

Scheme 7. Synthesis of skipped triepoxide **48**.



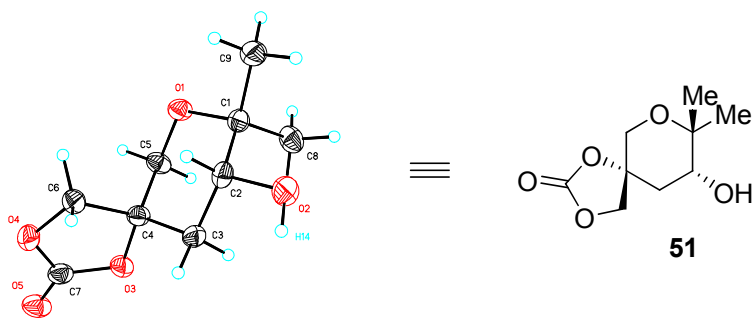
Diepoxide substrate **41** was designed with the *gem*-disubstituted epoxide at C2^{27a}, so that 5-*exo*-cyclization at C2 would not interfere with the anticipated *endo*-cyclization mode at C5 of the other epoxide. However, BF₃·OEt₂ as the Lewis acid promoter for oxabicyclization of **41** resulted in an acyclic aldehyde **50**, attributed to fragmentation of an epoxonium ion **49** intermediate (scheme 8).

Scheme 8. Oxacyclization of model substrate diepoxide **41**.



After evaluation of several other Lewis acids including ytterbium(III) triflate [$\text{Yb}(\text{OTf})_3$] and gadolinium(III) triflate [$\text{Gd}(\text{OTf})_3$],³³ we observed that TMSOTf-mediated reaction with diepoxide **41** resulted in the desired spirobicyclic product **51** as the only isolable product. The structure of product **51**, including stereochemistry, was conclusively confirmed by the single crystal X-ray analysis (figure 2). We attribute the strong silicon-oxygen covalent bond in the formation of epoxonium ion intermediate **49** to preventing the fragmentation observed with other Lewis acid promoters.

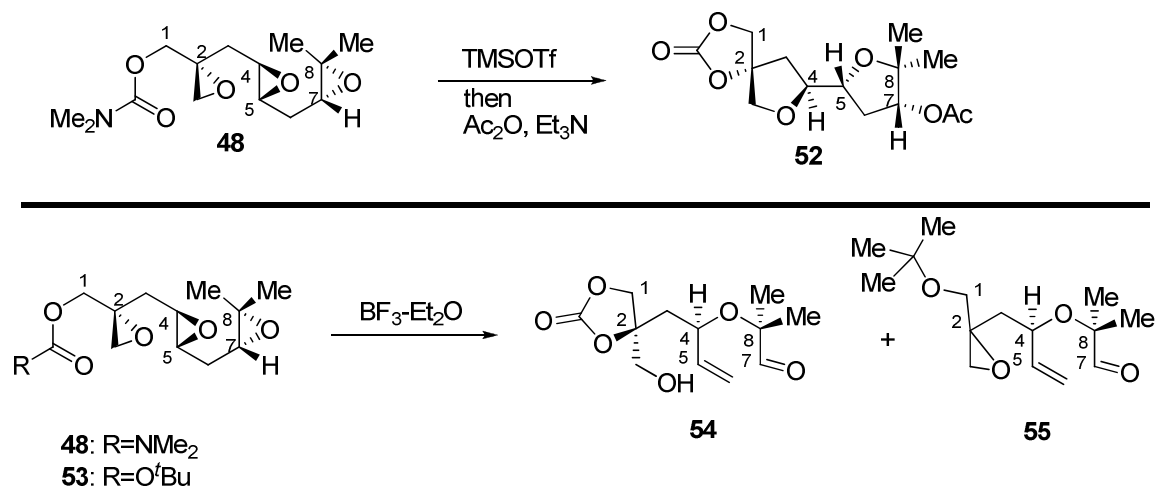
Figure 2. The thermal ellipsoid diagram for compound **51**.



We next explored the application of the same conditions with a more complex substrate, triepoxide **48** (Scheme 9). To our surprise, the product **52**, containing three five-membered rings from *exo*-mode oxacyclization of the internal

disubstituted C4-C5 epoxide, was obtained as the major product with TMSOTf after acetylating under standard conditions.

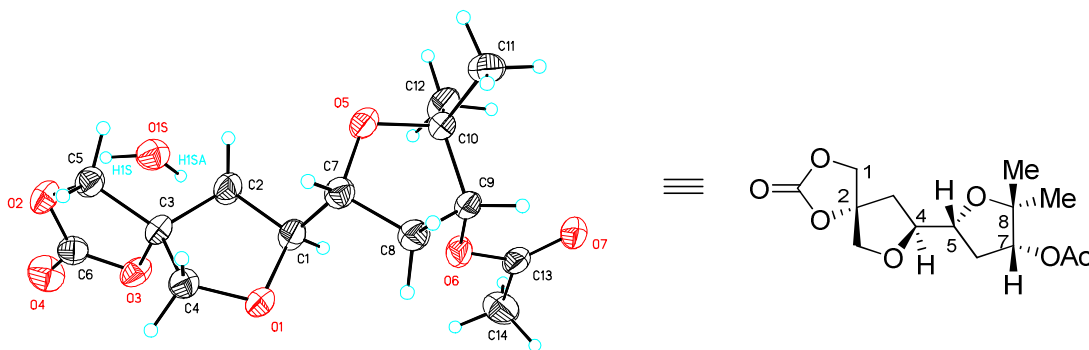
Scheme 9. Trialkylsilyl triflate-promoted oxacyclization of triepoxide **48** and **53**.



In addition to the undesired *exo*-mode of cyclization, crystallography of the **52** (figure 3) revealed that not only C5 and C7 chiral centers but also C2 corresponded to *retention* of configuration from **48**, whereas only C4 underwent the inversion of configuration expected from *anti*-addition of nucleophiles to epoxide carbons. Stoichiometric amount of BF₃-OEt₂-promoted reactions of substrate **48** gave similar results. The formation of product **52** was rationalized as possibly arising from protic acid catalysis and a carbenium ion or ion pair intermediate at C2, rather than selective activation of the terminal C7-C8 epoxide. While using catalytic amount of BF₃-Et₂O as Lewis acid promoter, oxacyclization of triepoxide **48** or **53** at various reaction temperatures only resulted in fragmentation to **54** (and **55** in the case triepoxide **53** was used) (Scheme 9). Activation of terminal C7-C8 epoxide was apparently selective, but the newly-

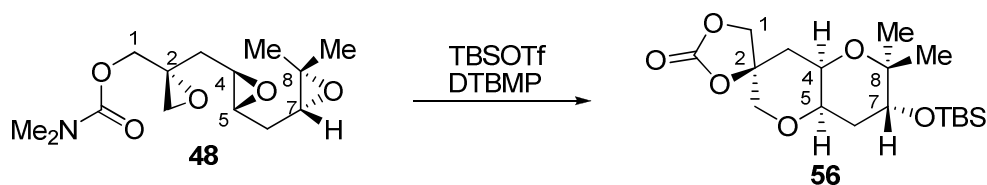
formed B-O bond with negative charge is easy to break due to the developing positive charge on C5.

Figure 3. The thermal ellipsoid diagram for compound **52**.



Thus we hypothesized that a sterically hindered and/or more robust silicon-oxygen adduct might provide selective activation of the terminal C7-C8 epoxide,³⁴ and if the silyl ether could be isolated, the reaction direction would be clarified. After screening several silyl Lewis acid promoters and conditions, we found that *tert*-butyldimethyl silyl triflate (TBSOTf) provided a substantially different outcome (scheme 10), affording the fused bis-pyran product **56** from *endo*-mode oxacyclization. Optimal yields were obtained in the presence

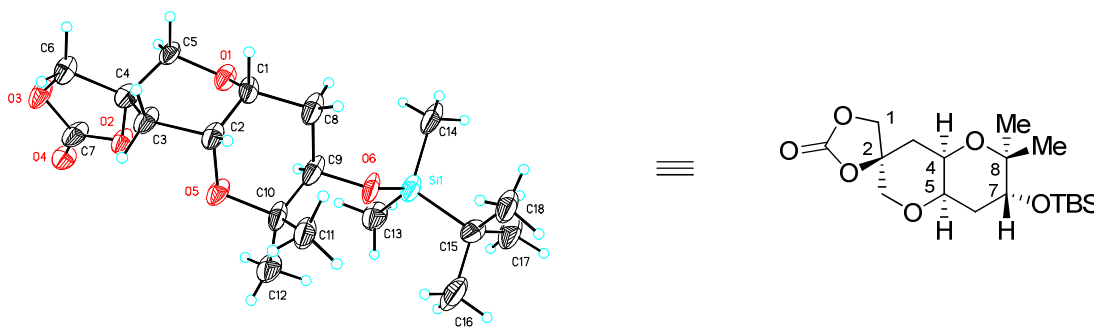
Scheme 10. TBSOTf-promoted oxacyclization of skipped triepoxide **48**.



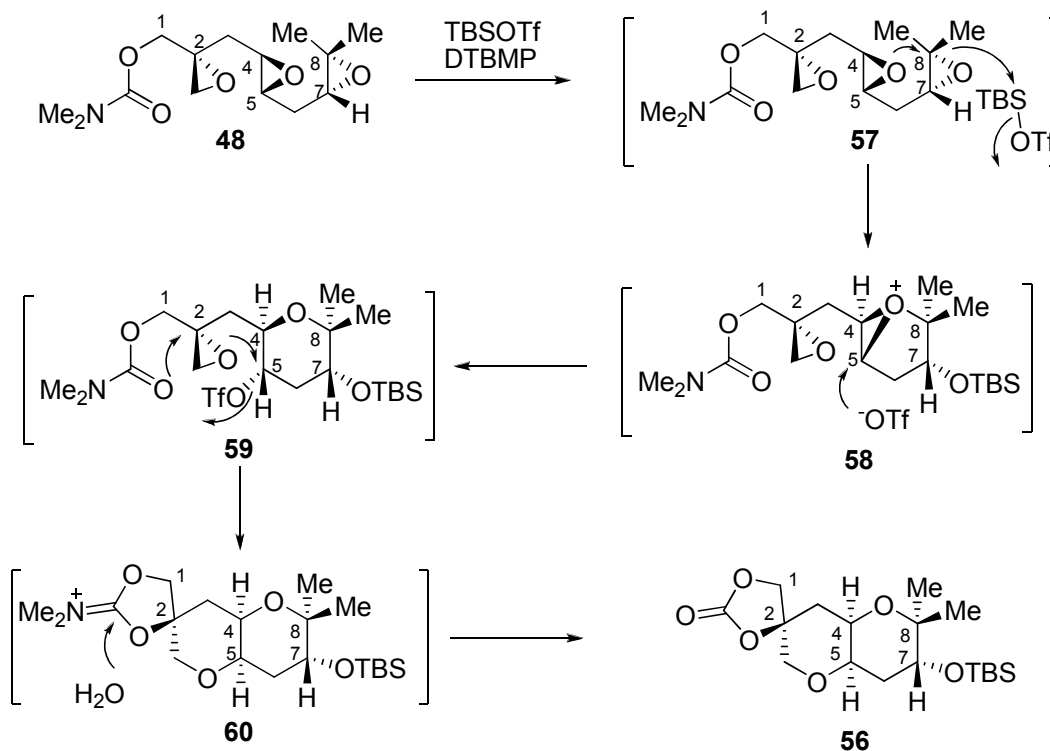
of aromatic amines to facilitate formation of the silyl ether and serving as a protic acid trap³⁵, imidazole and 2,6-lutidine were successfully employed, but the best results (including excellent reproducibility) were observed with 2,6-di-*tert*-

butylpyridine (DTBMP). Crystallographic studies of **56** (figure 4) demonstrated that the expected *trans*-fused product was *not* formed, but rather the *cis*-fusion as shown in **56** was obtained, resulting from apparent *retention* of configuration of stereochemistry at C5.

Figure 4. The thermal ellipsoid diagram for compound **56**.



Scheme 11. Mechanistic explanation of oxacyclization to bispyran **56**.



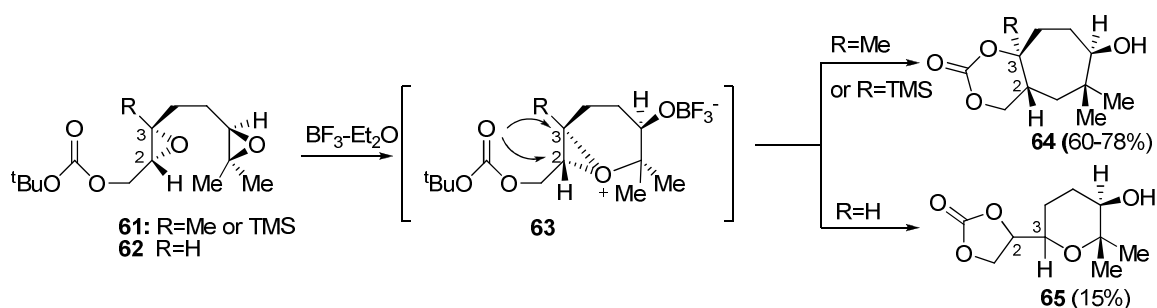
The formation of tricyclic product **56** *with apparent retention of configuration at both C4 and C5* is puzzling. 1,2-Disubstituted epoxides generally react with inversion of configuration at the site of nucleophilic addition, given the lack of stabilization for possible carbenium ion or ion pair intermediates at secondary carbons. However, the weakly nucleophilic triflate anion could be competing effectively with the C2 epoxide oxygen³⁶, undergoing direct nucleophilic addition at C5 via epoxonium ion **58** to possible triflate intermediate **59** (Scheme 11) with inversion of configuration at C5. This step would be followed by addition of the C2 oxygen to C5 with a second inversion of configuration, providing overall retention of configuration as observed at C5.

This mechanistic interpretation leads us to hypothesize that the energy of the reaction transition state required for synchronous cyclizations to form polypyran is much higher than that in the analogous synthesis of polyoxepanes, and thus the stepwise mechanism shown in scheme 10 may operate. The relative efficacy of this cyclization pathway might be generally useful in the synthesis of *cis*-fused bispyrans, as observed in the LM and NO substructures of maitotoxin³⁷.

2.2.2. Unexpected oxacyclization of skipped 2,3-disubstituted epoxides

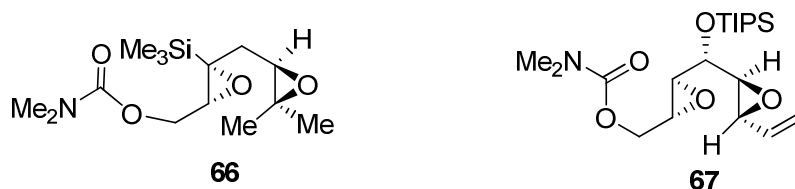
In an earlier study, McDonald's laboratory^{27c} demonstrated that 3-substituted diepoxide **61** underwent $\text{BF}_3\text{-Et}_2\text{O}$ promoted *endo* oxacyclization to provide only oxepane **64** in good yield, while under similar conditions 2,3-disubstituted epoxide **62** produced only *exo*-cyclization product **65** in much lower yield (scheme 12). These results apparently confirmed the substituent (R) effects that either methyl or removable silane (TMS) at the 2,3-epoxide is required to achieve the *endo*-oxacyclization to oxepane.

Scheme 12. McDonald's oxacyclization of isoprenoid-derived polyepoxide.



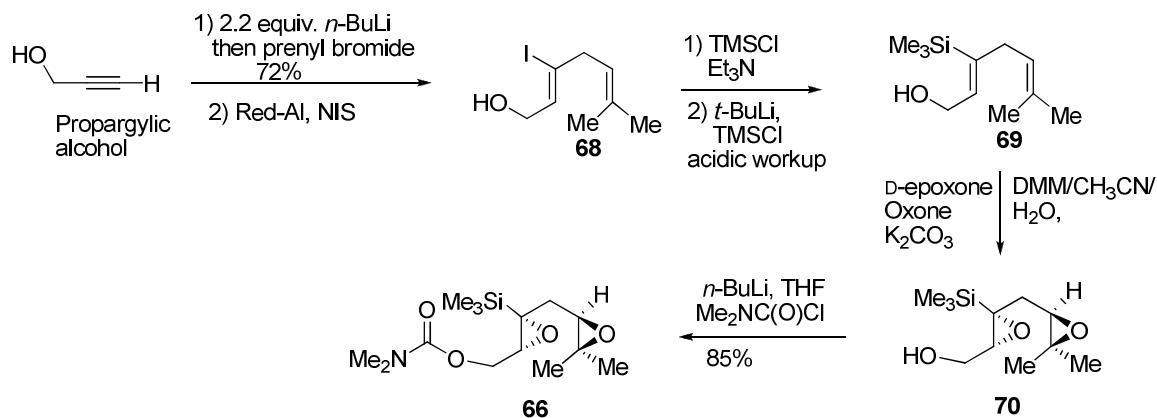
Similar substituents effects on the mode of epoxide opening in oxacyclization are expected for skipped polyepoxide. However, there is no evidence in support of this hypothesis. Hence, we undertook the studies on oxacyclization of skipped 2,3-disubstituted epoxides to polypyran. We began our studies with preparation of cyclization substrates diepoxide **67**, as well as **66** with trimethylsilyl on C3 for control studies (figure 5).

Figure 5. Cyclization substrate **62** and **63**.



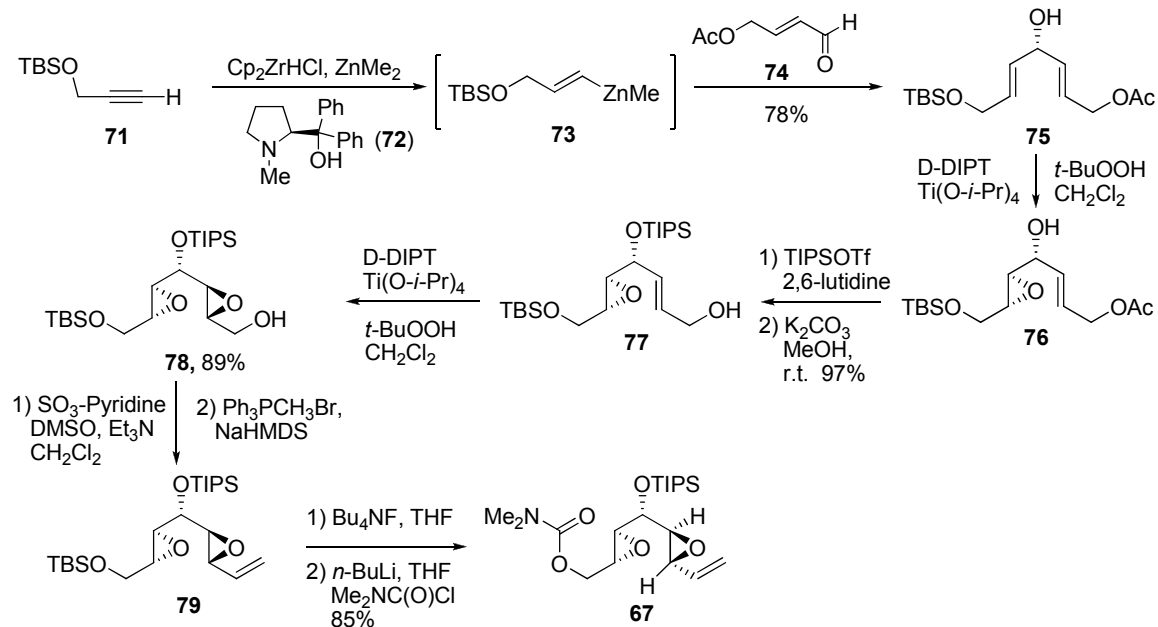
Alkylation of propargylic alcohol with prenyl bromide followed by reductive halogenation³⁸ of the resulting alkynol yielded vinyl iodide **68**, which was used for 1,4-*O-C* silyl migration under modified *Magriotis* conditions³⁹ to give vinyl silane **69** (scheme 13). Double Shi enantioselective epoxidation to diepoxy **70** and *O*-carbamate formation under classical conditions afforded the oxacyclization substrate diepoxide **66**.

Scheme 13. Synthesis of diepoxide **66**.



For the synthesis of diepoxide **67** (scheme 14), regioselective hydrozirconation⁴⁰ of alkyne **71** and subsequent transmetalation⁴¹ to organozinc **73** that underwent asymmetric addition⁴¹ to aldehyde **74** in the presence of chiral amino alcohol catalyst **72**, provided the desired skipped dienol **75**. Sharpless asymmetric epoxidation of **75** using D-diisopropyl tartrate (D-DIPT) as a chiral auxiliary yielded monoepoxide **76** as single isomer.

Scheme 14. Synthesis of diepoxide **67**.

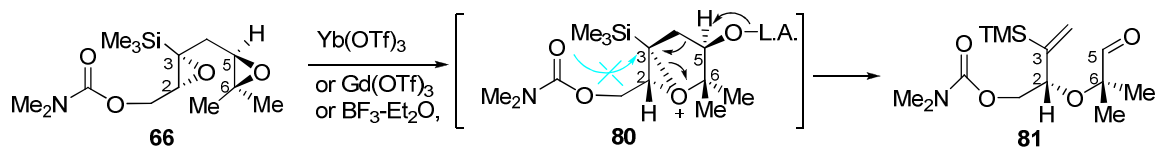


It is worthy of notice that Sharpless asymmetric epoxidation has been used to kinetically resolve racemic allylic secondary alcohol⁴², like **75**. Silylation of the secondary alcohol with triisopropylsilyl triflate (TIPSOTf) and deacetylation with potassium carbonate in methanol gave allylic alcohol **77**, which was epoxidized under Sharpless conditions using catalytic amounts of D-diisopropyl tartrate (D-DIPT) to diepoxide alcohol **74**. Vinyl group was then introduced via a two-step oxidation/methylenation sequence and placed to favor selective activation of the adjacent epoxide through π -electron donation.²³ Diepoxide **67** was then obtained in good yield by two-step protection/deprotection.

With the diepoxide substrates **66** and **67** in hand, we performed the studies of the Lewis acid-promoted oxacyclization. However, under our standard oxacyclization conditions, $\text{BF}_3\text{-OEt}_2$ as the Lewis acid promoter for oxacyclization of **67** resulted in an acyclic aldehyde **81**, probably due to fragmentation of an epoxonium ion **80**

intermediate (scheme 15), which is completely unexpected since trimethylsilyl of **66** was elected as a removable substituent and cation-stabilizing auxiliary on C-3 to favor the *endo*-oxacyclization of isoprenoid-derived epoxides to oxepanes.^{27b}

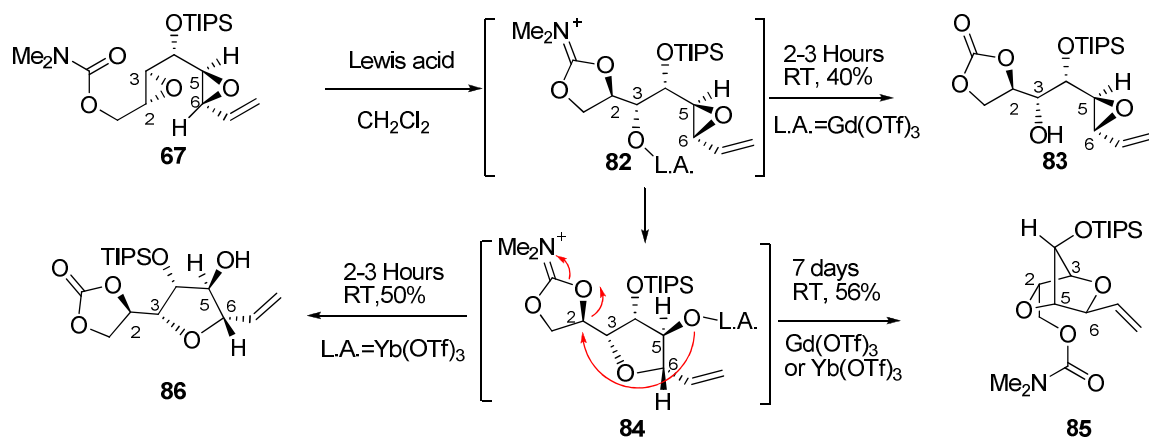
Scheme 15. Lewis acid promoted oxacyclization of diepoxide **66**.



Oxacyclization promoted by other Lewis acids including ytterbium(III) triflate [Yb(OTf)₃], gadolinium(III) triflate [Gd(OTf)₃] and trimethylsilyl triflate (TMSOTf), proceeded in the same way to give acyclic product **81**. One possible explanation for this unexpected result is that bulky substituent (TMS) on C-3 actually precluded carbamate from nucleophilic S_N2 attack on the congested epoxonium ion or S_N1 attack on congested carbon cation (C-3), thus resulting in fragmentation⁴³ that would be impossible to occur for isoprenoid-derived polyepoxide substrates.

2,3-Disubstituted epoxide **66** was synthesized as a cyclization substrate in this study because according to our mechanistic understanding of oxacyclization, epoxonium ion intermediate (such as **34** in scheme 5) from skipped polyepoxide may experience more ring strain [3.1.0] than that from isoprenoid-derived polyepoxide (such as **63** in scheme 12), which may result in favorable *endo*-regioselective oxacyclization without the assistance of substituents. Unfortunately, treatment of diepoxide **67** with Lewis acid Gd(OTf)₃ resulted in partial cyclization to afford compound **83** as a major isolated product (scheme 16).

Scheme 16. Oxacyclization of skipped triepoxide **67**.

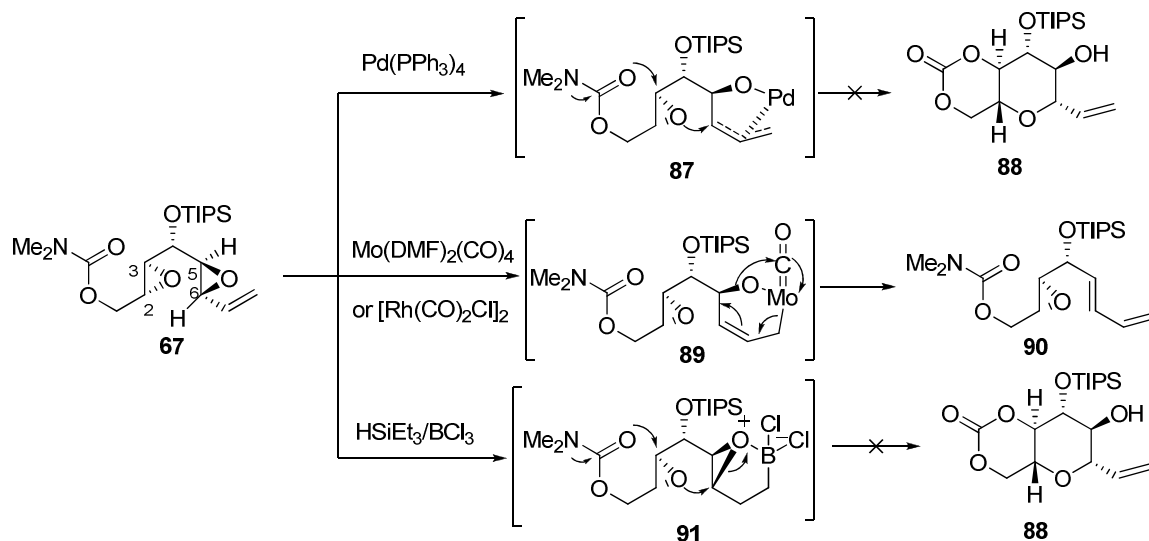


Extending the reaction time under identical conditions, however, provided another unexpected bicyclo[2.2.1] product **85** in 56% yield. $\text{Yb}(\text{OTf})_3$ promoted similar oxacyclization of skipped diepoxide **67** as $\text{Gd}(\text{OTf})_3$ to give bicyclic compound **85** after 7 days, while *exo*-cyclization product **86** was isolated when quenching the reaction within 2 to 3 hours after addition of the Lewis acid [$\text{Yb}(\text{OTf})_3$]. Other Lewis acids including $\text{BF}_3\text{-Et}_2\text{O}$ and TMSOTf or protic acid (Amberlyst 15) resulted in *exo*-cyclization to bicyclic product **86**. Taken these results together, we proposed a mechanism for the production of **85** that Lewis acid may activate the 2,3-epoxide first and induced the *exo*-cyclization to form intermediate **82**, which underwent another *exo*-cyclization to produce intermediate **84**. Slow $\text{S}_{\text{N}}2$ substitution on C-2 was followed to afford **85**, whose structure was determined by extensive NMR studies.

Transitional metal-promoted opening of epoxide, including $[\text{Rh}(\text{CO})_2\text{Cl}]_2$, $\text{Mo}(\text{DMF})_2(\text{CO})_4$, $\text{Pd}(\text{PPh}_3)_4$ and $\text{HSiEt}_3/\text{BCl}_3$, did not induce the subsequent cascade oxacyclization (Scheme 17). Palladium(0) did not induce cascade oxacyclization via intermediate **87** from oxidative addition of vinyl epoxide of **67**.

Crude ^1H NMR of the reaction mixture after aqueous workup indicated the presence of 2,3-epoxide. Molybdenum $[\text{Mo}(\text{DMF})_2(\text{CO})_4]$ or rhodium $[\text{Rh}(\text{CO})_2\text{Cl}]_2$ only triggered elimination of epoxide to form a diene through hypothetical intermediate **89**. $\text{HSiEt}_3/\text{BCl}_3$ resulted in complex unidentified mixtures.

Scheme 17. Transition metal promoted opening of epoxide **67**.



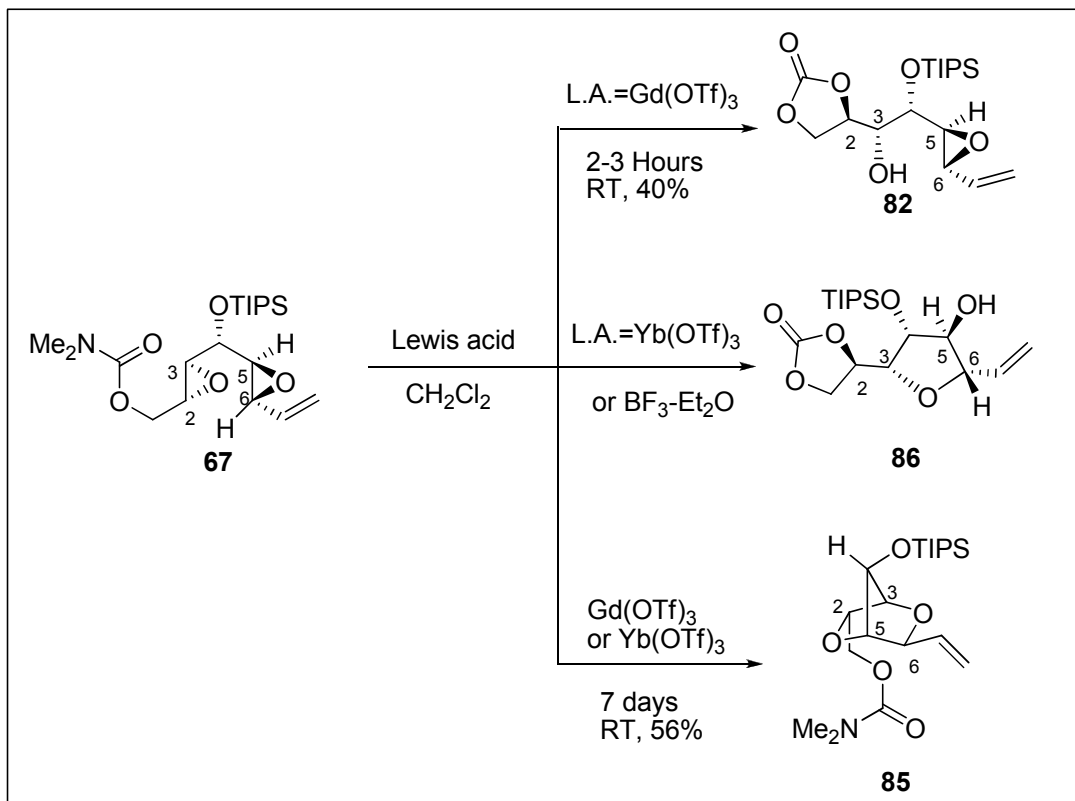
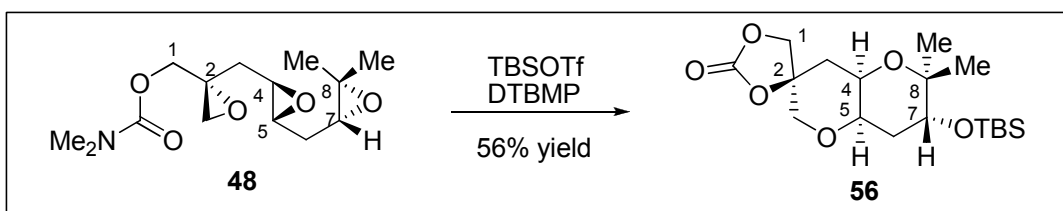
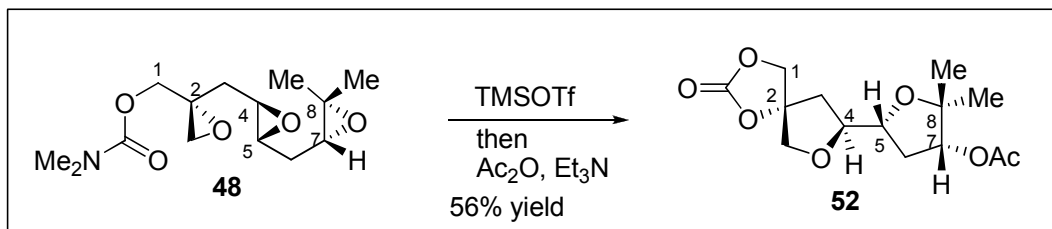
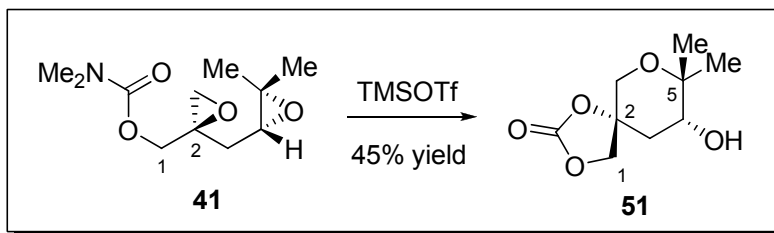
In summary, we have uncovered some novel mechanistic aspects of oxacyclization of skipped polyepoxide to polypyran or polytetrahydrofurans: 1) Fragmentation of polyepoxides with Lewis acid was unique to skipped polyepoxides, as compared with isoprenoid-derived polyepoxides; 2) the role of C-3 substituents on the oxacyclization is so critical that different mechanisms was followed with different substituents; 3) energy of the reaction transition state required for synchronous cyclizations of skipped polyepoxides is much higher than that in the analogous synthesis of isoprenoid-derived polyepoxides, and thus the stepwise mechanism may operate. 4) Lewis acid has pronounced effects on efficacy of oxacyclization of skipped polyepoxides.

2.3. Conclusions

We have achieved the silyl Lewis acid-promoted *endo*-selective oxacyclization of internal disubstituted epoxide to polypyranes via a novel mechanistic pathway.⁴⁴

The silyl Lewis acid was elected based on the mechanism and found to be generally effective on oxacyclization. The relative efficacy of this cyclization pathway might be generally useful in the synthesis of *cis*-fused bispyrans, as observed in the LM and NO substructures of maitotoxin.

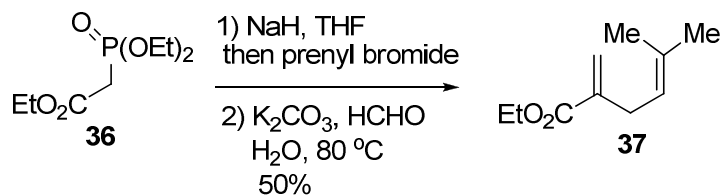
Oxacyclization of skipped polyepoxides with 3-TMS substituted epoxide resulted in fragmentation with various Lewis acid promoters. Cyclization of 2,3-disubstituted epoxide only proceeded in an *exo* mode to give cyclization products, which structures were highly dependent on the Lewis acid promoter and reaction time. These findings greatly expand our mechanistic understanding of oxacyclization of polyepoxides to polycyclic ethers. Further, these results will guide our development of novel oxacyclization in the future. The oxacyclizations of skipped polyepoxides explored in this part was summarized below.



2.4. Experiments

General information: ^1H and ^{13}C NMR spectra were recorded on an Inova-400 spectrometer (400 MHz for ^1H , 100 MHz for ^{13}C), or an Inova-600 spectrometer (600 MHz for ^1H , 150 MHz for ^{13}C). NMR spectra were recorded as solutions in deuterated chloroform (CDCl_3) with residual chloroform (7.27 ppm for ^1H NMR and 77.23 ppm for ^{13}C NMR) taken as the internal standard, and were reported in parts per million (ppm); or as specified in deuterated benzene (C_6D_6) (7.16 ppm for ^1H NMR, 128.2 ppm for ^{13}C NMR). Abbreviations for signal coupling are as follows: s, singlet; d, doublet; t, triplet; q, quartet; m, multiplet. IR spectra were collected on a Mattson Genesis II FT-IR spectrometer, with samples as neat films. Mass spectra (high resolution FAB) were recorded on a VG 70-S Nier Johanson Mass Spectrometer. Optical rotations were recorded at 23°C with a Perkin-Elmer Model 341 polarimeter. Melting point was recorded on FISHER-JOHNS melting point apparatus. Analytical thin layer chromatography (TLC) was performed on precoated glass backed plates purchased from Whatman (silica gel 60 F254; 0.25 mm thickness). Flash column chromatography was carried out with silica gel 60 (230-400 mesh ASTM) from EM Science. All reactions except as mentioned were conducted with anhydrous solvents in oven-dried or flame-dried and argon-charged glassware. All anhydrous solvents were dried over 3Å or 4Å molecular sieves. Trace water content was tested with Coulometric KF Titrator from Denver Instruments. Solvents used in workup, extraction and column chromatography were used as received from commercial suppliers without prior purification. All reagents were purchased from Sigma-Aldrich.

Alkylation of phosphonoacetate and methylenation to ester **37**²⁹

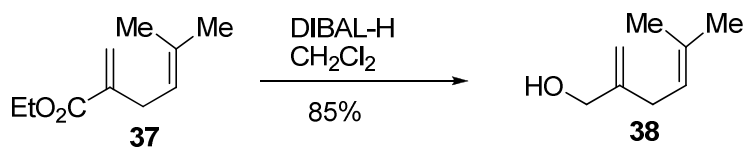


Triethyl phosphonoacetate **36** (4.59 g, 20.5 mmol) was dissolved in THF (20 mL) and cooled to 0 °C. NaH (60% in mineral oil, 1.05 g, 25.1 mmol) was added in 20 portions over a 20 min period with stirring. After 10 min, prenyl bromide (2.34 g, 15.7 mmol) was added over 20 min, and the mixture was stirred at 20 °C for 6 h. K₂CO₃ (4.55 g, 33.0 mmol), H₂O (2.5 mL) and formaldehyde (37% in water, 5.01 mL, 62.8 mmol) were added to the solution. The mixture was then heated to 80 °C and stirred at this temperature for 2 h. After cooling to 20 °C, the organic phase was separated and the aqueous phase was extracted twice with ether. The combined organic fractions were washed with water and brine, dried with anhydrous MgSO₄, and solvent was removed by rotary evaporation. The residue was purified by silica gel chromatography to give **37** (1.32 g, 50%) as a colorless liquid.

¹H NMR (400 MHz, CDCl₃): δ 6.11 (dd, *J*=2.8, 1.6 Hz, 1H), 5.49 (dd, *J*=3.6, 2.0 Hz, 1H), 5.15 (m, 1H), 4.18 (dd, *J*=14.4, 7.2 Hz, 2H), 2.96 (d, *J*=7.2 Hz, 2H), 1.71 (s, 3H), 1.61 (s, 3H), 1.28 (t, *J*=7.2 Hz, 3H).

¹³C NMR (100 MHz, CDCl₃): δ 167.5, 140.1, 134.2, 124.4, 120.8, 60.8, 30.5, 25.9, 17.8, 14.4.

Reduction of ester **37** with DIBAL-H²⁹

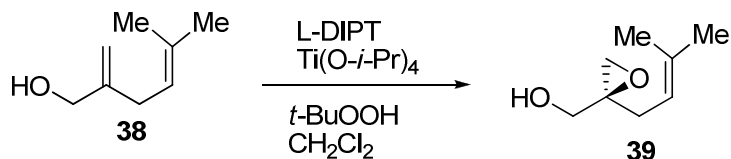


The diene ester **37** (923 mg, 5.49 mmol) was dissolved in CH₂Cl₂ (50 mL) and cooled to -78 °C. Diisobutylaluminum hydride (DIBAL-H, 1.0 M in CH₂Cl₂, 12.1 mL, 12.1 mmol) was added slowly. After stirring at -78 °C for 2 h, ethyl acetate (20 mL) was added dropwise to quench the excess DIBAL-H, followed by addition of sat. ammonium chloride (NH₄Cl, 20 mL) and sat. Rochelle's salt (20 mL). The mixture was stirred for several hours, until it became a clear solution, which was transferred to a separatory funnel. The organic fractions were collected, and the aqueous fractions were extracted with ethyl acetate (50 mL x 2). The combined organic fractions were washed with water and brine, dried with anhydrous MgSO₄, and solvent was removed by rotary evaporation. The residue was purified by silica gel chromatography to give analytical pure allylic alcohol **38** (558 mg, 85%) as a colorless oil.

¹H NMR (400 MHz, CDCl₃): δ 5.14 (m, 1H), 4.97 (d, *J*=1.2 Hz, 1H), 4.84 (d, *J*=1.2 Hz, 1H), 4.03 (s, 2H), 2.72 (d, *J*=7.6 Hz, 2H), 1.94 (s, br, OH), 1.69 (s, 3H), 1.60 (s, 3H).

¹³C NMR (100 MHz, CDCl₃): δ 148.8, 134.0, 121.7, 109.8, 66.3, 32.4, 26.2, 18.1.

Sharpless asymmetric epoxidation of allylic alcohol **38**^{29,30}

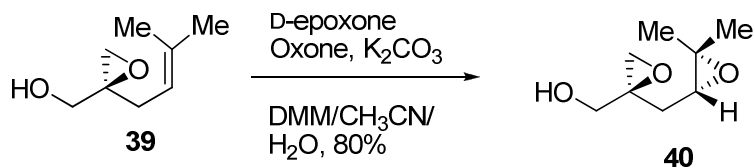


In a 50 mL, round-bottomed flask, 4 Å molecular sieves (1.86 g) were dispersed in anhydrous dichloromethane (25 mL). Then L-(+)-diisopropyl tartrate (L-DIPT, 117 mg, 0.56 mmol) was added to the reaction flask, and the mixture was cooled to -40 °C. After 10 min, Ti(O-*i*-Pr)₄ (138 mg, 0.47 mmol) was added, and the mixture was stirred at -40 °C for 20 min. After that time, *t*-BuOOH (5.0-6.0 M in decane, 1.69 mL, 9.32 mmol) was introduced, and the mixture was stirred at -40 °C for 30 min, after which time the allylic alcohol **38** (588 mg, 4.66 mmol) was added as a solution in dry dichloromethane (5 mL). The reaction mixture was warmed to -18 °C and kept at this temperature overnight. The reaction was quenched by addition of acetone containing 2% water (10 mL), and warmed to room temperature and stirred for 3 h. After filtering through Celite to remove the molecular sieves and salts, the filtrate was dried over MgSO₄, the solids were filtered, and the solvent was removed by rotary evaporation. Purification by column chromatography gave pure epoxy alcohol **39** (615 mg, 93%).

¹H NMR (600 MHz, CDCl₃): δ 5.06 (t, *J*=7.8 Hz, 1H), 3.71 (d, *J*=12 Hz, 1H), 3.56 (d, *J*=12 Hz, 1H), 2.81 (d, *J*=4.8 Hz, 1H), 2.63 (d, *J*=4.2 Hz, 1H), 2.45 (dd, *J*=14.4, 7.8 Hz, 1H), 2.18 (dd, *J*=15.6, 7.2 Hz, 2H), 1.67 (s, 3H), 1.58 (s, 3H).

¹³C NMR (150 MHz, CDCl₃): δ 135.5, 117.7, 63.1, 60.2, 49.4, 30.7, 25.9, 18.0.

Diastereoselective Shi epoxidation of epoxy alkene **39**

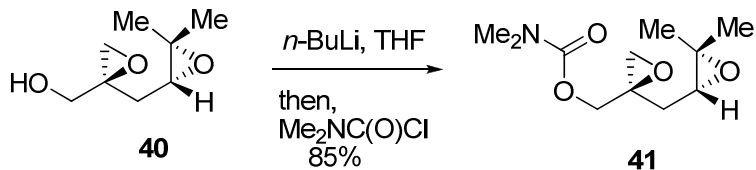


Allylic alcohol **39** (615 mg, 4.33 mmol) was dissolved in a 1: 2 mixture of acetonitrile: dimethoxymethane (68 mL). Under vigorous agitation, a 0.05 M solution of $\text{Na}_2\text{B}_4\text{O}_7$ in 4×10^{-4} M $\text{Na}_2(\text{EDTA})$ (44 mL), $\text{Bu}_4\text{NH}_4\text{SO}_4$ (60 mg, 0.18 mmol) and 1,2:4,5-di-*O*-isopropylidene-*D*-erythro-2,3-hexodiuro-2,6-pyranose (Shi catalyst, D-epoxone[®], 350 mg, 1.36 mmol), were sequentially added. The mixture was cooled to 0 °C, and then Oxone (3.80 g, 6.02 mmol), dissolved in 4×10^{-4} M $\text{Na}_2(\text{EDTA})$ (29.0 mL), and K_2CO_3 (3.60 g, 26.0 mmol), dissolved in water (29 mL), were simultaneously added to the mixture over 1.5 h. Once the addition was completed, the mixture was stirred for 15 min, diluted with water and extracted with ethyl ether. The organic extracts were dried over MgSO_4 , and the solvent was removed by rotary evaporation. Purification by column chromatography on silica gel yielded diepoxy alcohol **40** (547 mg, 80%) as a colorless oil.

^1H NMR (400 MHz, CDCl_3): δ 3.75 (dd, $J=12.4, 4.8$ Hz, 1H), 3.67 (dd, $J=12.8, 7.6$ Hz, 1H), 2.89 (dd, $J=8.8, 4.4$ Hz, 1H), 2.87 (d, $J=4.8$ Hz, 1H), 2.67 (d, $J=4.8$ Hz, 1H), 2.46 (br s, OH), 1.91 (dd, $J=14.8, 4.0$ Hz, 1H), 1.76 (dd, $J=14.8, 8.0$ Hz, 1H), 1.29 (s, 3H), 1.23 (s, 3H).

^{13}C NMR (100 MHz, CDCl_3): δ 64.4, 63.5, 60.7, 58.7, 51.0, 32.2, 24.8, 18.9.

Carbamate formation from diepoxy alcohol 40



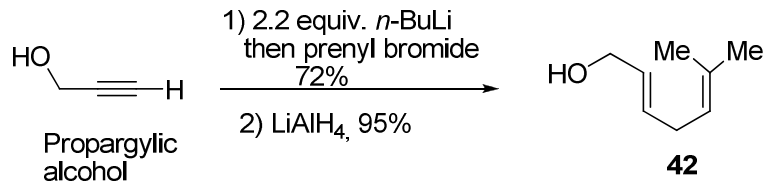
Diepoxy alcohol **40** (479 mg, 3.03 mmol) was dissolved in THF (50 mL) and cooled to $-78\text{ }^\circ\text{C}$. *n*-BuLi (2.5 M in hexane, 1.45 mL, 3.6 mmol) was added dropwise over 10 min. The mixture was stirred at $-78\text{ }^\circ\text{C}$ for 1 h, and dimethyl chlorocarbamate (648 mg, 6.06 mmol) was added to the solution. The mixture was allowed to warm up to room temperature and stirred overnight. The reaction was quenched with sat. NH_4Cl (20 mL) and diluted with Et_2O (50 mL). The organic fractions were collected and dried over anhydrous MgSO_4 , and the solvent was removed by rotary evaporation. The residue was purified by silica gel chromatography to afford diepoxy carbamate **41** (589 mg, 85%) as a colorless oil.

$[\alpha]_{\text{D}} = +5.0$ (*c* 0.7, CHCl_3).

$^1\text{H NMR}$ (600 MHz, CDCl_3): δ 4.33 (d, $J=12.0$ Hz, 1H), 4.03 (d, $J=12.6$ Hz, 1H), 2.89 (s, 6H), 2.86 (m, 1H), 2.78 (d, $J = 4.8$ Hz, 1H), 2.71 (d, $J = 4.8$ Hz, 1H), 1.97 (dd, $J=15, 6.0$ Hz, 1H), 1.75 (dd, $J = 15.0, 7.2$ Hz, 1H), 1.28 (s, 3H), 1.21 (s, 3H).

$^{13}\text{C NMR}$ (150 MHz, CDCl_3): δ 156.0, 66.8, 60.2, 58.1, 56.5, 50.9, 36.7, 36.0, 32.1, 24.7, 18.8.

Alkylation and Reduction with LAH to allylic alcohol 41



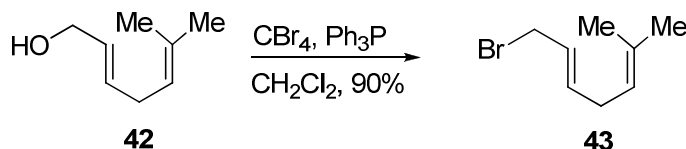
To a THF (25 mL) solution of propargylic alcohol (1.4 mL, 24 mmol) was added *n*-BuLi (2.5 M in hexane, 19.2 mL, 48 mmol) dropwise over 20 minutes at -78 °C. After stirred at -78 °C for 30 minutes, the reaction mixture was allowed to warm up to room temperature and stirred at this temperature for 30 minutes, and then cooled to 0 °C. Copper iodide (CuI, 114 mg, 0.6 mmol) was added to the cooled solution. After 30 minutes, prenyl bromide (2.33 mL, 20 mmol) was added as a THF (2 mL) solution at 0 °C -8 °C. The resulting mixture was allowed to warm up to room temperature and stirred overnight. The reaction was quenched with sat. NH₄Cl (10 mL) and diluted with Et₂O (10 mL). The organic fractions were collected and dried over anhydrous MgSO₄, and the solvent was removed by rotary evaporation. The residue was purified by silica gel chromatography to afford enyn alcohol (2.19 g, 72%) as colorless oil. To a 250 mL flask was charged THF (80 mL) and cooled to -78 °C. Lithium aluminum hydride (LAH, 1.0 M in diethyl ether, 20 mL, 20.0 mmol) was added to the cooled THF, resulting large amount of precipitate in the flask. A THF (5 mL) solution of the enyn alcohol (2.19 g, 19.6 mmol) obtained above was then added to the suspension with stirring at -78 °C. After 10 minutes, the dry ice-acetone cooling bath was removed to allow warming to room temperature and stirred overnight. Ethyl acetate (20 mL) was added dropwise to quench the excess LAH, followed by addition of sat.

ammonium chloride (NH₄Cl, 20 mL) and sat. Rochelle's salt (60 mL). The mixture was stirred for several hours, until it became a clear solution, which was transferred to a separatory funnel. The organic fractions were collected, and the aqueous fractions were extracted with ethyl acetate (80 mL x 2). The combined organic fractions were washed with water and brine, dried with anhydrous MgSO₄, and solvent was removed by rotary evaporation. The residue was purified by silica gel chromatography to give analytical pure allylic alcohol **42** (2.12 g, 95%) as a colorless oil.

¹H NMR (600 MHz, CDCl₃): δ 5.64 (m, 2H), 5.14 (m, 1H), 4.08 (d, *J* = 4.8 Hz, 2H), 2.72 (t, *J* = 7.2, 5.4 Hz, 2H), 1.69 (s, 3H), 1.60 (s, 3H).

¹³C NMR (150 MHz, CDCl₃): δ 133.2, 132.1, 129.0, 121.7, 64.0, 31.1, 25.9, 17.9.

Bromination of allylic alcohol 42³¹



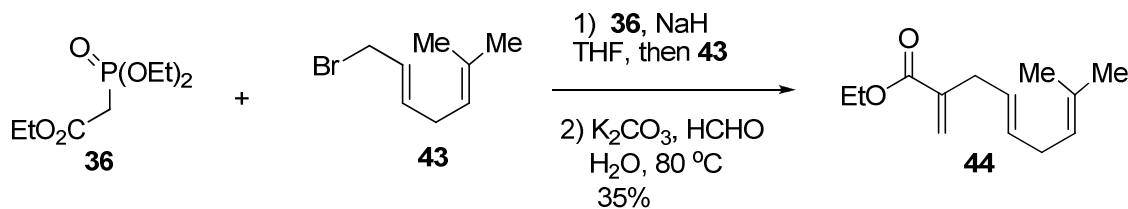
To a 250 mL round-bottomed flask was charged with dichloromethane (150 mL), allylic alcohol **42** (4.2 g, 36.8 mmol) and triphenylphosphine (11.6 g, 44.2 mmol). The solution was cooled with water-ice bath to 0 °C. After 20 minutes, carbon tetrabromide (14.7 g, 44.2 mmol) dissolved in CH₂Cl₂ (20 mL) was added dropwise to the reaction flask. After addition was complete, the reaction mixture was stirred for another two hours. Saturated Na₂S₂O₃ (30 mL) was added to quench the reaction. The organic fractions were collected, and the aqueous fractions were extracted with diethyl ether (80 mL x 2). The combined organic

fractions were washed with water and brine, dried with anhydrous MgSO_4 , and solvent was removed by rotary evaporation. 50 mL of hexane was added to the residue dissolved in ether (20 mL). The solid (most triphenylphosphine oxide) was filtered and washed with hexane (10 mL x 2). The filtrate was concentrated and purified by passing through a short silica gel column to give allylic alcohol **43** (5.8 g, 90%) as a yellow oil.

$^1\text{H NMR}$ (400 MHz, CDCl_3): δ 5.68 (m, 2H), 5.11 (m, 1H), 3.94 (d, $J = 7.2$ Hz, 2H), 2.74 (t, $J = 6.8, 6.0$ Hz, 2H), 1.70 (s, 3H), 1.60 (s, 3H).

$^{13}\text{C NMR}$ (100 MHz, CDCl_3): δ 135.3, 133.8, 126.3, 120.9, 33.8, 30.9, 25.9, 17.9.

Alkylation of phosphonoacetate and methylenation to ester **44**

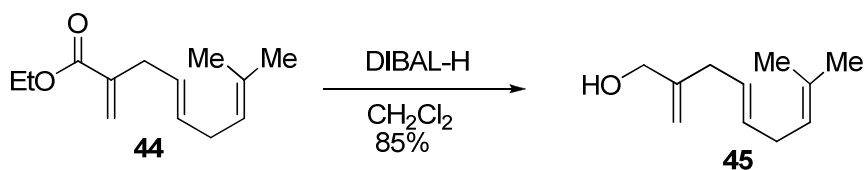


Prepared as described for compound **37**, from triethyl phosphonoacetate **36** (4.59 g, 20.5 mmol) in THF (20 mL), NaH (60% in mineral oil, 1.05 g, 25.1 mmol), 1-bromo-6-methylhepta-2,5-diene³ (**43**, 2.97 g, 15.7 mmol), K_2CO_3 (4.55 g, 33.0 mmol) in H_2O (2.5 mL), and formaldehyde (37% in water, 5.01 mL, 62.8 mmol). Yield: 1.14 g (35%); colorless liquid.

$^1\text{H NMR}$ (600 MHz, CDCl_3): δ 6.12 (s, 1H), 5.50 (d, $J = 1.2$ Hz, 1H), 5.43 (m, 2H), 5.10 (m, 1H), 4.18 (dd, $J = 15.0, 7.8$ Hz, 2H), 2.97 (d, $J = 5.4$ Hz, 2H), 2.68 (t, $J = 6.0, 5.4$ Hz, 2H), 1.68 (s, 3H), 1.59 (s, 3H), 1.27 (t, $J = 7.2$ Hz, 3H).

^{13}C NMR (150 MHz, CDCl_3): δ 167.3, 140.2, 132.6, 131.8, 126.5, 124.9, 122.3, 60.8, 34.9, 31.4, 25.9, 17.8, 14.4.

Reduction of ester 44 with DIBAL-H

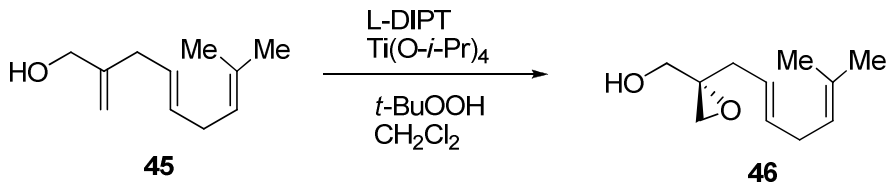


Prepared as described for compound **38**, from compound **44** (1.14 g, 5.48 mmol) in CH_2Cl_2 (50 mL), and DIBAL-H (1.0 M in CH_2Cl_2 , 12.1 mL, 12.1 mmol). Yield: 773 mg (85%), colorless oil.

^1H NMR (600 MHz, CDCl_3): δ 5.24 (m, 2H), 5.11 (m, 1H), 5.01 (s, 1H), 4.87 (s, 1H), 4.05 (s, 2H), 2.74 (d, $J = 6.0$ Hz, 2H), 2.68 (t, $J = 7.2, 6.0$ Hz, 2H), 1.69 (s, 3H), 1.59 (s, 3H).

^{13}C NMR (150 MHz, CDCl_3): δ 148.3, 132.7, 131.5, 127.1, 122.3, 110.2, 65.9, 36.6, 31.4, 25.9, 17.8.

Sharpless asymmetric epoxidation of allylic alcohol 45

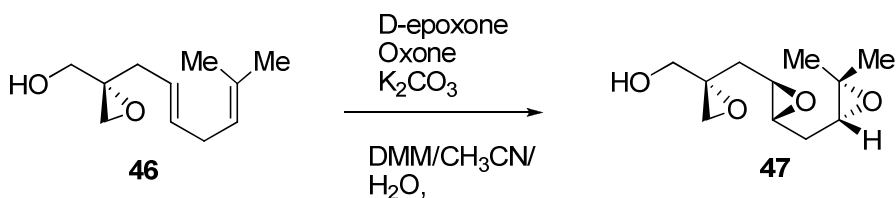


Prepared as described for compound **39**, from compound **45** (773 mg, 4.66 mmol) in CH_2Cl_2 (5 mL), 4 Å molecular sieves (1.86 g) in CH_2Cl_2 (25 mL), L-(+)-diisopropyl tartrate (117 mg, 0.56 mmol), $\text{Ti}(\text{O}-i\text{-Pr})_4$ (138 mg, 0.47 mmol), and *tert*-BuOOH (5.0-6.0 M in decane, 1.69 mL, 9.32 mmol). Yield: 788 mg (93%); colorless oil.

^1H NMR (600 MHz, CDCl_3): δ 5.49 (dt, $J=15, 7.2$ Hz, 1H), 5.33 (m, 1H), 5.08 (m, 1H), 3.73 (dd, $J=11.4, 4.2$ Hz, 1H), 3.60 (dd, $J=12, 8.4$ Hz, 1H), 2.84 (d, $J=4.8$ Hz, 1H), 2.66 (t, $J=6.6$ Hz, 2H), 2.65 (d, $J=4.2$ Hz, 2H), 2.42 (dd, $J=15, 7.8$ Hz, 1H), 2.22 (dd, $J=14.4, 6.6$ Hz, 1H), 1.91 (dd, $J=7.8, 4.2$ Hz, 1H), 1.67 (s, 3H), 1.58 (s, 3H).

^{13}C NMR (150 MHz, CDCl_3): δ 133.5, 132.9, 123.4, 121.9, 62.9, 59.7, 49.6, 35.4, 31.4, 25.8, 17.8.

Double Shi epoxidation of epoxy alkene 46



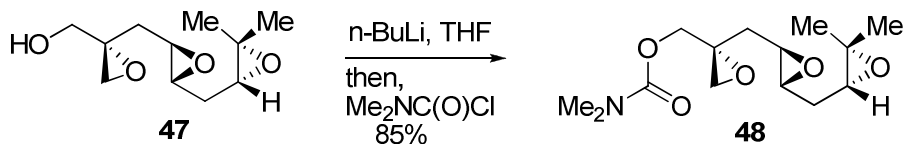
Monoepoxy dienyl alcohol **46** (788 mg, 4.33 mmol) was dissolved in a 1 : 2 mixture of acetonitrile : dimethoxymethane (68 mL). Under vigorous agitation, a

0.05 M solution of $\text{Na}_2\text{B}_4\text{O}_7$ in 4×10^{-4} M $\text{Na}_2(\text{EDTA})$ (44 mL), Bu_4NHSO_4 (60 mg, 0.18 mmol) and 1,2:4,5-di-*O*-isopropylidene-*D*-erythro-2,3-hexodiuoro-2,6-pyranose (Shi catalyst, D-epoxone, 700 mg, 2.72 mmol), were sequentially added. The mixture was cooled to 0 °C, and then Oxone (7.60 g, 12.0 mmol), dissolved in 4×10^{-4} M $\text{Na}_2(\text{EDTA})$ (58 mL), and K_2CO_3 (7.20 g, 52.0 mmol), dissolved in water (58 mL), were simultaneously added to the mixture over 2 hrs. Once the addition was completed, the mixture was stirred for 15 min, diluted with water and extracted with ethyl ether. The organic extracts were dried over anhydrous Na_2SO_4 , and the solvent was removed by rotary evaporation. Purification by column chromatography on silica gel yielded diepoxy alcohol **47** (648 mg, 3.03 mmol) as a colorless oil.

^1H NMR (600 MHz, CDCl_3): δ 3.79 (d, $J = 12.6$ Hz, 1H), 3.68 (dd, $J = 12.6, 4.2$ Hz, 1H), 2.90 (m, 3H), 2.88 (d, $J = 4.8$ Hz, 1H), 2.72 (d, $J = 4.8$ Hz, 1H), 2.25 (br, OH), 1.92 (dd, $J = 15.0, 4.8$ Hz, 1H), 1.82 (dd, $J = 14.4, 6.6$ Hz, 1H), 1.79 (m, 1H), 1.69 (m, 1H), 1.31 (s, 3H), 1.24 (s, 3H).

^{13}C NMR (150 MHz, CDCl_3): δ 64.1, 61.1, 58.6, 58.4, 56.3, 55.3, 51.0, 35.7, 32.1, 24.8, 19.0.

Carbamate formation from diepoxy alcohol 47



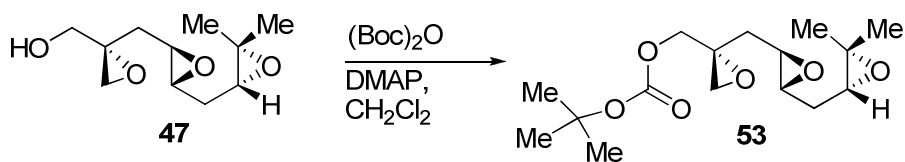
The triepoxy carbamate **48** was then prepared by following the carbamate formation as described for compound **41**, with triepoxy alcohol **47** (648 mg, 3.03 mmol) in THF (50 mL), $n\text{-BuLi}$ (2.5 M in hexane, 1.45 mL, 3.63 mmol), and dimethyl chlorocarbamate (648 mg, 6.06 mmol). Yield: 674 mg (85%, two steps from **48**) as a colorless oil.

$[\alpha]_{\text{D}} = +38.5$ (c 0.4, CHCl_3).

$^1\text{H NMR}$ (600 MHz, CDCl_3): δ 4.39 (d, $J=12.0$ Hz, 1H), 4.02 (d, $J=12.6$ Hz, 1H), 2.91 (s, 6H), 2.87 (m, 3H), 2.78 (dd, $J=11.4$, 4.8 Hz, 2H), 2.00 (dd, $J=14.4$, 4.8 Hz, 1H), 1.80-1.69 (m, 3H), 1.31 (s, 3H), 1.24 (s, 3H).

$^{13}\text{C NMR}$ (150 MHz, CDCl_3) δ : 156.1, 66.9, 61.0, 58.5, 56.4, 56.1, 54.8, 50.8, 36.8, 36.1, 35.3, 32.2, 24.9, 19.0.

Carbonate formation from triepoxy alcohol 47

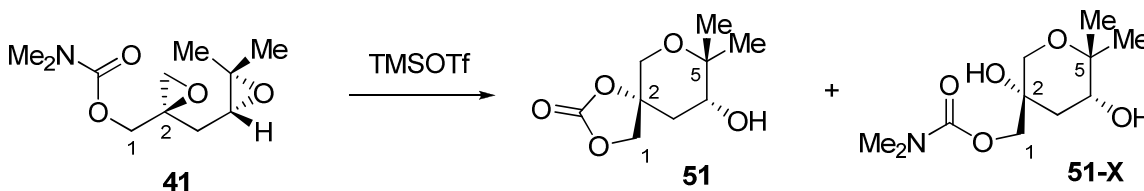


A round-bottomed flask was charged with triepoxy alcohol **47** (350 mg, 1.64 mmol), CH_2Cl_2 (15 mL), dimethylaminopyridine (DMAP, 300 mg, 2.45 mmol) and triethylamine (1.3 mL, 8.18 mmol), and was cooled to 0 °C. Di-*tert*-butyl dicarbonate [$(\text{Boc})_2\text{O}$, 1.43 g, 1.5 mL, 6.54 mmol] was added at 0 °C. The

reaction was stirred overnight while slowly warming up to room temperature. Saturated NaHCO₃ was then added to quench and let the stirring continue for 30 – 60 minutes. The organic fractions were collected, and the aqueous fractions were extracted with diethyl ether (20 mL x 2). The combined organic fractions were washed with water and brine, dried with anhydrous Na₂SO₄, and solvent was removed by rotary evaporation. The residue was purified by silica gel chromatography to give analytical pure allylic alcohol **53** (427 mg, 83%) as a colorless oil.

¹H NMR (400 MHz, CDCl₃): δ 4.24 (d, *J* = 12.0 Hz, 1H), 4.07 (d, *J* = 12.0 Hz, 1H), 2.86 (m, 3H), 2.79 (d, *J* = 4.4 Hz, 1H), 2.74 (d, *J* = 4.8 Hz, 1H), 2.00 (dd, *J* = 14.4, 4.8 Hz, 1H), 1.80-1.69 (m, 3H), 1.44 (s, 9H), 1.28 (s, 3H), 1.22 (s, 3H).

TMSOTf-promoted cascade oxacyclization of diepoxy carbamate **41**⁴⁴



Diepoxy carbamate **41** (50 mg, 0.22 mmol) was dissolved in anhydrous CH₂Cl₂ (5 mL, ~0.05 M) at room temperature, and trimethylsilyl triflate (TMSOTf, 0.05 mL, 0.26 mmol) was added. The reaction progress was monitored by TLC. After completion, sat. NaHCO₃ was added to quench the reaction and the mixture was diluted with Et₂O (10 mL). The organic fractions were collected and dried over anhydrous MgSO₄, and solvent was removed by rotary evaporation. The crude

product residue was purified by flash column chromatography on silica gel to give **51** (20 mg, 45%), along a small amount of **51-X** (4.0 mg, 8%).

m.p. 117-118 °C. $[\alpha]_D = +1.2$ (c 0.34, CHCl₃).

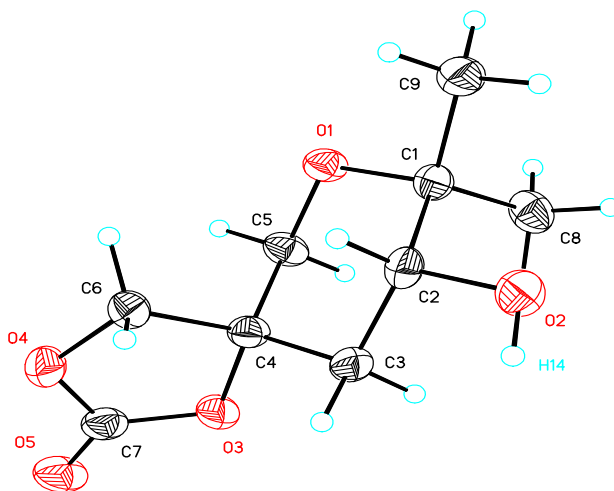
IR (neat, cm⁻¹): 3433, 2979, 2881, 1799, 1324, 1174, 1057.

¹H NMR (400 MHz, CDCl₃): δ 4.34 (d, $J=8.4$ Hz, 1H), 4.16 (dd, $J=8.4, 0.8$ Hz, 1H), 3.73 (d, $J=12.4$ Hz, 1H), 3.61 (d, $J=12.4$ Hz, 1H), 3.39 (br s, 1H), 2.16 (d, $J=6.8$ Hz, 2H), 1.26 (s, 3H), 1.25 (s, 3H).

¹³C NMR (100 MHz, CDCl₃): δ 153.7, 79.4, 75.2, 72.7, 70.9, 65.3, 37.1, 25.1, 19.2.

HRMS (FAB⁺) Calcd for C₉H₁₅O₅ [M+H⁺] 203.0914, found 203.0912.

X-Ray analysis: The structure of compounds **51** was established by X-ray analysis. The thermal ellipsoid diagrams and data for compound **51** are provided below:



For X-ray data of compound 51, see page 303-310.

Data for compound 51-X

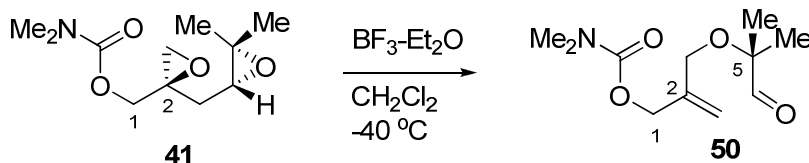
IR (neat, cm⁻¹): 3408, 2935, 2877, 1687, 1498, 1451, 1403, 1198, 1061, 768.

¹H NMR (600 MHz, CDCl₃): δ 4.03 (d, *J* = 12.0 Hz, 1H), 3.99 (d, *J* = 11.4 Hz, 1H), 3.63 (d, *J* = 12.0 Hz, 1H), 3.57 (dd, *J* = 12.0, 2.4 Hz, 1H), 3.47 (t, *J* = 4.2 Hz, 1H), 2.93 (s, 6H), 1.93 (dd, *J* = 14.4, 3.6 Hz, 1H), 1.85 (ddd, *J* = 14.4, 4.5, 2.4 Hz, 1H), 1.28 (s, 3H), 1.20 (s, 3H).

¹³C NMR (150 MHz, CDCl₃): δ 157.1, 75.1, 71.2, 70.2, 70.2, 67.0, 36.9, 36.2, 34.1, 24.1, 22.6.

HRMS (FAB⁺) Calcd for C₁₁H₂₂O₅N₁ [M+H⁺] 248.14925, found 248.14937.

BF₃-Et₂O-promoted cascade oxacyclization of diepoxy carbamate 41

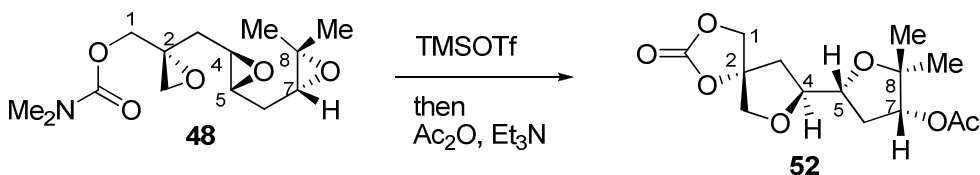


Following conditions generally utilized in our laboratory for the endo-selective cascade oxacyclization of polyepoxides, diepoxide **41** (80 mg, 0.35 mmol) was dissolved in dry CH₂Cl₂ (5 mL) and cooled to -40 °C. BF₃-Et₂O (0.2 M in CH₂Cl₂, 2.0 mL, 0.4 mmol) was subsequently added dropwise over 5 minutes. After stirred for 30 minutes at -40 °C, the reaction mixture was quenched with sat. NaHCO₃ (3 mL) and stirred overnight at room temperature. The organic layer was separated. Aqueous layer was extracted with CH₂Cl₂ (10 mL x 2). The combined organic layers were washed with brine (20 mL), dried with MgSO₄ and evaporated. The resulting crude product was purified by column chromatography on silica gel to give aldehyde **50** (60 mg, 75%) as a colorless oil.

^1H NMR (400 MHz, CDCl_3): δ 9.56 (s, 1H), 5.25 (d, $J = 1.2$ Hz, 1H), 5.20 (d, $J = 0.8$ Hz, 1H), 4.63 (s, 2H), 3.93 (s, 2H), 2.90 (s, 6H), 1.27 (s, 6H).

^{13}C NMR (100 MHz, CDCl_3): δ 204.4, 156.4, 141.7, 114.9, 80.6, 65.7, 65.3, 36.7 (2C), 20.9 (2C).

TMSOTf-promoted cascade oxacyclization of triepoxy carbamate **47⁴**



Following the general conditions utilized for oxacyclization of diepoxy carbamate to **51**, triepoxy carbamate **48** (55 mg, 0.19 mmol) was dissolved in anhydrous CH_2Cl_2 (5 mL, 0.04 M) at room temperature, and TMSOTf (0.04 mL, 0.23 mmol) was added. The reaction progress was monitored by TLC. After completion, sat. NaHCO_3 (5 mL) was added to quench the reaction and the mixture was diluted with Et_2O (10 mL). The organic fractions were collected and dried over anhydrous MgSO_4 , and solvent was removed by rotary evaporation. The crude product residue was purified by flash column chromatography on silica gel to provide bis-tetrahydrofuran, which was subjected to acetylation reaction. Specifically, bis-tetrahydrofuran product was dissolved in CH_2Cl_2 (10 mL) at room temperature. Acetic anhydride (38 mg, 0.38 mmol) and triethylamine (0.11 mL, 0.76 mmol) were added to the CH_2Cl_2 solution of bis-tetrahydrofuran with stirring. After stirring overnight, the reaction mixture was evaporated. Chromatography on silica gel afforded the acetylated product **52** (32 mg, 56%).

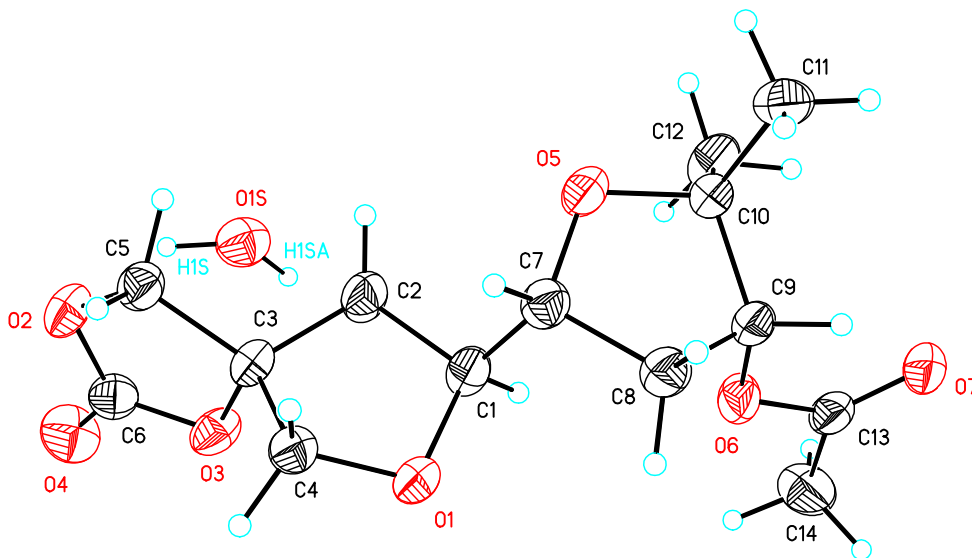
IR (neat, cm^{-1}): 2959, 2921, 2851, 1802, 1731, 1242, 1051.

^1H NMR (600 MHz, CDCl_3): δ 5.01 (dd, $J=6.6, 2.4$ Hz, 1H), 4.46 (d, $J=9.0$ Hz, 1H), 4.42 (d, $J=9.0$ Hz, 1H), 4.21 (m, 1H), 4.10 (m, 1H), 4.08 (d, $J=10.2$ Hz, 1H), 3.97 (d, $J=10.8$ Hz, 1H), 2.56 (m, 1H), 2.49 (dd, $J=13.2, 6.6$ Hz, 1H), 2.14 (dd, $J=13.2, 7.8$ Hz, 1H), 2.08 (s, 3H), 1.70 (ddd, $J=14.4, 6.0, 2.4$ Hz, 1H), 1.20 (s, 6H).

^{13}C NMR (150 MHz, CDCl_3) δ : 170.5, 154.1, 89.1, 83.7, 81.6, 78.6, 76.7, 76.0, 71.9, 38.9, 35.6, 25.4, 25.4, 22.4.

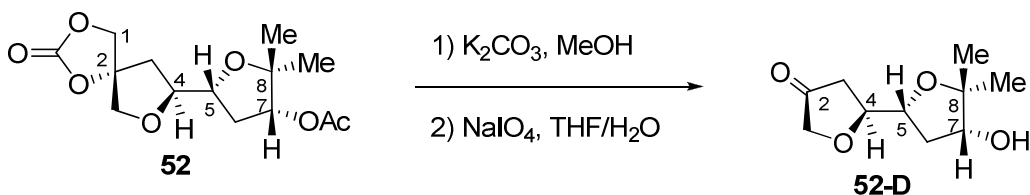
HRMS (FAB $^+$) Calcd for $\text{C}_{14}\text{H}_{21}\text{O}_7$ [(M+H $^+$)] 301.1282, found 301.1281.

X-Ray analysis: The structure of compounds **52** was established by X-ray analysis. The thermal ellipsoid diagrams and data for compound **52** are provided below:



For X-ray data of compound 52, see page 311-319.

Oxidative degradation of 52 to ketone 52-D



The cyclization product bis-tetrahydrofuran **52** (20 mg, 78 μ mol) was dissolved in methanol (5 mL) at room temperature. Anhydrous potassium carbonate (K_2CO_3 , 13.8 mg, 0.1 mmol) was added and the resulting reaction mixture was stirred for 60 minutes at room temperature. Solid ammonium chloride (NH_4Cl , 80 mg, 1.5 mmol) was added to neutralize the base. After 20 minutes, filtration was performed to remove the salts and the filtrate was evaporated. The residue was dissolved in THF (3 mL) and water (1 mL). $NaIO_4$ (100 mg, 0.47 mmol) was added to the solution with vigorous stirring at room temperature. After 60 minutes, saturated NH_4Cl (10 mL) was added to quench the reaction and ethyl acetate (5 mL) was added to dilute the reaction mixture. Organic layer was separated and aqueous layer was extracted with ethyl acetate (10 x 2). The combined organic fractions were washed with brine (20 mL), dried with $MgSO_4$ and evaporated under reduced pressure. Chromatography on silica gel gave the ketone **52-D** (14 mg, 90%). This method has been usually used in our group to confirm the product from *exo*-cyclization of polyepoxide.

IR (neat, cm^{-1}): 3450, 2972, 2926, 1758, 1448, 1178, 1147, 1063.

1H NMR (600 MHz, $CDCl_3$): δ 4.44 (ddd, $J = 10.4, 7.2, 2.4$ Hz, 1H), 4.27 (ddd, $J = 9.6, 3.6, 3.0$ Hz, 1H), 4.14 (d, $J = 16.8$ Hz, 1H), 3.91 (d, $J = 17.4$ Hz, 1H), 3.85 (t, $J = 7.2, 6.6$ Hz, 1H), 2.82 (d, $J = 9.0$ Hz, 1H), 2.50 (m, 1), 2.47 (d, $J = 6.6$ Hz, 1H),

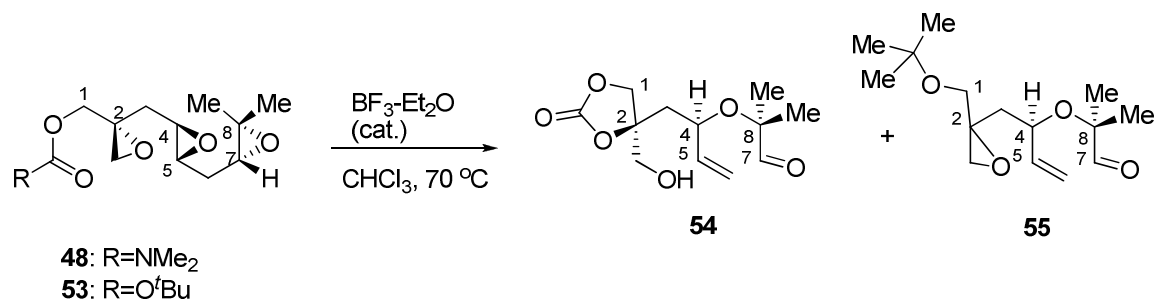
2.31 (dd, $J = 18.0, 10.4$ Hz, 1H), 1.82 (dd, $J = 13.8, 4.2$ Hz, 1H), 1.29 (s, 3H),
1.14 (s, 3H).

^{13}C NMR (150 MHz, CDCl_3) δ : 213.4, 85.0, 79.5, 77.3, 76.6, 71.7, 38.9, 34.9,
25.3, 22.1.

HRMS (FAB⁺) Calcd for $\text{C}_{10}\text{H}_{17}\text{O}_4$ [(M+H⁺)] 201.11214, found 201.11211.

For 2-D NMR spectra (H-H COSY) of compound 52-D, see page 293.

$\text{BF}_3\text{-Et}_2\text{O}$ -promoted cascade oxacyclization of triepoxy carbamate 48



Following conditions generally utilized in our laboratory for the endo-selective cascade oxacyclization of polyepoxides, triepoxide **48** (40 mg, 0.14 mmol) was dissolved in dry CH_2Cl_2 (10 mL) and cooled to -40 °C. $\text{BF}_3\text{-Et}_2\text{O}$ (0.2 M in CH_2Cl_2 , 1.1 mL, 2.2 mmol) was subsequently added dropwise over 5 minutes. After stirred for 30 minutes at -40 °C, the reaction mixture was quenched with sat. NaHCO_3 (5 mL) and the organic layer was separated. Aqueous layer was extracted with CH_2Cl_2 (10 mL x 2). The combined organic layers were washed with brine (20 mL), dried with MgSO_4 and evaporated. The resulting crude

product was purified by column chromatography on silica gel to give aldehyde **54** (20 mg, 50%) and **55** (5 mg, 10%) as colorless oils.

Data for compound 54

IR (neat, cm⁻¹): 3457, 2984, 2932, 1797, 1730, 1386, 1206, 1168, 1065, 772.

¹H NMR (400 MHz, CDCl₃): δ 9.46 (s, 1H), 5.66 (ddd, *J* = 17.2, 10.4, 9.2 Hz, 1H), 5.24 (d, *J* = 6.8 Hz, 1H), 5.21 (s, 1H), 4.42 (d, *J* = 9.2 Hz, 1H), 4.30 (d, *J* = 8.8 Hz, 1H), 4.29 (dd, *J* = 8.8, 2.4 Hz, 1H), 3.79 (t, *J* = 5.6 Hz, 2H), 2.64 (t, *J* = 7.2, 6.8 Hz, 1H), 2.20 (dd, *J* = 15.8, 9.6 Hz, 1H), 2.00 (dd, *J* = 15.8, 2.8 Hz, 1H), 1.34 (s, 3H), 1.23 (s, 3H).

¹³C NMR (100 MHz, CDCl₃): δ 203.2, 138.4, 119.9, 84.5, 81.1, 72.9, 72.2, 64.9, 41.4, 23.5, 20.6.

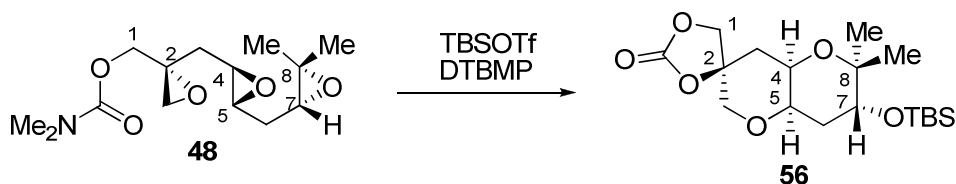
Data for compound 55

IR (neat, cm⁻¹): 2981, 2934, 1741, 1460, 1369, 1277, 1255, 1165, 1102, 930, 858.

¹H NMR (400 MHz, CDCl₃): δ 9.48 (s, 1H), 5.68 (ddd, *J* = 17.6, 10.4, 7.6 Hz, 1H), 5.10 (dd, *J* = 15.6, 10.4 Hz, 2H), 4.27 (d, *J* = 11.6 Hz, 1H), 4.17 (m, 1H), 4.07 (d, *J* = 12.0 Hz, 1H), 2.75 (d, *J* = 4.8 Hz, 1H), 2.66 (d, *J* = 4.4 Hz, 1H), 1.89 (dd, *J* = 14.4, 4.0 Hz, 1H), 1.76 (dd, *J* = 14.0, 8.0 Hz, 1H), 1.42 (s, 9H), 1.26 (s, 3H), 1.17 (s, 3H).

¹³C NMR (100 MHz, CDCl₃): δ 204.4, 139.8, 117.7, 82.7, 81.0, 73.2, 68.4, 55.6, 51.9, 39.8, 27.9 (3C), 23.2, 21.0.

TBSOTf-promoted oxacyclization of triepoxy carbamate 48



Triepoxy carbamate **48** (55 mg, 0.19 mmol) was dissolved in anhydrous CH_2Cl_2 (5 mL, 0.04 M) at room temperature. 2,6-Di-*tert*-butyl-4-methylpyridine (DTBMP, 46.7 mg, 0.23 mmol) was added, followed by *tert*-butyldimethylsilyl triflate (TBSOTf, 0.05 mL, 0.23 mmol). The reaction progress was monitored by TLC. After completion, sat. NaHCO_3 was added to quench the reaction, and the mixture was diluted with Et_2O (50 mL). The organic fractions were collected and dried over anhydrous MgSO_4 , and solvent was removed by rotary evaporation. The crude product residue was purified by flash column chromatography on silica gel to yield bis-tetrahydropyran **56** (39.6 mg, 56%).

m.p. 195-200 °C (sublimed). $[\alpha]_{\text{D}} = +18.0$ (*c* 0.1, CHCl_3).

IR (neat, cm^{-1}): 2958, 2882, 1786, 1249, 1059.

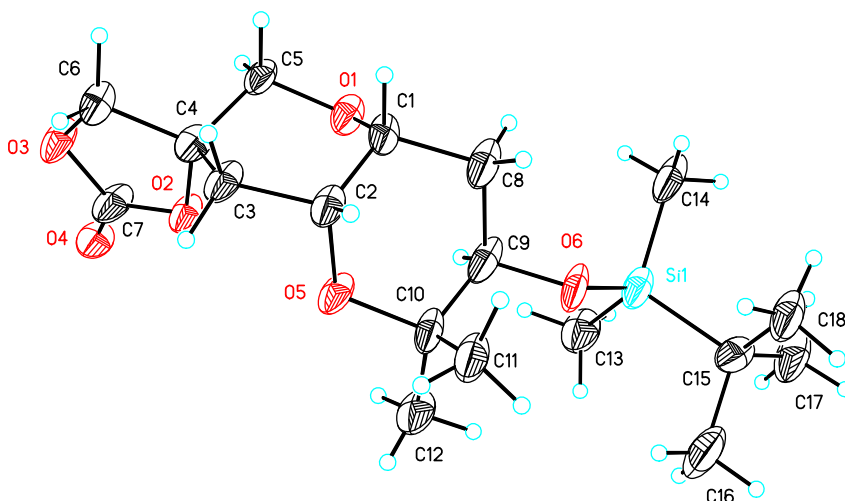
^1H NMR (400 MHz, CDCl_3): δ 4.03 (dd, $J=12.8, 3.2$ Hz, 1H), 3.92 (d, $J=2.0$ Hz, 2H), 3.75 (dd, $J=11.4, 5.0$ Hz, 1H), 3.66 (t, $J=2.0$ Hz, 1H), 3.43 (m 1H), 3.29 (d, $J=12.8$ Hz, 1H), 2.23 (dt, $J=15.4, 2.8$ Hz, 1H), 1.89 (m, 1H), 1.75 (dd, $J=15.2, 4.0$ Hz, 1H), 1.66 (ddd, $J=14.0, 12, 3.6$ Hz, 1H), 1.21 (s, 3H), 1.05 (s, 3H), 0.81 (s, 9H), 0.00 (d, $J=4.4$ Hz, 6H).

^{13}C NMR (100 MHz, CDCl_3): δ 154.5, 77.8, 76.3, 74.5, 72.7, 71.0, 69.3, 63.4, 37.2, 34.5, 28.3, 25.9, 18.0, 15.7, -3.8, -4.7.

HRMS (FAB⁺) Calcd for $\text{C}_{18}\text{H}_{33}\text{O}_6\text{Si}$ [(M+H⁺)] 373.2041, found 373.2034.

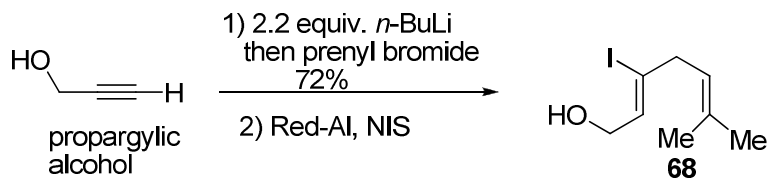
For 2-D spectra (H-H COSY, H-H NOESY and NOE) of compound 56, see page 294-296.

X-Ray analysis: The structure of compounds **56** was established by X-ray analysis. The thermal ellipsoid diagrams and data for compound **56** are provided below:



For X-ray data of compound 56, see page 320-329.

Alkylation and reductive iodination to vinyl iodide 68³⁸

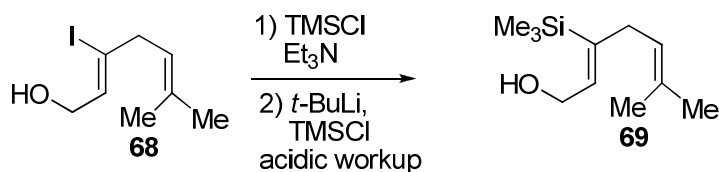


To a solution of sodium bis(2-methoxyethoxy)aluminum hydride (Red-Al, 65% in toluene, 7.7 mL, 25.2 mmol) in diethyl ether (10 mL) was added propargylic alcohol (1.88 g, 16.8 mmol) at 0 °C slowly over 30 minutes. After the addition was complete, the reaction mixture was stirred for 10 minutes at 0 °C and then the

water-ice cooling bath was removed. The reaction was allowed to warm up to room temperature and stirred overnight. The reaction was cooled to $-78\text{ }^{\circ}\text{C}$ with dry ice-acetone bath for 10 minutes. *N*-iodosuccinimide (NIS, 6.43 g, 28.6 mmol) in diethyl ether (10 mL) was added slowly to the reaction mixture. The reaction was allowed to warm up to room temperature and stirred for another 2-3 hours. Saturated Rochelle's salt was used to quench the reaction that was stirred for 1 or 2 hours, resulting in a clear solution. The organic layer was separated and aqueous layer was extracted with diethyl ether (50 mL x 2). The combined organic layers were washed with brine (50 mL), dried with MgSO_4 and evaporated. The resulting crude product was purified by column chromatography on silica gel to give vinyl iodide **68** (1.3 g, 31%).

$^1\text{H NMR}$ (400 MHz, CDCl_3): δ 5.84 (m, 1H), 5.13 (m, 1H), 4.17 (d, $J = 5.6$ Hz, 2H), 3.24 (d, $J = 6.8$ Hz, 2H), 2.02 (s, OH), 1.71 (s, 3H), 1.61 (s, 3H).

Silylation and O-C Silyl migration to vinyl silane **69**³⁹



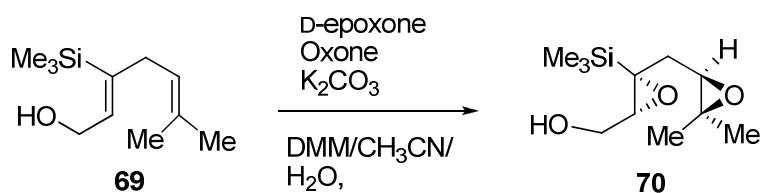
allylic alcohol **68** (1.26 g, 5.04 mmol) was silylated with trimethylsilyl chloride (1.28 mL, 10.1 mmol) in THF (10 mL) in the presence of triethylamine (1.4 mL, 10.1 mmol) at $0\text{ }^{\circ}\text{C}$. After aqueous workup (sat. NaHCO_3), the crude product was used for the O-C silyl migration reaction. Another round bottomed flask was charged with a stir bar and THF (30 mL), then cooled to $-78\text{ }^{\circ}\text{C}$. *tert*-Butyllithium (1.7 M in pentane, 6.4 mL, 11.0 mmol) was added to the THF solution slowly.

Silyl ether (1.62 g, 5.0 mmol) obtained above was added slowly as a THF (5 mL) solution. After stirred for 30 minutes at -78 °C, trimethylsilyl chloride (1.26 mL, 10.0 mmol) was added and the resulting reaction mixture was warmed up to room temperature slowly and stirred for another 1 hour at room temperature. Saturated NH₄Cl (20 mL) was added to quench the reaction. The organic layer was separated and aqueous layer was extracted with diethyl ether (30 mL x 2). The combined organic layers were washed with brine (50 mL), dried with MgSO₄ and evaporated. The resulting crude product was purified by column chromatography on silica gel to give vinyl iodide **69** (940 mg, 64% for 2 steps).

¹H NMR (600 MHz, CDCl₃): δ 5.97 (m, 1H), 4.90 (m, 1H), 4.05 (d, *J* = 7.2 Hz, 2H), 2.63 (d, *J* = 6.6 Hz, 2H), 1.56 (s, 3H), 1.45 (s, 3H), 0.00 (s, 9H).

¹³C NMR (100 MHz, CDCl₃): δ 143.5, 140.2, 132.6, 123.3, 62.3, 36.4, 25.9, 18.0, 0.39 (3C).

Double Shi epoxidation of epoxy alkene 46



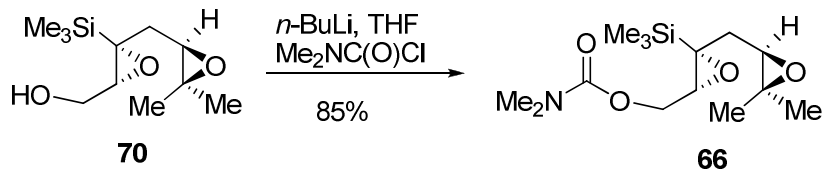
Following the Shi epoxidation conditions described for triepoxide **47**, dienylic alcohol **69** (94 mg, 0.5 mmol) was epoxidized to **70** (66 mg, 60%) with 4:1 diastereoselectivity based on the H NMR. Dienylic alcohol **69** (94 mg, 0.5 mmol) was dissolved in a 1 : 2 mixture of acetonitrile : dimethoxymethane (10 mL). Under vigorous agitation, a 0.05 M solution of Na₂B₄O₇ in 4 x 10⁻⁴ M Na₂(EDTA)

(6 mL), Bu₄NHSO₄ (10 mg, 0.29 μmol) and 1,2:4,5-di-*O*-isopropylidene-*D*-erythro-2,3-hexodiuro-2,6-pyranose (Shi catalyst, *D*-epoxone, 77.4 mg, 0.30 mmol), were sequentially added. The mixture was cooled to 0 °C, and then oxone (920 mg, 24.0 mmol), dissolved in 4 × 10⁻⁴ M Na₂(EDTA) (3.4 mL), and K₂CO₃ (7.20 g, 52.0 mmol), dissolved in water (3.4 mL), were simultaneously added to the mixture over 3 hrs. Once the addition was completed, the mixture was stirred for another hour, diluted with water and extracted with ethyl ether. The organic extracts were dried over anhydrous Na₂SO₄, and the solvent was removed by rotary evaporation. Purification by column chromatography on silica gel yielded diepoxy alcohol **70** (66 mg, 60%) as a colorless oil.

¹H NMR (600 MHz, CDCl₃): δ 3.70 (m, 1H), 3.47 (m, 1H), 2.94 (dd, *J* = 7.2, 3.6 Hz, 1H), 2.61 (dd, *J* = 7.2, 5.4 Hz, 1H), 2.29 (s, OH), 1.91 (dd, *J* = 15.0, 4.8 Hz, 1H), 1.34 (dd, *J* = 15.0, 7.2 Hz, 1H), 1.16 (s, 3H), 1.08 (s, 3H), 0.02 (s, 9H).

¹³C NMR (150 MHz, CDCl₃): δ 64.1, 62.8, 60.9, 58.7, 55.7, 36.1, 24.8, 18.9, -1.22 (3C).

Carbamate formation from diepoxy alcohol 70

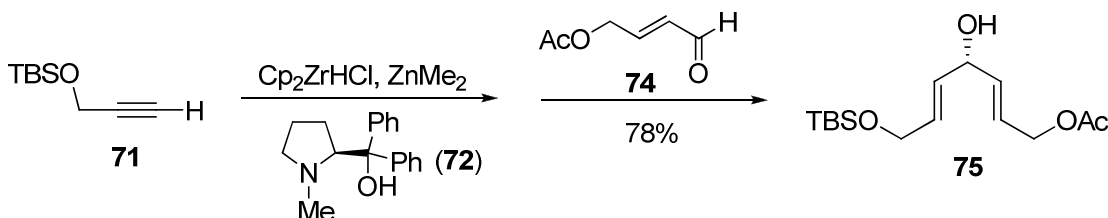


The diepoxy carbamate **66** was then prepared by following the carbamate formation as described for carbamates **41** and **48**, with diepoxy alcohol **70** (220 mg, 1.0 mmol) in THF (10 mL), $n\text{-BuLi}$ (2.5 M in hexane, 0.6 mL, 1.5 mmol), and dimethyl chlorocarbamate (321 mg, 3.0 mmol). Yield: 230 mg (79%) as colorless oil.

^1H NMR (400 MHz, CDCl_3): δ 4.17 (dd, $J = 11.6, 3.6$ Hz, 1H), 3.86 (dd, $J = 12.0, 7.6$ Hz, 1H), 2.99 (dd, $J = 7.6, 4.0$ Hz, 1H), 2.98 (s, 3H), 2.88 (s, 3H), 2.58 (dd, $J = 6.4, 5.6$ Hz, 1H), 1.81 (dd, $J = 14.4, 5.2$ Hz, 1H), 1.43 (dd, $J = 14.8, 6.8$ Hz, 1H), 1.13 (s, 3H), 1.05 (s, 3H), 0.01 (s, 9H).

^{13}C NMR (100 MHz, CDCl_3): δ 156.3, 65.3, 61.1, 60.7, 58.4, 55.0, 36.6, 36.1, 35.8, 24.8, 18.8, -1.43 (3C).

Hydrozirconation, transmetalation and addition to aldehyde 74^{41b}



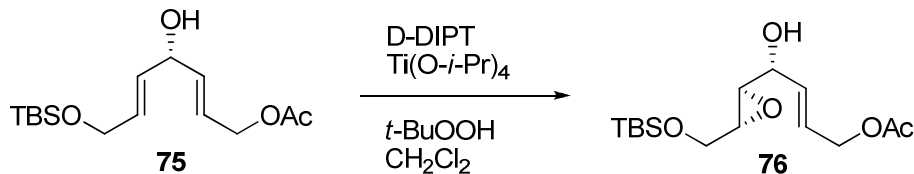
A solution of alkyne **71** (3.0 g, 17.6 mmol) in 150 mL CH_2Cl_2 (water: 2.1 ppm) was kept under argon atmosphere and treated with zirconocene hydrochloride (Cp_2ZrHCl , freshly prepared from reduction of Cp_2ZrCl_2 with lithium aluminum

hydride, 8.82 g, 35.3 mmol). The mixture was stirred at room temperature until homogenous solution was formed (about 10 to 20 minutes) and cooled to -65 °C with dry ice-acetone bath. Dimethylzinc (1.0 M in toluene, 30 mL, 30.0 mmol) was added over 30 minutes at -65 °C. After addition was complete, the reaction mixture was stirred for 40 minutes. Chiral amino alcohol **72** (470 mg, 1.76 mmol) was added as a CH₂Cl₂ (5 mL) solution. The resulting solution was warmed up to -30 °C over 30 minutes and aldehyde **74** (2.12 g, 17.6 mmol) dissolved in CH₂Cl₂ (5 mL) was added dropwise. After addition was complete, the reaction mixture was allowed to warm up to room temperature slowly and stirred overnight. Saturated NH₄Cl (80 mL) was added slowly at the beginnings to quench the reaction. The organic layer was separated and aqueous layer was extracted with diethyl ether (80 mL x 2). The combined organic layers were washed with brine (100 mL), dried with MgSO₄ and evaporated. The resulting crude product was purified by column chromatography on silica gel to give bis-allylic alcohol **75** (4.07 g, 77%) as colorless oil.

¹H NMR (600 MHz, CDCl₃): δ 5.74 (t, *J* = 17.4, 2.4 Hz, 2H), 5.73 (dt, *J* = 17.4, 4.2 Hz, 1H), 5.67 (ddt, *J* = 15.6, 9.6, 6.0, 1.2 Hz, 1H), 4.61 (m, 1H), 4.51 (d, *J* = 3.6 Hz, 2H), 4.12 (d, *J* = 4.2 Hz, 2H), 2.00 (s, 3H), 1.70 (d, *J* = 4.2 Hz, 1H), 0.84 (s, 9H), 0.00 (s, 6H).

¹³C NMR (150 MHz, CDCl₃): δ 170.9, 135.6, 131.5, 130.6, 125.1, 72.3, 64.4, 63.2, 26.1 (3C), 21.1, 18.6, -5.0 (2C).

Sharpless asymmetric epoxidation of bis-allylic alcohol 75

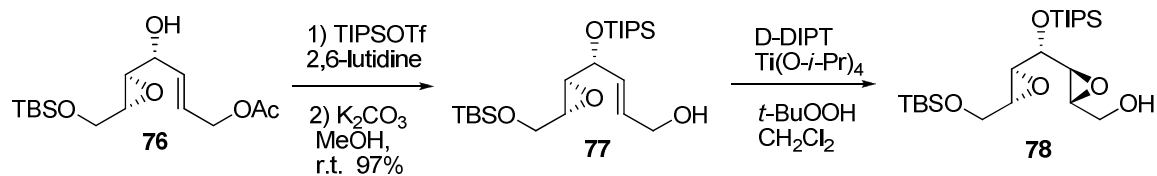


Following the conditions developed by Sharpless and described for compound **39**, from compound **75** (2.1 g, 7.00 mmol) in CH_2Cl_2 (5 mL), 4 Å molecular sieves (3.5 g) in CH_2Cl_2 (35 mL), D-(-)-diisopropyl tartrate (117 mg, 0.56 mmol), $\text{Ti}(\text{O-}i\text{-Pr})_4$ (138 mg, 0.47 mmol), and $t\text{-BuOOH}$ (5.0-6.0 M in decane, 2.8 mL, 14.0 mmol). Yield of **76**: 1.55 g (70%); colorless oil.

$^1\text{H NMR}$ (400 MHz, CDCl_3): δ 5.86 (m, 1H), 5.70 (m, 1H), 4.52 (d, $J = 5.6$ Hz, 2H), 4.30 (t, $J = 2.8$ Hz, 1H), 3.82 (dd, $J = 12.4, 3.2$ Hz, 1H), 3.63 (dd, $J = 12.4, 4.8$ Hz, 1H), 3.09 (ddd, $J = 4.4, 2.4$ Hz, 1H), 2.97 (dd, $J = 3.6, 2.4$ Hz, 1H), 2.42 (d, $J = 4.2$ Hz, 1H), 2.01 (s, 3H), 0.83 (s, 9H), 0.00 (d, $J = 3.2$ Hz, 6H).

$^{13}\text{C NMR}$ (100 MHz, CDCl_3): δ 170.9, 131.4, 127.3, 69.0, 64.2, 62.7, 57.3, 55.3, 26.0 (3C), 21.0, 18.5, -5.1, -5.2.

Preparation of diepoxy alcohol 78



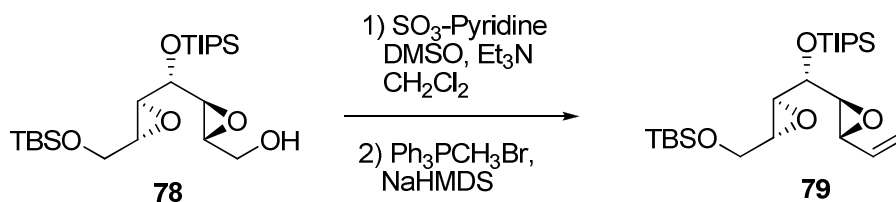
Allylic alcohol **76** (1.10g, 3.48 mmol) was silylated with triisopropylsilyl triflate (TIPSOTf, 1.07g, 3.48 mmol) in the presence 2,6-lutidine (0.8 mL, 6.9 mmol) in 12 mL CH_2Cl_2 at 0 °C for 30 minutes. Quenching the reaction with sat. NH_4Cl (20

mL). The organic layer was separated and aqueous layer was extracted with diethyl ether (80 mL x 2). The combined organic layers were washed with brine (100 mL), dried with MgSO₄ and evaporated. The residue was subjected to deacetylation with potassium carbonate (50 mg, 0.36 mmol) in dry methanol (20 mL) at room temperature for 30 minutes. The resulting allylic alcohol **77** (1.45 g, 3.38 mmol, 97% for 2 steps) was epoxidized using typical Sharpless asymmetric epoxidation conditions to give diepoxy alcohol **78** (1.36 g, 90%). CH₂Cl₂ (20 mL), 4 Å molecular sieves (2.0 g) in CH₂Cl₂ (35 mL), D-(-)-diisopropyl tartrate (117 mg, 0.56 mmol), Ti(O-*i*-Pr)₄ (138 mg, 0.47 mmol), and *tert*-BuOOH (5.0-6.0 M in decane, 1.35 mL, 6.76 mmol).

¹H NMR (400 MHz, CDCl₃): δ 4.05 (dd, *J* = 14.4, 7.6 Hz, 1H), 3.88 (m, 1H), 3.80 (dd, *J* = 12.0, 2.8 Hz, 1H), 3.59 (dd, *J* = 12.0, 4.8 Hz, 2H), 3.38 (t, *J* = 6.0 Hz, 1H), 3.08 (m, 2H), 2.97 (ddd, *J* = 4.8, 2.0 Hz, 1H), 2.90 (dd, *J* = 6.0, 2.4 Hz, 1H), 1.01 (m, 21H), 0.83 (s, 9H), 0.00 (d, *J* = 3.2 Hz, 6H).

¹³C NMR (100 MHz, CDCl₃): δ 73.6, 63.0, 61.4, 57.8, 57.6, 55.9, 55.8, 26.1 (3C), 18.5, 18.1 (3C), 18.1 (6C), 14.4, 12.5 (2C), -5.17, -5.22.

Parikh-Doering oxidation and Wittig methylenation to vinyl diepoxy **79**



Parikh-Doering oxidation of **78:** To a mixture of epoxy alcohol **78** (950 mg, 2.14 mmol), dry dimethylsulfoxide (DMSO, 1.75 mL, 24.7 mmol) and

triethylamine (Et₃N, 1.32 mL, 9.50 mmol) in dichloromethane (8 mL) at 0 °C was added sulfur trioxide-pyridine complex (SO₃-Pyr., 1.06 g, 6.67 mmol) in four portions. After 3.5 hours, the reaction mixture was diluted with ether (20 mL) and quenched with saturated NH₄Cl (20 mL). The organic layer was separated and aqueous layer was extracted with diethyl ether (20 mL x 2). The combined organic layers were washed with brine (50 mL), dried with MgSO₄ and evaporated to give epoxy aldehyde.

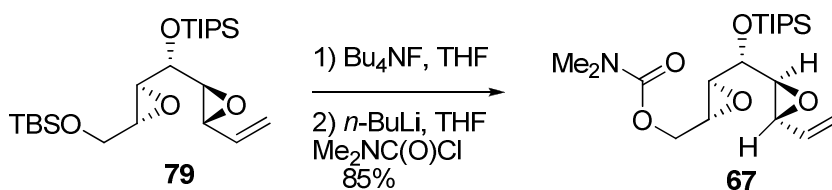
Wittig methylenation of epoxy aldehyde: In another flask was charged with methyltriphenylphosphonium bromide (Ph₃PCH₃Br, 1.14 g, 3.2 mmol) and THF (3 mL) and cooled to 0 °C. Sodium bis(trimethylsilyl)amide (NaHMDS, 1.0 M in THF, 3.0 mL, 3.0 mmol) was added to this cooled solution, which was then stirred for 30 minutes at 0 °C to form a Wittig reagent solution. The epoxy aldehyde obtained from the Parikh-Doering oxidation was added to this Wittig reagent solution. The reaction mixture was stirred for 40 minutes at 0 °C. The reaction mixture was diluted with ether (20 mL) and quenched with saturated NH₄Cl (20 mL). The organic layer was separated and aqueous layer was extracted with diethyl ether (20 mL x 2). The combined organic layers were washed with brine (50 mL), dried with MgSO₄ and evaporated. The residue was purified by column chromatography on silica gel to afford diepoxy alkene **79** (820 mg, 87% for 2 steps).

¹H NMR (400 MHz, CDCl₃): δ 5.49 (m, 2H), 5.23 (dd, *J* = 10.0, 1.6 Hz, 1H), 3.79 (dd, *J* = 12.0, 3.2 Hz, 1H), 3.61 (dd, *J* = 12.0, 3.2 Hz, 1H), 3.43 (t, *J* = 5.6 Hz, 1H),

3.27 (dd, $J = 7.6, 2.4$ Hz, 1H), 3.03 (ddd, $J = 4.4, 2.8$ Hz, 1H), 2.97 (dd, $J = 6.4, 2.0$ Hz, 1H), 2.91 (dd, $J = 5.2, 2.0$ Hz, 1H), 1.01 (m, 21H), 0.83 (s, 9H), 0.00 (d, $J = 3.2$ Hz, 6H).

^{13}C NMR (100 MHz, CDCl_3): δ 134.9, 120.1, 73.4, 63.1, 62.1, 57.2, 56.1, 55.9, 26.1 (3C), 18.6, 18.2 (9C), 12.6, -5.1 (2C).

Selective desilylation and carbamate formation from diepoxy alcohol 79



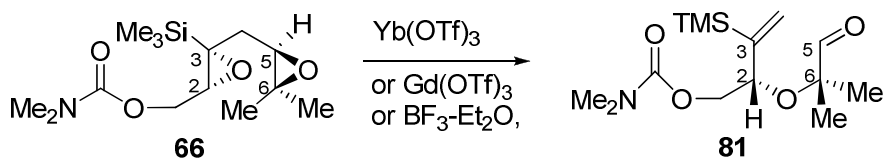
Selective removal of *tert*-butyldimethylsilyl of **79** was achieved by treatment of THF (30 mL) solution of **79** (250 mg, 0.566 mmol) with hydrofluoride-pyridine complex (HF-pyr., 9 mL of HF-pyridine stock solution, prepared by 2.0 g of Aldrich pyridiniumhydrofluoride, 4 mL of pyridine and 16 mL of THF) in a Nalgene container at room temperature. The reaction mixture was stirred for 1-2 hours and saturated NaHCO_3 (20 mL) was added dropwise to quench the reaction. The organic layer was separated and aqueous layer was extracted with diethyl ether (20 mL x 2). The combined organic layers were washed with brine (50 mL), dried with MgSO_4 and evaporated. The residue (137 mg, 75%) was dried under vacuum overnight and used for the carbamate formation without further purification. The diepoxy carbamate **67** was then prepared by following the carbamate formation as described for carbamates **41**, **48** and **66**.

IR (neat, cm^{-1}): 2943, 2866, 1710, 1462, 1399, 1187, 1149, 1061, 883.

^1H NMR (400 MHz, CDCl_3): δ 5.57 (m, 2H), 5.31 (dd, $J = 10.0, 2.0$ Hz, 1H), 4.40 (dd, $J = 12.4, 3.2$ Hz, 1H), 3.98 (dd, $J = 12.0, 6.4$ Hz, 1H), 3.49 (t, $J = 5.6$ Hz, 1H), 3.34 (dd, $J = 7.2, 2.0$ Hz, 1H), 3.24 (m, 1H), 3.04 (dd, $J = 6.0, 2.4$ Hz, 1H), 2.98 (dd, $J = 5.6, 2.0$ Hz, 1H), 2.93 (s, 6H), 1.08 (m, 21H).

^{13}C NMR (100 MHz, CDCl_3): δ 134.8, 120.3, 73.3, 65.2, 62.0, 56.4, 56.1, 54.5, 41.8, 36.8, 18.2 (6C), 12.6 (3C).

Lewis acid-promoted fragmentation of diepoxysilyl carbamate **66**

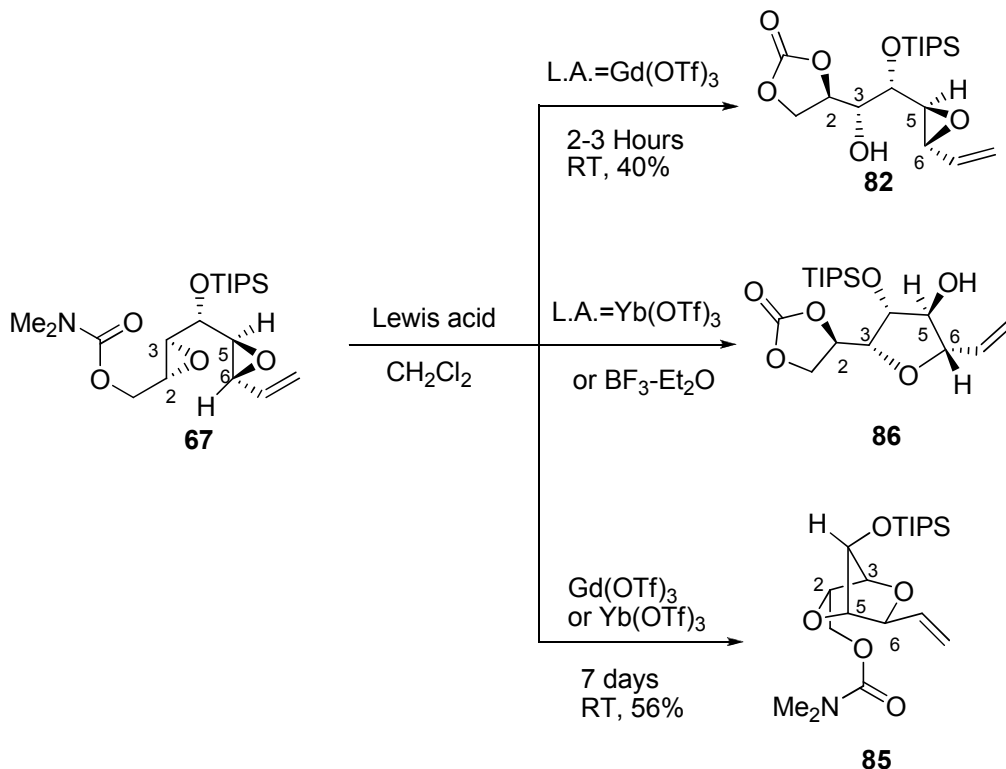


Procedure A: Following conditions generally utilized in our laboratory for the endo-selective cascade oxacyclization of polyepoxides, diepoxide **66** (50 mg, 0.172 mmol) was dissolved in dry CH_2Cl_2 (5 mL) and cooled to -40 °C. $\text{BF}_3\text{-Et}_2\text{O}$ (0.2 M in CH_2Cl_2 , 1.0 mL, 0.2 mmol) was subsequently added dropwise over 5 minutes. After stirred for 30 minutes at -40 °C, the reaction mixture was quenched with sat. NaHCO_3 (3 mL) and stirred overnight at room temperature. The organic layer was separated. Aqueous layer was extracted with CH_2Cl_2 (10 mL x 2). The combined organic layers were washed with brine (20 mL), dried with MgSO_4 and evaporated. The resulting crude product was purified by column chromatography on silica gel to give aldehyde **81** (27.5 mg, 65 %) as a colorless oil.

^1H NMR(400 M Hz, CDCl_3): δ 9.43 (s, 1H), 5.81 (d, $J=2.4$ Hz, 1H), 5.39 (d, $J=2.8$ Hz, 1H), 4.09 (dd, $J=8.4, 3.2$ Hz, 1H), 3.88 (dd, $J=11.6, 3.2$ Hz, 1H), 3.69 (dd, $J=12.0, 8.8$ Hz, 1H), 2.76 (s, 6H), 1.08 (s, 3H), 1.06 (s, 3H).

Procedure B: Diepoxide **66** (50 mg, 0.172 mmol) was dissolved in dry CH_2Cl_2 (5 mL). $\text{Yb}(\text{OTf})_3$ (320mg, 0.516 mmol) or $\text{Gd}(\text{OTf})_3$ (312 mg, 0.512 mmol) was subsequently added at room temperature and stirred for 2-4 hours at room temperature. After completion, the reaction mixture was quenched with sat. NaHCO_3 (3 mL) and stirred overnight at room temperature. Workup as procedure A, column chromatography on silica gel gave aldehyde **81** (32.5 mg, 65%) as a colorless oil. Treatment of diepoxide **66** with TMSOTf resulted in unidentified complex mixtures.

Lewis acid-promoted oxacyclization of diepoxy carbamate 67



Procedure A: Following conditions generally utilized in our laboratory for the endo-selective cascade oxacyclization of polyepoxides, diepoxide **67** (30 mg, 75 μmmol) was dissolved in dry CH_2Cl_2 (5 mL) and cooled to $-40\text{ }^\circ\text{C}$. $\text{BF}_3\text{-Et}_2\text{O}$ (0.53 M in CH_2Cl_2 , 0.15 mL, 80 μmol) was subsequently added dropwise over 5 minutes. After stirred for 30 minutes at $-40\text{ }^\circ\text{C}$, the reaction mixture was quenched with sat. NaHCO_3 (3 mL) and stirred overnight at room temperature. The organic layer was separated. Aqueous layer was extracted with CH_2Cl_2 (10 mL x 2). The combined organic layers were washed with brine (20 mL), dried with MgSO_4 and evaporated. The resulting crude product was purified by column chromatography on silica gel to give aldehyde **86** (13.5 mg, 45 %) as a colorless oil.

Procedure B: Diepoxide **67** (30 mg, 75 μ mol) was dissolved in dry CH_2Cl_2 (5 mL). $\text{Yb}(\text{OTf})_3$ (140 mg, 0.23 mmol) was subsequently added at room temperature and stirred for 2-4 hours at room temperature. After the starting material was completely consumed, the reaction mixture was quenched with sat. NaHCO_3 (3 mL) and stirred overnight at room temperature. Workup as procedure A, column chromatography on silica gel gave aldehyde **86** (18.0 mg, 60%) as a colorless oil.

Procedure C: Diepoxide **67** (40 mg, 0.10 mmol) was dissolved in dry CH_2Cl_2 (5 mL). $\text{Gd}(\text{OTf})_3$ (190 mg, 0.32 mmol) was subsequently added at room temperature and stirred for 2-4 hours at room temperature. The reaction mixture was quenched with sat. NaHCO_3 (3 mL) and stirred overnight at room temperature. Workup as procedure A, column chromatography on silica gel gave aldehyde **82** (16.0 mg, 40%) as a colorless oil.

Procedure D: Diepoxide **67** (40 mg, 0.1 mmol) was dissolved in dry CH_2Cl_2 (5 mL). $\text{Yb}(\text{OTf})_3$ (187 mg, 0.306 mmol) or $\text{Gd}(\text{OTf})_3$ (190 mg, 0.315 mmol) was subsequently added at room temperature and stirred for 7 days at room temperature. The reaction mixture was quenched with sat. NaHCO_3 (3 mL) and stirred overnight at room temperature. Workup as procedure A, column chromatography on silica gel gave aldehyde **85** (26.0 mg, 65%) as a colorless oil.

Data for compound 82

IR(neat, cm^{-1}): 3469, 3089, 2944, 2867, 1796, 1463, 1389, 1177, 1125, 1077, 883.

^1H NMR (600 MHz, CDCl_3): δ 5.53 (m, 2H), 5.33 (dd, J = 8.4, 3.0 Hz, 1H), 4.71 (q, J = 7.2, 4.8 Hz, 1H), 4.52 (dd, J = 7.8, 4.2 Hz, 2H), 3.91 (ddd, J = 6.6, 4.8, 4.2 Hz, 1H), 3.67 (dd, J = 7.2, 4.2 Hz, 1H), 3.35 (dd, J =6.6, 1.8 Hz, 1H), 3.03 (dd, J = 7.2, 2.4 Hz, 1H), 2.78 (d, J = 3.6 Hz, 1H), 1.20-1.02 (m, 21H).

^{13}C NMR (150 MHz, CDCl_3) δ 154.7, 134.3, 121.1, 75.0, 74.4, 73.8, 67.3, 59.9, 56.7, 18.2 (6C), 12.8 (3C).

for 2-D spectrum (H-H COSY) of compound 82, see page 271.

Data for compound 86

IR(neat, cm^{-1}): 3494, 3076, 2942, 2866, 1781, 1463, 1383, 1174, 1110, 1068, 881.

^1H NMR (600 MHz, CDCl_3): δ 5.98 (ddd, J = 17.2, 10.4, 7.6 Hz, 1H), 5.26 (dt, J = 16.8, 2.4 Hz, 1H), 5.16 (dt, J = 10.0, 1.6 Hz, 1H), 4.82 (ddd, J = 8.0, 6.0 Hz, 1H), 4.49 (m, 2H), 4.39 (d, J = 6.4 Hz, 1H), 4.32 (t, J = 1.6 Hz, 1H), 4.13 (d, J = 1.6 Hz, 1H), 4.12 (dd, J = 4.0, 1.2 Hz, 1H), 1.92 (d, J = 3.6 Hz, OH, 1H), 1.20-1.02 (m, 21H).

^{13}C NMR (150 MHz, CDCl_3) δ 154.8, 136.0, 117.4, 89.1, 86.8, 82.9, 80.3, 75.2, 67.6, 18.1 (6C), 12.1 (3C).

for 2-D spectrum (H-H COSY) of compound 86, see page 276.

Data for compound 85:

IR (neat, cm^{-1}): 3080, 2943, 2866, 1709, 1187, 1062.

^1H NMR (400 MHz, CDCl_3): δ 6.14 (m, 1H), 5.24 (d, J =17.2 Hz, 1H), 5.09 (d, J =10.4 Hz, 1H), 4.64 (m, 2H), 4.47 (s, 1H), 4.09 (s, 1H), 3.99 (dd, J =8.8, 7.2 Hz, 1H), 3.51 (dd, J =10.8, 10.0 Hz, 1H), 2.92 (s, 3H), 2.91 (s, 3H), 1.08 (m, 21H).

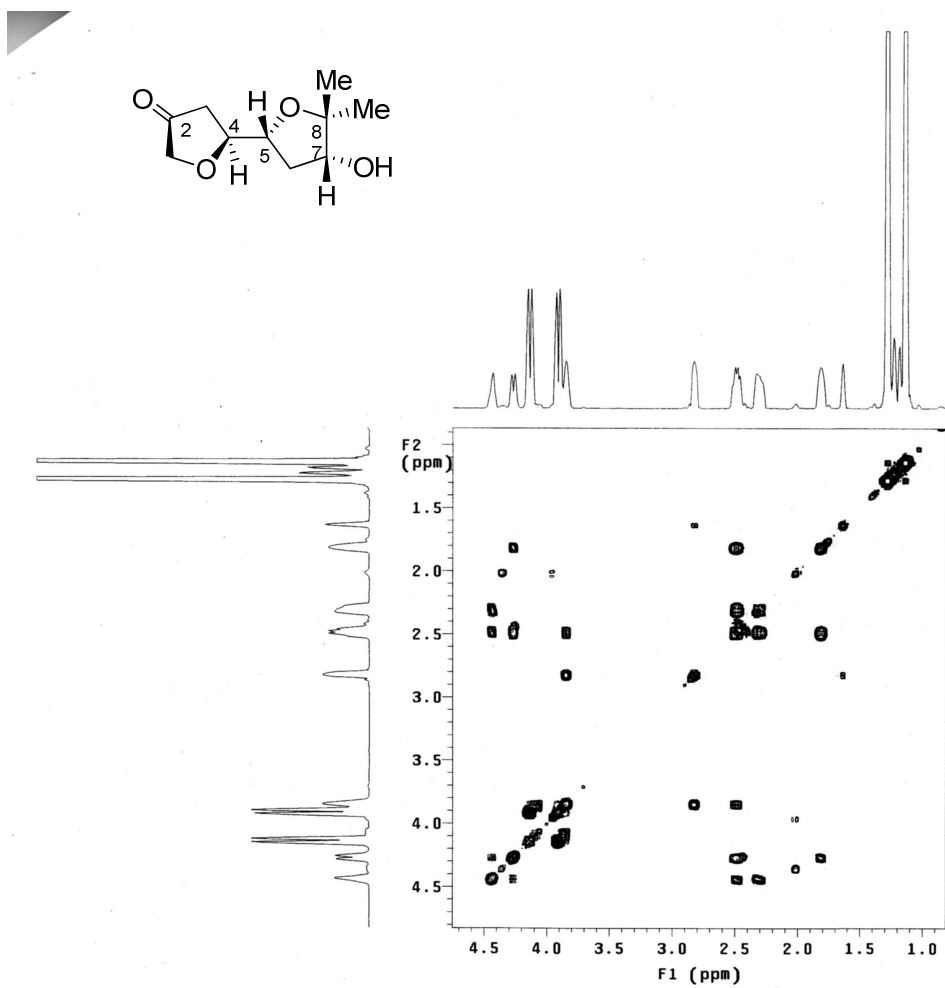
^{13}C NMR (100 MHz, CDCl_3) δ 155.7, 137.4, 116.8, 83.8, 83.4, 82.7, 76.1, 71.1, 62.2, 36.7, 36.3, 18.2, 12.1.

HRMS (FAB⁺) Calcd for $\text{C}_{20}\text{H}_{38}\text{O}_5\text{N}_1\text{Si}_1[(\text{M}+\text{H}^+)]$ 400.2514 found 400.2514.

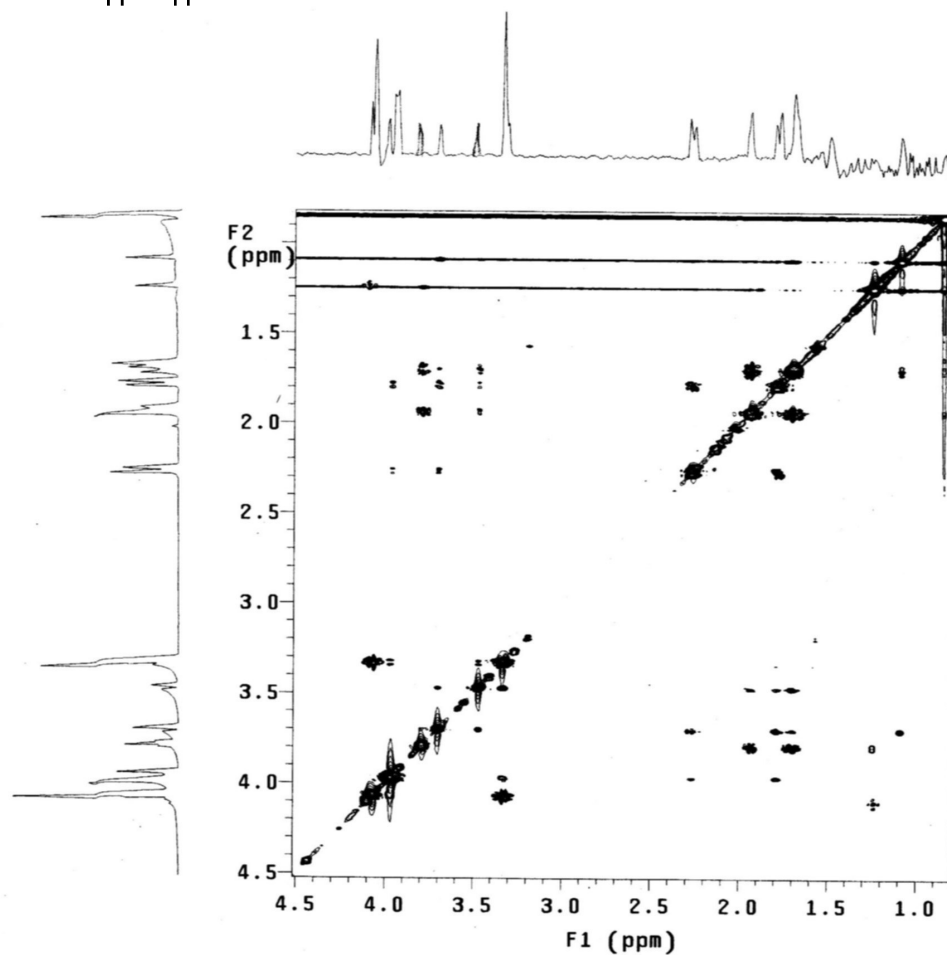
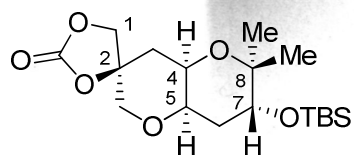
For NOE and 2-D NMR (H-H COSY and H-H NOESY, H-C HMQC) of compound 85, see page 272-275.

2-D NMR spectra (COSY, NOESY, HMQC, NOE)

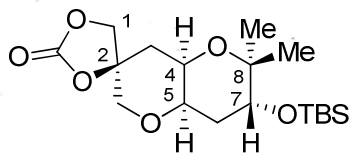
COSY spectra of compound 52-D



NOESY spectra of compound 56



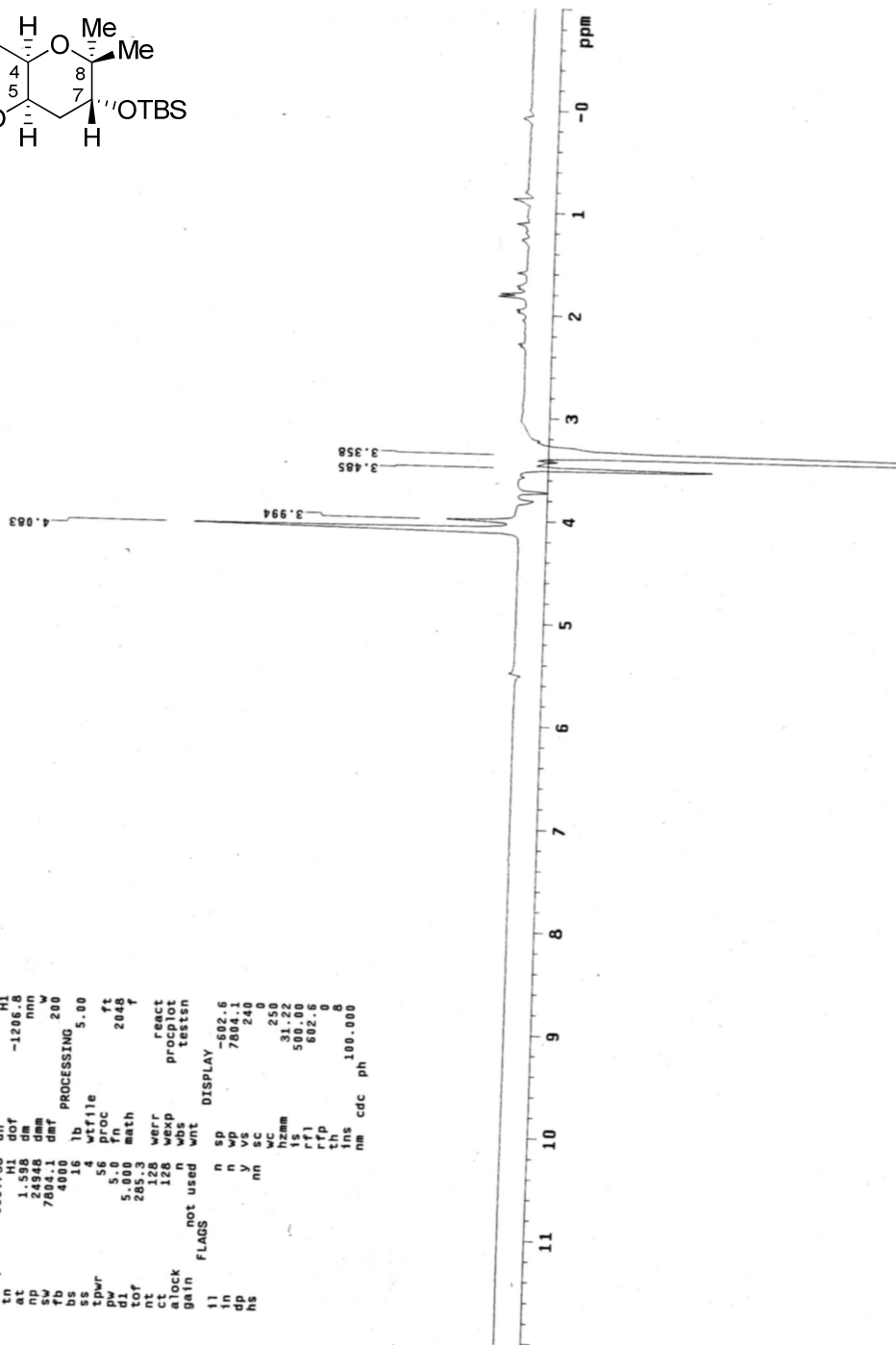
NOE spectra of compound 56



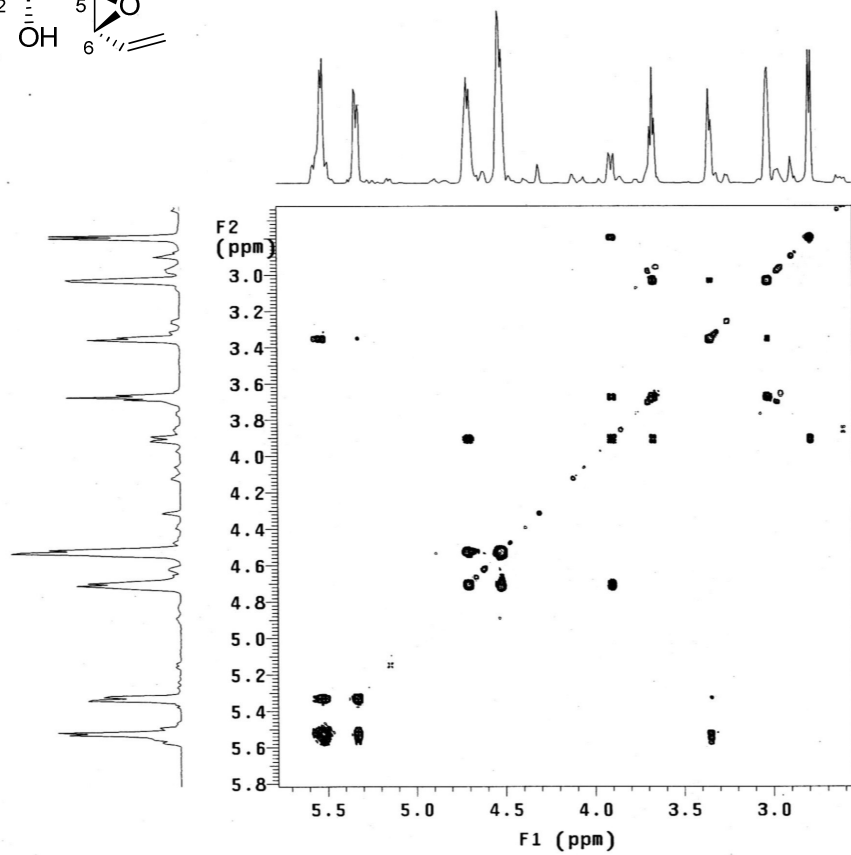
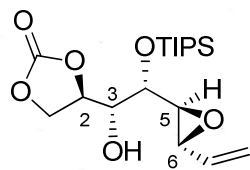
Standard Proton Parameters

```

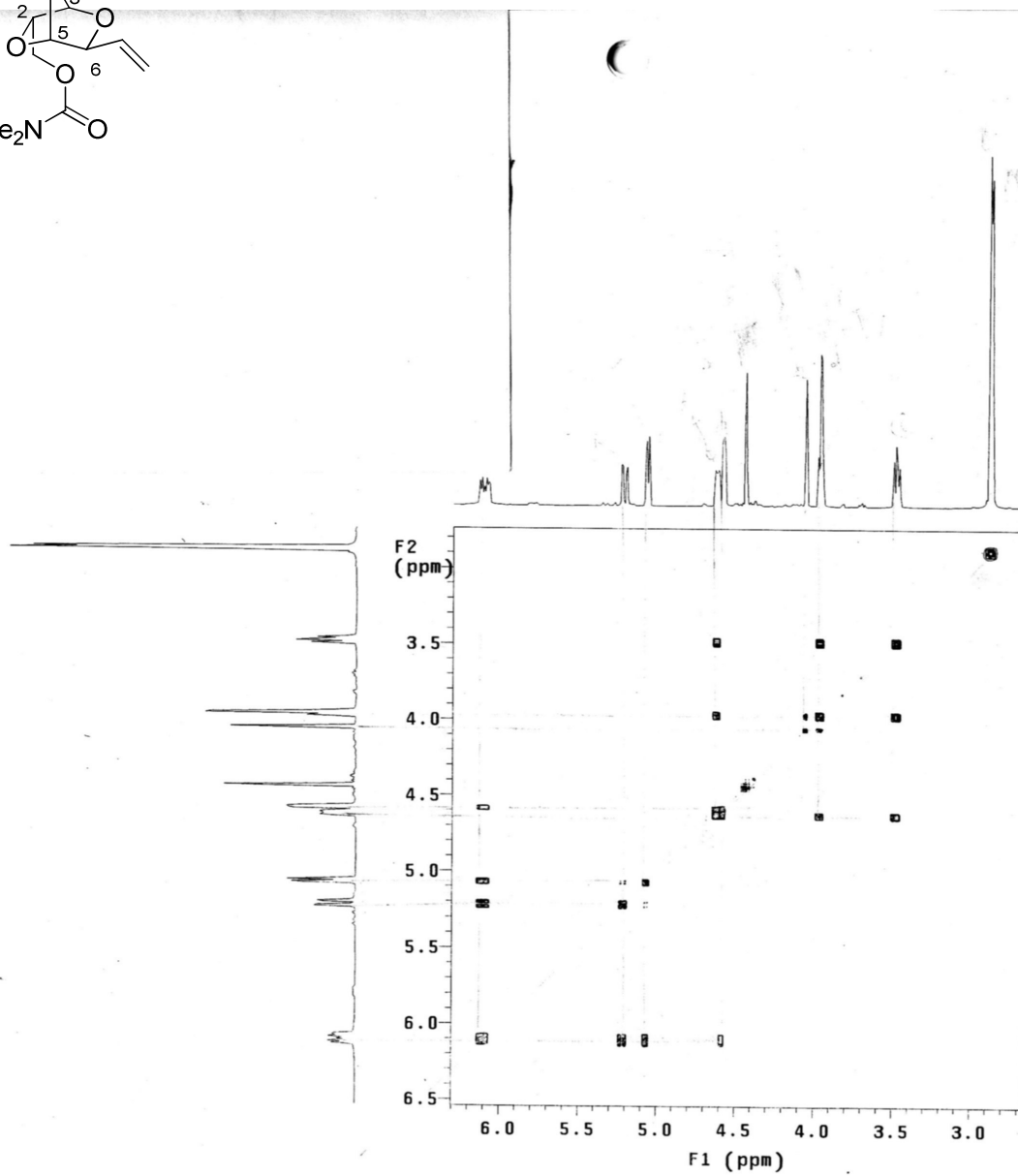
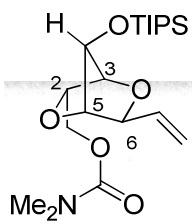
exp5 preset
SAMPLE SATURATION
date Oct 25 2005 sspul n
file cdc13 satpr 2
fileport/abw/- satfrq -993.4
nuser/mcdonag/- satfrq 2.000
ongbio/noe-cisfr- satcde ynn
cycle-1.fid composit n
ACQUISITION DEC. & VT
sfrq 599.738 dn H1
at 1.591 dof -1296.8
np 24948 dm nnn
sw 7804.1 dmf w
fz 4000 lb PROCESSING 5.00
ss 16 lb
tdwr 4 wfile
pw 5.0 proc ft
d1 5.000 math 2048
tor 285.3
ct 128 werr react
alock 128 wexp proplot
gain not used n wnt testen
FLAGS n SP -602.6
l1 n n wp 7804.1
n n y vs 240
hs nn sc 0
hzmm 31.250
ls 500.00
rfl 602.6
rff 0
th 0
nm cdc ph 100.000
  
```



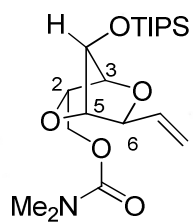
COSY spectra of compound 82



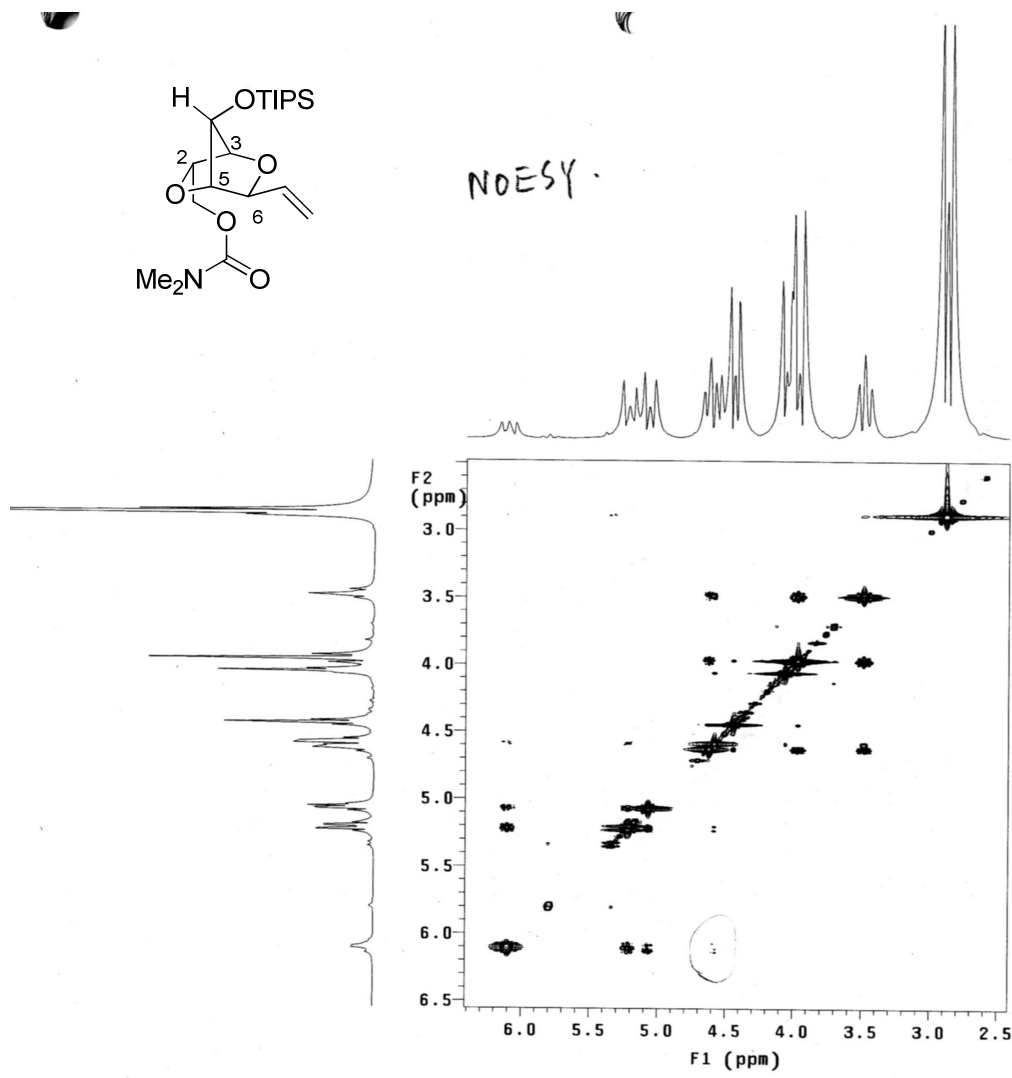
COSY spectra of compound 85



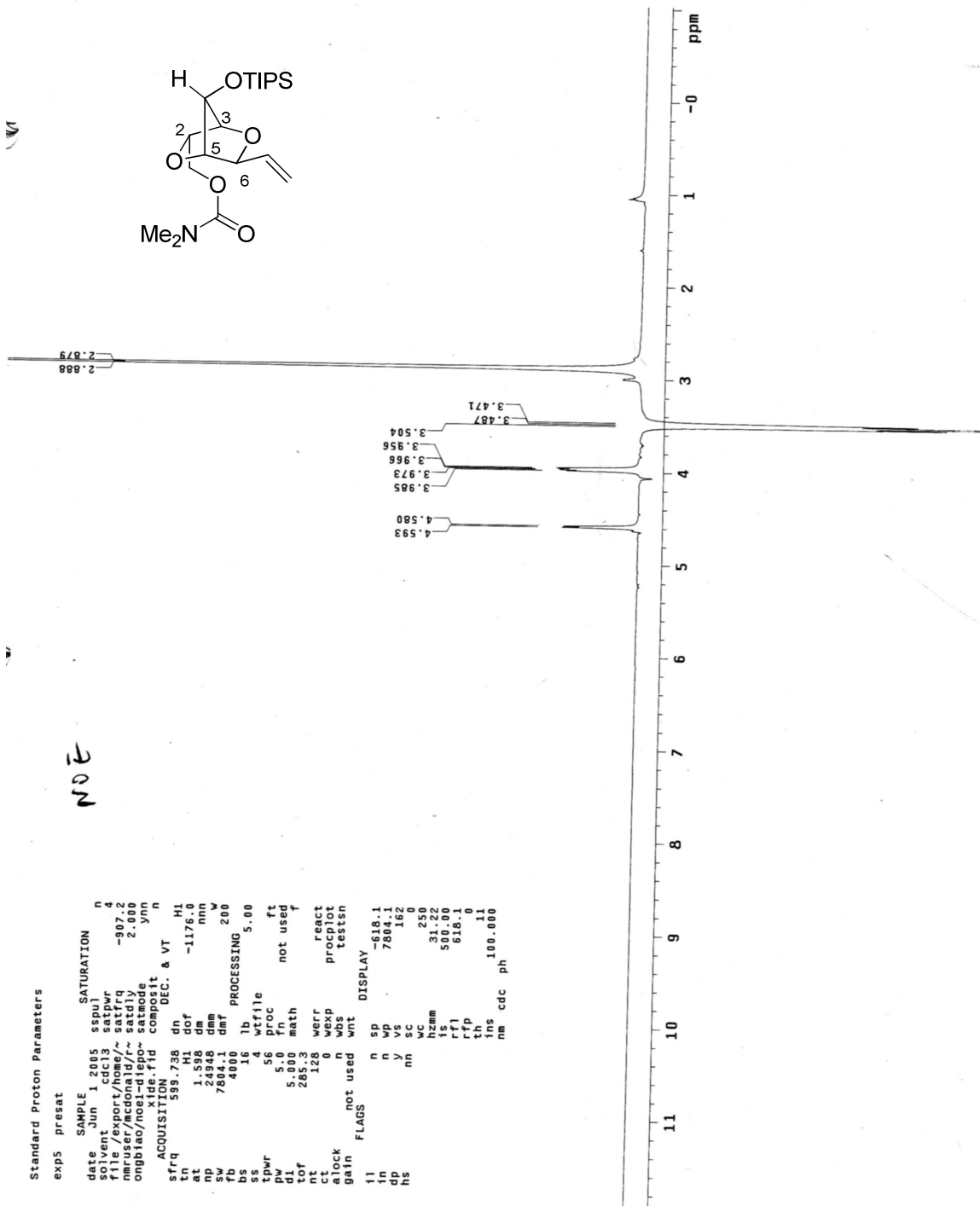
NOESY spectra of compound 85



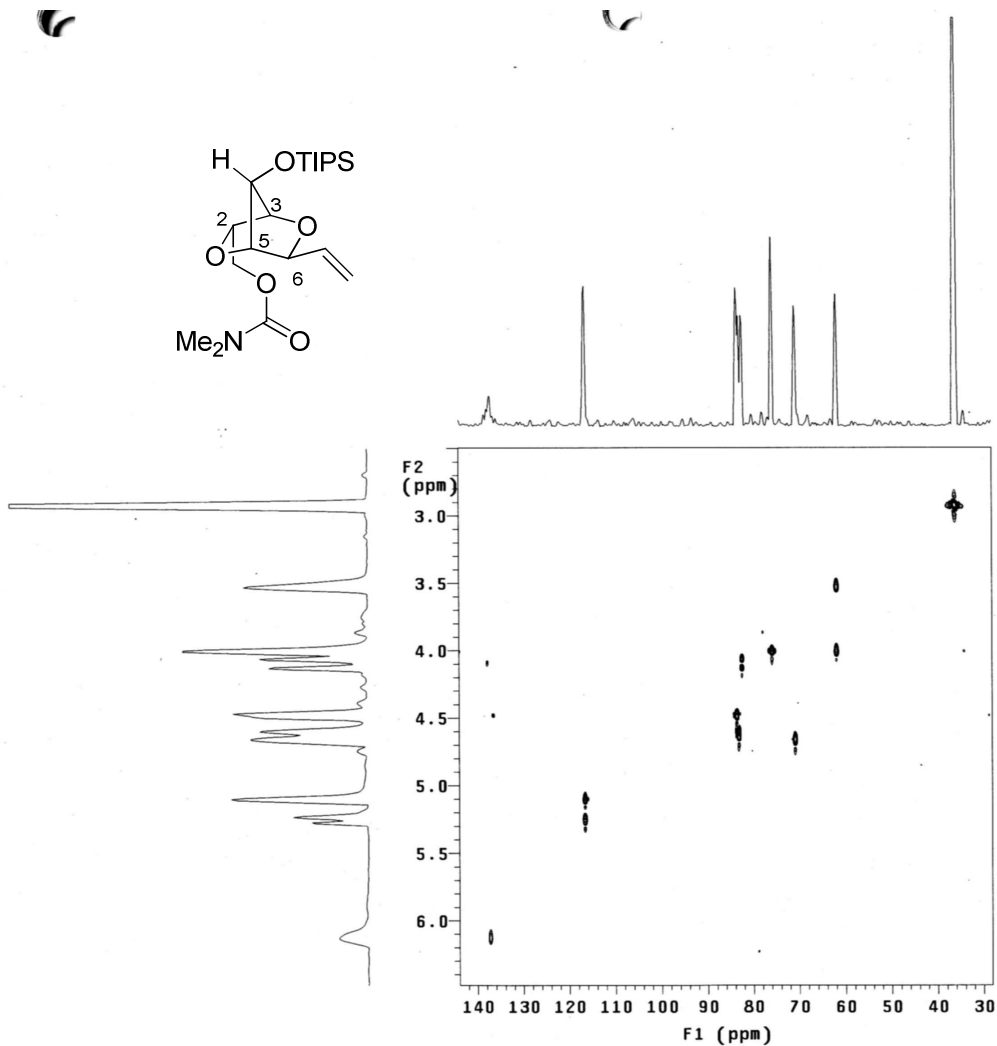
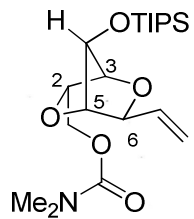
NOESY



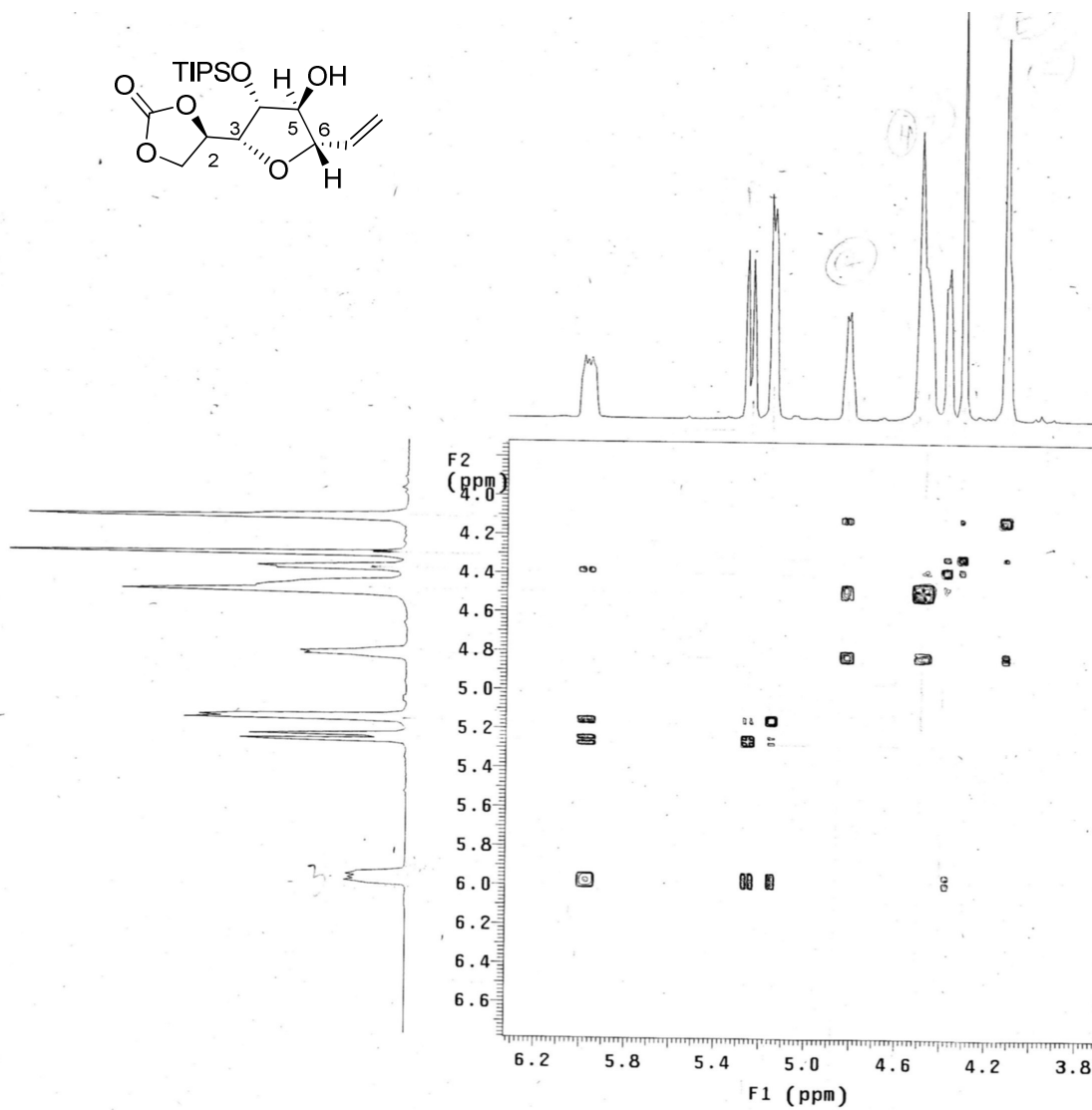
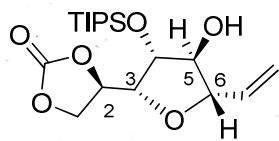
NOE spectra of compound 85



HMQC spectra of compound 85



COSY spectra of compound 86



X-Ray database in the biomimetic synthesis of fused polypyrrans

X-Ray data of compound 51

Table 1. Crystal data and structure refinement for **51**.

Identification code	T101	
Empirical formula	C ₉ H ₁₄ O ₅	
Formula weight	202.20	
Temperature	173(2) K	
Wavelength	1.54178 Å	
Crystal system	Orthorhombic	
Space group	P2(1)2(1)2(1)	
Unit cell dimensions	a = 6.1075(1) Å	α = 90°.
	b = 7.7931(2) Å	β = 90°.
	c = 19.7674(4) Å	γ = 90°.
Volume	940.86(3) Å ³	
Z	4	
Density (calculated)	1.427 Mg/m ³	
Absorption coefficient	0.994 mm ⁻¹	
F(000)	432	
Crystal size	0.50 x 0.20 x 0.10 mm ³	
Theta range for data collection	7.24 to 65.78°.	
Index ranges	-6<=h<=6, -9<=k<=8, -23<=l<=22	
Reflections collected	4082	
Independent reflections	1490 [R(int) = 0.0169]	
Completeness to theta = 65.78°	94.9 %	
Absorption correction	Semi-empirical from equivalents	
Max. and min. transmission	0.9071 and 0.6363	
Refinement method	Full-matrix least-squares on F ²	
Data / restraints / parameters	1490 / 0 / 184	
Goodness-of-fit on F ²	1.787	
Final R indices [I>2σ(I)]	R1 = 0.0254, wR2 = 0.0677	
R indices (all data)	R1 = 0.0260, wR2 = 0.0681	

Absolute structure parameter	0.13(17)
Extinction coefficient	0.0166(13)
Largest diff. peak and hole	0.147 and -0.174 e.Å ⁻³

Table 2. Atomic coordinates ($\times 10^4$) and equivalent isotropic displacement parameters ($\text{Å}^2 \times 10^3$) for **51**. $U(\text{eq})$ is defined as one third of the trace of the orthogonalized U^{ij} tensor.

	x	y	z	U(eq)
C(1)	2463(2)	2599(2)	6839(1)	23(1)
C(2)	4585(2)	1567(2)	6756(1)	24(1)
C(3)	5080(2)	1160(2)	6017(1)	25(1)
C(4)	3130(2)	281(2)	5698(1)	23(1)
C(5)	1073(2)	1338(2)	5803(1)	25(1)
C(6)	2854(3)	-1592(2)	5916(1)	26(1)
C(7)	2980(2)	-1461(2)	4760(1)	28(1)
C(8)	2607(3)	4400(2)	6550(1)	31(1)
C(9)	1791(3)	2644(2)	7576(1)	31(1)
O(1)	728(2)	1611(1)	6509(1)	25(1)
O(2)	6316(2)	2510(2)	7061(1)	33(1)
O(3)	3453(2)	131(1)	4969(1)	28(1)
O(4)	2561(2)	-2508(1)	5286(1)	32(1)
O(5)	2916(2)	-1907(2)	4184(1)	37(1)

Table 3. Bond lengths [\AA] and angles [$^\circ$] for **51**.

C(1)-O(1)	1.4633(16)	C(9)-C(1)-C(2)	110.15(11)
C(1)-C(9)	1.5143(18)	C(8)-C(1)-C(2)	113.32(11)
C(1)-C(8)	1.518(2)	O(2)-C(2)-C(3)	111.48(12)
C(1)-C(2)	1.534(2)	O(2)-C(2)-C(1)	108.17(11)
C(2)-O(2)	1.4213(18)	C(3)-C(2)-C(1)	112.30(11)
C(2)-C(3)	1.5245(19)	O(2)-C(2)-H(7)	110.5(9)
C(2)-H(7)	0.983(18)	C(3)-C(2)-H(7)	107.3(9)
C(3)-C(4)	1.512(2)	C(1)-C(2)-H(7)	107.0(10)
C(3)-H(8)	0.997(17)	C(4)-C(3)-C(2)	109.76(11)
C(3)-H(9)	0.965(18)	C(4)-C(3)-H(8)	108.1(9)
C(4)-O(3)	1.4581(15)	C(2)-C(3)-H(8)	111.8(8)
C(4)-C(5)	1.5162(19)	C(4)-C(3)-H(9)	111.8(10)
C(4)-C(6)	1.531(2)	C(2)-C(3)-H(9)	108.6(9)
C(5)-O(1)	1.4275(15)	H(8)-C(3)-H(9)	106.8(13)
C(5)-H(10)	0.985(17)	O(3)-C(4)-C(3)	109.99(11)
C(5)-H(11)	1.012(17)	O(3)-C(4)-C(5)	106.92(10)
C(6)-O(4)	1.4470(16)	C(3)-C(4)-C(5)	110.46(12)
C(6)-H(12)	0.946(18)	O(3)-C(4)-C(6)	102.50(11)
C(6)-H(13)	0.979(16)	C(3)-C(4)-C(6)	113.62(12)
C(7)-O(5)	1.1898(16)	C(5)-C(4)-C(6)	112.84(12)
C(7)-O(3)	1.3401(19)	O(1)-C(5)-C(4)	109.70(11)
C(7)-O(4)	1.3462(17)	O(1)-C(5)-H(10)	110.7(9)
C(8)-H(4)	0.951(19)	C(4)-C(5)-H(10)	108.9(9)
C(8)-H(5)	0.98(2)	O(1)-C(5)-H(11)	107.5(8)
C(8)-H(6)	0.976(18)	C(4)-C(5)-H(11)	108.7(10)
C(9)-H(1)	1.003(18)	H(10)-C(5)-H(11)	111.4(13)
C(9)-H(2)	1.02(2)	O(4)-C(6)-C(4)	103.98(10)
C(9)-H(3)	0.947(19)	O(4)-C(6)-H(12)	105.7(10)
O(2)-H(14)	0.82(2)	C(4)-C(6)-H(12)	111.1(11)
		O(4)-C(6)-H(13)	107.7(9)
O(1)-C(1)-C(9)	104.19(11)	C(4)-C(6)-H(13)	110.6(11)
O(1)-C(1)-C(8)	111.14(11)	H(12)-C(6)-H(13)	116.8(12)
C(9)-C(1)-C(8)	110.84(12)	O(5)-C(7)-O(3)	124.98(13)
O(1)-C(1)-C(2)	106.75(10)	O(5)-C(7)-O(4)	123.71(14)

O(3)-C(7)-O(4)	111.30(10)
C(1)-C(8)-H(4)	110.6(12)
C(1)-C(8)-H(5)	111.4(11)
H(4)-C(8)-H(5)	104.9(16)
C(1)-C(8)-H(6)	113.2(11)
H(4)-C(8)-H(6)	109.2(14)
H(5)-C(8)-H(6)	107.2(15)
C(1)-C(9)-H(1)	107.1(9)
C(1)-C(9)-H(2)	113.8(10)
H(1)-C(9)-H(2)	110.5(15)
C(1)-C(9)-H(3)	108.7(9)
H(1)-C(9)-H(3)	112.3(14)
H(2)-C(9)-H(3)	104.4(16)
C(5)-O(1)-C(1)	114.05(10)
C(2)-O(2)-H(14)	108.3(14)
C(7)-O(3)-C(4)	110.52(10)
C(7)-O(4)-C(6)	110.02(11)

Symmetry transformations used to
generate equivalent atoms:

Table 4. Anisotropic displacement parameters ($\text{\AA}^2 \times 10^3$) for **51**. The anisotropic displacement factor exponent takes the form: $-2\pi^2 [h^2 a^{*2} U^{11} + \dots + 2 h k a^* b^* U^{12}]$

	U11	U22	U33	U23	U13	U12
C(1)	21(1)	25(1)	24(1)	-3(1)	-1(1)	-2(1)
C(2)	21(1)	21(1)	28(1)	0(1)	-3(1)	-4(1)
C(3)	19(1)	24(1)	33(1)	-1(1)	4(1)	0(1)
C(4)	22(1)	26(1)	20(1)	-1(1)	3(1)	0(1)
C(5)	24(1)	32(1)	21(1)	-5(1)	-2(1)	4(1)
C(6)	30(1)	26(1)	23(1)	-4(1)	2(1)	-3(1)
C(7)	19(1)	35(1)	29(1)	-4(1)	2(1)	-2(1)
C(8)	38(1)	23(1)	33(1)	-1(1)	0(1)	5(1)
C(9)	30(1)	36(1)	26(1)	-4(1)	2(1)	-6(1)
O(1)	19(1)	33(1)	23(1)	-5(1)	0(1)	-1(1)
O(2)	20(1)	40(1)	41(1)	-12(1)	-4(1)	-3(1)
O(3)	35(1)	27(1)	22(1)	-2(1)	6(1)	-1(1)
O(4)	37(1)	28(1)	30(1)	-7(1)	4(1)	-9(1)
O(5)	31(1)	53(1)	27(1)	-14(1)	2(1)	-3(1)

Table 5. Hydrogen coordinates ($\times 10^4$) and isotropic displacement parameters ($\text{\AA}^2 \times 10^3$) for **51**.

	x	y	z	U(eq)
H(1)	3000(30)	3230(20)	7831(8)	36(4)
H(2)	330(40)	3250(30)	7661(9)	52(5)
H(3)	1560(30)	1510(20)	7727(7)	26(4)
H(4)	1200(30)	4920(30)	6537(8)	39(5)
H(5)	3480(30)	5150(30)	6839(9)	49(5)
H(6)	3250(30)	4440(20)	6099(9)	40(5)
H(7)	4370(30)	470(20)	6990(7)	24(4)
H(8)	6370(30)	390(20)	5970(7)	22(4)
H(9)	5440(30)	2210(20)	5788(8)	30(4)
H(10)	1240(20)	2440(20)	5564(8)	27(4)
H(11)	-220(30)	670(20)	5626(7)	25(4)
H(12)	4160(30)	-2030(20)	6107(8)	31(4)
H(13)	1510(30)	-1730(20)	6182(7)	26(4)
H(14)	7480(40)	2140(30)	6915(9)	43(5)

Table 6. Torsion angles [°] for **51**.

O(1)-C(1)-C(2)-O(2)	178.91(10)
C(9)-C(1)-C(2)-O(2)	-68.57(14)
C(8)-C(1)-C(2)-O(2)	56.23(14)
O(1)-C(1)-C(2)-C(3)	55.46(14)
C(9)-C(1)-C(2)-C(3)	167.99(12)
C(8)-C(1)-C(2)-C(3)	-67.21(15)
O(2)-C(2)-C(3)-C(4)	-175.59(12)
C(1)-C(2)-C(3)-C(4)	-54.01(16)
C(2)-C(3)-C(4)-O(3)	171.11(11)
C(2)-C(3)-C(4)-C(5)	53.32(16)
C(2)-C(3)-C(4)-C(6)	-74.65(15)
O(3)-C(4)-C(5)-O(1)	-176.90(11)
C(3)-C(4)-C(5)-O(1)	-57.24(16)
C(6)-C(4)-C(5)-O(1)	71.16(15)
O(3)-C(4)-C(6)-O(4)	-12.40(13)
C(3)-C(4)-C(6)-O(4)	-131.03(11)
C(5)-C(4)-C(6)-O(4)	102.24(12)
C(4)-C(5)-O(1)-C(1)	62.99(15)
C(9)-C(1)-O(1)-C(5)	-177.48(12)
C(8)-C(1)-O(1)-C(5)	63.10(14)
C(2)-C(1)-O(1)-C(5)	-60.92(14)
O(5)-C(7)-O(3)-C(4)	173.18(13)
O(4)-C(7)-O(3)-C(4)	-6.29(15)
C(3)-C(4)-O(3)-C(7)	132.85(13)
C(5)-C(4)-O(3)-C(7)	-107.18(12)
C(6)-C(4)-O(3)-C(7)	11.70(14)
O(5)-C(7)-O(4)-C(6)	177.93(13)
O(3)-C(7)-O(4)-C(6)	-2.60(16)
C(4)-C(6)-O(4)-C(7)	9.68(15)

Symmetry transformations used to generate equivalent atoms:

Table 7. Hydrogen bonds for **51** [Å and °].

D-H...A	d(D-H)	d(H...A)	d(D...A)	<(DHA)
O(2)-H(14)...O(1)#1	0.82(2)	2.18(2)	2.9905(15)	170.4(19)

Symmetry transformations used to generate equivalent atoms:

#1 x+1,y,z

X-Ray data of compound 52

Table 8. Crystal data and structure refinement for **52**.

Identification code	RT102_0m
Empirical formula	C14 H21 O7.50
Formula weight	309.31
Temperature	173(2) K
Wavelength	1.54178 Å
Crystal system	Monoclinic
Space group	C2
Unit cell dimensions	a = 20.8592(17) Å $\alpha = 90^\circ$. b = 6.4610(5) Å $\beta = 118.081(4)^\circ$. c = 12.5333(13) Å $\gamma = 90^\circ$.
Volume	1490.3(2) Å ³
Z	4
Density (calculated)	1.379 Mg/m ³
Absorption coefficient	0.953 mm ⁻¹
F(000)	660
Crystal size	0.56 x 0.12 x 0.10 mm ³
Theta range for data collection	8.84 to 58.72°.
Index ranges	-21 ≤ h ≤ 22, -6 ≤ k ≤ 7, -13 ≤ l ≤ 13
Reflections collected	2732
Independent reflections	1546 [R(int) = 0.0234]
Completeness to theta = 58.72°	85.6 %
Absorption correction	Semi-empirical from equivalents
Max. and min. transmission	0.9107 and 0.6173
Refinement method	Full-matrix least-squares on F ²
Data / restraints / parameters	1546 / 1 / 199
Goodness-of-fit on F ²	1.072
Final R indices [I > 2σ(I)]	R1 = 0.0357, wR2 = 0.0799
R indices (all data)	R1 = 0.0420, wR2 = 0.0825
Absolute structure parameter	0.1(3)
Largest diff. peak and hole	0.152 and -0.139 e.Å ⁻³

Table 9. Atomic coordinates ($\times 10^4$) and equivalent isotropic displacement parameters ($\text{\AA}^2 \times 10^3$) for **52**. $U(\text{eq})$ is defined as one third of the trace of the orthogonalized U^{ij} tensor.

	x	y	z	U(eq)
C(1)	-3737(2)	-1039(5)	-2037(3)	38(1)
C(2)	-4427(2)	-1887(6)	-3120(3)	45(1)
C(3)	-4914(2)	-2578(5)	-2590(3)	36(1)
C(4)	-4592(2)	-1511(6)	-1385(3)	39(1)
C(5)	-5729(2)	-2320(5)	-3399(3)	39(1)
C(6)	-5482(2)	-5751(6)	-3056(3)	41(1)
C(7)	-3638(2)	1266(5)	-2147(3)	39(1)
C(8)	-2926(2)	2136(5)	-1166(3)	41(1)
C(9)	-2411(2)	1937(5)	-1705(3)	38(1)
C(10)	-2898(2)	2219(5)	-3053(3)	37(1)
C(11)	-2907(2)	4497(6)	-3376(4)	56(1)
C(12)	-2735(2)	860(6)	-3880(3)	54(1)
C(13)	-1399(2)	-288(6)	-1224(3)	44(1)
C(14)	-1107(2)	-2400(6)	-820(4)	64(1)
O(1)	-3825(1)	-1423(4)	-979(2)	43(1)
O(2)	-6004(1)	-4382(3)	-3703(2)	43(1)
O(3)	-4844(1)	-4813(3)	-2385(2)	42(1)
O(4)	-5575(1)	-7563(4)	-3077(3)	60(1)
O(5)	-3622(1)	1673(3)	-3263(2)	46(1)
O(6)	-2083(1)	-105(3)	-1393(2)	44(1)
O(7)	-1062(1)	1124(4)	-1353(2)	51(1)
O(1S)	-5000	-6138(5)	-5000	56(1)

Table 10. Bond lengths [\AA] and angles [$^\circ$] for **52**.

C(1)-O(1)	1.443(4)	C(12)-H(12A)	0.9800
C(1)-C(7)	1.519(4)	C(12)-H(12B)	0.9800
C(1)-C(2)	1.540(5)	C(12)-H(12C)	0.9800
C(1)-H(1)	1.0000	C(13)-O(7)	1.208(4)
C(2)-C(3)	1.519(4)	C(13)-O(6)	1.345(4)
C(2)-H(2A)	0.9900	C(13)-C(14)	1.483(5)
C(2)-H(2B)	0.9900	C(14)-H(14A)	0.9800
C(3)-O(3)	1.462(4)	C(14)-H(14B)	0.9800
C(3)-C(4)	1.501(5)	C(14)-H(14C)	0.9800
C(3)-C(5)	1.523(4)	O(1S)-H(1S)	1.00(6)
C(4)-O(1)	1.434(3)		
C(4)-H(4A)	0.9900	O(1)-C(1)-C(7)	109.5(3)
C(4)-H(4B)	0.9900	O(1)-C(1)-C(2)	106.2(2)
C(5)-O(2)	1.430(4)	C(7)-C(1)-C(2)	112.3(3)
C(5)-H(5A)	0.9900	O(1)-C(1)-H(1)	109.6
C(5)-H(5B)	0.9900	C(7)-C(1)-H(1)	109.6
C(6)-O(4)	1.185(4)	C(2)-C(1)-H(1)	109.6
C(6)-O(3)	1.339(4)	C(3)-C(2)-C(1)	105.0(3)
C(6)-O(2)	1.340(4)	C(3)-C(2)-H(2A)	110.7
C(7)-O(5)	1.439(4)	C(1)-C(2)-H(2A)	110.7
C(7)-C(8)	1.522(4)	C(3)-C(2)-H(2B)	110.7
C(7)-H(7)	1.0000	C(1)-C(2)-H(2B)	110.7
C(8)-C(9)	1.519(4)	H(2A)-C(2)-H(2B)	108.8
C(8)-H(8A)	0.9900	O(3)-C(3)-C(4)	108.4(3)
C(8)-H(8B)	0.9900	O(3)-C(3)-C(2)	109.6(3)
C(9)-O(6)	1.453(4)	C(4)-C(3)-C(2)	103.3(3)
C(9)-C(10)	1.517(5)	O(3)-C(3)-C(5)	102.3(2)
C(9)-H(9)	1.0000	C(4)-C(3)-C(5)	116.8(3)
C(10)-O(5)	1.449(4)	C(2)-C(3)-C(5)	116.3(3)
C(10)-C(12)	1.514(5)	O(1)-C(4)-C(3)	105.7(3)
C(10)-C(11)	1.524(5)	O(1)-C(4)-H(4A)	110.6
C(11)-H(11A)	0.9800	C(3)-C(4)-H(4A)	110.6
C(11)-H(11B)	0.9800	O(1)-C(4)-H(4B)	110.6
C(11)-H(11C)	0.9800	C(3)-C(4)-H(4B)	110.6

H(4A)-C(4)-H(4B)	108.7	H(11A)-C(11)-H(11B)	109.5
O(2)-C(5)-C(3)	105.0(2)	C(10)-C(11)-H(11C)	109.5
O(2)-C(5)-H(5A)	110.8	H(11A)-C(11)-H(11C)	109.5
C(3)-C(5)-H(5A)	110.8	H(11B)-C(11)-H(11C)	109.5
O(2)-C(5)-H(5B)	110.8	C(10)-C(12)-H(12A)	109.5
C(3)-C(5)-H(5B)	110.8	C(10)-C(12)-H(12B)	109.5
H(5A)-C(5)-H(5B)	108.8	H(12A)-C(12)-H(12B)	109.5
O(4)-C(6)-O(3)	124.4(3)	C(10)-C(12)-H(12C)	109.5
O(4)-C(6)-O(2)	124.2(3)	H(12A)-C(12)-H(12C)	109.5
O(3)-C(6)-O(2)	111.5(3)	H(12B)-C(12)-H(12C)	109.5
O(5)-C(7)-C(1)	109.5(3)	O(7)-C(13)-O(6)	123.6(3)
O(5)-C(7)-C(8)	104.9(2)	O(7)-C(13)-C(14)	124.7(3)
C(1)-C(7)-C(8)	114.3(3)	O(6)-C(13)-C(14)	111.7(3)
O(5)-C(7)-H(7)	109.3	C(13)-C(14)-H(14A)	109.5
C(1)-C(7)-H(7)	109.3	C(13)-C(14)-H(14B)	109.5
C(8)-C(7)-H(7)	109.3	H(14A)-C(14)-H(14B)	109.5
C(9)-C(8)-C(7)	103.6(3)	C(13)-C(14)-H(14C)	109.4
C(9)-C(8)-H(8A)	111.0	H(14A)-C(14)-H(14C)	109.5
C(7)-C(8)-H(8A)	111.0	H(14B)-C(14)-H(14C)	109.5
C(9)-C(8)-H(8B)	111.0	C(4)-O(1)-C(1)	106.5(2)
C(7)-C(8)-H(8B)	111.0	C(6)-O(2)-C(5)	110.1(2)
H(8A)-C(8)-H(8B)	109.0	C(6)-O(3)-C(3)	110.4(2)
O(6)-C(9)-C(10)	113.1(3)	C(7)-O(5)-C(10)	111.5(2)
O(6)-C(9)-C(8)	107.4(3)	C(13)-O(6)-C(9)	116.9(2)
C(10)-C(9)-C(8)	104.0(3)		
O(6)-C(9)-H(9)	110.7		
C(10)-C(9)-H(9)	110.7		
C(8)-C(9)-H(9)	110.7		
O(5)-C(10)-C(12)	106.6(3)		
O(5)-C(10)-C(9)	105.5(3)		
C(12)-C(10)-C(9)	116.3(3)		
O(5)-C(10)-C(11)	107.8(3)		
C(12)-C(10)-C(11)	110.9(3)		
C(9)-C(10)-C(11)	109.3(3)		
C(10)-C(11)-H(11A)	109.5		
C(10)-C(11)-H(11B)	109.5		

Symmetry transformations used to generate equivalent atoms:

Table 11. Anisotropic displacement parameters ($\text{\AA}^2 \times 10^3$) for **52**. The anisotropic displacement factor exponent takes the form: $-2\pi^2 [h^2 a^{*2} U^{11} + \dots + 2 h k a^* b^* U^{12}]$

	U11	U22	U33	U23	U13	U12
C(1)	30(2)	46(2)	35(3)	-6(2)	13(2)	-2(2)
C(2)	38(2)	56(2)	35(3)	-9(2)	13(2)	-11(2)
C(3)	27(2)	40(2)	34(2)	-2(2)	8(2)	0(2)
C(4)	36(2)	45(2)	35(2)	1(2)	16(2)	0(2)
C(5)	33(2)	36(2)	43(3)	4(2)	13(2)	0(2)
C(6)	45(2)	42(2)	36(3)	-2(2)	18(2)	0(2)
C(7)	34(2)	46(2)	37(3)	-1(2)	17(2)	2(2)
C(8)	42(2)	41(2)	35(3)	-1(2)	15(2)	-4(2)
C(9)	33(2)	37(2)	32(3)	1(2)	6(2)	-7(2)
C(10)	32(2)	40(2)	33(3)	2(2)	11(2)	-4(2)
C(11)	58(2)	52(2)	42(3)	11(2)	11(2)	-2(2)
C(12)	39(2)	71(2)	45(3)	-8(2)	15(2)	1(2)
C(13)	28(2)	64(3)	34(3)	7(2)	9(2)	0(2)
C(14)	47(2)	72(3)	78(3)	36(3)	33(2)	24(2)
O(1)	32(1)	56(2)	31(2)	0(1)	8(1)	-6(1)
O(2)	31(1)	41(1)	45(2)	-7(1)	8(1)	-2(1)
O(3)	37(1)	35(1)	41(2)	1(1)	7(1)	5(1)
O(4)	76(2)	32(2)	70(2)	-3(1)	34(2)	-7(1)
O(5)	29(1)	66(2)	36(2)	3(1)	10(1)	-3(1)
O(6)	28(1)	42(1)	53(2)	9(1)	13(1)	1(1)
O(7)	35(1)	67(2)	46(2)	2(1)	16(1)	-11(1)
O(1S)	61(2)	51(2)	51(3)	0	21(2)	0

Table 12. Hydrogen coordinates ($\times 10^4$) and isotropic displacement parameters ($\text{\AA}^2 \times 10^3$) for **52**.

	x	y	z	U(eq)
H(1)	-3302	-1804	-1966	46
H(2A)	-4666	-797	-3736	53
H(2B)	-4307	-3067	-3498	53
H(4A)	-4795	-100	-1467	46
H(4B)	-4695	-2302	-806	46
H(5A)	-5953	-1591	-2964	47
H(5B)	-5827	-1525	-4136	47
H(7)	-4053	2034	-2143	46
H(8A)	-2981	3601	-993	49
H(8B)	-2749	1324	-410	49
H(9)	-2030	3038	-1382	45
H(11A)	-3006	5347	-2822	84
H(11B)	-3287	4730	-4208	84
H(11C)	-2434	4880	-3305	84
H(12A)	-3072	1194	-4724	80
H(12B)	-2792	-597	-3724	80
H(12C)	-2235	1105	-3726	80
H(14A)	-650	-2312	-63	96
H(14B)	-1018	-3065	-1441	96
H(14C)	-1459	-3217	-689	96
H(1S)	-5440(30)	-7010(130)	-5200(60)	200(30)

Table 13. Torsion angles [°] for **52**.

O(1)-C(1)-C(2)-C(3)	4.6(3)
C(7)-C(1)-C(2)-C(3)	-115.0(3)
C(1)-C(2)-C(3)-O(3)	-98.5(3)
C(1)-C(2)-C(3)-C(4)	16.9(3)
C(1)-C(2)-C(3)-C(5)	146.1(3)
O(3)-C(3)-C(4)-O(1)	83.0(3)
C(2)-C(3)-C(4)-O(1)	-33.2(3)
C(5)-C(3)-C(4)-O(1)	-162.2(3)
O(3)-C(3)-C(5)-O(2)	-8.3(4)
C(4)-C(3)-C(5)-O(2)	-126.5(3)
C(2)-C(3)-C(5)-O(2)	111.1(3)
O(1)-C(1)-C(7)-O(5)	-174.4(2)
C(2)-C(1)-C(7)-O(5)	-56.7(3)
O(1)-C(1)-C(7)-C(8)	68.2(3)
C(2)-C(1)-C(7)-C(8)	-174.1(3)
O(5)-C(7)-C(8)-C(9)	-29.0(3)
C(1)-C(7)-C(8)-C(9)	91.0(3)
C(7)-C(8)-C(9)-O(6)	-88.1(3)
C(7)-C(8)-C(9)-C(10)	32.1(3)
O(6)-C(9)-C(10)-O(5)	92.7(3)
C(8)-C(9)-C(10)-O(5)	-23.5(3)
O(6)-C(9)-C(10)-C(12)	-25.2(4)
C(8)-C(9)-C(10)-C(12)	-141.4(3)
O(6)-C(9)-C(10)-C(11)	-151.7(3)
C(8)-C(9)-C(10)-C(11)	92.1(3)
C(3)-C(4)-O(1)-C(1)	37.4(3)
C(7)-C(1)-O(1)-C(4)	95.6(3)
C(2)-C(1)-O(1)-C(4)	-25.8(3)
O(4)-C(6)-O(2)-C(5)	175.4(4)
O(3)-C(6)-O(2)-C(5)	-4.7(4)
C(3)-C(5)-O(2)-C(6)	8.2(4)
O(4)-C(6)-O(3)-C(3)	178.7(4)
O(2)-C(6)-O(3)-C(3)	-1.2(4)
C(4)-C(3)-O(3)-C(6)	130.0(3)

C(2)-C(3)-O(3)-C(6)	-118.0(3)
C(5)-C(3)-O(3)-C(6)	6.0(4)
C(1)-C(7)-O(5)-C(10)	-108.2(3)
C(8)-C(7)-O(5)-C(10)	14.9(3)
C(12)-C(10)-O(5)-C(7)	129.8(3)
C(9)-C(10)-O(5)-C(7)	5.5(3)
C(11)-C(10)-O(5)-C(7)	-111.1(3)
O(7)-C(13)-O(6)-C(9)	-2.3(5)
C(14)-C(13)-O(6)-C(9)	175.6(3)
C(10)-C(9)-O(6)-C(13)	97.9(3)
C(8)-C(9)-O(6)-C(13)	-147.9(3)

Symmetry transformations used to generate equivalent atoms:

Table 14. Hydrogen bonds for **52** [Å and °].

D-H...A	d(D-H)	d(H...A)	d(D...A)	<(DHA)
O(1S)-H(1S)...O(5)#1	1.00(6)	2.17(7)	3.018(3)	141(6)

Symmetry transformations used to generate equivalent atoms:

#1 -x-1,y-1,-z-1

X-Ray data of compound 56

Table 15. Crystal data and structure refinement for **56**.

Identification code	T103s
Empirical formula	C18.25 H33 O6.25 Si
Formula weight	380.54
Temperature	173(2) K
Wavelength	1.54178 Å
Crystal system	Monoclinic
Space group	C2
Unit cell dimensions	a = 41.999(9) Å $\alpha = 90^\circ$. b = 8.997(3) Å $\beta = 96.268(10)^\circ$. c = 6.4620(13) Å $\gamma = 90^\circ$.
Volume	2427.2(10) Å ³
Z	4
Density (calculated)	1.041 Mg/m ³
Absorption coefficient	1.077 mm ⁻¹
F(000)	826
Crystal size	0.55 x 0.12 x 0.04 mm ³
Theta range for data collection	2.12 to 61.85°.
Index ranges	-47<=h<=46, -10<=k<=9, -7<=l<=7
Reflections collected	5209
Independent reflections	2598 [R(int) = 0.0550]
Completeness to theta = 61.85°	82.5 %
Absorption correction	Semi-empirical from equivalents
Max. and min. transmission	0.9582 and 0.5890
Refinement method	Full-matrix least-squares on F ²
Data / restraints / parameters	2598 / 4 / 245
Goodness-of-fit on F ²	1.134
Final R indices [I>2sigma(I)]	R1 = 0.1049, wR2 = 0.2718
R indices (all data)	R1 = 0.1488, wR2 = 0.2946
Absolute structure parameter	0.33(14)
Extinction coefficient	0.0081(16)
Largest diff. peak and hole	0.733 and -0.431 e.Å ⁻³

Table 16. Atomic coordinates ($\times 10^4$) and equivalent isotropic displacement parameters ($\text{\AA}^2 \times 10^3$) for **56**. U(eq) is defined as one third of the trace of the orthogonalized U^{ij} tensor.

	x	y	z	U(eq)
C(1)	2929(2)	5980(19)	3896(14)	55(4)
C(2)	2884(2)	4400(20)	3271(15)	63(4)
C(3)	2533(2)	4008(18)	2799(14)	64(4)
C(4)	2333(2)	5162(17)	1576(12)	51(4)
C(5)	2417(2)	6734(17)	2343(15)	53(3)
C(6)	1978(2)	4882(17)	1490(13)	54(4)
C(7)	2105(2)	5200(20)	-1830(15)	74(5)
C(8)	3283(2)	6510(20)	4019(15)	79(5)
C(9)	3438(2)	5970(20)	2103(16)	67(4)
C(10)	3378(2)	4300(20)	1603(16)	60(4)
C(11)	3553(2)	3280(20)	3201(17)	74(5)
C(12)	3463(3)	3950(20)	-553(16)	87(5)
C(13)	3887(3)	7900(20)	-1147(16)	84(5)
C(14)	3916(3)	9330(20)	3064(19)	85(5)
C(15)	4410(3)	6978(16)	2291(17)	61(4)
C(16)	4463(3)	5480(30)	1070(30)	136(10)
C(17)	4638(3)	8160(20)	1630(20)	93(6)
C(18)	4481(3)	6690(30)	4654(18)	101(7)
O(1)	2753(2)	6982(11)	2417(9)	63(3)
O(2)	2383(1)	5142(11)	-648(8)	55(2)
O(3)	1856(2)	5092(12)	-675(9)	68(3)
O(4)	2066(2)	5368(11)	-3670(9)	61(3)
O(5)	3031(1)	4075(11)	1412(9)	62(3)
O(6)	3770(2)	6239(13)	2473(11)	75(3)
Si(1)	3988(1)	7590(5)	1662(4)	68(1)
O(1S)	4236(7)	2160(50)	7810(50)	84(10)
C(1S)	4527(10)	1630(70)	7510(80)	80(15)

Table 17. Bond lengths [\AA] and angles [$^\circ$] for **56**.

C(1)-O(1)	1.456(15)	C(12)-H(12A)	0.9800
C(1)-C(2)	1.48(2)	C(12)-H(12B)	0.9800
C(1)-C(8)	1.553(14)	C(12)-H(12C)	0.9800
C(1)-H(1)	1.0000	C(13)-Si(1)	1.840(11)
C(2)-O(5)	1.441(11)	C(13)-H(13A)	0.9800
C(2)-C(3)	1.516(15)	C(13)-H(13B)	0.9800
C(2)-H(2)	1.0000	C(13)-H(13C)	0.9800
C(3)-C(4)	1.503(18)	C(14)-Si(1)	1.847(19)
C(3)-H(3A)	0.9900	C(14)-H(14A)	0.9800
C(3)-H(3B)	0.9900	C(14)-H(14B)	0.9800
C(4)-O(2)	1.474(9)	C(14)-H(14C)	0.9800
C(4)-C(6)	1.509(12)	C(15)-C(17)	1.53(2)
C(4)-C(5)	1.527(19)	C(15)-C(18)	1.545(17)
C(5)-O(1)	1.425(11)	C(15)-C(16)	1.59(3)
C(5)-H(5A)	0.9900	C(15)-Si(1)	1.857(11)
C(5)-H(5B)	0.9900	C(16)-H(16A)	0.9800
C(6)-O(3)	1.449(10)	C(16)-H(16B)	0.9800
C(6)-H(6A)	0.9900	C(16)-H(16C)	0.9800
C(6)-H(6B)	0.9900	C(17)-H(17A)	0.9800
C(7)-O(4)	1.192(12)	C(17)-H(17B)	0.9800
C(7)-O(2)	1.325(12)	C(17)-H(17C)	0.9800
C(7)-O(3)	1.354(12)	C(18)-H(18A)	0.9800
C(8)-C(9)	1.539(16)	C(18)-H(18B)	0.9800
C(8)-H(8A)	0.9900	C(18)-H(18C)	0.9800
C(8)-H(8B)	0.9900	O(6)-Si(1)	1.642(10)
C(9)-O(6)	1.412(13)	O(1S)-C(1S)	1.349(18)
C(9)-C(10)	1.55(2)	O(1S)-H(1S)	0.6433
C(9)-H(9)	1.0000	C(1S)-H(1S1)	0.9800
C(10)-O(5)	1.465(11)	C(1S)-H(1S2)	0.9800
C(10)-C(12)	1.507(14)	C(1S)-H(1S3)	0.9800
C(10)-C(11)	1.508(19)		
C(11)-H(11A)	0.9800	O(1)-C(1)-C(2)	111.9(9)
C(11)-H(11B)	0.9800	O(1)-C(1)-C(8)	105.0(11)
C(11)-H(11C)	0.9800	C(2)-C(1)-C(8)	113.7(11)

O(1)-C(1)-H(1)	108.7	C(9)-C(8)-C(1)	110.3(10)
C(2)-C(1)-H(1)	108.7	C(9)-C(8)-H(8A)	109.6
C(8)-C(1)-H(1)	108.7	C(1)-C(8)-H(8A)	109.6
O(5)-C(2)-C(1)	111.7(11)	C(9)-C(8)-H(8B)	109.6
O(5)-C(2)-C(3)	106.2(9)	C(1)-C(8)-H(8B)	109.6
C(1)-C(2)-C(3)	112.0(12)	H(8A)-C(8)-H(8B)	108.1
O(5)-C(2)-H(2)	108.9	O(6)-C(9)-C(8)	107.8(10)
C(1)-C(2)-H(2)	108.9	O(6)-C(9)-C(10)	109.7(11)
C(3)-C(2)-H(2)	108.9	C(8)-C(9)-C(10)	113.7(12)
C(4)-C(3)-C(2)	114.7(12)	O(6)-C(9)-H(9)	108.5
C(4)-C(3)-H(3A)	108.6	C(8)-C(9)-H(9)	108.5
C(2)-C(3)-H(3A)	108.6	C(10)-C(9)-H(9)	108.5
C(4)-C(3)-H(3B)	108.6	O(5)-C(10)-C(12)	103.1(8)
C(2)-C(3)-H(3B)	108.6	O(5)-C(10)-C(11)	112.4(10)
H(3A)-C(3)-H(3B)	107.6	C(12)-C(10)-C(11)	111.2(13)
O(2)-C(4)-C(3)	112.0(9)	O(5)-C(10)-C(9)	106.7(11)
O(2)-C(4)-C(6)	101.9(6)	C(12)-C(10)-C(9)	110.1(12)
C(3)-C(4)-C(6)	113.3(11)	C(11)-C(10)-C(9)	112.9(10)
O(2)-C(4)-C(5)	106.0(10)	C(10)-C(11)-H(11A)	109.5
C(3)-C(4)-C(5)	112.0(9)	C(10)-C(11)-H(11B)	109.5
C(6)-C(4)-C(5)	111.0(10)	H(11A)-C(11)-H(11B)	109.5
O(1)-C(5)-C(4)	110.4(9)	C(10)-C(11)-H(11C)	109.5
O(1)-C(5)-H(5A)	109.6	H(11A)-C(11)-H(11C)	109.5
C(4)-C(5)-H(5A)	109.6	H(11B)-C(11)-H(11C)	109.5
O(1)-C(5)-H(5B)	109.6	C(10)-C(12)-H(12A)	109.5
C(4)-C(5)-H(5B)	109.6	C(10)-C(12)-H(12B)	109.5
H(5A)-C(5)-H(5B)	108.1	H(12A)-C(12)-H(12B)	109.5
O(3)-C(6)-C(4)	105.0(6)	C(10)-C(12)-H(12C)	109.5
O(3)-C(6)-H(6A)	110.8	H(12A)-C(12)-H(12C)	109.5
C(4)-C(6)-H(6A)	110.8	H(12B)-C(12)-H(12C)	109.5
O(3)-C(6)-H(6B)	110.8	Si(1)-C(13)-H(13A)	109.5
C(4)-C(6)-H(6B)	110.8	Si(1)-C(13)-H(13B)	109.5
H(6A)-C(6)-H(6B)	108.8	H(13A)-C(13)-H(13B)	109.5
O(4)-C(7)-O(2)	126.7(9)	Si(1)-C(13)-H(13C)	109.5
O(4)-C(7)-O(3)	121.9(9)	H(13A)-C(13)-H(13C)	109.5
O(2)-C(7)-O(3)	111.4(8)	H(13B)-C(13)-H(13C)	109.5

Si(1)-C(14)-H(14A)	109.5	O(6)-Si(1)-C(14)	110.1(5)
Si(1)-C(14)-H(14B)	109.5	C(13)-Si(1)-C(14)	108.8(8)
H(14A)-C(14)-H(14B)	109.5	O(6)-Si(1)-C(15)	105.2(6)
Si(1)-C(14)-H(14C)	109.5	C(13)-Si(1)-C(15)	112.0(5)
H(14A)-C(14)-H(14C)	109.5	C(14)-Si(1)-C(15)	110.3(6)
H(14B)-C(14)-H(14C)	109.5	C(1S)-O(1S)-H(1S)	116.8
C(17)-C(15)-C(18)	109.7(12)	O(1S)-C(1S)-H(1S1)	109.5
C(17)-C(15)-C(16)	109.1(11)	O(1S)-C(1S)-H(1S2)	109.5
C(18)-C(15)-C(16)	109.0(14)	H(1S1)-C(1S)-H(1S2)	109.5
C(17)-C(15)-Si(1)	110.1(10)	O(1S)-C(1S)-H(1S3)	109.5
C(18)-C(15)-Si(1)	110.0(7)	H(1S1)-C(1S)-H(1S3)	109.5
C(16)-C(15)-Si(1)	109.0(8)	H(1S2)-C(1S)-H(1S3)	109.5
C(15)-C(16)-H(16A)	109.5		
C(15)-C(16)-H(16B)	109.5		
H(16A)-C(16)-H(16B)	109.5		
C(15)-C(16)-H(16C)	109.5		
H(16A)-C(16)-H(16C)	109.5		
H(16B)-C(16)-H(16C)	109.5		
C(15)-C(17)-H(17A)	109.5		
C(15)-C(17)-H(17B)	109.5		
H(17A)-C(17)-H(17B)	109.5		
C(15)-C(17)-H(17C)	109.5		
H(17A)-C(17)-H(17C)	109.5		
H(17B)-C(17)-H(17C)	109.5		
C(15)-C(18)-H(18A)	109.5		
C(15)-C(18)-H(18B)	109.5		
H(18A)-C(18)-H(18B)	109.5		
C(15)-C(18)-H(18C)	109.5		
H(18A)-C(18)-H(18C)	109.5		
H(18B)-C(18)-H(18C)	109.5		
C(5)-O(1)-C(1)	110.9(8)		
C(7)-O(2)-C(4)	110.6(6)		
C(7)-O(3)-C(6)	109.2(7)		
C(2)-O(5)-C(10)	114.5(8)		
C(9)-O(6)-Si(1)	130.5(10)		
O(6)-Si(1)-C(13)	110.5(6)		

Symmetry transformations used to generate equivalent atoms:

Table 18. Anisotropic displacement parameters ($\text{\AA}^2 \times 10^3$) for **56**. The anisotropic displacement factor exponent takes the form: $-2\pi^2 [h^2 a^{*2} U^{11} + \dots + 2 h k a^* b^* U^{12}]$

	U11	U22	U33	U23	U13	U12
C(1)	37(6)	108(13)	18(4)	-3(6)	-1(4)	-13(6)
C(2)	35(5)	127(15)	27(5)	-11(7)	8(4)	-9(6)
C(3)	35(5)	132(14)	25(4)	-5(7)	7(4)	1(7)
C(4)	41(5)	92(12)	19(4)	6(7)	1(4)	6(6)
C(5)	33(5)	87(11)	42(5)	-1(7)	14(4)	-5(5)
C(6)	36(5)	101(12)	23(4)	16(6)	-4(4)	-3(6)
C(7)	44(6)	149(16)	31(5)	-11(8)	8(4)	8(8)
C(8)	34(6)	166(17)	38(5)	2(8)	4(4)	-12(7)
C(9)	28(5)	132(15)	42(6)	13(8)	5(4)	3(7)
C(10)	28(5)	107(14)	45(6)	0(7)	4(4)	-14(6)
C(11)	36(6)	127(15)	58(7)	-11(8)	0(5)	-6(6)
C(12)	48(6)	166(17)	52(6)	-32(9)	22(5)	-10(8)
C(13)	60(7)	136(17)	56(6)	2(9)	14(6)	-1(8)
C(14)	31(5)	156(17)	68(7)	17(9)	1(5)	10(7)
C(15)	51(6)	71(11)	62(6)	1(7)	15(5)	10(6)
C(16)	41(7)	240(30)	128(13)	-45(16)	4(8)	32(11)
C(17)	39(6)	145(17)	96(9)	14(11)	15(6)	-14(8)
C(18)	35(6)	210(20)	57(6)	-22(10)	5(5)	3(8)
O(1)	39(4)	115(9)	33(3)	-2(4)	1(3)	-4(4)
O(2)	32(3)	110(8)	24(3)	0(4)	6(2)	-4(4)
O(3)	36(3)	137(9)	33(3)	10(5)	10(3)	-10(4)
O(4)	54(4)	103(8)	28(3)	-3(4)	5(3)	2(4)
O(5)	33(4)	120(9)	35(3)	-5(4)	14(3)	-3(4)
O(6)	23(3)	141(10)	59(4)	-6(5)	3(3)	-15(4)
Si(1)	32(1)	132(4)	41(2)	-2(2)	6(1)	-1(2)

Table 19. Hydrogen coordinates ($\times 10^4$) and isotropic displacement parameters ($\text{\AA}^2 \times 10^3$) for **56**.

	x	y	z	U(eq)
H(1)	2852	6120	5291	66
H(2)	2982	3756	4427	75
H(3A)	2516	3062	2011	77
H(3B)	2442	3838	4130	77
H(5A)	2301	7466	1395	64
H(5B)	2348	6873	3748	64
H(6A)	1935	3858	1949	65
H(6B)	1877	5593	2391	65
H(8A)	3291	7607	4084	95
H(8B)	3404	6114	5301	95
H(9)	3349	6566	869	81
H(11A)	3551	3717	4590	111
H(11B)	3775	3160	2896	111
H(11C)	3447	2312	3155	111
H(12A)	3455	2876	-777	131
H(12B)	3679	4318	-697	131
H(12C)	3309	4441	-1586	131
H(13A)	3989	7139	-1928	125
H(13B)	3963	8886	-1519	125
H(13C)	3654	7848	-1490	125
H(14A)	3724	9815	2392	128
H(14B)	4101	9990	3032	128
H(14C)	3887	9095	4512	128
H(16A)	4442	5680	-426	205
H(16B)	4302	4749	1380	205
H(16C)	4678	5092	1516	205
H(17A)	4598	9106	2312	139
H(17B)	4603	8293	113	139
H(17C)	4860	7852	2028	139
H(18A)	4692	6226	4945	151

H(18B)	4317	6027	5109	151
H(18C)	4478	7635	5406	151
H(1S)	4180	2689	7208	125
H(1S1)	4690	2099	8500	119
H(1S2)	4572	1846	6088	119
H(1S3)	4531	550	7736	119

Table 20. Torsion angles [°] for **56**.

O(1)-C(1)-C(2)-O(5)	67.9(11)
C(8)-C(1)-C(2)-O(5)	-50.8(12)
O(1)-C(1)-C(2)-C(3)	-51.1(10)
C(8)-C(1)-C(2)-C(3)	-169.9(8)
O(5)-C(2)-C(3)-C(4)	-80.2(14)
C(1)-C(2)-C(3)-C(4)	42.0(11)
C(2)-C(3)-C(4)-O(2)	76.6(13)
C(2)-C(3)-C(4)-C(6)	-168.7(9)
C(2)-C(3)-C(4)-C(5)	-42.2(10)
O(2)-C(4)-C(5)-O(1)	-70.1(9)
C(3)-C(4)-C(5)-O(1)	52.2(9)
C(6)-C(4)-C(5)-O(1)	180.0(7)
O(2)-C(4)-C(6)-O(3)	-13.3(14)
C(3)-C(4)-C(6)-O(3)	-133.8(10)
C(5)-C(4)-C(6)-O(3)	99.2(10)
O(1)-C(1)-C(8)-C(9)	-77.7(15)
C(2)-C(1)-C(8)-C(9)	44.9(15)
C(1)-C(8)-C(9)-O(6)	-169.5(13)
C(1)-C(8)-C(9)-C(10)	-47.6(15)
O(6)-C(9)-C(10)-O(5)	175.4(7)
C(8)-C(9)-C(10)-O(5)	54.6(11)
O(6)-C(9)-C(10)-C(12)	-73.4(11)
C(8)-C(9)-C(10)-C(12)	165.8(9)
O(6)-C(9)-C(10)-C(11)	51.5(11)
C(8)-C(9)-C(10)-C(11)	-69.3(11)
C(4)-C(5)-O(1)-C(1)	-62.7(11)
C(2)-C(1)-O(1)-C(5)	63.3(10)
C(8)-C(1)-O(1)-C(5)	-172.9(9)
O(4)-C(7)-O(2)-C(4)	171.3(16)
O(3)-C(7)-O(2)-C(4)	-7.2(18)
C(3)-C(4)-O(2)-C(7)	134.3(12)
C(6)-C(4)-O(2)-C(7)	12.8(16)
C(5)-C(4)-O(2)-C(7)	-103.4(12)
O(4)-C(7)-O(3)-C(6)	179.2(15)

O(2)-C(7)-O(3)-C(6)	-2.2(17)
C(4)-C(6)-O(3)-C(7)	10.2(16)
C(1)-C(2)-O(5)-C(10)	61.3(14)
C(3)-C(2)-O(5)-C(10)	-176.3(12)
C(12)-C(10)-O(5)-C(2)	-177.3(13)
C(11)-C(10)-O(5)-C(2)	62.9(16)
C(9)-C(10)-O(5)-C(2)	-61.3(13)
C(8)-C(9)-O(6)-Si(1)	-99.8(12)
C(10)-C(9)-O(6)-Si(1)	136.0(10)
C(9)-O(6)-Si(1)-C(13)	-46.9(13)
C(9)-O(6)-Si(1)-C(14)	73.3(11)
C(9)-O(6)-Si(1)-C(15)	-167.9(10)
C(17)-C(15)-Si(1)-O(6)	-179.4(9)
C(18)-C(15)-Si(1)-O(6)	-58.4(12)
C(16)-C(15)-Si(1)-O(6)	61.0(11)
C(17)-C(15)-Si(1)-C(13)	60.5(12)
C(18)-C(15)-Si(1)-C(13)	-178.5(12)
C(16)-C(15)-Si(1)-C(13)	-59.0(13)
C(17)-C(15)-Si(1)-C(14)	-60.7(10)
C(18)-C(15)-Si(1)-C(14)	60.3(13)
C(16)-C(15)-Si(1)-C(14)	179.7(11)

Symmetry transformations used to generate equivalent atoms:

2.5 References

1. Murata, M.; Yasumoto, T. *Nat. Prod. Rep.* **2000**, *17*, 293. (b) Deranas, A. H.; Norte, M.; Fernandez, J. J. *Toxicon* **2001**, *39*, 1101. (c) Nakata, T. *Chem. Rev.* **2005**, *105*, 4314. (d) Inoue, M. *Chem. Rev.* **2005**, *105*, 4379.
2. Fernandez, J. J.; Souto, M. L.; Norte, M. *Bioorg. Med. Chem.* **1998**, *6*, 2237. and references therein.
3. (a) Nicolaou, K. C.; Rutjes, F. P. J. T.; Theodorakis, E. A.; Tiebes, J.; Sato, M.; Untersteller, E. *J. Am. Chem. Soc.* **1995**, *117*, 1173. (b) Nicolaou, K. C.; Rutjes, F. P. J. T.; Theodorakis, E. A.; Tiebes, J.; Sato, M.; Untersteller, E. *J. Am. Chem. Soc.* **1995**, *117*, 10252. (c) Matsuo, G.; Kawamura, K.; Hori, N.; Matsukura, H.; Nakata, T. *J. Am. Chem. Soc.* **2004**, *126*, 14374. (d) Kadota, I.; Takamura, H.; Nishii, H.; Yamamoto, Y. *J. Am. Chem. Soc.* **2005**, *127*, 9246.
4. (a) Nicolaou, K. C.; Yang, Z.; Shi, G.; Gunzner, J. L.; Agrios, K. A.; Gartner, P. *Nature* **1998**, *392*, 264. (b) Nicolaou, K. C.; Gunzner, J. L.; Shi, G.-q.; Agrios, K. A.; Gartner, P.; Yang, Z. *Chem. Eur. J.* **1999**, *5*, 646.
5. (a) Hirama, M.; Oishi, T.; Uehara, H.; Inoue, M.; Maruyama, M.; Oguri, H.; Satake, M. *Science* **2001**, *294*, 1904. (b) Inoue, M.; Uehara, H.; Maruyama, M.; Hirama, M. *Org. Lett.* **2002**, *4*, 4551.

6. (a) Fuwa, H.; Sasaki, M.; Satake, M.; Tachibana, K. *Org. Lett.* **2002**, *4*, 2981. (b) Fuwa, H.; Kainuma, N.; Tachibana, K.; Sasaki, M. *J. Am. Chem. Soc.* **2002**, *124*, 14983. (c) Kadota, I.; Takamura, H.; Sato, K.; Ohno, A.; Matsuda, K.; Yamamoto, Y. *J. Am. Chem. Soc.* **2003**, *125*, 46. (d) Kadota, I.; Takamura, H.; Sato, K.; Ohno, A.; Matsuda, K.; Satake, M.; Yamamoto, Y. *J. Am. Chem. Soc.* **2003**, *125*, 11893. (e) Johnson, H. W. B.; Majumder, U.; Rainier, J. D. *J. Am. Chem. Soc.* **2005**, *127*, 848.
7. (a) Tsukano, C.; Sasaki, M. *J. Am. Chem. Soc.* **2003**, *125*, 14294. (b) Tsukano, C.; Ebine, M.; Sasaki, M. *J. Am. Chem. Soc.* **2005**, *127*, 4326.
8. (a) Fujiwara, K.; Murai, A. *Bull. Chem. Soc. Jpn.* **2004**, *77*, 2129. (b) Kadota, I.; Yamamoto, Y. *Acc. Chem. Res.* **2005**, *38*, 423. (c) Sasaki, M.; Fuwa, H. *Synlett.* **2004**, *11*, 1851. (d) Marmsater, F. P.; West, F. G. *Chem. Eur. J.* **2002**, *8*, 4346.
9. (a) Nicolaou, K. C.; Duggan, M. E.; Hwang, C.-K. *J. Am. Chem. Soc.* **1986**, *108*, 2468. (b) Nicolaou, K. C.; Prasad, C. V. C.; Hwang, C.-K.; Duggan, M. E.; Veale, C. A. *J. Am. Chem. Soc.* **1989**, *111*, 5321.
10. (a) Fujiwara, K.; Saka, K.; Takaoka, D.; Murai, A. *Synlett* **1999**, 1037. (b) Fujiwara, K.; Sato, D.; Watanabe, M.; Morishita, H.; Murai, A.; Kawai, H.; Suzuki, T. *Tetrahedron Lett.* **2004**, *45*, 5243.
11. Sasaki, M.; Fuwa, H.; Inoue, M.; Tachibana, K. *Tetrahedron Lett.* **1998**, *39*, 9027. (b) Sasaki, M.; Fuwa, H. *Synlett* **2004**, 1851.
12. Cieplak, A. S. *J. Am. Chem. Soc.* **1981**, *103*, 4540.

13. (a) Fujiwara, K.; Morishita, H.; Saka, K.; Murai, A. *Tetrahedron Lett.* **2000**, *41*, 507. (b) Matsuo, G.; Hinou, H.; Koshino, H.; Suenaga, T.; Nakata, T. *Tetrahedron Lett.* **2000**, *41*, 903. (c) Mori, Y.; Mitsuoka, S.; Furukawa, H. *Tetrahedron Lett.* **2000**, *41*, 4161.
14. (a) Mori, Y.; Nogami, K.; Hayashi, H.; Noyori, R. *J. Org. Chem.* **2003**, *68*, 9050. (b) Mori, Y.; Hayashi, H. *Tetrahedron* **2002**, *58*, 1789.
15. (a) Inoue, M.; Sasaki, M.; Tachibana, K. *Tetrahedron Lett.* **1997**, *38*, 1611. (b) Inoue, M.; Sasaki, M.; Tachibana, K. *Tetrahedron* **1999**, *55*, 10949. (c) Inoue, M.; Sasaki, M.; Tachibana, K. *Angew. Chem. Int. Ed.* **1998**, *37*, 965. (d) Inoue, M.; Sasaki, M.; Tachibana, K. *J. Org. Chem.* **1999**, *64*, 9416.
16. (a) Hori, N.; Matsukura, H.; Matsuo, G.; Nakata, T. *Tetrahedron Lett.* **1999**, *40*, 2811. (b) Matsuo, G.; Hori, N.; Nakata, T. *Tetrahedron Lett.* **1999**, *40*, 8859. (c) Hori, N.; Matsukura, H.; Nakata, T. *Org. Lett.* **1999**, *1*, 1099. (d) Hori, N.; Matsukura, H.; Matsuo, G.; Nakata, T. *Tetrahedron* **2002**, *58*, 1853.
17. (a) Clark, J. S.; Kettle, J. G. *Tetrahedron Lett.* **1997**, *38*, 123. (b) Clark, J. S.; Kettle, J. G. *Tetrahedron Lett.* **1997**, *38*, 127. (c) Clark, J. S.; Kettle, J. G. *Tetrahedron* **1999**, *55*, 8231.
18. McDonald, F. E.; Bowman, J. L. *J. Org. Chem.* **1998**, *63*, 3680.
19. (a) Rainier, J. D.; Allwein, S. P. *J. Org. Chem.* **1998**, *63*, 5310. (b) Rainier, J. D.; Allwein, S. P.; *Tetrahedron Lett.* **1998**, *39*, 9601. (c) Rainier, J. D.; Allwein, S. P.; Cox, J. M. *Org. Lett.* **2000**, *2*, 231. (d) Rainier, J. D.; Allwein, S. P.; Cox, J. M. *J. Org. Chem.* **2001**, *66*, 1380.

20. (a) Marmsäter, F. P.; West, F. G. *J. Am. Chem. Soc.* **2001**, *123*, 5144. (b) Marmsäter, F. P.; Vanecko, J. A.; West, F. G. *Tetrahedron* **2002**, *58*, 2027.
21. (a) Nakanishi, K. *Toxicon* **1985**, *23*, 473. (b) Shimizu, Y. *Natural Toxins: Animal, Plant, and Microbial* ed. by Harris, J. B.; Clarendon Press, Oxford **1986**, 123. (c) Lee, M. S.; Repeta, D. J.; Nakanishi, K.; Zagorski, M. G. *J. Am. Chem. Soc.* **1986**, *108*, 7855. (d) Chou, H.-N.; Shimizu, Y. *J. Am. Chem. Soc.*, **1987**, *109*, 2184. (e) Lee, M. S.; Qin, Q.-W.; Nakanishi, K.; Zagorski, M. G. *J. Am. Chem. Soc.* **1989**, *111*, 6234.
22. (a) Baldwin, J. E.; Thomas, R.C.; Kruse, L. I.; Silberman, L. *J. Org. Chem.* **1977**, *42*, 3846. (b) Baldwin, J. E.; Cutting, J.; Dupont, W.; Kruse, L. I.; Silberman, L.; Thomas, R.C. *J. Chem. Soc., Chem. Commun.* **1976**, 736. (c) Baldwin, J. E. *J. Chem. Soc., Chem. Commun.* **1976**, 738.
23. (a) Nicolaou, K. C.; Duggan, M. E.; Hwang, C.-K.; Somers, P. K. *J. Chem. Soc., Chem. Commun.*, **1985**, 1359. (b) Nicolaou, K. C.; Prasad, C. V. C.; Somers, P. K.; Hwang, C.-K. *J. Am. Chem. Soc.* **1989**, *111*, 5330. (c) Nicolaou, K. C.; Shi, G.-Q.; Gumzner, J. L.; Gartner, P.; Wallace, P. A.; Ouellette, M. A.; Shi, S.; Bunnage, M. E.; Agrios, K. A.; Veale, C. A., Hwang, C.-K.; Hutchinson, J.; Prasad, C. V. C.; Ogilvie, W.W.; Yang, Z. *Chem. Eur. J.*, 1999, *5*, 628.
24. (a) Suzuki, T.; Sato, O.; Hirama, M. *Tetrahedron Lett.* 1990, *31*, 4747. (b) Oishi, T.; Maeda, K.; Hirama, M. *Chem. Commun.* **1997**, 1289.

25. (a) Mori, Y.; Yaegashi, K.; Furukawa, H.; *J. Am. Chem. Soc.* **1996**, *118*, 8158. (b) Mori, Y.; Furuta, H.; Takase, T.; Mitsuoka, S.; Furukawa, H. *Tetrahedron Lett.* **1999**, *40*, 8019. (c) Furuta, H.; Takase, T.; Hayashi, H.; Noyori, R.; Mori, Y. *Tetrahedron*, **2003**, *59*, 9767. (d) Mori, Y.; Yaegashi, K.; Furukawa, H. *J. Am. Chem. Soc.* **1997**, *119*, 4557. (e) Mori, Y.; Yaegashi, K.; Furukawa, H. *J. Org. Chem.* **1998**, *63*, 6200.
26. Bartlett, P. A.; Ting, P. C. *J. Org. Chem.* **1986**, *51*, 2230.
27. (a) McDonald, F. E.; Bravo, F.; Wang, X.; Wei, X.; Toganoh, M.; Rodríguez, J. R.; Do, B.; Neiwert, W. A.; Hardcastle, K. I. *J. Org. Chem.* **2002**, *67*, 2515. (b) Valentine, J. C.; McDonald, F. E.; Neiwert, W. A.; Hardcastle, K. I. *J. Am. Chem. Soc.* **2005**, *127*, 4586, and references therein. (c) Valentine, J. C.; McDonald, F. E. *Synlett* **2006**, *12*, 1816. (d) McDonald, F. E.; Tong, R.; Valentine, J. C.; Bravo, F. *Pure Appl. Chem.*, **2007**, *79*, 281.
28. Bravo, F.; McDonald, F. E.; Neiwert, W. A.; Do, B.; Hardcastle, K. I. *Org. Lett.* **2003**, *5*, 2123.
29. Ferraboschi, P.; Grisenti, P.; Casati, S.; Santaniello, E. *Synlett* **1994**, 754.
30. (a) Gao, Y.; Hanson, R. M.; Klunder, J. M.; Ko, S. Y.; Masamune, H.; Sharpless, K. B. *J. Am. Chem. Soc.* **1987**, *109*, 5765. (b) Wang, X.; Tu, Y.; Frohn, M.; Zhang, J.; Shi, Y. *J. Am. Chem. Soc.* **1997**, *119*, 11224.
31. (a) Yadav, J. S.; Praveen Kumar, T. K.; Maniyan, P. P. *Tetrahedron Lett.* **1993**, *34*, 2965. (b) Descotes, G.; Menet, A.; Collonges, F. *Tetrahedron* **1973**, *29*, 2931.

32. (a) Chan, K.; Cohen, N.; De Noble, J. P.; Specian, A. C.; Saucy, G. *J. Org. Chem.* **1976**, *41*, 3497. (b) Denmark, S. E.; Jones, T. K. *J. Org. Chem.* **1982**, *47*, 4595. (c) Miller, C. H.; Hatzenellenbogen, J. A.; Bowlus, S. B. *Tetrahedron Lett.* **1973**, *24*, 1737.
33. Bravo, F.; McDonald, F. E.; Neiwert, W. A.; Hardcastle, K. I. *Org. Lett.* **2004**, *6*, 4487.
34. Morimoto, Y.; Nishikawa, Y.; Ueba, C.; Tanaka, T. *Angew. Chem. Int. Ed.* **2006**, *45*, 810.
35. Tong, R.; Valentine, J. C.; McDonald, F. E.; Cao, R.; Fang, X.; Hardcastle, K. I. *J. Am. Chem. Soc.* **2007**, *129*, 1050.
36. (a) Hayashi, N.; Fujiwara, K.; Murai, A. *Chem. Lett.* **1996**, 341. (b) Hayashi, N.; Fujiwara, K.; Murai, A. *Tetrahedron Lett.* **1996**, *37*, 6173.
37. (a) Nonomura, T.; Sasaki, M.; Matsumori, N.; Murata, M.; Tachibana, K.; Yasumoto, T. *Angew. Chem. Int. Ed.* **1996**, *35*, 1675. (b) Zheng, W. J.; DeMattei, J. A.; Wu, J. P.; Duan, J. J. W.; Cook, L. R.; Oinuma, H.; Kishi, Y. *J. Am. Chem. Soc.* **1996**, *118*, 7946.
38. (a) Corey, E. J.; Katzenellenbogen, J. A.; Posner, G. H. *J. Am. Chem. Soc.* **1967**, *89*, 4245. (b) Corey, E. J.; Kirst, H. A.; Katzenellenbogen, J. A. *J. Am. Chem. Soc.* **1970**, *92*, 6314.
39. Kim, K. D.; Magriotis, P. A. *Tetrahedron Lett.* **1990**, *31*, 6173.
40. Labinger, J. A.; Hart, D. W.; Seibert, W. E.; Schwartz, J. *J. Am. Chem. Soc.* **1975**, *97*, 3851.

41. (a) Wipf, P.; Xu, W. *Tetrahedron Lett.* **1994**, *35*, 5197. (b) Wipf, P.; Jahn, H. *Tetrahedron* **1996**, *52*, 12853.
42. Robinson, D. E. J. E.; Bull, S. D. *Tetrahedron: Asymmetry* **2003**, *14*, 1407.
43. (a) Taguchi, H.; Tanaka, S.; Yamamoto, H.; Nozaki, H. *Tetrahedron Lett.* **1973**, 2465. (b) Oshima, K.; Yamamoto, H.; Nozaki, H. *J. Am. Chem. Soc.* **1973**, *95*, 4446. Tong, R.; McDonald, F. E.; Fang, X.; Hardcastle, K.I. *Synthesis* **2007**, 2337.